ABSTRACT

GAO, HUIPU. The Effects of Materials and Environmental Factors on Heat Loss Indexes Used to Characterize the Contribution of Turnout Suits to Heat Strain in Structural Firefighting. (Under the direction of Dr. Roger L. Barker).

Firefighter protective clothing contributes to heat stress, considered as one major thermal hazard for firefighters. The NFPA 1971 standard for structural firefighter protective clothing establishes a minimum heat strain requirement for turnout suits materials based on Total Heat Loss (*THL*), measured at 25 °C, 65% RH. It cannot accurately predict the heat strain potential of turnout materials in hot environments, and NFPA 1971 is considering R_{ef}, which is evaporative resistance measured at 35 °C, 40% RH. This research aims to understand the relationship between these heat strain measures and, more generally, how heat loss through turnout materials is affected by environmental factors and turnout system features.

The first area addressed was understanding the effects of turnout materials on heat transfer in different environmental exposures encountered by firefighters. A dynamic hotplate system with a cooling mechanism and a heat flux sensor was used. This allowed the characterization of heat exchange in hot environments, which is impossible for a traditional sweating guarded hotplate.

The exploration of the relationship between thermal comfort indexes showed no correlation between *THL* and R_{ef}, demonstrating that the heat release properties of turnout materials depend on testing environments. The heat transfer through firefighter composite materials with different moisture barriers and air gap sizes were tested under various environmental conditions. It was found that in a cool environment, all moisture barrier systems performed similarly due to a large amount of moisture gain. In hot and dry conditions, or with air gaps, the evaporative resistance of bicomponent moisture barriers increased due to moisture loss.

The investigation on the effect of outer shells (color, texture, and smoke contaminant) and moisture barriers on heat loss under solar radiation revealed that dark-colored or dirty gear significantly impacted heat gain from solar radiation. In addition, bicomponent moisture barriers increased resistance with exposure to solar load. A new test method involving the application of simulated solar radiation was investigated.

Fabric level testing could not account for clothing reinforcement, design, fit, and pumping effect, and this led to the second objective, which was to investigate how heat strain indexes measured at the fabric level correlated with physiological parameters associated with turnout-related firefighter heat stress.

Turnout garments with differences in moisture barrier, reinforcement, thermal liner, and finishes were tested with a physiological sweating manikin. The results demonstrated that *THL* was a better index to predict firefighter physiological response in a mild environment. In comparison, R_{ef} performed better in warm conditions. This revealed the potential of using fabric level tests (*THL* and R_{ef}) to predict human heat strain. The results also showed that the durable water repellent finishing applied to thermal liners did not affect heat strain, while adding large quantities of thick impermeable material to the turnout garment could increase the risk of heat stress.

The Effects of Materials and Environmental Factors on Heat Loss Indexes Used to Characterize the Contribution of Turnout Suits to Heat Strain in Structural Firefighting

by
Huipu Gao

A dissertation submitted to the Graduate Faculty of
North Carolina State University
in partial fulfillment of the
requirements for the degree of
Doctor of Philosophy

Fiber and Polymer Science

Raleigh, North Carolina
2021

APPROVED BY:

Dr. Roger L. Barker
Committee Chair

Dr. Emiel DenHartog

Dr. Sharon Lubkin

Dr. Warren Jasper

Dr. Xiaomeng Fang

DEDICATION

To my parents, my wife, and my sisters.

BIOGRAPHY

Huipu Gao was born to Yueying Hu and Fengyou Gao. He has a younger sister Jiajia Gao, a Ph.D. student in law, and an elder sister Dr. Zhenzhen Gao working in a hospital. He was married to Ying Zhou on Christmas day 2017. Huipu was born and raised in Handan, one of China's oldest cities.

With his father in the textile business, he developed a strong interest in textiles. He attended Inner Mongolia University of Technology (Hohhot, China), majoring in Textile Engineering, and received a Bachelor of Science degree in 2013. He received a Master of Science in Nonwoven Materials and Engineering from Donghua University (Shanghai, China) in 2016, and an M.S. in Textile, Fiber and Polymer Since from the University of Georgia (Athens, GA, USA) in 2018. During his graduate study at UGA, he received the first prize in the American Association of Textile Colorists and Chemists (AATCC) Herman and Myrtle Goldstein Student Paper Competition.

Following the completion of his Master's degree, Huipu was fortunate to have the opportunity to pursue his Ph.D. in Fiber and Polymer Science at North Carolina State University (Raleigh, NC) beginning 2018. During his Ph.D., he worked at TPACC, a world leader in textile comfort and protection.

ACKNOWLEDGMENTS

First of all, I wish to express my deepest gratitude to my supervisor, Dr. Roger L. Barker, for his endless support and encouragement. He has been a perfect mentor and a role model. His patience and illuminating guidance are greatly appreciated. I would also like to give my very special thanks to Mr. Shawn Deaton for his great mentorship throughout my research. He has been a constant source of support and knowledge.

I am very grateful to my committee members Dr. Emiel DenHartog, Dr. Sharon Lubkin, Dr. Warren Jasper, and Dr. Xiaomeng Fang, for guiding me with their expertise. Their valuable insights contributed immensely to my dissertation.

I must thank Kyle Watson for his tremendous amount of help with the experimental devices. I wish to thank Sophie, John, Mark, and Michelle for their help.

I must also thank the Federal Emergency Management Agency, Assistance to Firefighters Grants (AFG) program, for their sponsorship and support in conducting the research project: Developing a New Basis for Rating the Heat Strain of Firefighter Turnout Gear.

Finally, I would like to thank my family. I could not have done this without the love and support from them.

TABLE OF CONTENTS

LIST OF TABLES

LIST OF FIGURES

LIST OF SYMBOLS

R_{ef}^{A}: intrinsic apparent evaporative resistance (kPa·m²/W)

R_{et}^{A}: total apparent evaporative resistance (kPa·m²/W)

C: convective heat transfer (W/m²)

CO: predicted cardiac output (L/min)

f_{cl}: clothing area factor (dimensionless)

h_c: convective heat transfer coefficient (W/m²/K)

H_d: heat loss measured during dry test (W/m²)

H_{dry}: dry heat loss (W/m²)

H_{eva}: wet heat loss (W/m²)

HL_0: heat loss measured without radiation (W/m²)

HL_R: heat loss measured under radiation (W/m²)

H_t: heat loss measured during wet test (W/m²)

k: thermal conductivity (W/m/K)

L: thickness (m)

P: vapor pressure (kPa)

q'': heat loss (W/m²)

$Q_{manikin}$: predicted heat loss value from manikin test (W/m²)

R: radiative heat exchange (W/m²)

R_{cbp}: thermal resistance of boundary air layer tested with bare plate (K·m²/W)

R_{cf}: intrinsic thermal resistance (K·m²/W)

R_{ct}: total thermal resistance (K·m²/W)

R_{ebp}: evaporative resistance of boundary air layer measured with bare plate (kPa·m²/W)

R_{ef}: intrinsic evaporative resistance ($kPa \cdot m^2/W$)

R_{et}: total evaporative resistance ($kPa \cdot m^2/W$)

Swa: predicted sweating rate (g/min)

T: temperature (°C)

T_a: air temperature (°C)

T_{cl}: clothing surface temperature (°C)

T_f: the temperature of outer shell fabrics (°C)

THL: total heat loss (W/m^2)

TPP: thermal protection performance (cal/cm^2)

Tre: predicted core body temperature (°C)

T_s: area-weighed manikin surface temperature (°C)

Tsk: predicted skin temperature (°C)

W: weight gain of samples after wet tests (g)

W_1: weight of samples before wet tests (g)

W_2: weight of samples after wet tests (g)

v: wind speed (m/s)

ε: surface emissivity (dimensionless)

σ: Stefan-Boltzmann constant (5.67×10^{-8} $W/m^2/K^4$)

1 Introduction

1.1 Research goal

Heat stress is important to firefighters' safety and health. A recent survey paper devoted to gathering firefighter input on the factors associated with heat strain in structural firefighting operations was generated from this project[1].The survey showed that about 50% of firefighters had experienced heat stress while on the job, and most heat stress cases were associated with environmentally stressful conditions[1]. NFPA 1971 (Standard on Protective Ensembles for Structural Fire Fighting and Proximity Fire Fighting) establishes minimum levels of performance requirements for firefighter turnout gear in the United States. NFPA 1971 relies on *THL* (total heat loss) to address turnout gear related heat stress problems. Nevertheless, *THL* tested at 25 °C, 65% RH (relative humidity), may not be able to predict firefighter heat strain in hot environments. Currently, the NFPA 1971 committee is considering R_{ef}, which is an index of evaporative resistance measured in hotter conditions (35 °C, 40% RH). However, there is a perceived lack of scientific data showing the value of any new heat strain metric for predicting turnout-related heat strain. Which is a better index for rating the heat strain of turnout materials, *THL* or R_{ef}? The goal of this research is to understand the relationships between these heat strain measures and, more generally, how heat loss through turnout materials is affected by environmental factors including ambient temperature, humidity, solar exposure, and turnout system features (e.g. moisture barrier types, thermal liner thickness, reinforcements, outer shell color, etc.) as well as smoke contamination of the outer shell. Gaining this understanding requires a comprehensive understanding of the mechanisms that control the heat loss through turnout systems in different exposure conditions. Achieving this goal would provide the technical basis for advancing the NFPA 1971 requirements for firefighter heat strain.

1.2 Research objectives

Reaching the goal requires achievement of the following objectives:

1. Understanding of the effects of specific turnout materials, including outer shell color and texture, and thermal liner composites as well as air layers, on heat transfer in different environmental exposures encountered by firefighters. Specific tasks include:

- Exploring the relationship between different indexes regarding thermal protection and thermal comfort properties of a wide range of firefighter turnout composites.
- Quantifying the impact of environmental temperature and relative humidity on heat transfer through firefighter composites incorporating semipermeable and permeable moisture barriers.
- Investigating the role of clothing air gaps on heat loss in different ambient conditions.
- Evaluating the effect of outer shell color, texture, and smoke contaminant level on heat gain from incident radiation emanating from the sun.
- Examining the effects of incident solar radiation on heat loss through turnout composites incorporating bicomponent and microporous moisture barriers.

2. Understanding how heat strain indexes measured at the fabric level translate to physiological responses associated with turnout-related firefighter heat stress. Specific tasks include:

- Investigating the effect of clothing reinforcement and durable water repellent finishing in turnout gear on heat loss and their potential impact on wearer thermal comfort.
- Relating the heat loss properties of turnout materials measured on bench level with predicted human physiological responses.

1.3 Research Approach

Accomplishing these objectives will require the applications of advanced equipment and the development of new test methods for measuring heat loss through turnout systems in various environmental conditions. A novel device called a dynamic hotplate system was used to measure the heat loss through flat swatches of clothing materials. Unlike a conventional hotplate, this dynamic hotplate is equipped with a cooling mechanism and a heat flux sensor, which allows it to function when used in hot conditions. New testing methods were also developed by applying simulated solar radiation and creating air gaps between the hotplate and fabric samples.

However, the fabric level testing is not enough as these measurements cannot account for reinforcements, garment design and fit, or pumping effect. Thus, it is necessary to investigate the effect of turnout gear on physiological responses. A sweating manikin coupled with a validated physiological model was used to assessing how the turnout systems perform in various working and environmental conditions. The following graph summarized the role of each chapter in achieving the research objectives.

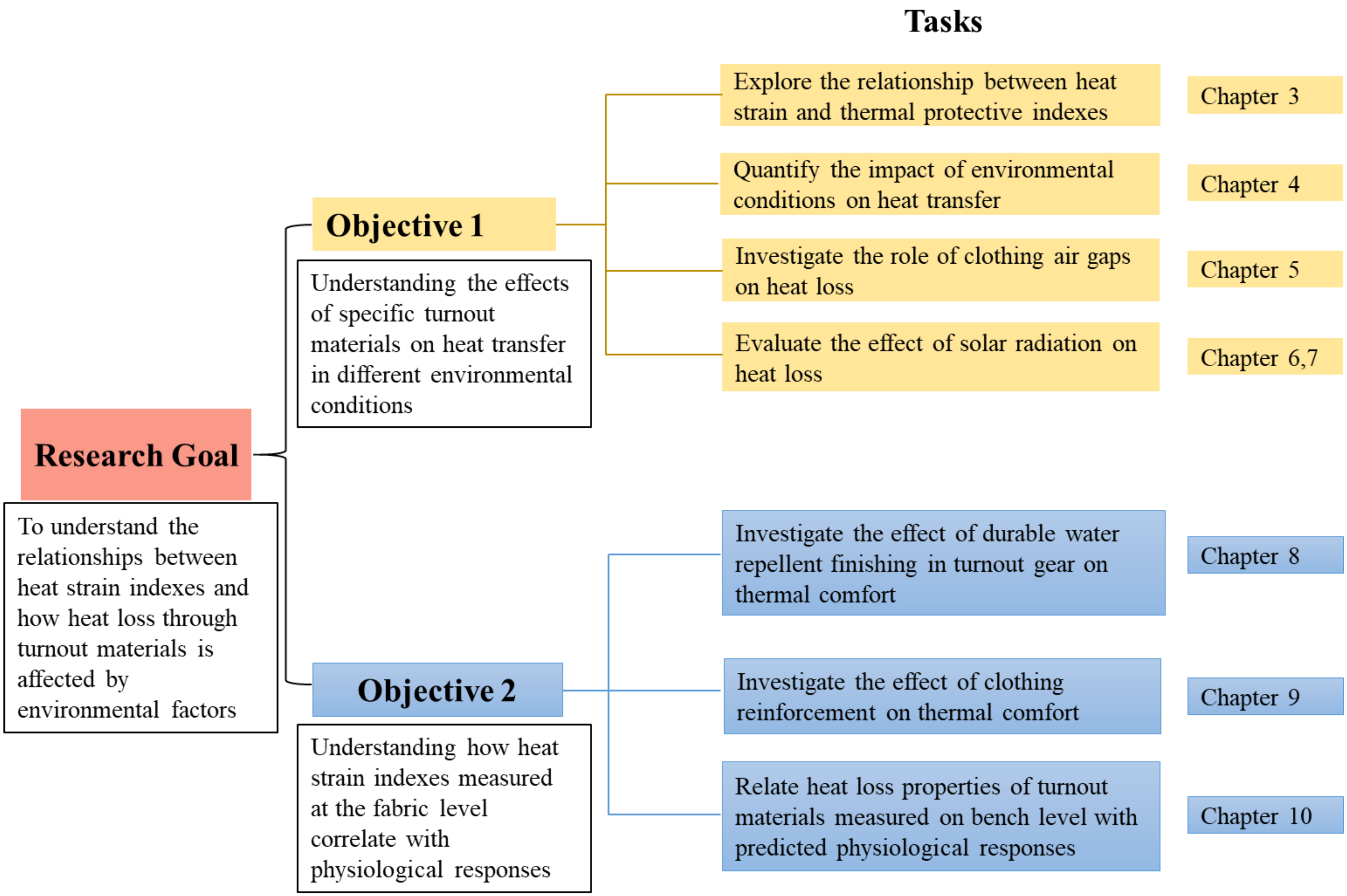

Figure 1-1. Research approach

2 Literature Review

2.1 Firefighter heat stress and its impact on the human body

Firefighting is one of the most strenuous of occupations[2]. The requirement to wear thick protective clothing places a substantial thermal burden on the wearer, contributing to heat stress[3].

The human body is in a continuous and dynamic interaction with the environment and it attempts to maintain a core temperature of 37 °C by balancing the amounts of heat produced in the body with the amounts continuously exchanged with the environment[4, 5]. The thermal energy causing heat stress is the sum of the heat generated in the body (metabolic heat) plus the net heat gain from the environment[6]. Heat stress is defined by NIOSH (National Institute for Occupational Safety and Health) as “the net heat load to which a worker is exposed to from the combined contributions of metabolic heat, environmental factors and clothing”[7]. Heat strain is the physiological reactions of human body to heat stress. Sweating is one of the mechanisms that the human body uses to increase heat loss to the environment to maintain a stable body temperature. Heat stress can cause acute disorders, such as heat stroke, heat exhaustion, heat cramps, heat syncope, and heat rashes[7]. Heat stress may also cause permanent damage to a person’s organs, such as the heart, kidneys, and liver[7]. Mild heat stress related illness, such as heat exhaustion, is associated with a core body temperature ranging from 38 °C to 40 °C[8], and heatstroke may happen when human core body temperature is above 40 °C[9]. Figure 2-1 lists the factors that contribute to heat-related illness, of which clothing is an important factor.

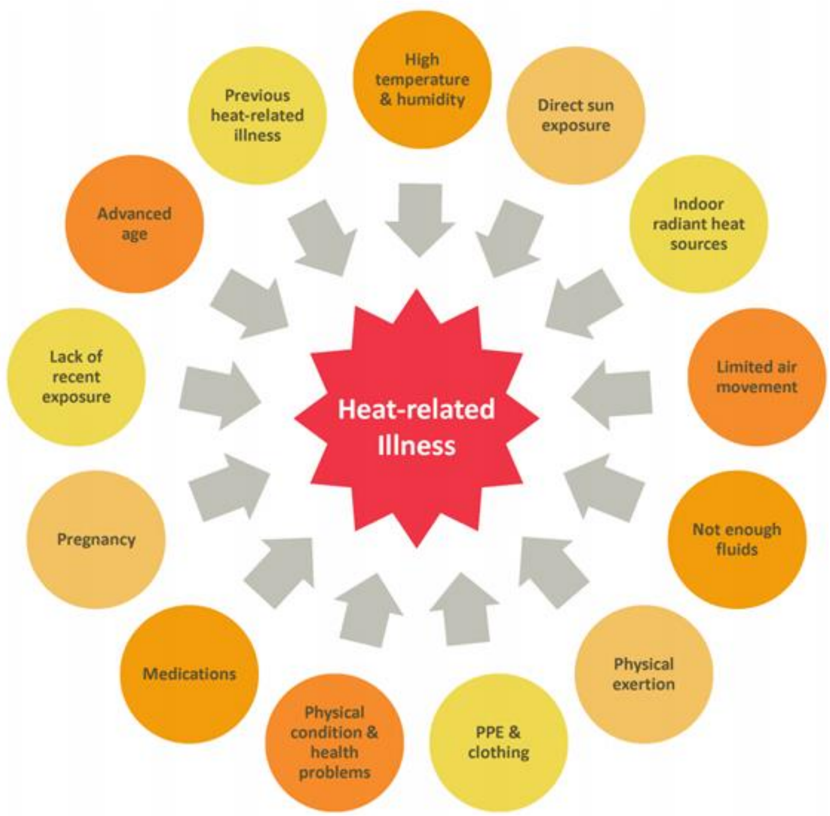

Figure 2-1. Factors that contribute to heat-related illness. From National Institute for Occupational Safety and Health[7]

Firefighters frequently need to perform strenuous work in hot environments while wearing bulky and highly insulative turnout gear, creating a significant physiological strain on firefighters[10]. Heart attacks are the leading causes of firefighter fatalities[11]. In 2019, 46% of firefighter fatalities were due to sudden cardiac events (Figure 2-2)[12]. Cardiac-related events accounted for 48 % of the on-duty fatalities over the past 17 years, as shown in Figure 2-3. Heat stress can exacerbate the cardiovascular strain experienced by firefighters and is considered one of the leading factors that can increase the risk of sudden cardiac events[13].

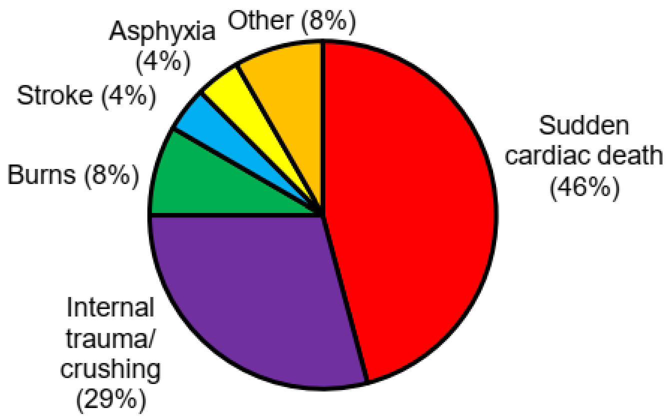

Figure 2-2. Firefighter deaths in 2019. From National Fire Protection Association[12]

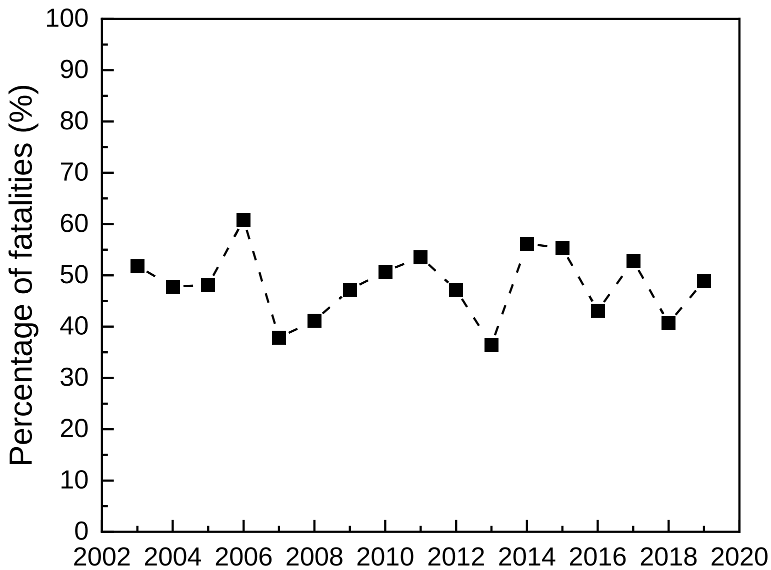

Figure 2-3. Percentage of firefighter fatalities due to sudden cardiac events from 2003 to 2019. Based on data from National Fire Protection Association[14].

It was reported that one of the leading categories of firefighter injury is slips, trips, and falls, and heat stress may be a common factor[10]. Heat stress and the resulting elevation in body temperature hasten muscular fatigue, increase cardiovascular strain, interfere with cognitive function, and reduce gait stability[15,16]. These changes in gait performance can lead to an increased risk for trips and falls[15,16]. The influence of heat stress on firefighter injuries and sudden cardiac events is summarized in Figure 2-4.

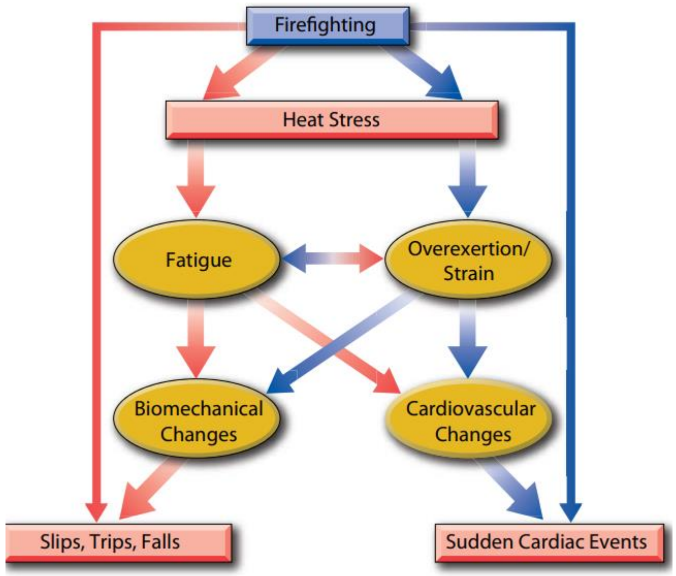

Figure 2-4. The role of heat stress in contributing to firefighter injuries and fatalities. From [10]

2.2 Ambient environments firefighters may encounter

2.2.1 Firefighting

To combat heat stress experienced by firefighters, it is critical to examine their working environments and activities. During firefighting, thermal environments faced by firefighting can be classified as routine, hazardous, and emergency (Figure 2-5)[17-19]. Routine conditions happen when firefighters operate hoses or fight against fire from a certain distance[20, 21]. Firefighters experience the lower range of hazardous conditions when operating from a very close distance to fire, and a higher range when they enter a fire hazard to rescue victims or property. Emergency condition is encountered mostly when flashfire happens[22]. During live-fire training, the local thermal environment of firefighters was found to be around 50 °C and heat flux about 1 kW/m^2

for mild training. For severe training, the temperature can reach between 150 to 200 °C with heat flux between 3 to 6 kW/m^2 [23].

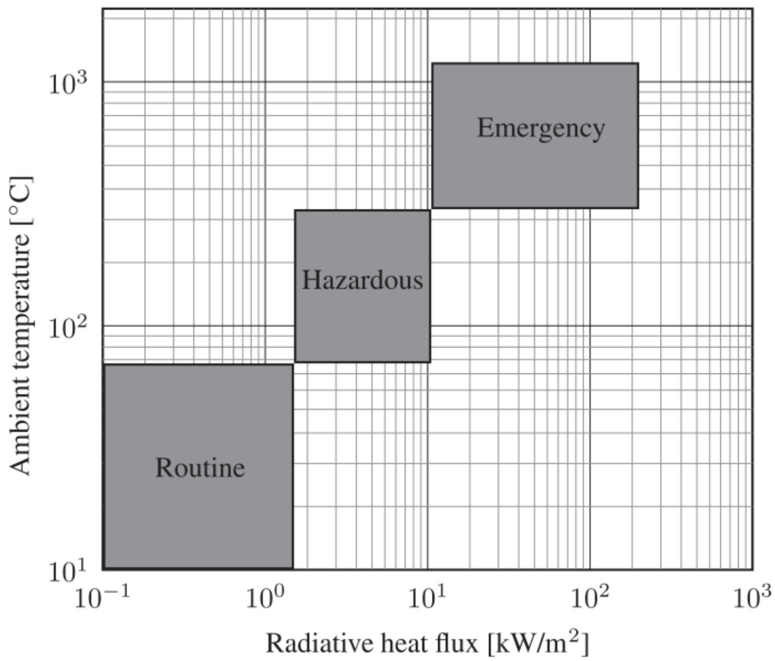

Figure 2-5. Exposure conditions encountered by firefighters[19]. Copyright 2015. Reproduced with permission from Elsevier

The spectral distribution of radiation from a fire may be approximated by a black body source at 1100-1400 K[20]. The heat flux ranges from a few kW/m^2 to 200 kW/m^2 [19]. Figure 2-6 is a typical flame spectrum and *y* axis is radiation intensity (W/m^2· steradian ·cm^{-1}) This spectrum extends approximately from 1 to 10 µm[24].

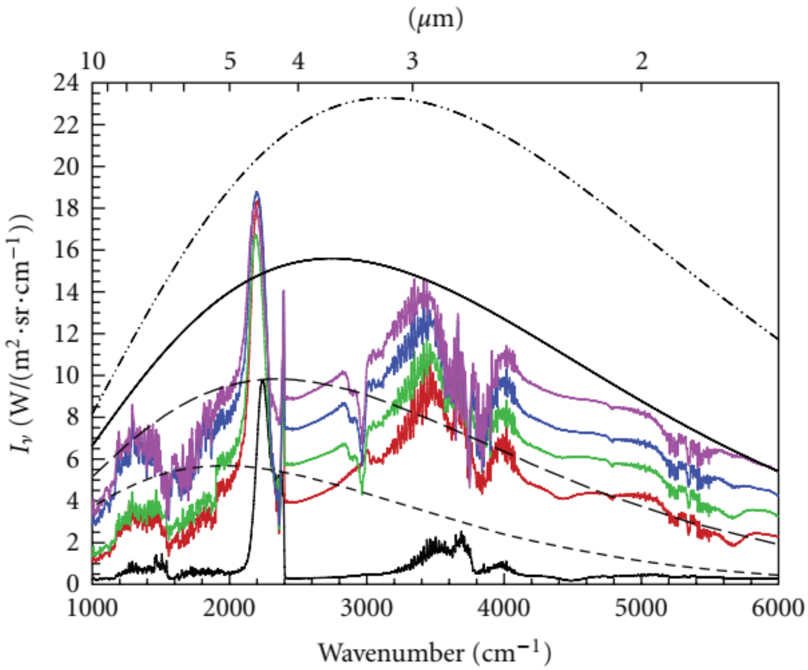

Figure 2-6. Emission spectra from wood shavings fuel beds.[24] Copyright 2011. Reproduced with permission from Hindawi

2.2.2 Non-firefighting activities

Apart from firefighting activities, firefighters respond to multiple types of emergencies, such as vehicle/industrial/aircraft accidents, medical calls, public assistance, technical rescue, hazardous materials spills, search and rescue operations during disasters[25-27]. Only 1%-5% of their time is engaged in firefighting activities[25]. During these activities, heat stress can also occur, especially in summer. Most U.S. fire departments operate in locations that can subject them to occasional summer environmental temperatures over 90 °F (32.2 °C). Many southern regions regularly endure temperatures over 100 °F (37.8 °C) for extended portions of the year[27]. In some cities, like in Phoenix, Arizona, the average maximum temperature in summer of 2019 (June to September) is 113.5 °F (45.3 °C)[28]. Relative humidity also varies enormously. For example, in Orlando, Florida, the average RH in July 2020 is 78% RH, while in Las Vegas, Nevada, it is only 11% RH, according to the historical weather data from Weather Underground[28].

In addition to high temperatures, the radiation from the sun exacerbates the situation. Solar radiation arrives at the surface of the Earth's atmosphere at an intensity of around 1370 W/m^2. After passing through the atmosphere, this provides a maximum of approximately 1000 W/m^2 at the earth's surface in full sun.[4] The spectrum of standard global solar irradiance with an Air Mass of 1.5 (AM 1.5, dimensionless) was plotted using the data provided by ASTM G173 - 03(2012),[29] as shown in Figure 2-7. By integration, the distribution of solar light can be found as: Ultra Violet (UV, 4.61%), Visible (50.15%), Near Infrared (NIR, 35.01%), and Medium Infrared (MIR, 9.50%).

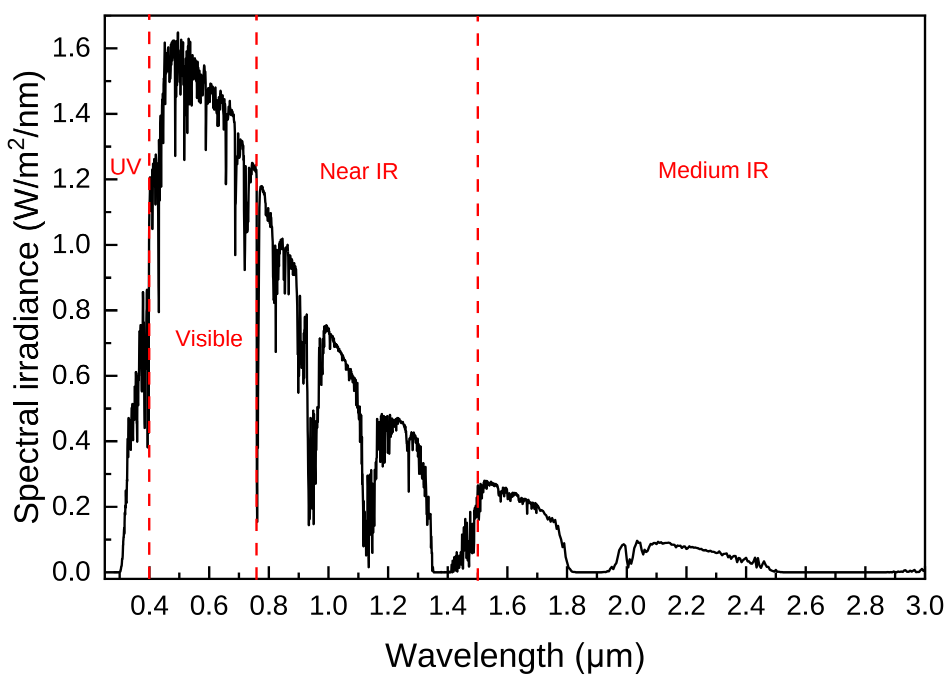

Figure 2-7. The solar spectrum of AM 1.5 Global. Based on data from ASTM G173 - 03(2012)[29]

2.3 Heat exchange between human body and environment through clothing

The human body is in continuous and dynamic interaction with its dynamic environment. It attempts to maintain a core temperature of 37 °C by balancing the amounts of heat produced in the body with the amounts continuously exchanged with the environment [4, 5], which can be described by the following heat balance equation:

Heat storage=heat production- heat loss

=(metabolic rate- external work)-(conduction + radiation + convection+ Evaporation + breathing)[5]

Heat production is determined by metabolic activity. When working, the muscles burn nutrients for mechanical activities. Part of the energy is liberated outside the body as external work (<10%), but most of it is released in the muscle as heat. In practice, external work is often neglected[4, 5]. The human body can exchange heat with the environment through evaporation, conduction, radiation, and convection. In addition, by breathing in cool and dry air, and breathing out hot and humid air, up to 10% of the total heat production can be lost through breathing[5]. If the heat production by metabolic activity is higher than the sum of all the heat losses, heat storage will be positive and body temperature rises. If the heat storage is negative, more heat is lost than produced and the body cools[5]. Clothing functions as a resistance to heat and moisture transfer between human skin and the environment, and it affects humans' thermal regulation[5].

2.3.1 Heat transfer through clothing

2.3.1.1 Thermal insulation

Clothing materials consist of air and fibers. For most clothing materials, the volume of air enclosed is far greater than that of fibers. The insulation is very much dependent on material thickness[5]. The convective component of heat transfer can usually be neglected except for textile materials with extremely low density[30]. The radiation portion of thermal conductivity is also very small, only contributing to about 5% of the total thermal conductivity for a 100 K temperature difference across the fabric[31]. The heat transfer through materials is mainly by conduction. The rate of heat loss q'' (W/m^2) by conduction is governed by the temperature difference between skin and clothing surface ΔT (K), thickness L (m), and thermal conductivity k (W/m/K)[32]:

$$q'' = -k\frac{\Delta T}{L} \tag{2.1}$$

2.3.1.2 Evaporative heat transfer

Evaporative heat exchange takes place by the transfer of latent heat of evaporated sweat from the skin to the environment[33]. The amount of heat transferred is determined by the vapor pressure difference between the skin and the environment, and the resistance of clothing to moisture transfer. Under steady-state conditions, the following equation applies.

$$H_{\mathrm{eva}} = \frac{\Delta P}{R_{\mathrm{et}}} \tag{2.2}$$

where H_{eva} is the evaporative heat exchange (W/m^2), ΔP is the water vapor pressure difference between skin and ambient environment (kPa). R_{et} is the total evaporative resistance of clothing and surface air layer (kPa·m^2/W). For normal and permeable materials, clothing material thickness determines the major part of the clothing vapor resistance[5]. When added with coatings or membranes, the evaporative resistance of textile fabrics will be largely determined by such components[34].

2.3.1.3 Radiation

Thermal radiation is electromagnetic waves emitted by matter that is at a nonzero temperature, and does not need a medium to transfer[35]. Radiative heat exchange rate R (W/m^2) on clothing surface can be calculated by equation 2.3:[36]

$$R = \sigma\varepsilon(T_{cl}^4 - T_a^4) \quad (2.3)$$

where σ is the Stefan-Boltzmann constant (5.67 x 10^{-8} W/m^2/K^4), ε is the surface emissivity (dimensionless). T_{cl} is the clothing surface temperature (K) and T_a is the ambient temperature (K). ε is dependent on the wavelength. For protective clothing, the emissivity of the outer shell under the range of infrared radiation is similar. While under solar radiation, the emissivity depends on color and appearance.

2.3.1.4 Convective heat transfer

Convective heat transfer is executed by the flow of a fluid, and is governed by random molecular motion (diffusion) and bulk motion of the fluid[37]. The convective heat transfer C (W/m^2) between a clothed body and the environment can be written as [38, 39]

$$C = h_c f_{cl}(T_{cl} - T_a) \quad (2.4)$$

where h_c is convective heat transfer coefficient, W/m^2/K, f_{cl} is clothing area factor (dimensionless), defined as the ratio between clothing surface area and body surface area. T_a is the air temperature (°C). h_c can be estimated by wind speed v (m/s)[39, 40]:

$$h_c = Bv^n \quad (2.5)$$

where n (dimensionless) and B (W·m^{-2-n}·s^n/K) are empirical coefficients. The reported empirical equations for estimating h_c were summarized by Wang[40], with B ranging from 6.7 to 12.2, and n from 0.4 to 0.9.

In summary, clothing reduces the rate of heat exchange between skin and the environment by adding a barrier of thermal resistance and evaporative resistance. The resistance to thermal and moisture transfer through clothing is not only dependent on material properties, but is also affected by moisture content, garment design, human posture, movement, wind speed, clothing fit[41-48].

2.4 Composition of firefighter protective clothing

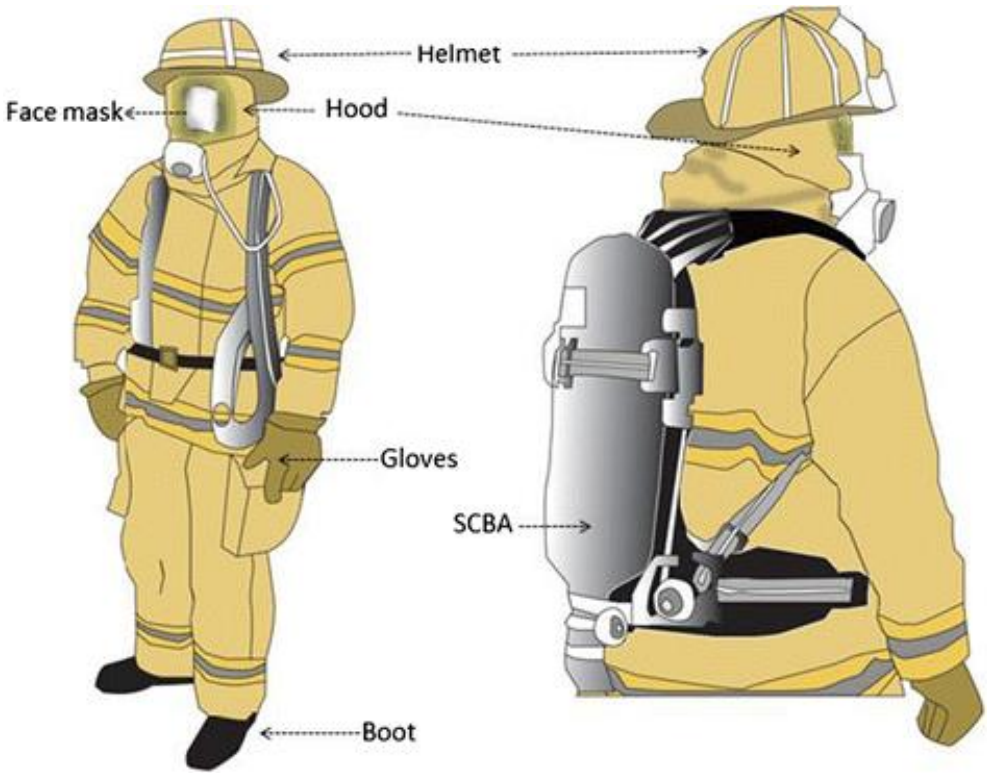

Figure 2-8. Configuration of firefighter PPE. Reproduced with permission[49]. Copyright 2014. Reproduced with permission from Springer Nature

To protect firefighters against external hazards, typically protective clothing along with a helmet, a self-contained breathing apparatus (SCBA), gloves, and a hood, are required gear (Figure 2-8). The turnout suit is a three-layer system, consisting of an outer shell, moisture barrier, and thermal liner, as shown in Figure 2-9.

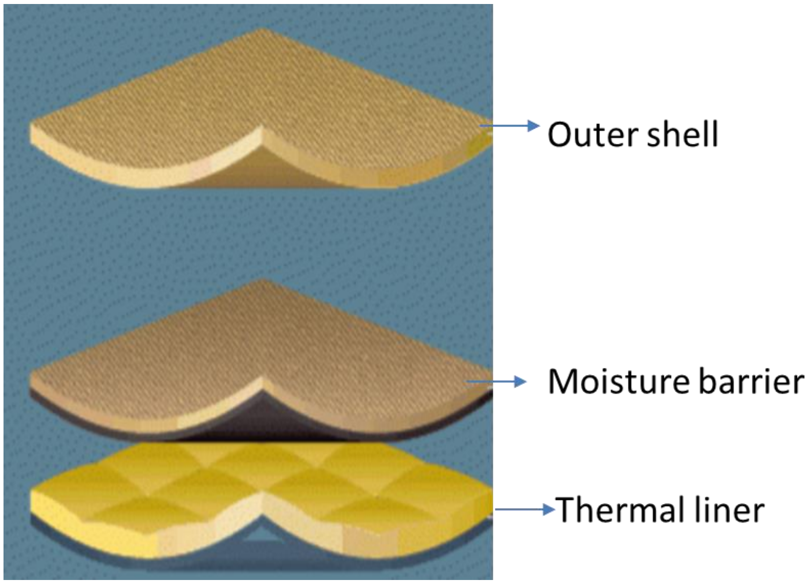

Figure 2-9. Typical components of structural firefighter suit.
(Source: https://www.goreprotectivefabrics.com/fire/parallon)

2.4.1 Outer shell

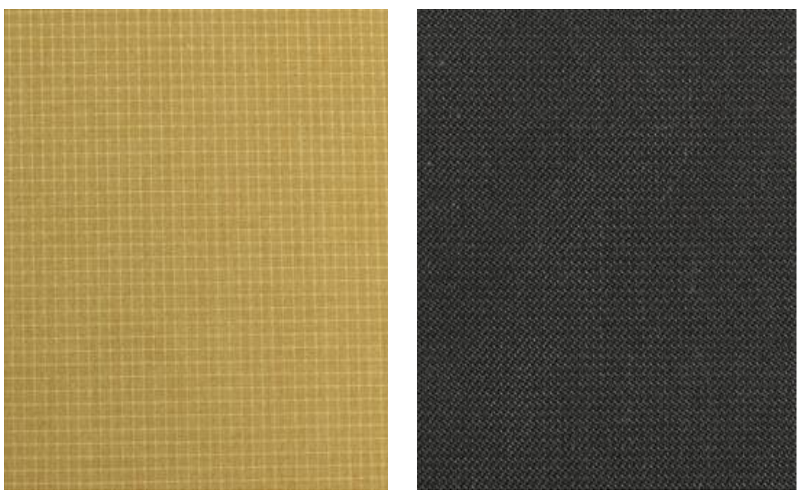

Figure 2-10. Pictures of commercial outer shells

The outer shell is the first line of protection, as shown in Figure 2-10. It should provide basic protection against flame and heat, and have sufficient mechanical resistance to cuts, snags, tears and abrasion[50]. Shells are typically composed of woven fabrics made with blends of inherently flame-resistant fibers, such as polyaramid, polybenzimidazole (PBI), and polybenzoxazole (PBO) as well as a water-repellent coating[51].

The properties of the outer shell strongly affect heat gain from radiation. It has been reported that shell color has a strong effect on solar heating load, where fabrics with light color absorb less heat compared with those with deep colors[19, 52]. Under flame radiation (infrared wavelength), color plays a negligible effect. For most protective clothing, the emissivity is about 0.9 in the range of infrared radiation[53], except for those with special finishes, such as aluminum coating. However, the impacts of fabric texture, washing, and contamination on radiative properties against solar and flame radiation are unknown.

2.4.2 Moisture barrier

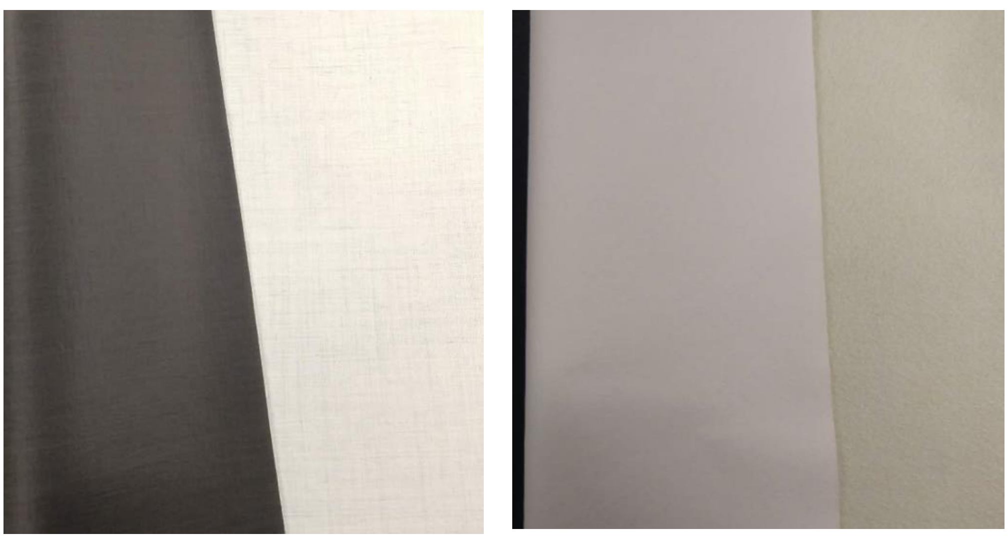

Figure 2-11. Pictures of commercial moisture barriers

The moisture barrier is typically the next layer (Figure 2-11). Most moisture barriers are composed of a thin semipermeable membrane laminated to a fire-resistant base fabric. This layer is responsible for protecting firefighters from liquids, such as water, biological materials and chemicals, while still allowing the transmission of sweat vapor from the body[54]. Moisture barriers largely determine the evaporative resistance of firefighter composites[55], and current technologies fall into three categories: microporous, non-porous hydrophilic, and bicomponent membranes[51], as illustrated in Figure 2-12.

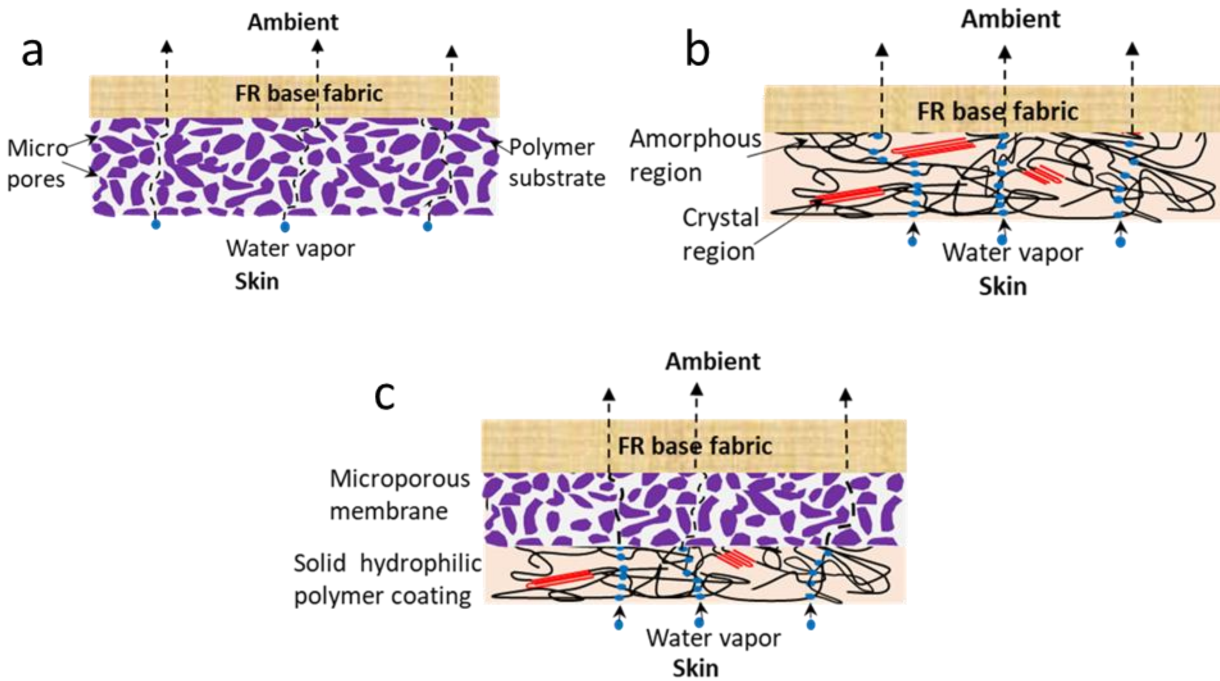

Figure 2-12. Schematic of water vapor diffusion through (a) microporous, (b) non-porous hydrophilic and (c) bicomponent moisture barrier

2.4.2.1 Microporous membranes

Microporous membranes have a pore size ranging from 0.02 to 1 µm, about 20,000 times larger than moisture vapor molecules (~0.0004 µm), but much smaller than water droplets (>100 µm)[56-58]. Thus, microporous membranes can withstand the penetration of liquid water but allow vapor molecules to diffuse through the interconnected channels easily, as shown in Figure 2-12a. Polyurethanes and poly(tetrafluoroethylene) are the two most widely used polymers[56, 57]. Various methods, such as wet coagulation, thermo-coagulation, melt-blown technology, solvent extraction, salt extraction, and electrospinning, can be used to induce such microporous structure[56, 57]. Among these, expanded poly(tetrafluoroethylene) is widely used in firefighter clothing. The porous structure, typically with a porosity of 80% and pore size ranging from 0.2

to 0.5 μm, is induced by biaxial stretching and annealing at high temperature, and it was claimed to have 9 billion pores per square inch[59]. The fundamental mechanism behind the vapor transfer through a microporous membrane is Fick's first law.

2.4.2.2 Solid hydrophilic membrane

Transmissions of gases and vapors through solid film occurs by the absorption-diffusion-desorption mechanism[59]: initially, water vapor is absorbed on the membrane surface with higher vapor pressure, migrated by forming transient hydrogen bonding with the hydrophilic groups on polymer chains (e.g., -OH, -COOH, $-NH_2$) in amorphous regions, and desorbed on the surface with lower water vapor concentration, as shown in Figure 2-12b[60]. The migration can be visualized as a sequence of steps which the water molecules pass over a potential barrier separating one another,[61] described as the molecular stepping-stone mechanism[59]. Polyurethanes (PU) containing hydrophilic components are broadly used as hydrophilic breathable, waterproof membranes[59]. The hydrophilic components are to provide polar groups, and are responsible for the water vapor transmission[59]. Compared with microporous films, solid hydrophilic membranes can provide better resistance against liquid penetration, and more windproofness[62]. However, the water vapor diffusion resistance is strongly dependent on the water vapor absorption within the polymer[63,61]. Moisture absorbed by the hydrophilic polymer can facilitate the transmission of water vapor by swelling the membrane (provide more free volume between polymer chains), and providing more hydrophilic sites[64].

2.4.2.3 Bicomponent membranes

This category of membranes features a fine hydrophilic layer coated on top of a microporous film (Figure 2-12c), with aims to protect the porous structure from blocking by contaminants, to provide enough resistance to high-pressure water penetration, to increase the film toughness, etc[65, 66]. Almost all commercially available moisture barriers for firefighter suits in USA market fall into this category. However, this surface coating of solid hydrophilic layer adds to the stiffness, and reduces the evaporative resistance, particularly making the breathability strongly dependent on the moisture content inside the hydrophilic layer[61].

2.4.3 Thermal liner

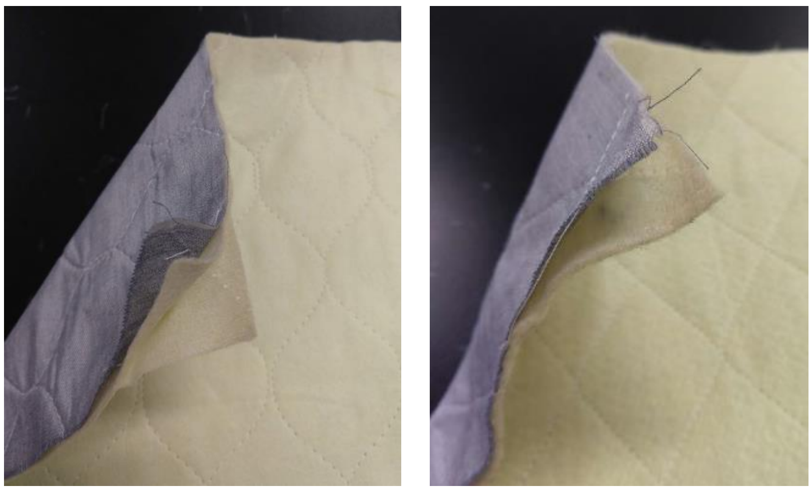

Figure 2-13. Pictures of commercial thermal liners

The thermal liner, generally composed of nonwoven fabrics made of flame-retardant/resistant fibers quilted to a light-weight woven fabric, is the innermost layer[67], as shown in Figure 2-13. It provides the majority of thermal protection against extreme heat[68]. Two conflicting requirements need to be addressed when developing firefighter protective clothing: thermal protection and heat stress[69]. Normally, firefighter heat stress could be reduced by developing lighter and thinner thermal liners[30], but this will be at the cost of thermal protection[69, 70]. Moreover, decreasing the thickness of composites may not necessarily decrease heat stress in certain conditions, such as under strong radiant heat load[71].

In addition, there are some turnout clothing versions available with durable water repellent finishing inside the thermal liner. The purpose of this finishing is to decrease sweat absorption from the skin and maintain a dry thermal liner. The effect of such finishing on firefighter thermal comfort is unknown.

2.5 Standards to characterize thermal comfort performance of firefighter composites

Currently, there are two indexes that are used widely to compare the capabilities of firefighter composites to release heat. *THL* is required by NFPA 1971-2018 (Standard on protective ensembles for structural fire fighting and proximity fire fighting)[72], and evaporative resistance is required by EN 469-2020 (Protective clothing for firefighters. Performance requirements for protective clothing for firefighting activities)[73]. In ISO 11999-3 (PPE for firefighters - Test methods and requirements for PPE used by firefighters who are at risk of exposure to high levels of heat and/or flame while fighting fires occurring in structures - Part 3: Clothing), both *THL* and water vapor resistance standards are required[74].

2.5.1 Total Heat Loss

Total heat loss (*THL*) is used to specify the heat transfer through firefighter composites and is regulated in the NFPA 1971[72]. It consists of dry heat loss through conduction, radiation, and convection, and wet heat loss by evaporation. It can be calculated according to ASTM F1868, part C, by measuring thermal resistance (R_{ct}) and apparent evaporative resistance ($R_{\mathrm{et}}^{\mathrm{A}}$)[75]. Total thermal resistance R_{ct} (K·m^2/W) can be calculated with the following equation:[75]

$$R_{\mathrm{ct}} = \frac{\Delta T}{H_{\mathrm{d}}} \tag{2.6}$$

where ΔT is the temperature difference between hotplate surface and ambient, 10°C; H_{d} is the electrical power supplied to maintain the hotplate at a constant temperature during the dry test, W/m^2.

Intrinsic thermal resistance R_{cf} (K·m^2/W) can be calculated with[75]:

$$R_{\mathrm{cf}} = R_{\mathrm{ct}} - R_{\mathrm{cbp}} \tag{2.7}$$

R_{cbp} is the thermal resistance of air layer tested with a bare plate, K·m^2/W.

Total apparent evaporative resistance R_{et}^A (kPa·m^2/W) is given by[75]:

$$R_{\mathrm{et}}^{\mathrm{A}} = \frac{\Delta P}{H_{\mathrm{t}} - \frac{\Delta T}{R_{\mathrm{ct}}}} \tag{2.8}$$

where ΔP is the vapor pressure difference between the hotplate surface and chamber, kPa; H_t is the heat loss measured by hotplate in the wet test, W/m^2. The term apparent was added to modify the evaporative resistance term to reflect that condensation might occur in the ensemble during the wet test[76].

Intrinsic apparent evaporative resistance R_{ef}^A (kPa·m^2/W) can be obtained from equation 2.10[75]:

$$R_{\mathrm{ef}}^{\mathrm{A}} = R_{\mathrm{et}}^{\mathrm{A}} - R_{\mathrm{ebp}} \tag{2.9}$$

R_{ebp} is the evaporative resistance of boundary air layer measured with bare plate, kPa·m^2/W.

THL (Total heat loss, W/m^2) is calculated by[75]:

$$THL = \frac{\Delta T}{R_{\mathrm{cf}}+0.04} + \frac{\Delta P}{R_{\mathrm{ef}}^{\mathrm{A}}+0.0035} \tag{2.10}$$

where the values of 0.04 (K·m^2/W) and 0.0035 (kPa·m^2/W) are standard bare plate values for dry and wet tests at a wind speed of 2 m/s, respectively[76].

THL was designed to reflect the capabilities of firefighter composites to transfer heat. Initially, *THL* was included as an index in the NFPA 1971-1991, and in 2000, a minimum heat loss of 130 W/m^2 was specified in the NFPA 1971-2000, based on two wear trials conducted at North Carolina State University[77, 78]. The wear trials in mild and warm conditions found that an impermeable suit (97 W/m^2) was statistically different in terms of work tolerance time and skin temperature rise when compared to breathable systems, which set the first *THL* requirement at 130 W/m^2 [77, 78]. In 2007, the *THL* requirement was further increased to 205 W/m^2, based on the wear trial performed by the International Association of Fire Fighters. It was found that *THL* between 170 to 210 W/m^2 would be the best breakpoint value[79]. In ISO 11999-3, the minimum *THL* requirement for performance level *d1* and *d2* is 200 W/m^2 and 300 W/m^2, respectively[74].

2.5.2 R_{ef} (Intrinsic evaporative resistance)

The water vapor resistance requirement of firefighter protective clothing was incorporated in EN-469 at 2005[73]. It characterizes the ability to release heat through evaporation measured in isothermal conditions, where the hotplate and environment are both maintained at 35 °C.

Total evaporative resistance R_{et} (kPa·m^2/W): [75]

$$R_{\mathrm{et}} = \frac{\Delta P}{H_{\mathrm{t}}} \tag{2.11}$$

where ΔP is the vapor pressure difference between the hotplate surface and chamber, kPa; H_t is the heat loss measured by hotplate in wet test, W/m^2.

Intrinsic evaporative resistance R_{ef} (kPa·m^2/W) can be obtained from equation:

$$R_{\mathrm{ef}} = R_{\mathrm{et}} - R_{\mathrm{ebp}} \tag{2.12}$$

where R_{ebp} is the evaporative resistance of the boundary air layer measured with bare plate, kPa·m^2/W.

EN 469 requires that the intrinsic evaporative resistance of firefighter composites shall be no larger than 30 Pa·m^2/W for performance level *Z2* and 45 Pa·m^2/W for performance level *Z1*[69, 73]. In ISO 11999-3, maximum water vapor resistance requirement for performance level d1 and d2 is 40 m^{2}Pa/W and 30 m^{2}Pa/W, respectively[74]. Does *THL* performs better than R_{ef} in predicting heat strain caused by firefighter clothing? This is to be investigated in this thesis.

2.6 Characterization methods of heat transfer

2.6.1 Sweating guarded hotplate

NFPA 1971 requires that firefighter composites should possess a *THL* of at least 205 W/m^2, according to ASTM F1868[75]. The sweating guarded hot plate, as shown in Figure 2-14 and Figure 2-15, is used to test *THL* and R_{ef}. The device consists of a square test zone, surrounded by a guard ring which is heated to the same temperature as the test zone to prevent heat loss laterally. The bottom guard is to prevent heat loss downward. Thus, the heat can only transfer upward through a specimen. During testing, a specimen was placed on the plate surface, maintained at skin temperature (35 °C). The electrical power needed to keep the hotplate at a set temperature is recorded, which equals the heat loss through the fabric. The hotplate is also able to emit water to the surface to simulate human sweating. The sweating is generally controlled gravitationally, with the water level in the reservoir being higher than the plate surface. A piece of water vapor permeable but liquid water impermeable membrane was covered on the hotplate surface to prevent wicking effect[80].

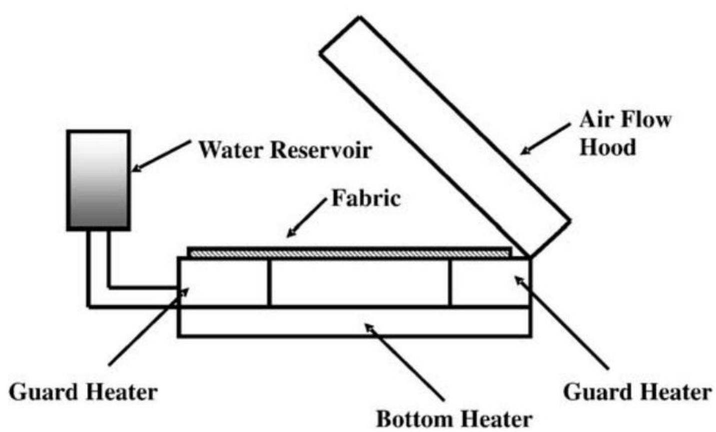

Figure 2-14. Schematic of a sweating guarded hot plate[80]. Copyright 2006. Reproduced with permission from Elsevier

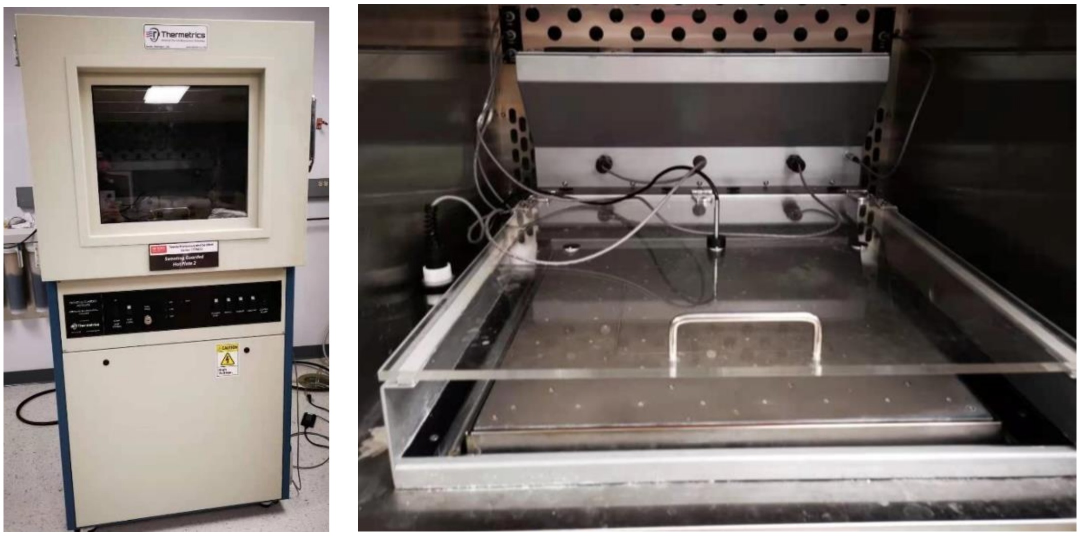

Figure 2-15. A sweating guarded hotplate housed in an environmental chamber

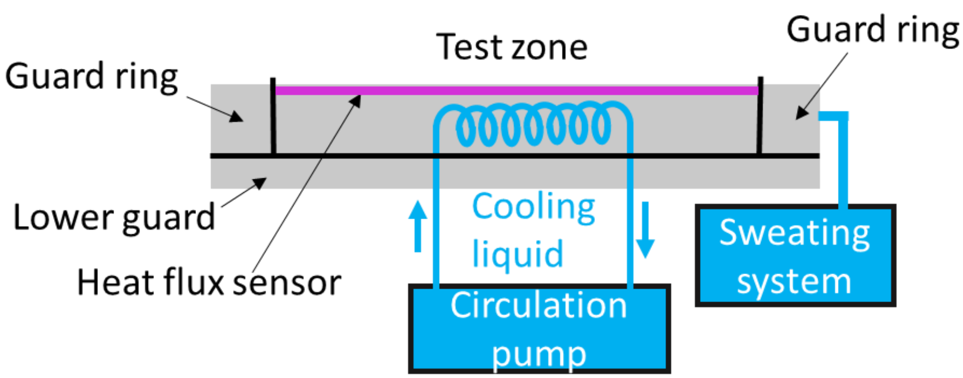

Figure 2-16. Schematic of a dynamic hotplate system

The conventional sweating guarded hotplate is only applicable to steady-state measurements. Dynamic hotplate systems (Figure 2-16) developed by Thermetrics, are equipped with a surface heat flux sensor, which extends its ability to measure instantaneous heat flux. The prerequisite for the proper functioning of a conventional hotplate is the continuous heat loss from the hotplate to the environment, making it only applied for the cool environments. For a dynamic hotplate system, there is a cooling system circulating in the plate to prevent overheating when testing at an elevated temperature[81]. With the dynamic hotplate, the performance of heat and moisture transfer through the hotplate can be studied at a higher temperature, or with external radiation load (solar light, or flame exposure).

2.6.2 Sweating manikin tests

A sweating manikin measures thermal resistance and evaporative resistance using most of the same principles as the sweating guarded hot plate[82]. The most prominent difference is the sweating manikin has a human form. It can be viewed as a human form made from many individual small hotplates. A sweating manikin could account for reinforcements, garment design, fit, the air layers between garments and the human body[82]. The first one-segment manikin was developed for the US Army in the 1940s[83]. To date, more than 100 manikins have been developed to measure the thermal-physiological properties of clothing, such as Coppelius, Walter, ADAM, Newton, SAM[84]. Among them, Newton is one of the most widely used manikins, which was developed in 2005 by Thermetrics, United States (Figure 2-17). This manikin is 175 cm in height, with a skin surface area of 1.8 m^2, to simulate an adult male. The manikin shell is made of thermally conductive carbon-epoxy composite materials. Resistance heating wires are embedded into the shell to heat the manikin. 134 sweating holes are evenly distributed. [84] Standard zone configurations include 20, 26, or 35-zone models[84].

Figure 2-17. Picture of a Newton manikin

The thermal resistance and evaporative resistance can be tested according to ASTM F1291 (Standard test method for measuring the thermal insulation of clothing using a heated manikin) and ASTM F2370 (Standard test method for measuring the evaporative resistance of clothing using a sweating manikin), respectively. The total thermal resistance R_{ct} ($K \cdot m^2/W$) can be calculated with the parallel method using the following equation[85, 86]:

$$R_{\mathrm{ct}} = \frac{(T_{\mathrm{s}} - T_{\mathrm{a}})}{H_{\mathrm{d}}} \tag{2.13}$$

where T_s is the area-weighed surface temperature (°C); T_a is the ambient temperature (°C); H_d is the power required to heat the manikin during the dry test (W/m^2). The ambient temperature should be at least 12 °C lower than the manikin surface (35 °C), and relative humidity should be between 30 and 80% RH, preferably 50% RH, for the thermal resistance test.

Evaporative resistance R_{et} (kPa·m^2/W) can be calculated with the parallel method using the following equation:[87]

$$R_{et} = \frac{\Delta P}{H_t - \frac{(T_s - T_a)}{R_{ct}}} \tag{2.14}$$

where ΔP is the water vapor pressure difference between the manikin surface and ambient (kPa), H_t is the power required to heat the manikin during the wet test. The ambient condition is required to be around 35 °C/40% RH for the evaporative resistance test in the standard ASTM F2370.

Manikin heat loss at specific environmental conditions can be estimated similarly to the *THL* calculations in a hotplate test[88]. However, since R_{ct} and R_{et} are measured by a manikin in two different environments, heat loss values are predictive rather than actual measurements[82]. The advantage of a manikin over a hotplate is that air layer, reinforcements, and pumping effect can be accounted for. Both dynamic tests and static tests can be conducted. Dynamic tests involve the walking of the manikin and can create forced convection through the body motion[68]. Compared with the static test, larger heat loss through both evaporative heat transfer and dry heat transfer was observed[68].

2.6.3 Virtual modeling

It is essential to know the physiological response of a human wearing different garments in certain environments. Human wear trials are demanding due to the high costs and ethical restrictions, and are often difficult to interpret due to the intra- and inter-subject variability[89]. Physiological modeling is a good option. The thermo-physiological model consists typically of a passive system and an active system. The passive system simulates the physical human body and models heat transfer within the human body, and between the human body and its environment. The passive system is controlled by an active system, which is a set of algorithms simulating human thermophysiological response[89,90]. Various thermal thermophysiological models have been developed, such as one-node thermal models, two-node thermal models, multi-node thermal models, and multi-element thermal models, as was summarized by Katic[90].

The Fiala Thermal Physiology and Comfort (FPC) model is a multi-segmental, multi-layered representation of the human body, and has gained popularity over the last decade in a wide range of applications[91, 92]. Its passive system is modeled by simulating the environmental heat exchange including local variations of surface convection, radiation exchange, evaporation at the skin, and the nonuniformity of clothing ensembles[93]. The active system of the model predicts the four essential overall responses of the central nervous system: constriction and dilatation of cutaneous blood flows, shivering, and sweating[94]. Skin and head core temperatures are considered as the main driving impulses for the regulatory actions[92, 94].

However, one limitation of virtual physiological modeling is that such models usually include simplified clothing models that assume that the evaporation resistance and thermal resistance of garments are constant during simulation[90, 95].

2.6.4 Physiological manikin test

A physiological manikin is a manikin coupled with a human physiological model. There are two approaches for the coupling of a manikin with a model, including type -2 and type-1 approach (Figure 2-18)[89]. In the type-1 coupling method, the manikin provides local heat loss data to the physiological model and the model uses this data to predict the physiological state of the body. Then the manikin sets the predicted skin temperatures and sweat rates from the physiological model[96]. In the type-2 coupling method, the model provides metabolic rate and sweating rate setpoints to the manikin. The skin temperatures for each segment on the manikin are sent to the model for physiological state prediction[96]. Burke et al. compared human subjects data with the response of a Newton thermal manikin coupled with a physiological regulation system based on the Fiala model, and found generally good agreement[97].

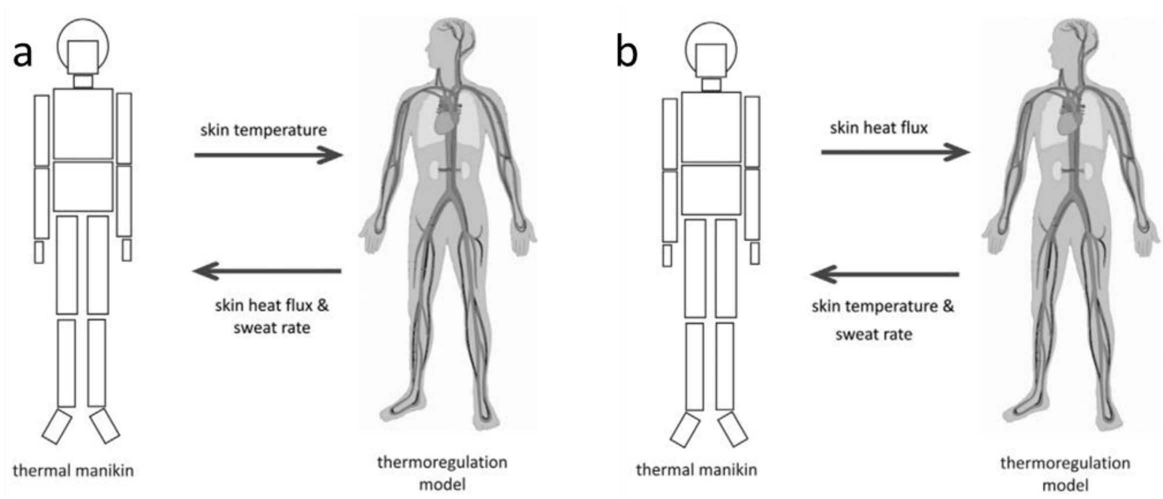

Figure 2-18. The coupling methodologies of the manikin and the thermoregulation model: (a) type 1 and (b) type 2 [89]. Copyright 2017. Reproduced with permission from Elsevier

It has been well established that the physiologically controlled sweating manikins act similar to a real human, and could generate reasonable results on physiological responses[98]. They are very useful in representing the dynamic interactions between the environment, clothing and the human body[98].

2.7 Influence of materials and ambient conditions on heat exchange between the human body and environment

2.7.1 Influence of the ambient temperature and humidity

Working conditions are very diverse for firefighters, so it is vital to understand how firefighter protective suits perform in different operational environments. Many firefighting operations include moderate to heavy work rates within environments where evaporative cooling is the primary mechanism to reduce physiological heat strain. As the human is a homeotherm, it needs to maintain its internal body temperature around 37 °C by releasing enough heat to the environment[4]. While the three functional layers in structural suits protect users from extreme threats in the environment, they also limit the heat release from the body. It is not surprising that the combination of high insulation value and limitation of vapor transport can contribute to the heat stress that is one of the leading contributors to firefighter fatalities.

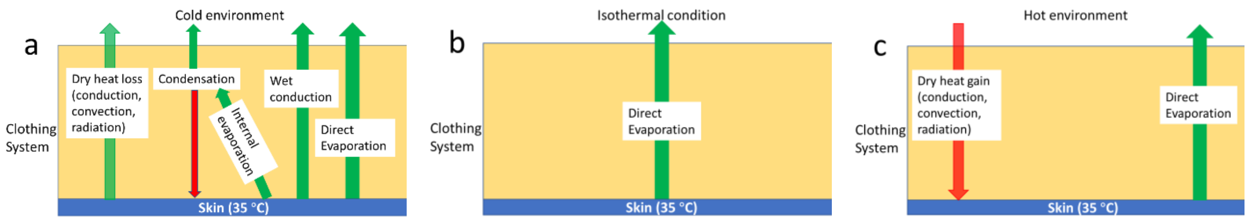

Figure 2-19. Pathways of heat loss through clothing in (a) cold environment, (b) isothermal condition (35 °C), and (c) hot environment (>35 °C)

Under heat stress, the first response of the human body is to increase skin temperature by pumping more blood to the skin[4]. If insufficient heat is released, then sweating begins[4]. Evaporative heat loss takes place by the transfer of latent heat of evaporated sweat from the skin to the environment[33]. When ambient temperatures approach and surpass skin temperature, evaporative heat loss becomes the only way to dissipate heat[4] (Figure 2-19b,c). When the ambient temperature is below the skin temperature (Figure 2-19a), dry heat loss is another basic way to release heat. Condensation happens when the moisture content at some region of the clothing exceeds the saturated moisture content for the local temperature[99-101]. When clothing is less permeable and the vapor pressure difference is steep (such as in cold environments), condensation tends to occur[33]. During condensation, heat will be given off and increase the local temperature[102, 103]. Part of the heat released by condensation will be liberated to the environment, defined as the heat pipe effect[104], and some part will be released back to the human body, which reduces the efficiency of evaporative heat loss[33]. In addition, when condensation happens, water will replace the air voids inside the fabric, leading to a decrease in thermal insulation, since the thermal conductivity of water (0.6 W/m/K) is about 25 times higher than air (0.024 W/m/K)[105]. This results in enhanced heat loss by wet conduction[100, 106, 107]. Among all the heat transfer pathways, evaporative heat transfer is considered as the main mechanism for heat loss when the subject is under thermal stress[108, 109].

Since evaporative heat transfer is predominant in hot conditions and moisture barriers largely determine evaporative resistance of firefighter composites[55], it is critical to study how properties of moisture barriers affect evaporative heat loss when used in different environments.

2.7.2 Heat exchange in firefighter clothing under solar radiation and flame radiation

In many scenarios, on-duty firefighters are subject to the radiation from heated items, flame, and the sun, which are major contributors to firefighter heat stress. The characteristics of radiation from the Sun and fire are listed in Table 2-1. To maintain the thermal homeostasis of human body and prevent heat stress, the external heat load from such radiation must be limited[110].

Table 2-1. Characteristics of the radiation from sun and flame

	Solar[29, 111]	Flame[19, 20]
Color temperature	5800 K	1100 K-1400 K
Wavelength range	0.3-2.5 μm	1-6 μm
Peak wavelength	~0.5 μm	~2 μm
Radiation intensity	< 1000 W/m^2	a few kW/m^2 to 200 kW/m^2

During firefighting, longwave radiation from flame can be encountered. Protective and comfort properties related to flame radiation have been well explored. Bröde et al. studied the influence of surface reflectivity, insulation, and vapor permeability of protective clothing on the heat gain from longwave radiation, and found that heat gain is relatively independent of fabric materials and color, except for fabrics with aluminized surfaces[53].

While on a fire scene or doing other jobs, such as car extrication, firefighters often work in direct sunlight. This solar radiation intensity has been measured as high as 1000 W/m^2 on a day with a clear sky[112]. A series of studies on the interaction between protective clothing and solar radiation was conducted within the European Union project THERMPROTECT[113-116]. One of the findings was that protective clothing with dark color tended to absorb more heat from solar radiation than the suits with light color or aluminized surface. Quintiere[52] and Collin et al.[19] measured the reflectivity of various firefighter clothing fabrics in the range of visible and longwave radiation using spectrometers, and found that color has a strong effect on solar heating load, but only a minor effect in the range of flame radiation.

However, many important questions remain unanswered, such as the influence of fabric texture on heat transfer between the human body and environment. In addition, almost all the studies mentioned above used new samples. During use, firefighter clothing is subject to washing and contaminants, such as soot, giving the appearance a darker look. The radiative properties of used clothing have seldom been addressed.

Heat gained from radiation constitutes a major part of heat stress, and has to be released from the body through evaporation[53]. The performance of firefighter composites with different moisture barriers under radiant heat load is unknown. Current moisture barriers are mostly bicomponent membranes, featuring a thin hydrophilic layer coated on top of a microporous film. For the surface hydrophilic nonporous layer in a bicomponent moisture barrier, it was reported that its water vapor resistance highly depends on moisture content in the membrane. The radiant heat load may decrease moisture content inside bicomponent moisture barriers and result in larger evaporative resistance, and this is to be investigated in this thesis.

2.7.3 Influence of air gap on heat transfer through firefighter composites

Air gaps exist in the microclimate of human body and clothing, and between fabric layers in multilayer turnout systems[117, 118]. The presence of air gaps plays a positive role in thermal protection[117, 118 119] but it may negatively influence on the wear comfort in terms of heat and water vapor transfer from the human body to the ambient environment[120]. Heat transfer through the air gap is mainly by radiation, heat conduction/ convection, and evaporation, as illustrated in Figure 2-20.

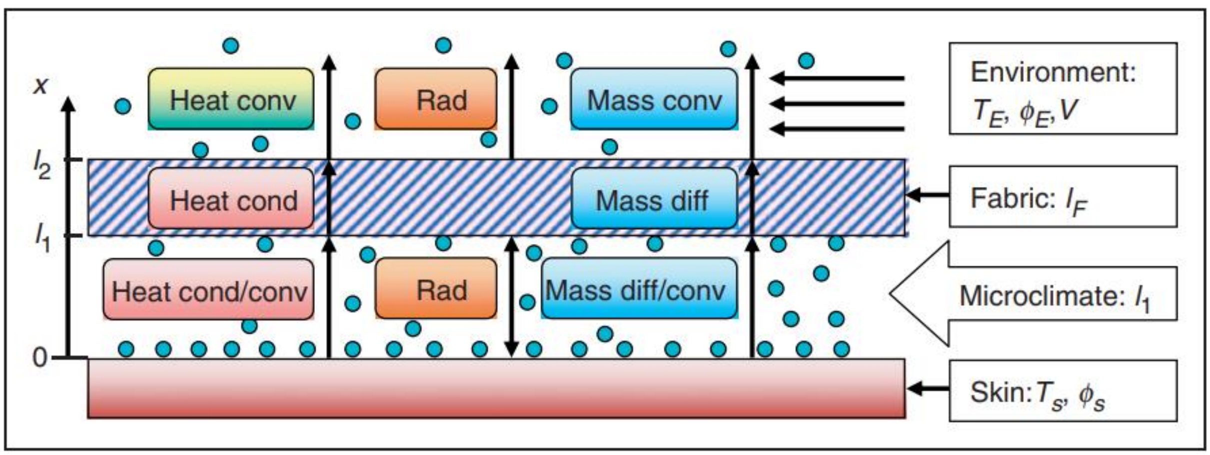

Figure 2-20. Heat and mass transfer through the air gap in a single layer system[121]. Copyright 2011. Permission granted from SAGE publishing

2.7.3.1 Heat and moisture transfer through a still air gap

Heat conduction and radiation are the primary modes of dry heat transfer within a smaller air gap.[118] The conductive heat loss rate through a stagnant air layer depends linearly on air gap size and the temperature difference. After the air gap size is increased to a certain threshold, natural convection occurs when the buoyancy force overcomes the shear and tensile forces in the fluid,[122,118] which may decrease the insulation value. The principle of the natural convection underneath the fabric includes the rise of warmer air (lighter due to lower density) to the top of the homogenous air gap along the heated surface, and sinking of the cooler air along the fabric inner surface[123]. Critical thickness in the range of 7 mm to 14 mm[119, 120, 123-125] was reported.

Similarly, the air gap can increase the evaporative resistance in the clothing system when the air gap is small[126]. When the air gap exceeds a certain value, water vapor resistance may decrease with the increases in the air gap due to the presence of natural convection[126]. In the absence of natural convection, the mass flux in the microclimate layer can be expressed using Fick's law[121]. In the presence of natural convection, the water vapor transfer mode changed from molecular diffusion to convective mass transfer, thereby enhancing the moisture transfer abilities[120].

2.7.3.2 Heat and moisture transfer through air gap via forced convection

In many cases, forced convection in air gaps can be created by human body movements (pumping effect)[41, 44-46, 127-130], incoming winds[44, 45, 128-130], or incorporating fans[131-133], which could decrease the evaporative and thermal resistance of air gaps.

Jasper et al. analyzed the convective and evaporative heat transfer on the skin surface when wearing a convective cooling system involving a series of micro fans with different sizes and amounts using COSMOL Multiphysics[132, 133]. The effects of air gap size between the undergarment and skin, the inlet airflow velocity, and the fan configuration on heat transfer were studied. It was found that convective and evaporative heat transfer along the skin surface was fully coupled and could be enhanced by the formation of eddy flows when the inlet airflow velocity was high, or the air gap size was large. Lu et al. investigated the influence of walking and wind on the insulation values of different clothing ensembles using a thermal manikin, and found that the total insulation values were reduced remarkably by the wind and body movements, especially for thin and light ensembles. In addition, the effects of wind and body movement on local resultant thermal resistance differed distinctively among different body parts[128, 129].

It is possible that the presence of air gaps with different sizes, in either still state or under forced convection, could affect the microenvironment of the moisture barrier, which could impact moisture absorption. This could further influence the evaporative resistance of bicomponent moisture barriers. To the best of our knowledge, this has never been studied.

2.8 Summary of critical gaps in current knowledge

The literature review identified the following gaps:

- Lack of knowledge of how NFPA 1971 certified turnout garments perform in different humidity and temperature conditions.
- It is unclear how firefighter composites incorporating different outer shells (contamination levels, texture, color) and moisture barriers perform under thermal radiation.
- The effects of an air gap between the skin of the wearer and clothing materials on the evaporative resistance of bicomponent moisture barriers also need further investigation.
- It is also important that the results from bench-level sweating plate tests be verified at the garment level to predict their impact on human thermal comfort.

Filling these gaps would contribute to understanding the relationships between heat strain indexes (*THL* and R_{ef}) and, more generally, how heat loss through turnout materials is affected by environmental factors including ambient temperature and humidity, as well as solar exposure and smoke contamination of the outer shell of the turnout system, which is the goal of this research. It requires a better understanding of the performance of specific turnout materials in different environmental exposures encountered by firefighters. It requires understanding about how smoke contamination of outer shell materials affects heat transfer through turnout composites. Finally, it requires understanding about how heat strain indexes measured at the fabric level translate to physiological responses associated with turnout-related firefighter heat stress. The outcomes of this research will be useful for improving testing protocols and establishing performance criteria for certifying the potential heat strain of turnout clothing at the NFPA 1971.

3 Relationship Between Total Heat Loss, Evaporative Resistance, and Thermal Protection Performance of Firefighter Protective Clothing

3.1 Introduction

Firefighting is a dangerous profession as firefighters need to perform strenuous work in hostile conditions[2]. Firefighter protective clothing, compromised of an outer shell, moisture barrier, and thermal liner, is required to protect firefighters from fire. Meanwhile, the protective clothing should be able to release enough metabolic heat to prevent heat stress issues. It was reported that heat stress is a major reason behind the cardiac events among firefighters, which accounts for 44% of all on-duty firefighter fatalities over the past decade[12, 13].

In the USA, two of the most critical factors when selecting firefighter protective clothing are total heat loss (*THL*) and thermal protective performance (*TPP*), as in NFPA 1971-Standard on Protective Ensembles for Structural Fire Fighting and Proximity Fire Fighting[72]. *THL* measures the capability of fabric systems to release heat by dry heat loss (conduction, convection, and radiation), and evaporation in the environment of 25 °C, 65% RH. It is measured with a sweating guarded hotplate with a surface maintained at 35 °C to simulate skin temperature[75]. *THL* was included in the NFPA 1971 in 2000, with a minimum requirement of 130 W/m^2. In 2007, *THL* was increased to 205 W/m^2. In comparison, *TPP* is defined as the total exposure energy that could cause a sufficient amount of heat transfer through the fabric system to human skin, inducing a second-degree burn[134]. It is tested under heat exposure of 2 cal/cm^2/s (84 kW/m^2), composed of 50/50 convective and radiation heat[72]. *TPP* rating is the product of heat exposure intensity with predicted time to a second-degree burn. The higher the *TPP* value, the more thermal protection the fabrics can provide. A minimum value of 35 cal/cm^2 is required in the NFPA 1971[72].

Apart from *THL*, intrinsic evaporative resistance (R_{ef}) is another index related to heat stress management in firefighter clothing. R_{ef} measures the ability to release heat in a fabric by evaporation in an isothermal condition where both the skin and ambient air are kept at 35 °C, according to ASTM F 1868, part B[75]. Both *THL* and water vapor resistance are required in ISO 11999-3[74]. There is current debate on including R_{ef} as an additional index in NFPA 1971. It is essential to understand the relationship between *THL* and R_{ef}. Li et al. investigated the relationship between thermal comfort and thermal protection properties of five firefighter composites, and found discordance between *THL* and R_{ef}. For some samples, the water vapor resistance fulfilled the performance requirement in ISO 11999-3, while *THL* failed to meet the requirement[69]. In addition, a negative correlation was found between *THL* and R_{ef} for the five composites studied[69]. DenHartog et al. found that three firefighter composites with similar *THL* values showed large differences in R_{ef}, which caused a significant difference in human physiological thermal comfort[135]. However, more samples are required to understand the relationship between *THL* and R_{ef}.

An ideal firefighter suit should have superior thermal protective performance while maintaining good thermal comfort properties. However, these usually are conflicting factors[33, 69]. Many studies on the relationship between *THL* and *TPP* have been conducted, and it was reported that *THL* was inversely correlated with *TPP*[69, 136, 137]. In contrast, there is little data available on the correlation between *TPP* and R_{ef} which is an important factor regarding thermal comfort in hot conditions.

In this thesis, thirteen firefighter turnout clothing composites were selected to investigate the relationship between thermal protection (*TPP*) and thermal comfort (*THL*, and R_{ef}) properties. In addition, the influence of outer shell, moisture barrier, and thermal liner on the performance of *TPP*, *THL*, and R_{ef} were explored. The results can be of significant importance for manufacturers to design firefighter protective clothing with good thermal protection and thermal comfort properties.

3.2 Methods

3.2.1 Materials

In this study, three kinds of outer shells (Natural, Black, Textured), seven types of moisture barriers (Bi-CompA, B, C, D/A, E, neoprene, and PTFE), and four kinds of thermal liners (2layer, DWR, needle-punched, and 1 layer), shown in Table 3-2, were employed to construct thirteen firefighter turnout clothing systems, as listed in Table 3-1. Out of the samples, six ensembles (#1, #2, #3, #7, #11, #12) are commercially available and are NFPA 1971 certified. They are representative of what freighters may wear when on duty. Some non-certified systems (#4, 5, 6, 8, 9, 10, 13) were included to expand the *THL* and R_{ef} range. In addition, with these samples, we could determine how DWR (durable water repellent) treatment in the thermal liner (#1, 2), thermal liner thickness (#1, 3, 4), outer shell color and texture (#1, 11, 12), and moisture barrier (#1, 5, 7, 8, 10,13) affect heat loss through firefighter ensembles as well as thermal protection.

Table 3-1. Compositions of firefighter ensembles

ID #	Thermal Liner	Moisture Barrier	Outer Shell	Weight (g/m^2)	Thickness (mm)
1	2 layer	Bi-CompA	Natural	674±1.9	2.15±0.07
2	DWR	Bi-CompA	Natural	665±0.5	2.20±0.05
3	Needle punched	Bi-CompA	Natural	693±6.3	2.68±0.07
4	1 layer	Bi-CompA	Natural	621±1.4	1.72±0.05
5	2 layer	Neoprene	Natural	869±4.4	2.11±0.06
6	2 layer/2 layer	ePTFE	Natural	924±4.1	3.54±0.08
7	2 layer	Bi-CompB	Natural	666±1.4	2.46±0.04
8	2 layer	Bi-CompC	Natural	660±5.2	2.51±0.07
9	1 layer	Bi-CompD/A	Natural	831±1.7	2.12±0.04
10	2 layer	ePTFE	Natural	652±2.1	2.15±0.06
11	2 layer	Bi-CompA	Black	677±0.2	2.16±0.06
12	2 layer	Bi-CompA	Textured	683±1.1	2.20±0.03
13	2 layer	Bi-CompE	Natural	736±2.5	2.24±0.02

Table 3-2. Physical properties of individual component

Code	Fiber contents	Weight (g/m^2)	Thickness (mm)
Natural	65% para-aramid,35% PBI, twill weave	239±0.6	0.40±0.01
Black	It is the same with the outer shell **Natural** except color	242±0.7	0.41±0.01
Textured	40% PBI, 60% para-aramid, plain weave	248±1.5	0.41±0.01
Bi-CompA	Bicomponent e-PTFE membrane attached on meta-aramid woven fabric	163±1.4	0.36±0
Bi-CompB	Bicomponent e-PTFE membrane attached on a meta-aramid nonwoven	155±1.4	0.67±0.02
Bi-CompC	European bicomponent e-PTFE membrane on a nonwoven	149±3.5	0.72±0.06
Neoprene	Neoprene laminated to a polyester/cotton woven fabric	358±5.5	0.32±0
Bi-CompE	Developed Bicomponent e-PTFE membrane attached on meta-aramid woven fabric	226±3.3	0.45±0.01
Bi-CompD/A	Developed e-PTFE bicomponent membrane attached on meta-aramid woven fabric (**Bi-CompD)** plus **Bi-CompA**	372±1.4	0.76±0.01
PTFE	Microporous e-PTFE membrane attached on meta-aramid woven fabric	141±0.5	0.36±0
2 layer	Two layers of aramid spunlace nonwoven quilted to a twill weave facecloth consisting of meta-aramid filament and meta-aramid /FR viscose spun yarns	272±2.2	1.39±0.04
DWR	Two layers of durable water repellant (DWR) finished aramid spunlace nonwoven quilted to a twill weave facecloth consisting of meta-aramid filament and meta-aramid/ FR viscose spun yarns	263±1.1	1.44±0.04
Needle punched	50% para-aramid/ 50% meta-aramid needle punch batt quilted to 60% meta-aramid filament / 40% spun twill weave (meta-aramid, FR viscose)	291±4.9	1.92±0.05
1 layer	One layer of aramid spunlace nonwoven quilted to a twill weave facecloth consisting of meta-aramid filament and meta-aramid /FR viscose spun yarns	219±0.7	0.96±0.03
2layer / 2layer	**PTFE** moisture barrier is sandwiched between two **2layer** thermal liners	543±4.4	2.78±0.09

3.2.2 Measurements

3.2.2.1 Total heat loss (THL) and intrinsic evaporative resistance (R_{ef})

THL and R_{ef} of firefighter composites (20 by 20 inches) were measured with a sweating guarded hotplate (Thermetrics, Seattle, USA) following ASTM F1868[75]. During tests, the hotplate surface was maintained at 35 °C to simulate human skin temperature. Total thermal resistance R_{ct} (K·W/m^2), intrinsic thermal resistance R_{cf} (K·W/m^2), intrinsic apparent evaporative resistance R_{ef}^A (kPa·W/m^2), *THL* and intrinsic evaporative resistance (R_{ef}, kPa·W/m^2) were calculated according to equations 2.6-2.12[75].

3.2.2.2 Thermal protection performance (TPP)

TPP was tested according to NFPA 1971[72]. A *TPP* tester (Custom Scientific Instrument Co.) containing two Meker burners and a bank of nine quartz tubes was used to produce a thermal exposure of 84 kW/m^2 (2.0 cal/cm^2/s), including 50% convective and 50% radiative heat. *TPP* is the product of heat exposure intensity with the time to a predicted a second-degree burn based on the Stoll Curve, which quantities the time needed for a second-degree burn at a certain heat level[138]. For each firefighter ensemble, *TPP* of three new specimens (6 × 6 inches) and three specimens that underwent five washing/drying cycles was tested. During the tests, an air gap of 6.3 mm was created between the *TPP* copper calorimeter and sample. According to NFPA 1971, the average *TPP* rating shall be no less than 35 cal/cm^2.

3.2.3 Statistical analysis

The statistical analysis was performed using JMP Pro 14 (SAS, Cary, NC, USA). The *THL*, *TPP*, and R_{ef} of different composites were compared using one-way analysis of variance (ANOVA), followed by Tukey's honestly significant difference (HSD). Comparison of materials ranking based on *THL* and R_{ef} was analyzed through Spearman Rank-Order Correlation. A *p*-value less than 0.05 was considered significant.

3.3 Results

3.3.1 Total heat loss (*THL*)

The intrinsic thermal resistance (R_{cf}) and intrinsic apparent evaporative resistance (R_{ef}^{A}) values measured with sweating guarded hotplate are shown in Figure 3-1a,b. Composites 4 and 6 demonstrated the highest and lowest insulation value, respectively. Sample #5 (Neoprene) showed an apparent evaporative resistance of 95 Pa·W/m^2, and the rest of the composites had a narrow distribution from 16 to 25 Pa·W/m^2. *THL* is illustrated in Figure 3-1c. The 13 samples covered a *THL* range from 111 to 271 W/m^2. Among them, sample 5 with an impermeable moisture barrier (Neoprene) and garment 6 with two thermal liners did not meet the minimum requirement of 205 W/m^2, as in NFPA 1971-2018[72]. Composite 4 with a thin thermal liner and a bicomponent moisture barrier had the highest *THL* of 271 W/m^2.

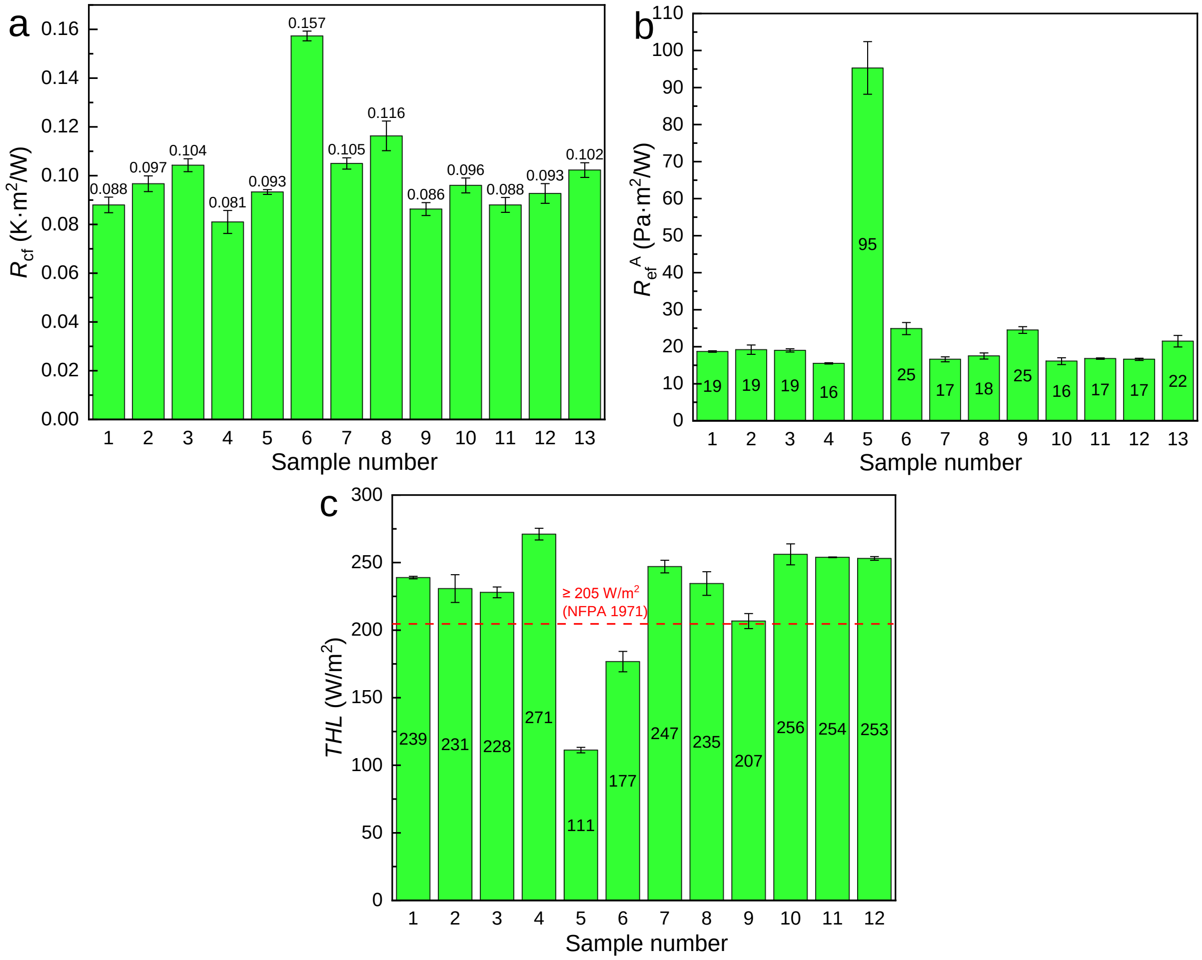

Figure 3-1. (a) Intrinsic thermal resistance (R_{cf}), (b) apparent evaporative resistance (R_{ef}^{A}) and (c) total heat loss (*THL*) of 13 turnout ensembles measured with a sweating guarded hotplate in the environment of 25 °C, 65% RH

3.3.2 R_{ef} (Intrinsic evaporative resistance)

R_{ef} was measured in an isothermal condition where both hotplate and chamber environment were kept at 35 °C, and the results are shown in Figure 3-2. We were able to obtain composites with R_{ef} ranging from 17 to 70 Pa·m^2/W excluding Neoprene (#5). Neoprene sample is impermeable, and a steady state during the R_{ef} test was not reached. An infinity R_{ef} value was assumed for this sample. Sample #13 possessed the highest R_{ef} value and might cause heat stress problems among firefighters. The best composite was sample #10 which showed a value of 17

Pa·m^2/W. Interestingly, for composites with bicomponent moisture barrier (#1, 2, 3, 4, 7, 8, 9, 11, 12, and 13), R_{ef} increased to some degree compared with R_{ef}^A (Figure 3-1b) (p<0.05).

In contrast, for sample 6 and 10 with the same microporous e-PTFE moisture barrier, their R_{ef}^A was similar with R_{ef} (p<0.05).

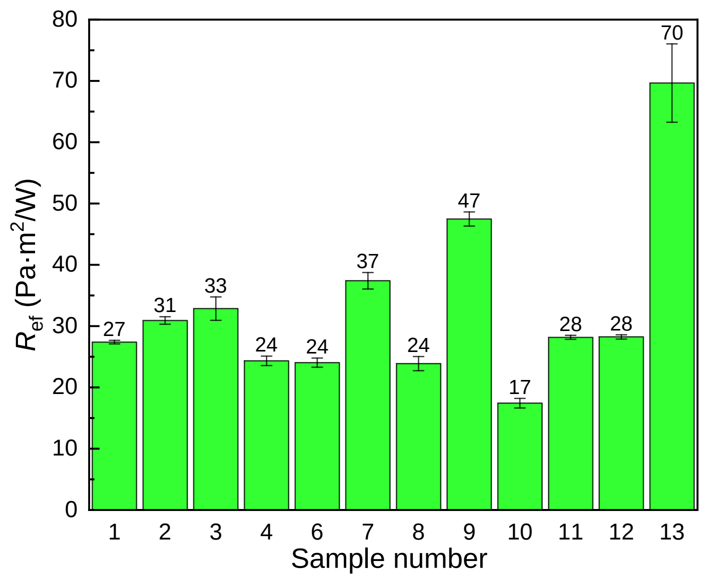

Figure 3-2. Intrinsic evaporative resistance (R_{ef}) of turnout ensembles measured with sweating guarded hotplate in the environment of 35 °C, 40% RH

3.3.3 *TPP* (Thermal protective performance)

TPP ratings of the thirteen turnout clothing systems are illustrated in Figure 3-3. A range from 33 to 61 cal/cm^2 was observed. Sample #4, with a thin thermal liner, was the only sample the did not meet the minimum requirement of 35 cal/cm^2 as in NFPA 1971-2018[72]. Sample 6 with two thermal liners possessed the highest *TPP* value, meaning superior thermal protection.

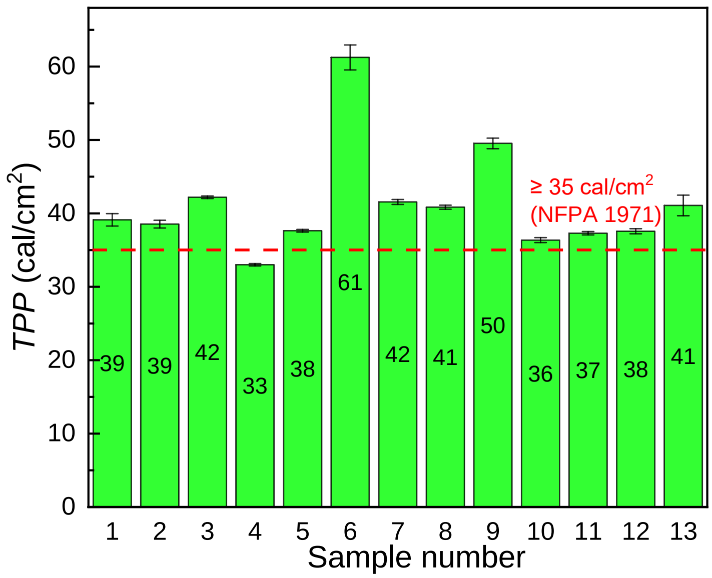

Figure 3-3. *TPP* ratings of turnout ensembles measured with a *TPP* tester

3.3.4 Correlation between *THL* and R_{ef}

The scatter points of *THL* and R_{ef} distribution are shown in Figure 3-4a.No relationship was found between *THL* and R_{ef} ($R^2 = 0.03$). In other words, a high *THL* did not necessarily mean low R_{ef}. For example, composite 13 showed a passing *THL* of 213 W/m^2 while exhibiting a high R_{ef} value of 70 Pa·m^2/W. In contrast, composite 6, a two thermal liner system with microporous e-PTFE moisture barrier, showed a low *THL*, and a low R_{ef} value. *THL* was calculated with insulation (R_{cf}) and apparent evaporative resistance (R_{ef}^A). It is of interest to see how evaporative resistance changed with test condition and the results are displayed in Figure 3-4b. No correlation was observed between R_{ef}^A and R_{ef} ($R^2 = 0.08$).

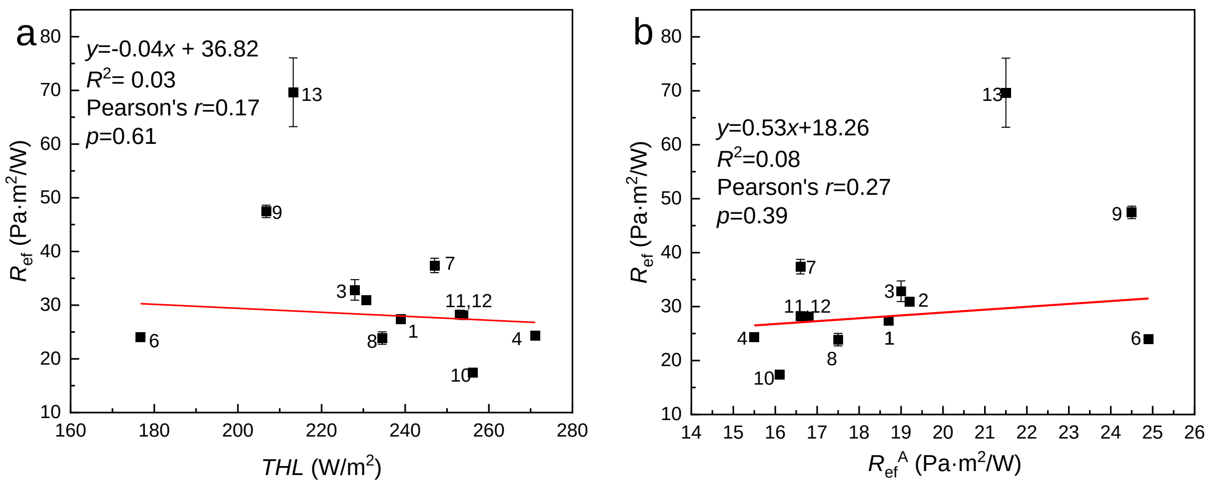

Figure 3-4. Correlation between (a) *THL* and R_{ef}, and (b) R_{ef}^{A} with R_{ef}

Table 3-3 lists the thermal comfort rankings of the thirteen firefighter composites which differed based on *THL* and R_{ef}. For example, garment 6 was the second worst in *THL* ranking but the third best in R_{ef} ranking. Through Spearman Rank-Order Correlation analysis, there was no significant correlation between the rankings based on *THL* and R_{ef} (p<0.05).

Table 3-3. Thermal comfort rankings of firefighter ensembles based on *THL* and R_{ef}

ID#	1	2	3	4	5	6	7	8	9	10	11	12	13
Ranking (*THL*)	6	8	9	1	13	12	5	7	11	2	3	4	10
Ranking (R_{ef})	5	8	9	4	13	3	10	2	11	1	6	7	12

3.3.5 Relationships between thermal comfort properties (*THL* & R_{ef}) and *TPP*

An ideal firefighter turnout suit should possess both good thermal protection and thermal comfort properties. We investigated the correlation between clothing thermal comfort (*THL*, and R_{ef}) with the thermal protection performance (*TPP*), and the results are shown in Figure 3-5. It is clearly revealed that *THL* is inversely correlated with *TPP*. However, sample 5 (Neoprene) was not included. If added, the correlation would be dropped from R^2 = 0.92 to 0.05. This means the inverse relationship is only valid between *THL* and *TPP* if all composites contain breathable moisture barriers. In contrast, there was little correlation between R_{ef} and *TPP* (R^2=0.42).

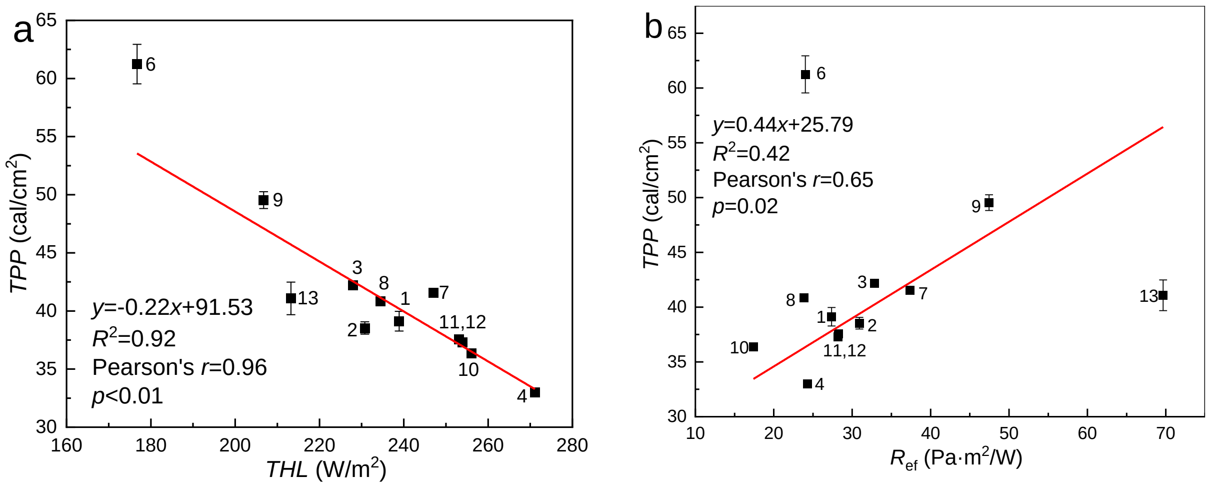

Figure 3-5. The relationship between (a) *THL* and *TPP*, and (b) R_{ef} and *TPP*

3.3.6 Influence of thickness

The influence of composite thickness on *THL*, R_{ef}, and *TPP* is displayed in Figure 3-6. No correlation was observed between thickness and *THL* or R_{ef} (Figure 3-6a, d). Intrinsic thermal resistance (R_{cf}) and apparent evaporative resistance (R_{ef}^A), with which *THL* was calculated, were also investigated. As expected, insulation was strongly correlated with the thickness (R^2=0.95), which was consistent with previous publications[30, 139]. In contrast, little correlation was observed between the thickness and R_{ef}^A (R^2=0.44). We also found a strong positive correlation between *TPP* and the thickness (R^2=0.84). Samples #6 and #9 were outliers, and a potential reason was that the two composites had four layers, which added an extra air layer, inducing a higher *TPP* value.

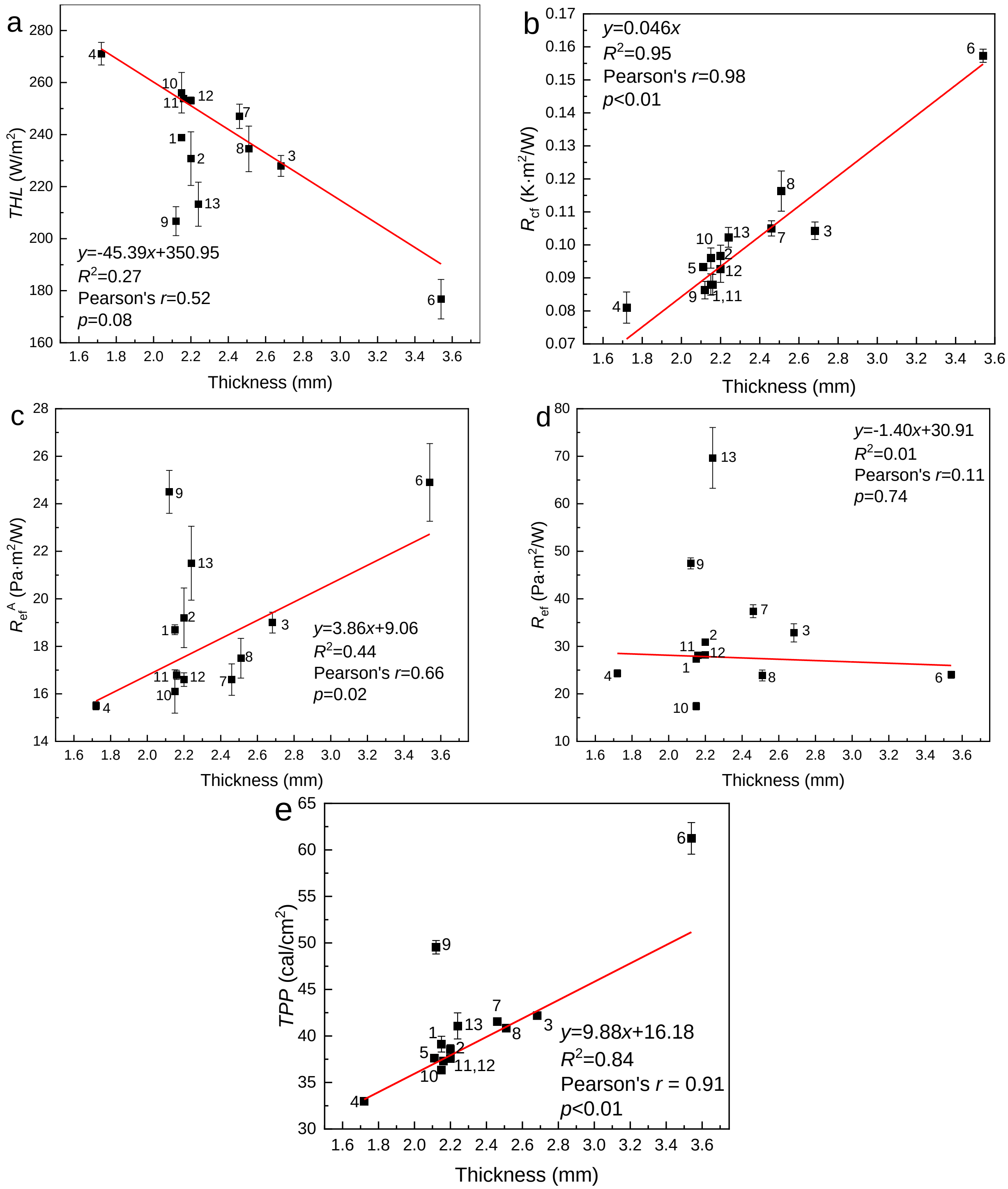

Figure 3-6. Correlation between the thickness with (a) *THL*, (b) R_{cf}, (c) R_{ef}^{A}, (d) R_{ef}, and (e) *TPP*

3.4 Discussion

Both *THL* and R_{ef} can be used to characterize the heat release properties of firefighter protective clothing. However, there is no correlation between them. During the *THL* test, it includes dry heat transfer through conduction, radiation, and convection, and wet heat transfer through evaporation in an environment of 25 °C, 65% RH. Condensation could happen during the *THL* test due to the temperature difference (10 °C) between the hotplate surface and chamber environment. For the R_{ef} test, which uses an isothermal condition, evaporation is the only method to lose heat. The reason why there was no correlation between *THL* and R_{ef} is that composites with a bicomponent moisture barrier strongly depend on the user environment. For example, R_{ef}^{A} values of composites 6 and 10 were similar with R_{ef}, while the rest of the composites showed much higher R_{ef} values than R_{ef}^{A}. Our previous study demonstrated that when tested in a cool environment (e.g. 25 °C), a larger amount of weight gain happened and could make bicomponent moisture barrier more breathable, reflected by small R_{ef}^{A} values. In the 35 °C test, due to moisture loss inside bicomponent moisture barriers, the composites became less breathable (large R_{ef}). As a result, the composites with bicomponent moisture barriers showed similar R_{ef}^{A} but different R_{ef} values. In comparison, the evaporative resistance of firefighter composites containing microporous moisture barriers did not depend on moisture absorption and was relatively independent of ambient conditions. Firefighter composites must possess a high *THL* and low R_{ef} value to ensure good heat release properties in both mild and hot environments.

Different from thermal comfort, the *TPP* test mainly relies on dry heat transfer. The heat from the flame could be transferred to the human body by infrared radiation and convective heat transfer. The emissivity of the outer shell surface is an important factor for radiative heat absorption from flame. For protective clothing fabrics, an approximate emissivity about 0.9 in the far infrared spectrum was reported, independent of color or materials[53]. The amount of heat absorbed from radiation and convective heat by the human body can be attenuated by insulation provided by protective clothing[71]. Thus, *TPP* is strongly correlated with thickness, which correlates with insulation[30, 140]. Sample #6 with two thermal liners and # 4 with a thin thermal liner had the highest and lowest *TPP* values, respectively. R_{ef} is mainly determined by the evaporative resistance of moisture barriers[55]. As a result, no correlation was observed between R_{ef} and *TPP* or thickness. For *THL*, at room temperature, composites with different moisture barriers showed similar evaporative resistance values (Figure 1b) and the difference in *THL* values was largely caused by the insulation component. Thus, a strong inverse correlation was observed with *TPP*. However, the premise of the conclusion is that all composites have similar apparent evaporative resistance. If the impermeable neoprene sample (#5) is included, the correlation becomes very poor. Since *TPP* is strongly correlated with the insulation value, but not correlated with evaporative resistance, one viable way to reach both high *TPP* and large *THL* or small R_{ef} is to use highly permeable moisture barriers without compromising insulation. It is also possible to achieve the goal by modifying the emissivity of the outer shell surface. Naeem et al. presented a nano-silver coated outer shell, and the resultant firefighter composites showed great thermal protection performance without affecting air and vapor permeability[141].

Another contribution of this study is the investigation of the effect of different components on *THL*, R_{ef}, and *TPP*. For *TPP*, thickness is the most important factor. Any way to increase the thickness could enhance *TPP*, like increasing the thickness of thermal liner (1, 3, and 4) or moisture barrier (1, and 7) (p<0.05). For *THL* and R_{ef}, the moisture barrier has the largest influence as it could affect evaporative resistance, and this can be revealed by comparing samples 1, 5, 7, 8, 10, and 13 (p<0.05). The microporous moisture barrier (Composite 10) showed the best performance while Bi-CompE (composite 13) possessed a poor performance at 35 °C. Outer shell color or texture (1, 11 and 12) has a minor influence on *THL*, R_{ef} or *TPP*. Durable water repellent finishing inside thermal liner (2) showed similar performance regarding all three indexes. The thickness of the thermal liner plays an important role. The thinner the thermal liner, the higher *THL* or lower R_{ef}, as can be observed from composite 1, 3, and 4 ($p<0.05$). A smaller thickness is correlated with lower insulation value. Composites with a smaller thickness can reduce evaporative resistance by decreasing the distance moisture vapor transfer through.

3.5 Limitations

We only investigated the relationship between *THL*, R_{ef}, and *TPP* on fabric using standard testing methods. Thermal comfort and thermal protection are complicated, as they can be affected by moisture content, garment design, posture, movement, air gaps, and environmental conditions[41-43, 45, 47, 119, 137, 142-145]. These factors should be taken into account in future studies.

3.6 Conclusions

In this study, the relationships between indexes for thermal comfort (*THL* and R_{ef}) and thermal protection (*TPP*) were investigated thoroughly by measuring fabric level properties of thirteen firefighter ensembles. The results show that *THL* is inversely correlated with *TPP* for composites with breathable moisture barriers, while no relationship was observed between R_{ef} and *TPP*. For *THL* and R_{ef}, little correlation was found, meaning that firefighter composites perform differently with the environment. In addition, we also found that *TPP* is mainly determined by thickness, while *THL* and R_{ef} can be improved by optimizing moisture barrier properties or decreasing thermal liner thickness. In order to have good thermal comfort properties in both mild and hot environmental conditions, as well as a high *TPP* rating, one of the best ways is to optimize the evaporative resistance of moisture barriers without comprising insulation value.

4 Effects of Environmental Temperature and Humidity on Evaporative Heat Loss through Firefighter Suit Materials Made with Semipermeable and Microporous Moisture Barriers

4.1 Introduction

The thermal burden of firefighter turnout suits is a primary contributor to firefighter heat strain and heat-related injuries that occur in structural firefighting[3, 10]. The NFPA 1971 Standard for Structural Firefighter PPE establishes a minimum heat strain requirement for turnout suits materials based on measured Total Heat Loss or *THL*[72]. Because the *THL* requirement is strictly valid only for predicting turnout related heat strain in mild environmental conditions (25 °C, 65% RH), there is interest in examining performance metrics across a broader range of environmental temperature and humidity conditions. This has led to the consideration of an evaporative resistance or R_{et} requirement. R_{et} is an index of water vapor resistance measured in hotter conditions (35 °C, 40% RH) according to standard ASTM F1868, Part B[75] R_{et} is an isothermal measurement wherein the only heat loss possible is by evaporative heat transfer. *THL* and R_{et} test conditions can produce different breathability rankings of tested turnout materials, depending on the technology of the moisture barrier incorporated in the turnout composite construction[146].

Heat loss through turnout materials is measured in the laboratory using a guarded sweating hot plate apparatus, sometimes called a sweating skin model. Sweating guarded hot plates are called sweating skin models because they measure heat loss through clothing fabrics using the same mechanisms responsible for heat loss from the human body through clothing, or by conductive, convective, and radiant heat transfer, and by heat loss through sweat evaporation

---

Gao H, Deaton AS, Fang X, Watson K, DenHartog E, Barker R. Textile Research Journal 2021. (Accepted)

from the skin. The testing principle is simple: heat loss is measured as the power, in W/m^2, needed to maintain the guarded heated plate surface at 35 °C (roughly skin temperature) as heat is lost from the plate surface through the test sample into an environmentally controlled test chamber. The guarded plate itself "sweats" or delivers a controlled source of evaporative heat energy. The test chamber can be set to maintain air temperature and humidity and to control airflow across the surface of the fabric test sample. *THL* is the sum of dry heat transfer and wet heat transfer. "Dry" heat transfer results from the temperature differential between the simulated skin surface and a cooler ambient environment. The second (and usually larger) fraction of *THL* comes from heat loss through evaporative heat transfer occurring because of the differences in the moisture vapor pressure on the skin or sweating plate side of the test material (assumed to be moisture saturated, or 100% RH) and the less humid ambient test environment.

The NFPA 1971 Standard for Structural Firefighter protective clothing[72] specifies non-isothermal testing conditions (25 °C, 65% RH) or ASTM F1868, Part C[75] for measuring the *THL* of firefighter suit materials. This enables the assessment of the insulation as well as the evaporative properties of turnout materials. Because of the 10 °C temperature difference across the turnout test sample and ambient environment, it is possible for moisture condensation to occur in the test sample. This phenomenon results in a higher reading of heat loss. This is why the evaporative resistance measured in non-isothermal conditions is called "apparent" evaporative resistance. Because of moisture condensation in the test sample, some test materials can appear to become more moisture vapor permeable when tested in cooler environments.

R_{et} is an index of evaporative heat resistance measured using a guarded sweating hot plate method (ASTM F1868, Part B) that is configured for isothermal environmental testing conditions (35 °C, 40% RH)[75]. Because it is an isothermal test, R_{et} is a "truer" or "pure" measure of the evaporative resistance of clothing materials since moisture condensation effects in this method avoid these complications. On the other hand, R_{et} does not measure the thermal insulation, or the resistance to "dry" heat transfer of turnout materials.

Turnout suit constructions consist of a woven heat-resistant outer shell fabric with inner layers including moisture barrier and thermal liner components. The moisture barrier functions to protect the firefighter from liquids, such as water, biological materials, and chemicals, while allowing transmission of evaporated sweat from the body[147]. Evaporative heat transfer is the primary mechanism of body heat loss in hot conditions, and the moisture barrier layer is the main determinant of the evaporative resistance of turnout systems[55]. The composition and structure of moisture barriers are key to understanding how environmental conditions may affect the evaporative heat resistance of different moisture barrier technologies.

Moisture barriers are typically composed of thin semipermeable membranes laminated to a fire-resistant woven or nonwoven base fabric. Current membrane technologies fall into three categories: microporous, solid hydrophilic, and bicomponent membranes. Among microporous membranes, expanded poly (tetrafluoroethylene) (e-PTFE) membranes are widely used in firefighter clothing constructions. These membranes have pore sizes ranging from 0.02 to 50 micrometers[57]. They resist the penetration of liquid water while allowing water vapor to diffuse through the interconnected channels[56]. Nonporous films, such as polyurethanes (PU) containing hydrophilic components, are also commonly used as breathable, waterproof membranes in firefighter suits. Vapor transmission through solid film barriers occurs by an absorption-diffusion-desorption mechanism[58, 59]. The diffusion coefficient of water vapor through hydrophilic polymers depends on the moisture content of the membrane[65, 66, 148]. Bicomponent membranes are the combination of the microporous membrane with solid hydrophilic film.

Almost all commercially available moisture barriers in firefighter suits are bicomponent e-PTFE moisture barriers, which feature a fine coating of solid hydrophilic film on e-PTFE microporous membrane. The addition of solid hydrophilic layer provides more durability to the moisture barrier and resistance to water penetration, but this surface coating increases the evaporative resistance, particularly making the evaporative resistance strongly dependent on the moisture content inside the hydrophilic layer[61].

Ding et al. developed a heat and mass transfer model and studied the influence of environmental conditions, materials properties, and air gap on the thermal and evaporative resistance of a single-layer fabric system. One of the findings was that ambient conditions including temperature, humidity, and wind speed have little effect on the evaporative resistance of the fabric itself without air gap[121, 149]. He et al. investigated the effect of ambient temperatures on evaporative resistance of firefighter turnout composite using sweating guarded hotplate and found that there was no obvious change in evaporative resistance under the chamber temperature from 20 to 40 °C[120]. But only one sample with a PTFE moisture barrier was selected. The above-mentioned studies did not address the effect of ambient conditions on mass transfer through different moisture barriers. Gibson studied the effect of temperature and humidity on vapor diffusion through polymer membranes or membrane/textile laminates with a Dynamic Moisture Permeation Cell[66]. It was reported that the diffusion resistance of water molecules through hydrophilic membranes strongly depended on the moisture content[66]. However, there was no temperature difference applied across membranes during testing, and the influence of ambient conditions on moisture gain in the membranes was unknown. It is therefore necessary to investigate how ambient conditions affect moisture gain inside moisture barriers, and how the moisture absorption would affect the evaporative resistance of firefighter composites containing different moisture barrier types.

It is critically important to understand how firefighter protective clothing with different moisture barriers transfers heat in different environmental conditions. In this paper, firefighter turnout composites with four different moisture barriers, including three bicomponent and one microporous moisture barrier, were selected. We explored how environmental conditions (temperature and humidity) affect the water uptake in each layer of firefighter fabric systems along with how cooling through evaporative heat loss changed in different conditions. We also considered the relationship between evaporative resistance and the moisture content inside moisture barriers.

4.2 Experimental method

We conducted experiments designed to quantify environmentally related differences in heat transfer in firefighter turnout materials incorporating different breathable moisture barrier technologies.

4.2.1 Test materials

The turnout composites studied utilize different membrane compositions to achieve a range of evaporative resistance (Table 4-1). Three of the samples are examples of e-PTFE (expanded Polytetrafluoroethylene) bicomponent membranes (Samples A, B, and C). Bicomponent membranes incorporate a fine hydrophilic layer coated onto a microporous e-PTFE film, as shown in Figure 4-1a. The nonporous hydrophilic coating increases resistance to high-pressure water penetration but impacts the evaporative resistance of the membrane. It makes the evaporative resistance of the membrane strongly dependent on the moisture content of this hydrophilic layer[61]. Two of the semipermeable bicomponent membranes (Samples B and C) are commercially available products compliant with the NFPA 1971 Standard for Structural Firefighter PPE. Sample A is a specially designed bicomponent e-PTFE membrane coated with a proprietary nonporous layer. Sample MM is an example of a truly moisture vapor permeable e-PTFE microporous membrane (no hydrophilic coating), as shown in Figure 4-1b. Membranes A and MM are moisture barrier constructs specially obtained for this study.

Table 4-1. Moisture barriers

Moisture barrier	Membrane type and composition	Weight (g/m^2)	Thickness (mm)	Images
A	**Bicomponent** e-PTFE membrane, bonded to woven aramid fabric	216±0.1	0.42±0.02	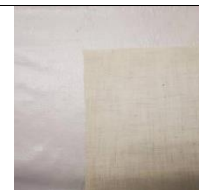
B	**Bicomponent** e-PTFE membrane, bonded to spun laced-aramid base fabric	167±1.6	0.76±0.02	
C	**Bicomponent** e-PTFE membrane, bonded to woven aramid fabric	170±2.5	0.40±0.01	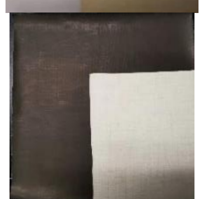
MM	**Microporous** e-PTFE membrane, bonded to woven aramid fabric	144±0.7	0.38±0.02	

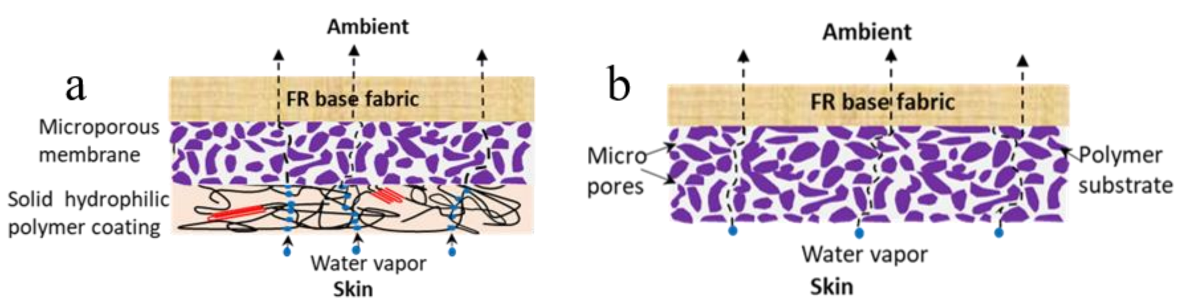

Figure 4-1. Schematic of (a) bicomponent moisture barrier (A, B, and C) and (b) microporous moisture barrier (MM)

We tested each of the four different moisture barrier technologies as inner-layer components of layered turnout fabric systems that were otherwise identical, as shown in Figure 4-2. They used the same outer shell fabric (meta-aramid blend, plain weave, weight: 256 g/m^2 and thickness: 0.61 mm) and thermal liner (needle punched aramid nonwoven quilted to 100% meta-aramid woven fabric, weight: 287 g/m^2, and thickness: 1.99 mm). During use, the base fabric of the moisture barrier faced outward, and the membrane surface faced human skin. Since the only difference between firefighter composites is the moisture barrier, we use the moisture barrier name to represent each firefighter composite. Unless specified, the notation of A, B, C, and MM refer to firefighter composite.

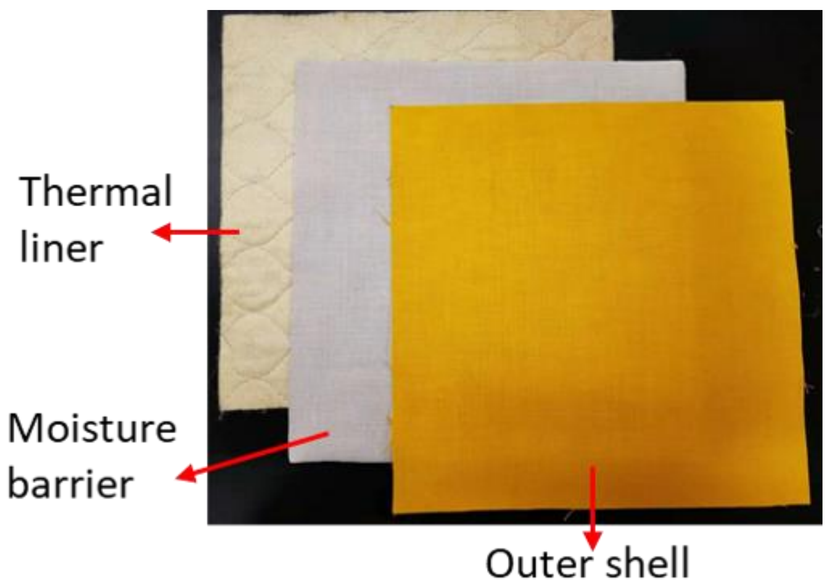

Figure 4-2. Firefighter turnout fabric system

4.2.2 Measuring heat loss of turnout systems in different ambient temperatures and humidity

We measured heat loss through turnout samples in different environmental temperatures and humidity using a sweating plate housed in an environmental chamber (Figure 4-3). The hot plate apparatus incorporates specialized instrumentation, including an embedded heat flux sensor, liquid-cooled hot plate, and thermal control system that enables measurements not possible using a standard hot plate apparatus, specifically when ambient air temperature exceeds the surface temperature of the guarded sweating plate.

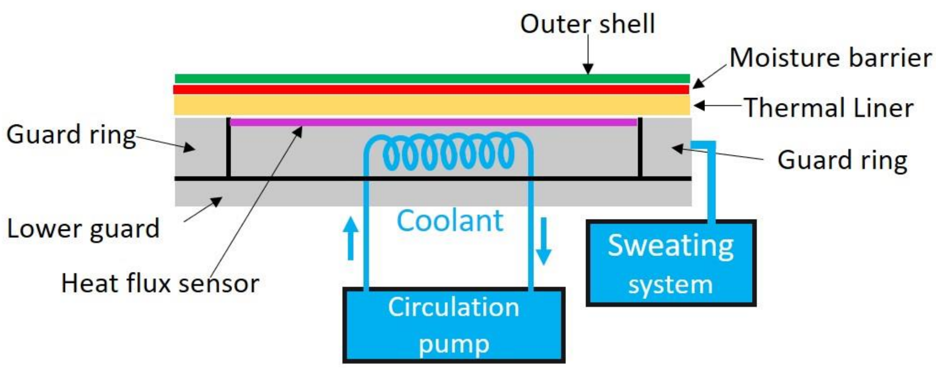

Figure 4-3. Schematic of sweating guarded hot plate

The hot plate system consisted of a 20.3 × 20.3 cm heated plate surrounded by a 5.1-cm guard ring (Figure 4-3). Twenty-five volumetrically controlled sweat ports supplied moisture to the plate. An integrated liquid-cooling loop and an embedded heat flux sensor enabled heat flux measurements in ambient conditions above the plate set temperature. An embedded heat flux sensor measured heat loss in the hottest testing condition (45 °C). Power supplied to the hotplate indicated heat loss for other ambient temperatures (20 °C, 25 °C, and 35 °C). We maintained the surface of the hot plate at 35 °C to simulate human skin temperature during the tests. The device used (DHS–8.2, Thermetrics, USA) fulfills all requirements in ASTM F1868-17, but it does not meet the requirement of ISO 11092-2014. The ISO standard requires the use of porous metal for the construction of hotplate surface, and the device test surface in this study was made of composite materials[19].

We measured heat loss at four different chamber conditions (20 °C, 88.1% RH; 25 °C, 65% RH; 35 °C, 36.6% RH; 45 °C, 21.5% RH). We set the relative humidity levels to maintain a constant ambient vapor pressure difference of 3.57 kPa between the wet hotplate surface and the chamber environment to eliminate the influence of a vapor pressure difference on evaporative resistance measurements. When tested at 45 °C, the incorporated cooling system was activated by circulating coolant under the hotplate surface to prevent it from overheating. With the additional cooling, the power required to keep the plate at a constant temperature could no longer be used as it included the power required to overcome the cooling. Therefore, the heat loss measured by the embedded heat flux sensor was utilized at the condition of 45 °C.

We also conducted tests at five different levels of ambient relative humidity (25% RH, 40% RH, 55% RH, 70% RH, and 85% RH) to study the effects of environmental humidity on heat loss. Tests were conducted at isothermal temperature conditions (35 °C) to determine the influence of ambient humidity levels on evaporative resistance. The test duration was one hour. Steady state heat transfer through test samples typically occurred within 30 minutes of initiating the test. Average heat loss was measured after achieving steady-state conditions.

Test samples were preconditioned at 21 °C and 65 % relative humidity for at least 12 hours prior to hot plate testing. The duration of all wet tests was controlled to be one hour. After the wet test, each layer of firefighter composites was weighed immediately, starting with the outer shell, then moisture barrier, and liner. The weight of each layer of the turnout composite was measured on a precision scale (Mettler PM460). Before measurement, all samples were sealed inside a plastic bag to minimize moisture loss.

4.2.3 Calculations

Total heat loss (*THL*) from the hot plate to the environment through the composites measured in the environment of 25 °C, 65% RH was calculated with equations 2.6-2.10[75].

The weight gain W (g) after wet test for each sample was calculated with

$$W = W_2 - W_1 \tag{4.1}$$

where W_1 (g) is the weight of the preconditioned sample before wet tests, and W_2 (g) is the weight after wet tests. To reduce the evaporation during measurement, we placed the digital scale near the hotplate device so that samples after wet tests could be weighed immediately. The weight measurements occurred at room temperature with minimal airflow, which can help to reduce evaporation. However, some evaporation during the weight measurements is unavoidable.

4.2.4 Statistical analysis

The statistical analysis was performed using JMP Pro 15 (SAS, Cary, NC, USA). The evaporative resistances measured at different environmental conditions for the firefighter composites were compared using one-way analysis of variance (ANOVA), followed by Tukey's honestly significant difference (HSD). The sample size is three. A p value of less than 0.05 was chosen to indicate a significant difference.

4.3 Results and Discussion

Table 4-2 shows the measured Total Heat Loss (*THL*) and evaporative resistance of the turnout study materials. *THL*, intrinsic thermal resistance (R_{cf}) and apparent evaporative resistance (R_{et}^{A}) were measured in non-isothermal conditions (25 °C, 65% RH) following ASTM F1868, Part C. Evaporative resistance (R_{et}) was measured in isothermal conditions (35 °C, 40% RH) following procedures described in ASTM F1868, Part B[75]. These data indicated only about 12 W/m^2 difference in total heat transmitted by the bicomponent membrane systems A, and C. However, the system that incorporated a microporous moisture barrier (Composite MM) transmitted 28 W/m^2 more heat than composite C in these non-isothermal test conditions. All the turnout systems exceeded the 205 W/m^2 minimum *THL* performance level required by the NFPA 1971 Standard[72]. In comparison, significant differences were found in the ability to transmit evaporative heat in isothermal conditions, as shown by measured R_{et} values. The system containing the microporous membrane (MM) had one third the evaporative resistance of the system with the monolithic hydrophilic coating layer (Composite A), when tested at 35 °C.

Table 4-2. Total heat loss and evaporative resistance of firefighter turnout materials

Composite	Weight (g/m^2)	Thickness (mm)	R_{cf} (K·m^2/W)	R_{et}^A (Pa·m^2/W)	*THL* (W/m^2)	R_{et} (Pa·m^2/W)
A	747±3	3.11±0.09	0.135±0.004	23.2±0.1	220±1.7	56.7±0.8
B	711±10	3.58±0.14	0.158±0.002	22.7±0.4	218±3.3	40.3±0.7
C	695±5	3.15±0.08	0.144±0.004	21.3±0.3	233±2.8	31.0±0.8
MM	666±8	3.07±0.07	0.138±0.020	18.8±0.4	261±4.7	18.7±0.4

Note: R_{cf} (intrinsic thermal resistance), R_{et}^A (total apparent evaporative resistance), and *THL* (total heat loss), R_{et} (total evaporative resistance) were tested three times according to ASTM F1868.

Significant differences in R_{et} values were observed in all three of the systems that incorporated bicomponent membranes (A > B > C) (p<0.05). Therefore, these data confirmed a material-dependent relationship between heat loss through turnout systems and environmental testing conditions.

4.3.1 Influence of air temperature on heat loss and evaporative resistance

Figure 4-4 shows heat loss through the turnout systems and environmental temperature in guarded hot plate tests conducted at 20, 25, 35 and 45 °C. The vapor pressure difference between the sweating plate and chamber environment was held constant at 3.57 kPa for these tests.

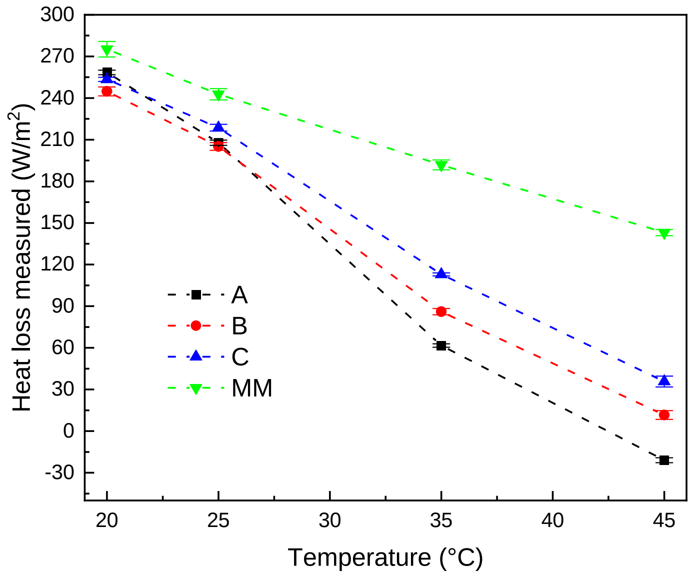

Figure 4-4. Heat loss through turnout composites measured by hotplate at different ambient air temperatures

These data show that higher air temperature had a more pronounced effect on lowering heat loss through turnout systems that contain semipermeable bicomponent moisture barriers (Composites A, B and C) than on the system incorporating a more vapor permeable microporous moisture barrier (Composite MM). We could observe that the heat loss was similar through the turnout systems in cool environments (20-25 °C). However, significant differences in composite heat loss appeared when ambient temperatures exceeded 30 °C. The observed differences were substantial at air temperature above 35 °C.

Figure 4-5 shows that the apparent evaporative resistance of the composites increased with temperature, following the same trend as total heat loss. This finding confirmed the effects of moisture barrier composition on the relationship between system heat loss and environmental temperature.

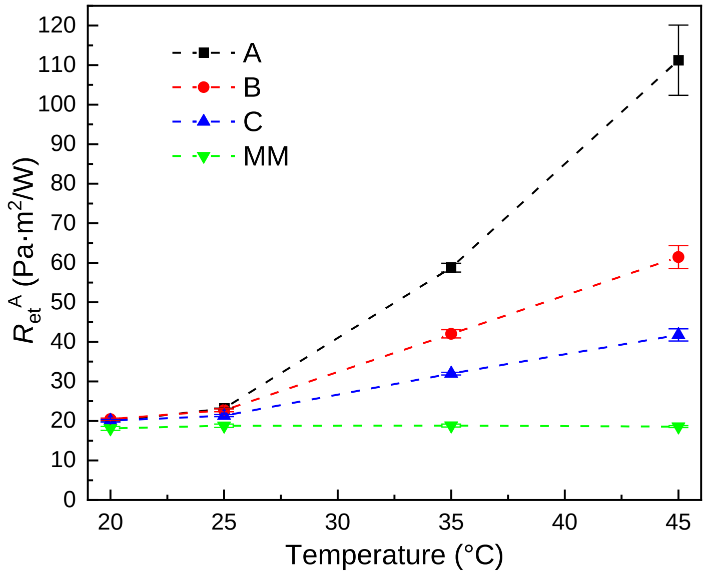

Figure 4-5. Evaporative resistance of turnout composites at different ambient temperatures

Figure 4-5 shows that, while the apparent evaporative resistance of the turnout systems was similar when measured in cool environments (20-25 °C), it increased sharply with ambient air temperature for composites containing bicomponent membranes (A, B and C). In contrast, apparent evaporative resistance (R_{et}^{A}) remained constant for the composite made with the microporous membrane (MM) ($p<0.05$).

Figure 4-6 shows the calculated fraction of the total heat loss through the composites broken out by evaporative heat transfer (wet heat loss) and by dry heat loss.

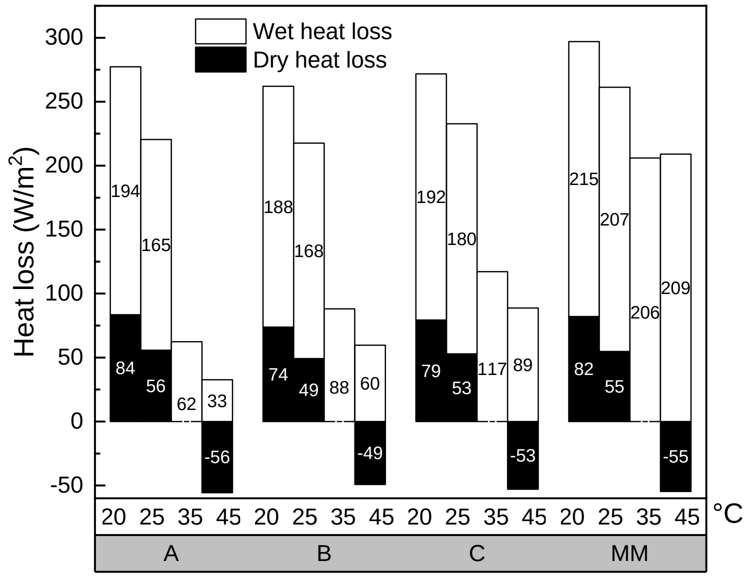

Figure 4-6. Calculated dry and wet heat loss under different ambient temperatures at a constant vapor pressure difference of 3.57 kPa

At cooler ambient temperatures (20-25 °C), the largest fraction of heat loss came through evaporative heat transfer through all the systems tested. The primary cause of the lower heat loss in composites containing bicomponent moisture barriers was the observed increase in the apparent evaporative resistance of these systems when ambient air temperatures exceeded about 30 °C. Significantly, reduced evaporative heat loss was not present in the composite that incorporates the microporous membrane barrier.

Therefore, we can attribute the effect of ambient temperature on heat loss in some turnout systems to reduced apparent evaporative heat transfer associated with moisture condensation in the composite. Figure 4-7 shows moisture absorption of the different systems measured at different ambient temperatures.

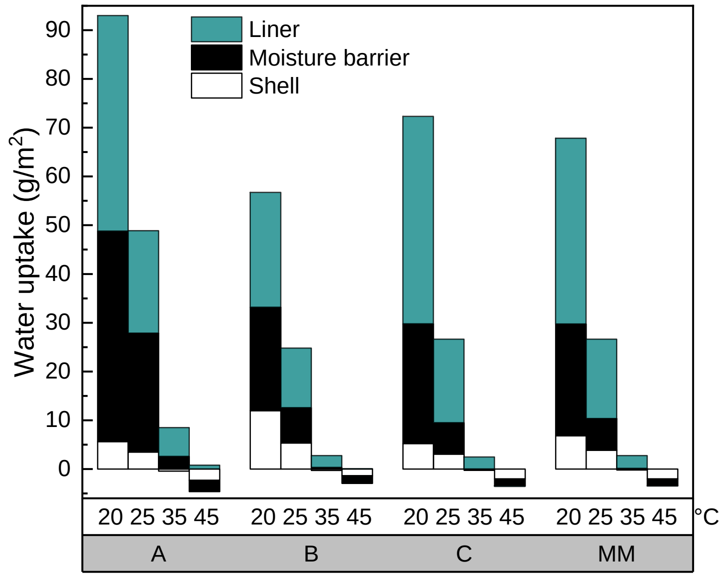

Figure 4-7. Water uptake of individual layers after wet tests conducted at different ambient temperatures

The data shows that all the turnout systems absorbed significant amounts of moisture through condensation when the ambient air temperature was cool (20-25 °C ambient temperatures), or when a positive temperature difference existed between the sweating plate surface temperature (35 °C) and the air in the test chamber. Most of the absorbed moisture resided in the moisture barrier and thermal liner layers of the turnout composites. Higher ambient air temperatures, or temperatures greater than 30 °C, significantly reduced moisture absorption in all of the semipermeable bicomponent and vapor permeable microporous membrane systems. Weight gain at 20 °C and 25 °C observed in Figure 4-7 was likely due to moisture condensation in the composite. Condensation occurs when the water vapor pressure reaches the saturation point in the fabric due to lower local temperature[150]. The amount of moisture uptake measured decreased with temperature, as was also observed by Rossi[151]. Interestingly, at 45 °C with the same vapor pressure in the environment, all composites showed a weight loss. This is because water absorption is an exothermic reaction, and water uptake decreases as temperature increases[152]. The results suggest that R_{et} is advantageous over *THL* in predicting heat loss at hot conditions. *THL* is measured at 25 °C, 65% RH, and would cause a large amount of condensation during test, making the bicomponent moisture barriers more breathable. Compared with the *THL* test, R_{et} is measured at a higher temperature (35 °C, 40% RH), and could reduce the moisture absorption inside moisture barriers and produce an evaporative resistance value for bicomponent moisture barrier systems (A, B, and C) closer to that at the hotter environment. For example, if we want to predict the wet heat loss of sample A in 45 °C, 21.5% RH using *THL* (25 °C), the predicted wet heat loss would be 165 W/m^2, indicating a large difference of 132 W/m^2 from the measured value (33 W/m^2) at 45 °C. In contrast, if using R_{et}, the difference between the predicted value (62 W/m^2) and measured evaporative heat loss (33 W/m^2) is only 29 W/m^2, as shown in Figure 4-6. This reveals the advantage of using R_{et} in predicting heat loss at high temperatures.

We can attribute observed differences between bicomponent systems (A, B, and C) and the microporous system (MM) to the effects that absorbed water had on swelling the hydrophilic coating layer present in bicomponent moisture barriers. Moisture induced swelling and produced more free volume between polymer chains, thereby facilitating the transmission of water vapor. This led to lower evaporative resistance, as indicated by Figure 4-5. In addition, absorbed water acted as a plasticizer, potentially lowering the activation energy of diffusion through the membrane[65]. In comparison, the evaporative resistance of firefighter composite containing microporous moisture barrier (MM) did not depend on moisture absorption and was relatively constant. Apart from the influence of moisture content, temperature could increase water diffusion rate through bicomponent membranes. However, compared with the effect of moisture content on evaporative resistance of bicomponent moisture barriers, the temperature effect was much less important, especially for the small temperature range we studied (20 to 45 °C). A similar conclusion was reported by Gibson[66].

It is arguable that higher evaporative heat loss at 20 °C or 25 °C (Figure 4-6) might be due to the increase in wet heat conduction caused by the moisture condensation in the system, instead of the change in evaporative resistance observed in Figure 4-5. For example, because of condensation at 20 °C the moisture content in composite A was 13%. The moisture condensation increased the thermal conductivity of the system, causing a corresponding decrease in the insulation value. The real evaporative heat loss of composite A at 20 °C might have been 33 W/m^2 instead of 194 W/m^2 as shown in Figure 4-6. The difference between 194 W/m^2 and 33 W/m^2, which is 161 W/m^2, could be due to extra thermal conduction caused by water condensation in the environment of 20 °C, instead of the dependence of evaporative resistance on moisture gain for bicomponent moisture barriers. Therefore, dry heat loss, defined as the heat loss pathways by conduction, radiation, and convection, should be the sum of 161 W/m^2 heat transfer by wet conduction and 84 W/m^2 by dry insulation. As a result, the total insulation value, including air layer resistance (0.04 $K{\cdot}m^2/W$) was 0.061 $K{\cdot}m^2/W$. This means that the intrinsic insulation of the fabric with 13% moisture content was reduced to 0.021 $K{\cdot}m^2/W$. This represented a significant 85% insulation loss compared to the insulation of the dry fabric (0.135 $K{\cdot}m^2/W$), which was not realistic. Hes et al. studied the insulation properties of woven fabric in wet state with the Alambeta instrument, and it was found that a 13% moisture gain in a wool/polyester woven fabric only resulted in about 8% decrease in thermal resistance[153]. Romeli et al. reported a 9% decrease in thermal resistance for a cotton woven fabric containing 12% moisture, measured with ThermoTex[154]. Thus, it is safe to conclude that the larger evaporative resistance or less wet heat loss at higher temperatures for firefighter composites containing bicomponent moisture barriers (A, B, and C) was mainly due to the dependence of evaporative resistance on the amount of water uptake.

3.2 Influence of relative humidity on heat loss and evaporative resistance

Figure 4-8a shows heat loss at relative humidity levels ranging from 25% to 85%, measured in sweating plate tests conducted in isothermal conditions (35 ^{o}C). Because of the reduced vapor pressure difference, an expected reduction in heat loss occurred at higher ambient humidity levels. Figure 4-9a shows that the evaporative resistance (R_{et}) of the systems decreased with ambient humidity. Although differences persisted across a range of humidity levels, moisture barrier related differences in evaporative resistance decreased at high humidity levels (>80% RH). Figure 4-8b shows that moisture absorption in turnout systems increased with ambient humidity. Smaller evaporative resistance, combined with a lower moisture vapor pressure difference, explained the reduction in the differences in total heat loss through the turnout composites observed at higher humidity levels (Figure 4-9b). Differences in heat loss among turnout systems were minimal at the highest humidity testing condition (85% RH).

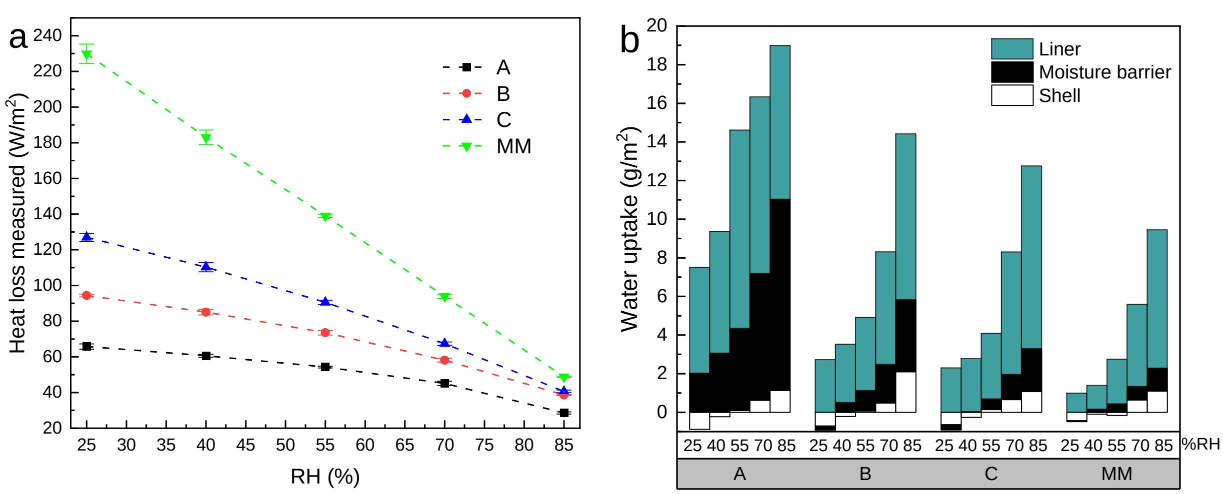

Figure 4-8. (a) Heat loss measured by hotplate, and (b) the water uptake of individual layers after wet tests conducted with varied relative humidity (25%, 40%, 55%, 70%, 85% RH) at a constant temperature of 35 °C

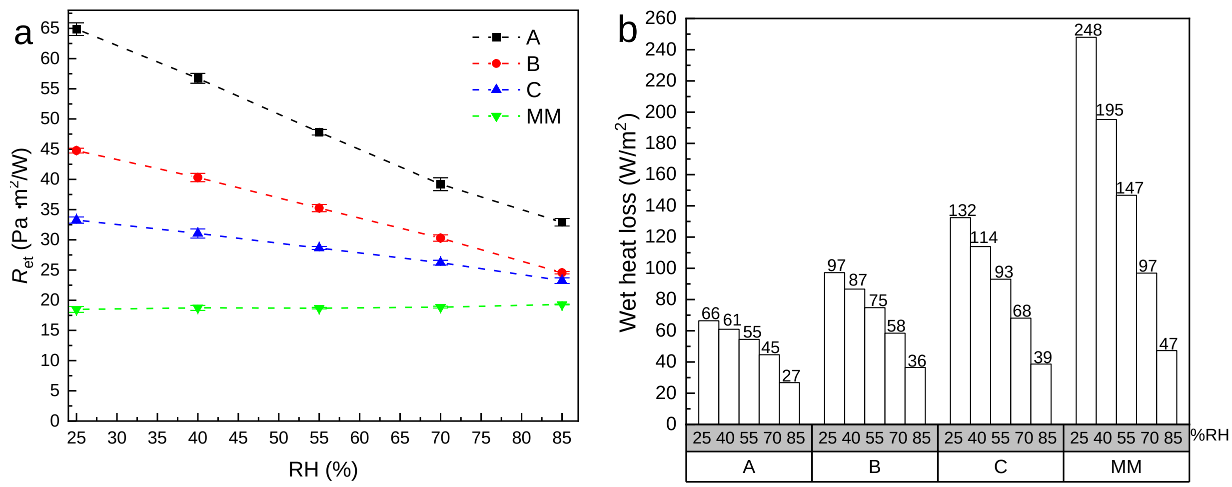

Figure 4-9. (a) Evaporative resistance and (b) calculated wet heat loss under different levels of relative humidity (25%, 40%, 55%, 70%, and 85%) at a constant ambient temperature of 35 °C

4.3.2 Relationships between moisture absorption and evaporative resistance in turnout systems

The experiments conducted to study the effects of ambient temperature and humidity on the heat loss and evaporative resistance of turnout composites have clearly demonstrated the effects of moisture pickup by turnout samples during sweating plate tests on their measured heat loss. Figure 4-10 shows the strongly significant inverse correlations observed between moisture absorbed by the moisture barrier in turnout systems and their evaporative resistance.

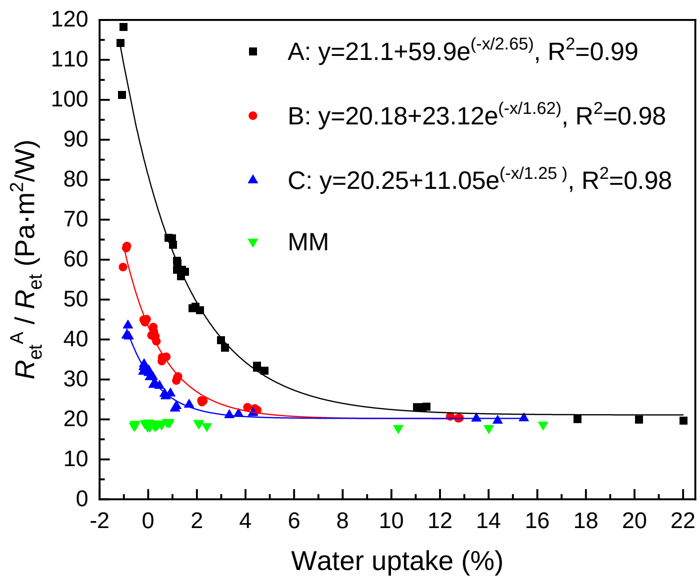

Figure 4-10. Relationships between evaporative resistances and water uptake in moisture barriers

Figure 4-10 shows that the evaporative resistance of the microporous barrier system (MM) was unchanged by absorbed moisture. In comparison, evaporative resistance dropped off exponentially with absorbed moisture for semipermeable barrier systems (A, B and C), reaching a minimum level when the system saturated with moisture. These data indicated that relatively small amounts of absorbed moisture were required to produce saturation and to minimize the evaporative resistance of semipermeable barrier systems. Commercial systems B and C achieved the minimum evaporative resistance level with 3-5% moisture uptake. System A saturated at about 10% water uptake. It is necessary to study the chemical composition and morphology of the moisture barriers in order to explain the observed differences among semipermeable bicomponent moisture barriers in Figure 4-10, and this is to be conducted in our future research. The exponential regression models developed for relating the evaporative resistance of semipermeable turnout systems to absorbed moisture are a useful outcome of this analysis (Figure 4-10). They could be used to predict the evaporative cooling and *THL* of firefighter turnout systems based on the moisture barrier type and moisture uptake.

The predicated heat loss at different chamber temperatures (20 °C, 25 °C, 35 °C, and 45 °C) under the same vapor pressure difference was calculated, as shown in Figure 4-11. The green bar shows the predicted *THL* in different environments calculated with the apparent evaporative resistance value measured at 25 °C, 65% RH, as in the standard *THL* measurement. The blue bar displays the predicted *THL* calculated with the actual evaporative resistance values shown in Figure 4-5, which was measured at the chamber condition to be predicted. It illustrates how measurements of evaporative resistance in a mild environment (25 °C) led to the significant overestimates of potential heat loss through turnout systems containing bicomponent moisture barriers at elevated testing temperatures (35 and 45 °C). This means that relative comparisons of the heat strain performance of different turnout materials could have dramatically different outcomes, depending on which of the indexes is used for the ranking.

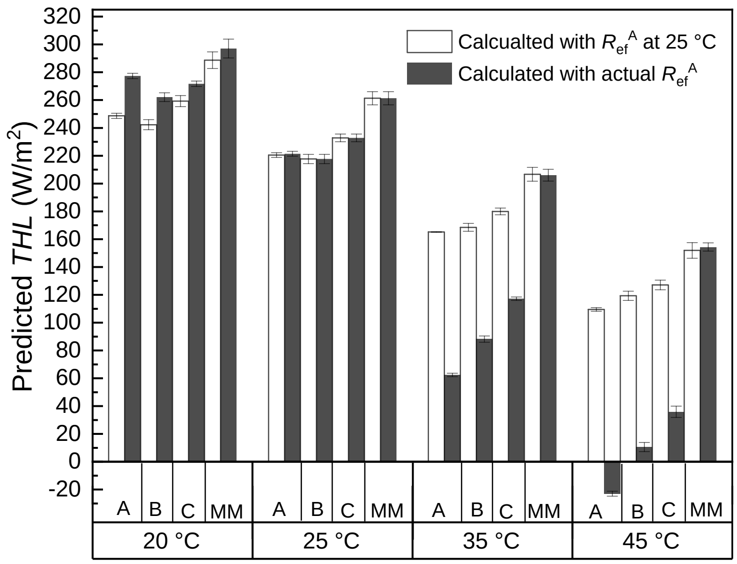

Figure 4-11. Calculated total heat loss based on R_{ef}^A measured at 25 °C and R_{ef}^A measured at prevailing conditions

4.4 Limitations

In this paper, we studied the effect of ambient temperature and relative humidity on the evaporative resistance of firefighter turnout composites on fabric level. Three bicomponent e-PTFE (A, B and C) and one microporous e-PTFE (MM) moisture barriers were selected, with only two samples (B, C) NFPA 1971 certified. It is important to include more commercially available moisture barriers in future research. Firefighter composites are multi-layer systems. Air gaps exist between the human body and clothing, as well as between fabric layers[117, 118]. The presence of air gaps influences the wear comfort negatively in terms of heat and water vapor transfer from the human body to the environment[120]. We will investigate how air gap sizes along with environmental conditions could affect heat transfer through firefighter turnout composites. Apart from fabric level test, garment level characterization is necessary. Heat exchange between the human body and the environment through clothing is complicated, and can be affected by moisture content, garment design, human posture, movement, wind, clothing fit, evaporation efficiency, etc[42-48, 120]. In addition, for *THL* and R_{et} test, the hotplate surface was kept as water saturated, which cannot reflect human thermoregulation actions. In mild conditions or in light activities, human skin may be dry due to less heat stress. In order to fully understand the influence of different turnout clothing on the human body in various environments, physiological manikin and human wear trials are required, which will be conducted in the future. Exploring the relationships between the evaporative resistance of turnout composites with bicomponent moisture barrier A, B, and C (observed in Table 4-2, Figure 4-5, Figure 4-9a and Figure 4-10) and their chemical composition and membrane structure was beyond the scope of this study. Research to better understand these relationships would be an excellent topic for future study. Characterization including Scanning Electron Microscope (SEM), Fourier Transform Infrared Spectroscopy (FTIR), and Differential Scanning Calorimetry (DSC) can be used.

4.5 Conclusions

Which is the better index for rating the heat strain of turnout materials, *THL* or R_{et}? We have shown that the answer to this question depends on the assumptions made about the temperature and humidity of the intended operating environment. Each heat loss index strictly correlates to a single set of conditions: *THL* predicts apparent evaporative heat and insulation in mild working conditions (25 °C, 65% RH). R_{et} predicts best for hotter conditions (35 °C, 40% RH). Each index provides complementary information about the potential heat strain contribution of turnout materials. Our study has demonstrated the significant effects that ambient temperature has on the evaporative resistance of firefighter turnout materials that contain semipermeable moisture barriers.

These findings reveal limitations in using *THL*, the current testing method used to characterize the capabilities for firefighter clothing to release heat specified by the NFPA 1971 Standard, as the only index for evaluating materials related heat strain potential. Because structural firefighters work in a range of environmental conditions, including mild and hot environments, they support the need to measure turnout evaporative thermal resistance at 35 °C (R_{et}), in addition to total heat loss (*THL*) at 25 °C. The environmental condition used in the *THL* test (25 °C, and 65% RH) can result in condensation and makes firefighter composites with bicomponent moisture barriers appear to be more breathable than they actually are without condensation. In some real-world firefighting scenarios, working conditions can be very hot. This study has definitively shown that hot environments produce less water inside moisture barriers, causing turnout systems with bicomponent moisture barriers to have much higher evaporative resistance.

5 Experimental Study on the Effect of Air Gap on Heat Loss through Firefighter Composites

5.1 Introduction

Firefighting is considered as one of the most strenuous occupations and together with the requirement to wear heavy protective clothing, substantial demands can be placed on the body, leading to heat stress[3]. Heart attacks have always been the leading cause of firefighter fatalities[11]. Heat stress can exacerbate the cardiovascular strain experienced by firefighters and is considered as one of the leading factors that can increase the risk of sudden cardiac events[13].

Firefighter composites include thermal liner, moisture barrier, and outer shell. Air gaps exist between the body and clothing, as well as between fabric layers in a multilayer system[117, 118]. The presence of air gaps plays a positive role on thermal protection[117-119], but it may influence the wear comfort[120]. It is paramount to understand the effect of air gap on heat loss through firefighter composites under various environmental conditions in order to address the heat stress issues among firefighters.

Heat conduction and radiation are the primary modes of dry heat transfer within a smaller air gap[118]. After the air gap size increase to a certain threshold, natural convection occurs when the buoyancy force overcomes the shear and tensile forces in the fluid,[122,118] which may reduce insulation value. Critical air gap thickness in the range of from 7 mm to 14 mm[119, 120, 123-125] was reported. The onset of natural convection is controlled by a critical Rayleigh number, and for the case of a horizontal rectangular enclosure, critical Raleigh number = 1708[121]. Similarly, air gaps can increase the evaporative resistance in clothing systems when the air gap is small[126]. When the air gap exceeds a certain value, vapor resistance may decrease with increases in the air gap due to the presence of natural convection[126]. In the absence of natural convection, the mass flux in the microclimate layer can be expressed using Fick's law[121]. In the presence of natural convection, the water vapor transfer mode changes from molecular diffusion to convective mass transfer, thereby enhancing the moisture transfer abilities[120].

The influence of air gaps on the total evaporative resistance of clothing systems has been well studied[120, 121, 125, 149]. He et al. investigated the effect of air gap on evaporative resistance of firefighter clothing under a range of ambient temperature and humidity using a sweating guarded hotplate, and found an overall increase in evaporative resistance with increasing air gap size. However, the evaporative resistance decreased when the air gap size reached up to 12 mm and increased again thereafter, due to the occurrence of natural convection in the multilayer fabric system[155].

There are different kinds of moisture barriers, and our previous study revealed a strong dependence of evaporative resistance of bicomponent moisture barriers on the ambient conditions. It is possible that the presence of an air gap could affect the evaporative resistance of bicomponent moisture barriers. Nevertheless, to the best of our knowledge, the influence of air gap on evaporative resistance of firefighter composites composed of different moisture barriers in cool and hot conditions has never been studied systematically.

The aim of the study was to investigate the effect of the air gap size on wet heat loss through firefighter composites with different moisture barriers under various environmental conditions. Three firefighter composites with different moisture barriers were selected. Heat loss through the fabric systems was studied in the ambient environments of 25 °C to 45 °C using a sweating guarded hotplate, with air gap size from 0 mm to 25 mm.

5.2 Methodology

5.2.1 Materials

Three kinds of turnout composites consisted of the same outer shell (40% polybenzimidazole, 60% para-aramid, plain weave) and thermal liner (two layers of meta-aramid spunlace nonwoven quilted to a twill woven facecloth consisting of para-aramid filament yarn and meta-aramid /FR cellulose spun yarn), but different moisture barriers were evaluated. Moisture barrier A was a specially designed bicomponent membrane, composed of a microporous e-PTFE (expanded polytetrafluoroethylene) membrane coated with a proprietary hydrophilic nonporous layer. This membrane is not a commercial product, but it is assumed that it could pass all the other NFPA 1971 requirements. Moisture barrier B is a commercially available bicomponent moisture barrier with a similar structure to A. Moisture barrier MM (abbreviation for microporous membrane) used a microporous e-PTFE membrane without any coating applied to the surface. Although it would pass the *THL* (Total Heat Loss) requirement, it would not pass other requirements such as viral penetration test within the NFPA 1971 standard. All membranes were attached to the same fire-resistant base woven fabric. More information about the moisture barriers is listed in Table 5-1.

Table 5-1. Physical properties of moisture barriers

Moisture barrier	Composition	Weight (g/m^2)	Thickness (mm)
A	Bicomponent e-PTFE, bonded to woven fabric made with meta-aramid spun yarn	226±3.3	0.45±0.01
B	Bicomponent e-PTFE, bonded to woven fabric made with meta-aramid spun yarn	163±1.4	0.36±0
MM (Microporous membrane)	e-PTFE, bonded to woven fabric made with meta-aramid spun yarn	141±0.5	0.36±0

5.2.2 Experimental design

All samples were preconditioned in 21 °C, 65% relative humidity (RH) for at least 12 hours before the test. Heat exchange between hotplate surface and environments through firefighter composites was characterized using a dynamic hotplate (Thermetrics, Seattle, WA), as shown in Figure 5-1. The main features of the dynamic hotplate include a surface heat flux sensor, and an internal cooling system. A detailed description of the dynamic hotplate system can be found in our previous publication[156]. Tests were conducted at 25 °C, 65% RH; 35 °C, 36.6% RH; and 45 °C, 21.5% RH, where the different relative humidity was chosen to ensure a constant vapor pressure difference between hotplate surface and ambient air (3.57 kPa). During all tests, the plate surface was maintained at 35 °C to simulate human skin temperature. Heat loss was measured by the embedded heat flux sensor in place of power demand. Air gap spacer made of polylactic acid (Figure 5-1a) was used to create air gaps of 5 mm, 10 mm and 25 mm between hotplate surface and firefighter composite. The thickness of the air spacer frame is 2 cm and this can limit the heat transfer through the air spacer horizontally.

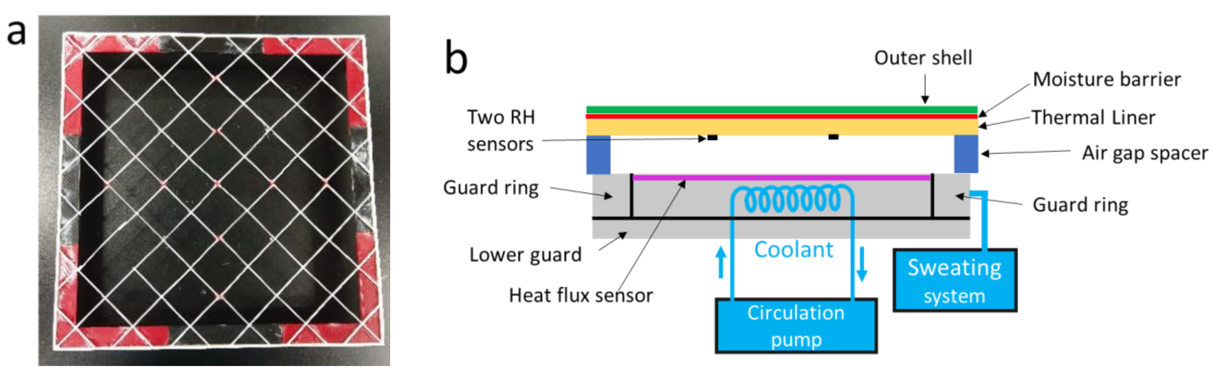

Figure 5-1. (a) Picture of air layer spacer and (b) schematic of test apparatus

Dry tests were conducted to find insulation values at 25 °C and 45 °C. All composites were tested 3 times with no air gap. When adding an air gap of 5, 15, and 25 mm, only composite

A was tested. The insulation value of air gaps was estimated by subtracting the insulation values of firefighter composites from the total insulation. For wet tests, a microporous membrane was covered on water saturated hotplate surface. All samples were tested 3 times at 25, 35, and 45 °C, with air gap of 0mm, 5 mm, 15 mm, and 25 mm. The duration of all wet tests was controlled to 1h. Heat loss measured from the heat flux sensor was average over the last 30 mins. Following the wet tests, the individual layer in composites was weighed using a digital scale (PB 303-S, Mettler Toledo, USA) immediately. To prevent moisture loss, samples were sealed in a plastic bag before weighing. During the wet tests with air gaps, the temperature and relative humidity close to the face cloth of thermal liner were monitored with two relative humidity sensors (±2 % RH, MSR Electronics GmbH, Swiss). Sensors were attached to face cloth of thermal liner using porous tape, as shown in Figure 5-1b. Both temperature and RH data were stored in a data logger (MSR 145, MSR Electronics GmbH, Swiss), and average reading during steady state was used.

5.2.3 Calculations

Heat loss from the hot plate to environment was measured with the heat flux sensor. During dry tests, measured heat loss can be used to calculate the total insulation value, including air gap, firefighter composite, and outer shell surface air layer.

Intrinsic thermal resistance R_{cf} (K·m^2/W), intrinsic apparent evaporative resistance R_{ef}^{A} (kPa·m^2/W), and intrinsic evaporative resistance (R_{ef}) were calculated by equations 2.6-2.9, and 2.12[75].

During evaporative resistance tests, the heat loss measured from the heat flux sensor includes two parts - wet heat loss and dry heat loss[75]:

Dry heat loss H_{dry} (W/m^2):

$$H_{\mathrm{dry}} = \frac{\Delta T}{R_{\mathrm{cf}}+0.04} \tag{5.1}$$

Wet heat loss H_{eva} (W/m^2):

$$H_{\text{eva}} = \frac{\Delta P}{R_{\text{ef}}^{\text{A}} + 0.0035} \tag{5.2}$$

The values of 0.04 (K·m^2/W) and 0.0035 (kPa·m^2/W) are the standard bare plate values for dry and wet tests at a wind speed of 2 m/s, respectively[76].

5.2.4 Statistical analysis

The average and the standard deviation of heat flux, temperature, and relative humidity data, etc. of three repetitions were calculated. The results were analyzed through one-way ANOVA (analysis of variance), followed by Tukey's HSD test (honestly significant difference) using JMP Pro V.14 (SAS Institute Inc., Cary, NC, USA). The significance level p was set as 0.05.

5.3 Results

Table 5-2. Properties of fabric ensembles

Ensemble	Weight (g/m^2)	Thickness (mm)	*THL* (W/m^2)
A	736±2.5	2.24±0.02	213±8.5
B	674±1.9	2.15±0.07	239±0.9
MM	652±2.1	2.15±0.06	256±7.8

Note: *THL* (total heat loss) was tested according to ASTM F1868, part C[75]

The results of the material tests with a sweating guarded hot plate are listed in Table 5-2. All the composites passed the NFPA 1971 requirement on the minimum *THL* (205 W/m^2). The study focused on the influence of air gaps and ambient conditions on heat transfer through three firefighter composites with different moisture barriers in both dry and wet tests.

5.3.1 Dry tests

Sample A was used to study the influence of air gap on insulation, and heat loss from hotplate during the dry tests was measured. The results are shown in Figure 5-2a. Heat loss measured from hotplate at 25 °C decreased gradually from 70 W/m^2 to 36 W/m^2 with air gap until 15 mm and then increased slightly to 38 W/m^2 (p<0.05). At 45 °C, a negative heat flux was observed due to the negative temperature difference, representing net heat gain from the environment. Measured heat flux increased gradually from -71.2 to -38.8 W/m^2 as air gap increased (p<0.05). The insulation value of air gap and firefighter composite are shown in Figure 5-2b. At 25 °C, the total insulation value increased with the air gap, and then decreased (p<0.05). At 45 °C, insulation value showed an increasing trend with the air gap (p<0.05). Since the firefighter composite insulation was constant, the change in total insulation was due to air gap size.

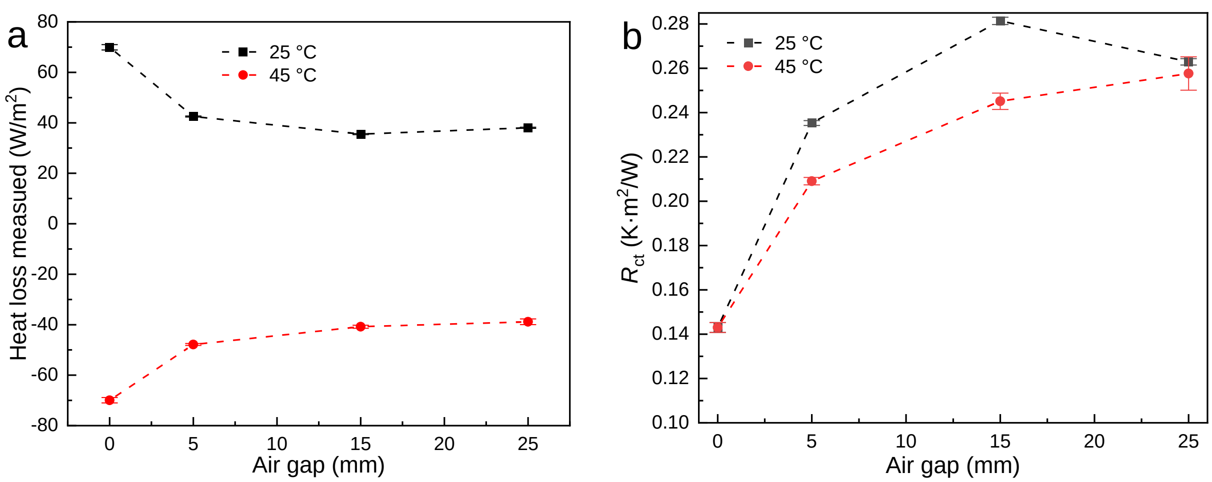

Figure 5-2. (a) Heat loss measured during dry tests under 25 °C and 45 °C; (b) calculated total insulation value including air gap and firefighter composite

5.3.2 Wet tests

Figure 5-3 presented the heat loss measured at 25 °C, 35 °C, and 45 °C during wet tests. As shown in Figure 5-3a,b, heat loss measured was attenuated by air gap during the wet tests at 25 °C and 35 °C for all composites. Different trends were observed at 45 °C (Figure 5-3c), where composite A and B was able to release 112 W/m^2 and 30 W/m^2 respectively, while composite A showed a net heat gain of 36 W/m^2 at 0 mm air gap. The existence of an air gap decreased heat loss for composites MM and B, while the air gap played a positive role for composite A as it can help mitigate the heat gain. When the air gap increased to 25 mm, heat release through composites MM and B decreased to 21 and 5 W/m^2, respectively, whereas heat gain for composite A decreased from 36 to 17 W/m^2. Note that the difference in heat transfer with air gap narrowed at 35 °C and 45 °C. For example, at 35 °C, composite MM released 116 W/m^2 more heat than composite A under 0 mm air gap, while the difference decreased to 43 W/m^2 at an air gap of 25 mm.

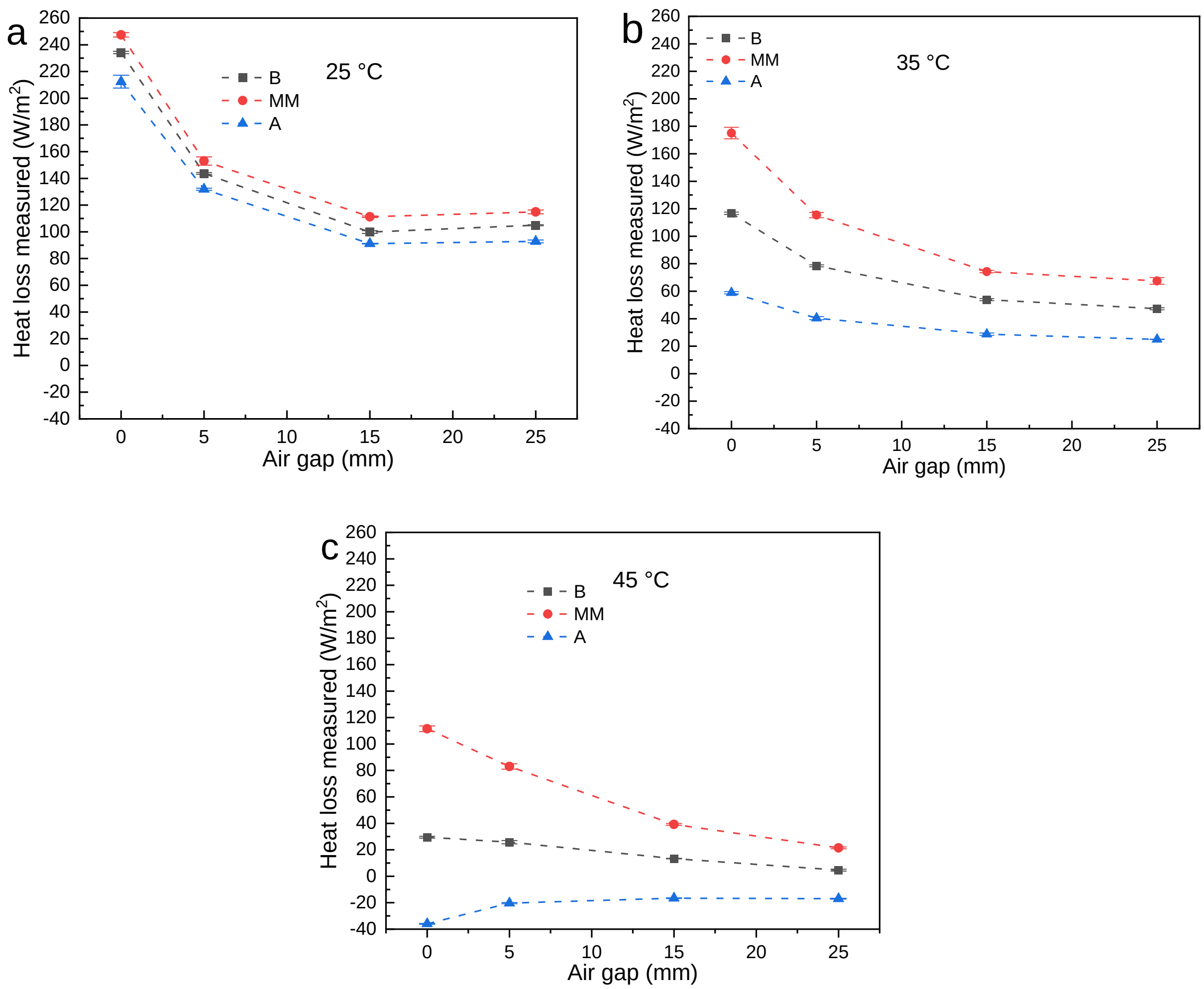

Figure 5-3. Heat loss measured at (a) 25 °C, (b) 35 °C, and (c) 45 °C during wet tests at constant vapor difference of 3.57 kPa

The weight of each layer in firefighter composites after the one-hour wet tests was compared to the samples preconditioned at 21 °C, 65% RH, and the results are illustrated in Figure 5-4a-c. The largest weight gain was observed at 25 °C compared to other conditions. At 25 °C, water uptake decreased dramatically when air gap size increased from 0 mm to 5 mm. The water uptake decreased with air gap until 15 mm and then reached a steady state (p<0.05). While at 35 °C and 45 °C, a constant decrease in water uptake was observed. The moisture content inside the moisture barrier was displayed separately in Figure 5-4d-f. With the presence of a 5 mm air gap, a large weight loss was observed in all conditions. At 25 °C, the percentage of water uptake of all moisture barriers kept decreasing to an air gap of 15 mm and then reached stable state (p<0.05). At 35 °C, water uptake declined gradually with air gap size (p<0.05). At 45 °C, water uptake decreased dramatically from 0 mm to 5 mm and then at a much slower rate. For moisture barrier B, its water uptake decreased from -1.22% to -1.38 % when the air gap size enlarged from 15 mm to 25 mm (p<0.05). While, for composites A and MM, the water uptake reached a steady state after 15 mm air gap (p<0.05).

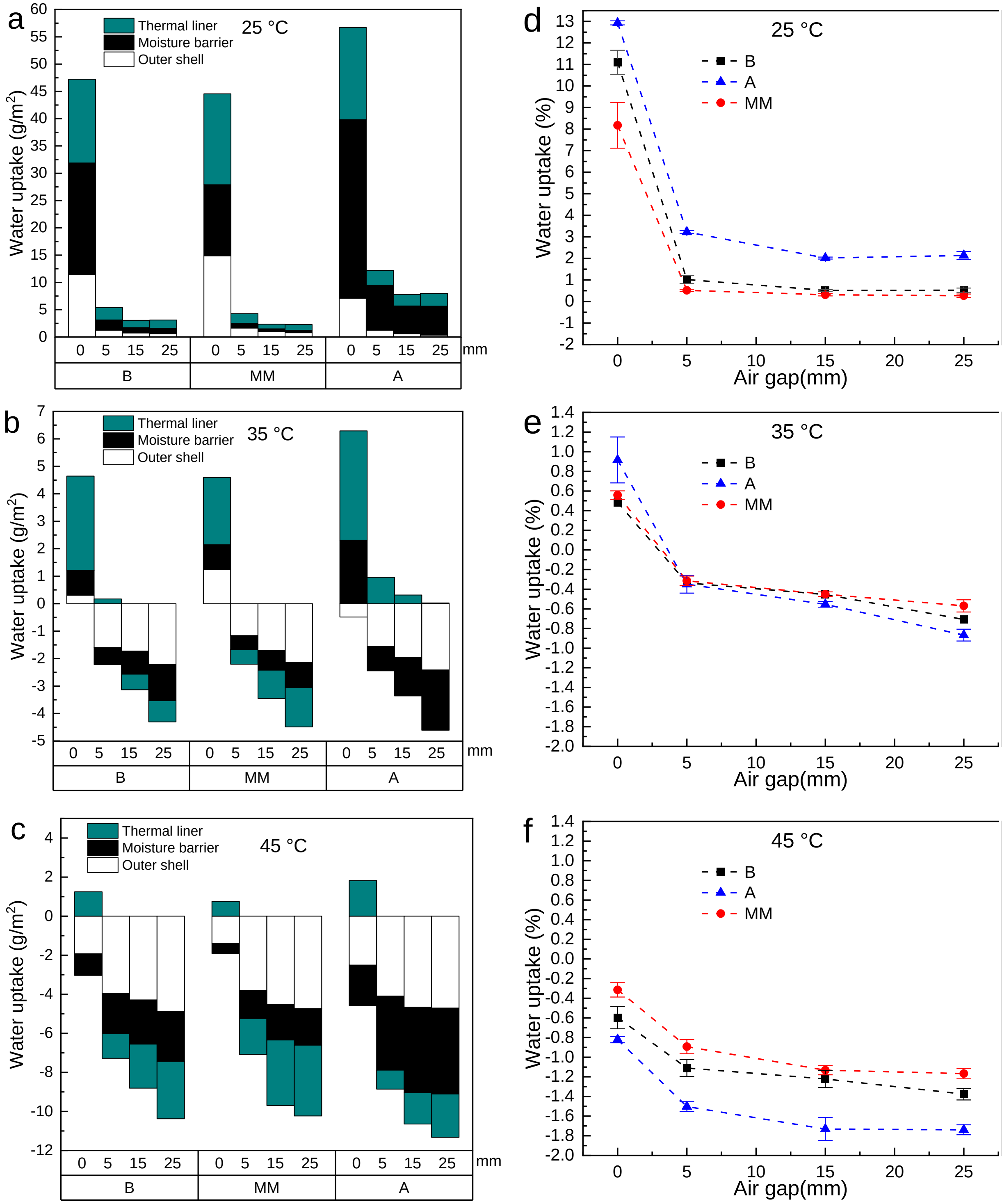

Figure 5-4. Water uptake of individual layers after wet tests conducted at (a) 25 °C, (b) 35 °C, and (c) 45 °C; percentage of water uptake in moisture barrier after wet tests conducted at (d) 25 °C, (e) 35 °C, and (f) 45 °C

During the wet tests, humidity sensors were employed to measure the relative humidity close to the face cloth of the thermal liner. In addition to RH data, the sensors could also measure temperature. The temperature and RH data are shown in Figure 5-5. At 25 °C, temperature on the face cloth of thermal liner for all composites decreased with air gap, and became relatively steady after 15 mm, while at 45 °C, the temperature increased with the air gap size. The relative humidity for composite A is the highest and composite MM is the lowest for most tests (Figure 5-5d-f). At 25 °C, the difference between all the composites is smaller than at 35 °C and 45 °C. For example, with an air gap of 25 mm, the difference between composite A and MM is 18.7, 90.1, and 102.4 Pa·m^2/W at 25 °C, 35 °C and 45 °C, respectively. Vapor pressure on the face cloth was estimated with temperature and relative humidity, and the results are shown in Figure 5-5g-i. It was interesting that the vapor pressure at 25 °C dropped with air gap and then became steady. In other conditions, the vapor pressure dropped with the air gap size. Among all the tests, composite A showed the highest vapor pressure while MM showed the lowest vapor pressure.

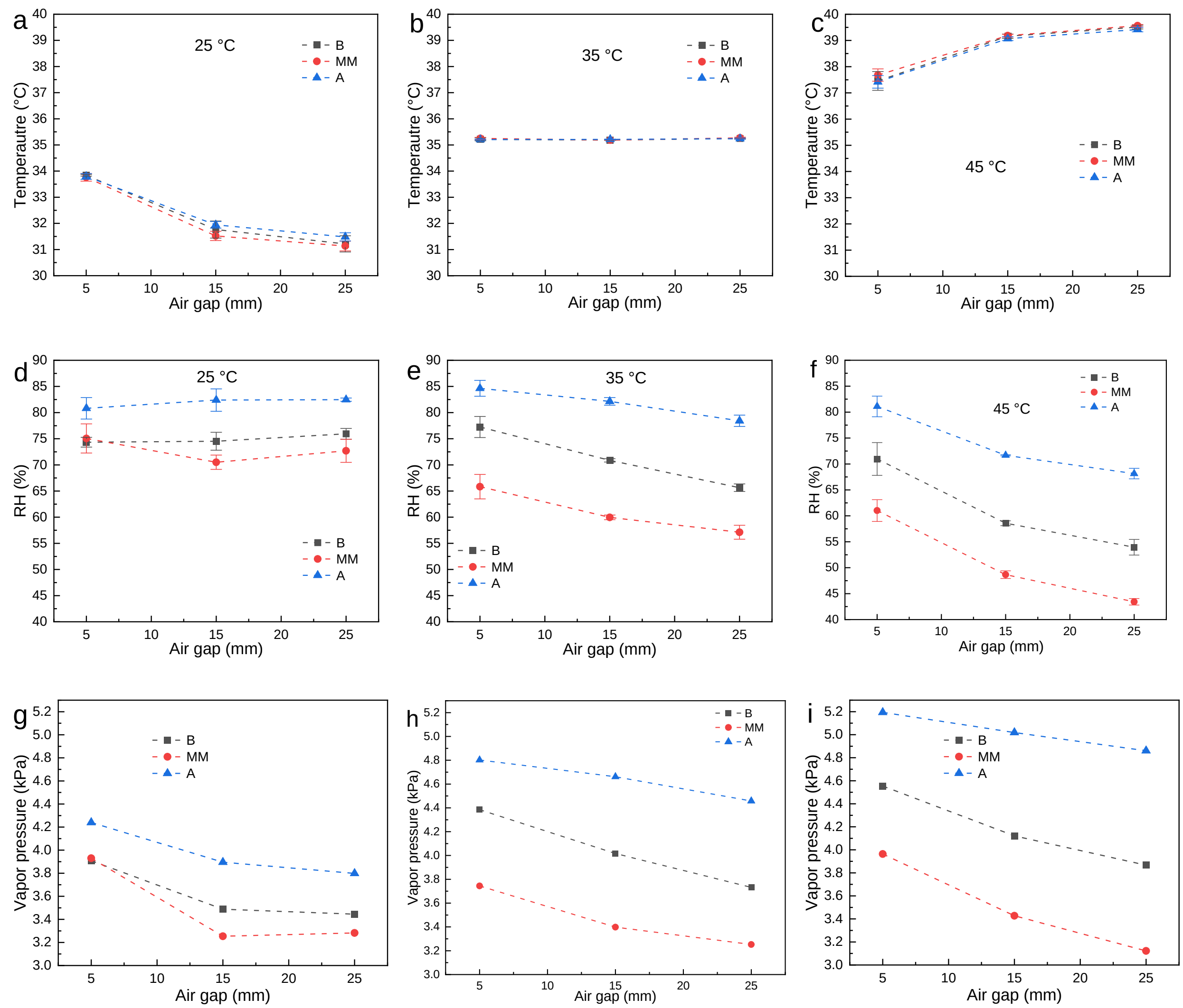

Figure 5-5. Temperature, humidity and vapor pressure on the face cloth of thermal liner at 25 °C (a,d,g), 35 °C (b, e, h), and 45 °C (c,f,i) during wet tests

The total evaporative resistance of air gap plus fabric composite are displayed in Figure 5-6. It was shown that at 25 °C, the evaporative resistance of all composites increased first with the air gap. For composite A and MM, the evaporative resistance reached a steady state after 15 mm, while B showed a slight decrease of 2.2 Pa·m^2/W when the air gap enlarged from 15 mm to 25 mm (p<0.05). At 35 and 45 °C, the evaporative resistance showed a consistent increasing trend with the air gap (p<0.05). We found that the evaporative resistance of composite MM is relatively constant[156] and the evaporative resistance of the air gap can be estimated by subtracting the evaporative resistance of composite MM from the total evaporative resistance value. The results are displayed in Figure 5-6. The evaporative resistance of the air gap increased from 5 mm to 10 mm for all conditions ($p<0.05$). At 25 °C, evaporative resistance of the air gap became steady after reaching 15 mm while for 35 and 45 °C, evaporative resistance increased with the air gap.

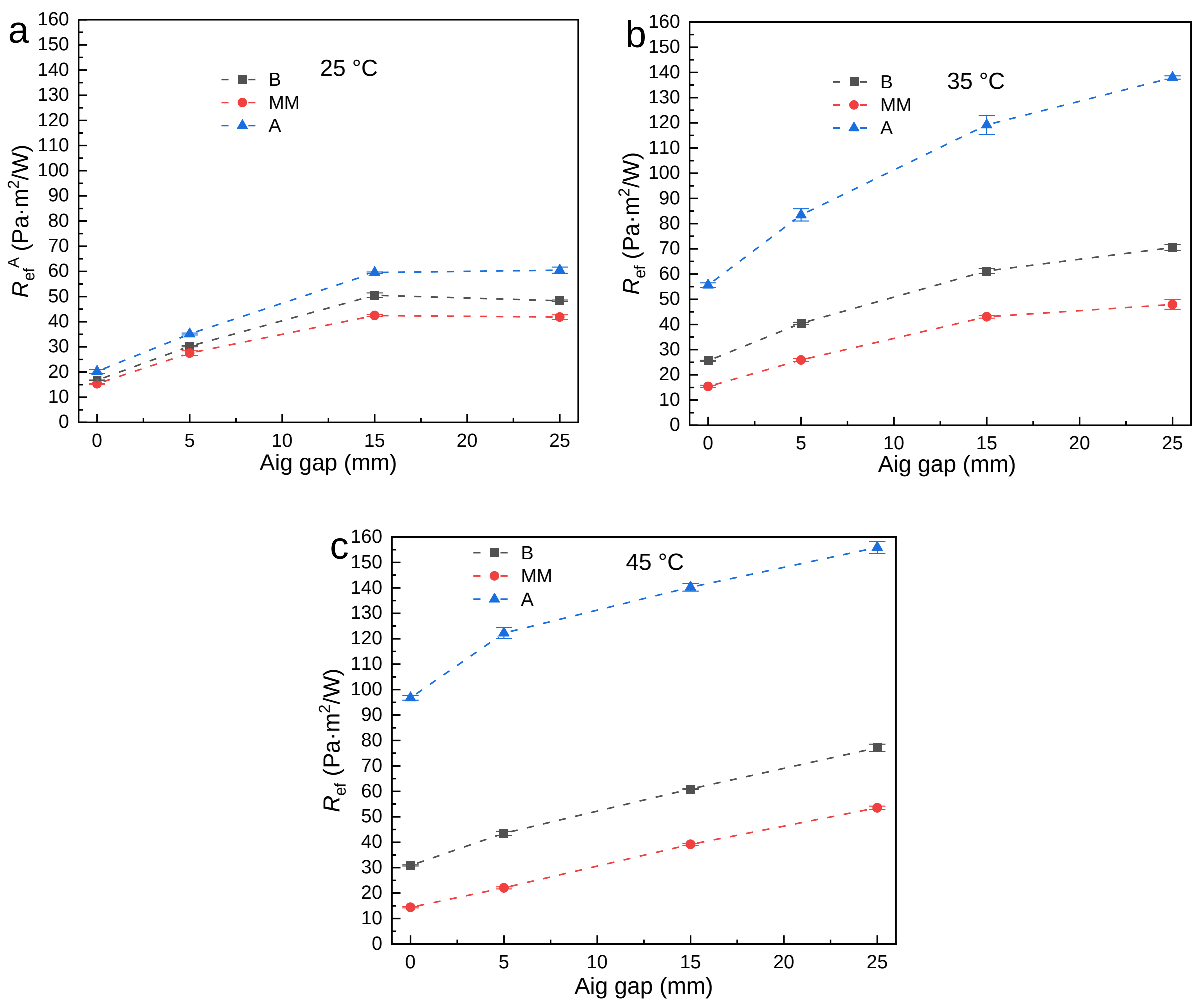

Figure 5-6. Total evaporative resistance of the air gap and firefighter composite under (a) 25 °C, (b) 35 °C, and (c) 45 °C

With the evaporative resistance of air gap shown in Figure 5-7, the evaporative resistance of firefighter composites A and B without air gap at 25, 35, and 45 °C can be separated from the total evaporative resistance. The results are shown in Figure 5-8. At 25 °C, evaporative resistance of composites A and B increased first with the air gap, and then became steady. For example, at 0 mm air gap, evaporative resistance of A and B increased by 5 and 10 Pa·m^2/W respectively when reaching an air gap of 15 mm, and then became relatively consistent. Under 35 °C, composites A and B kept increasing, but composite A increased at a faster rate. At 45 °C, composites A and B started with a higher evaporative resistance than other conditions, increased gradually with air gap and then reached a steady state after 5 mm.

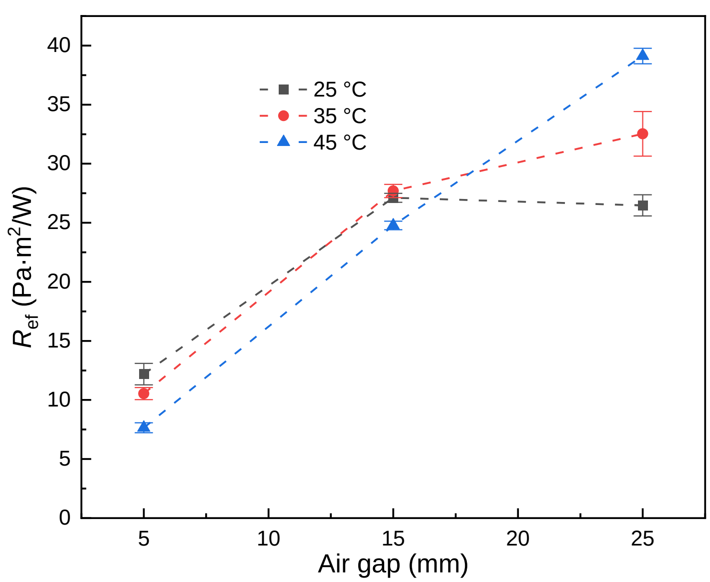

Figure 5-7. Evaporative resistance of the air gap under 25 °C, 35 °C, and 45 °C.

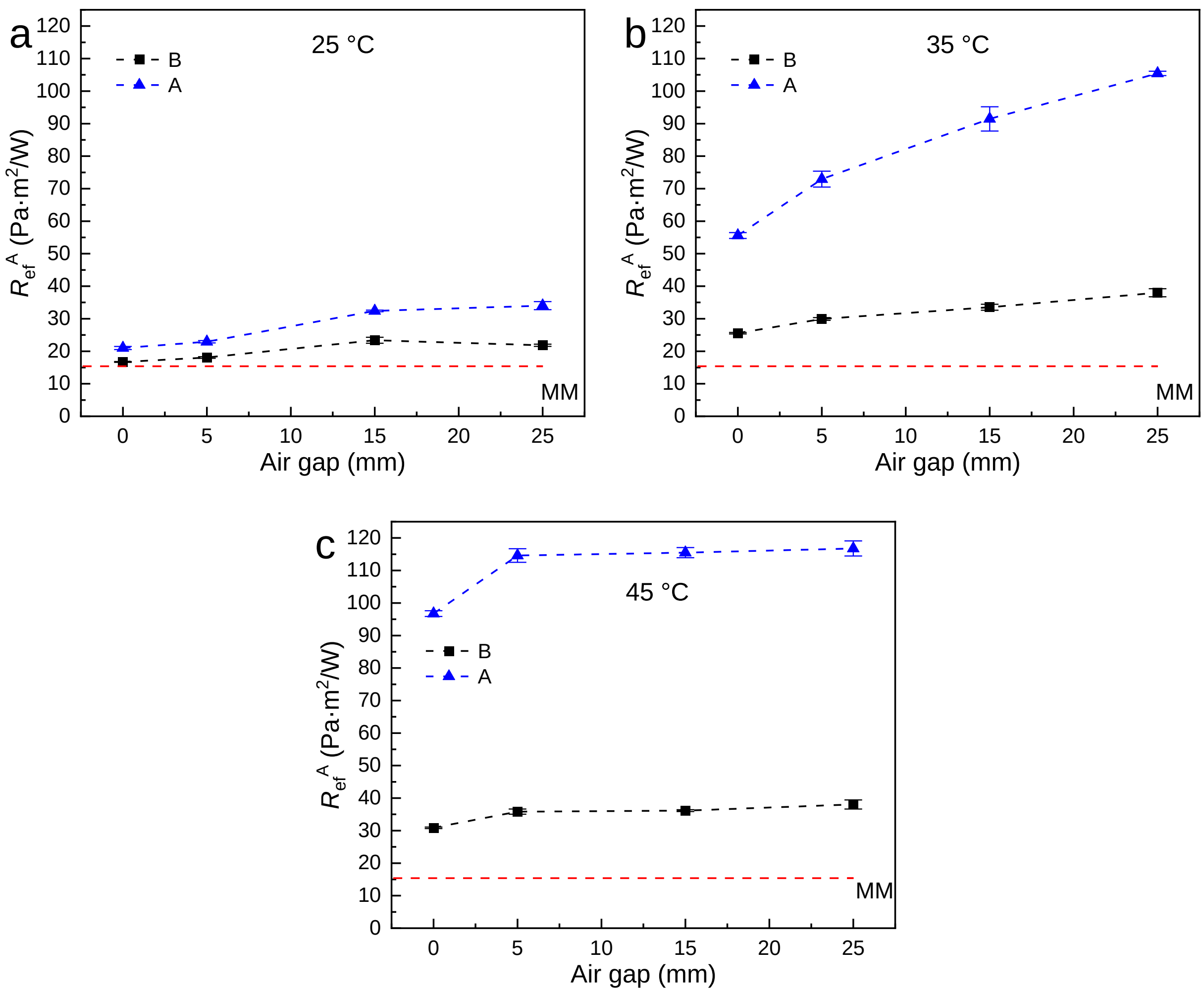

Figure 5-8. Evaporative resistance of firefighter composite as a function of air gap size at (a) 25 °C, (b) 35 °C, and (c) 45 °C

Dry heat loss and wet heat loss of all samples at different temperatures with the same vapor pressure difference are presented in Figure 5-9. At 0 mm air gap, with the increase of temperature, the amount of wet heat loss was consistent for composite MM, but decreased for composite A, and B. This was due to the dependence of evaporative resistance of composites A and B on environmental conditions, as reflected in Figure 5-8. For example, composite A was able to release about 150 W/m^2 at 25 °C through evaporation, but only 36 W/m^2 at 45 °C. The effect of air gap on heat loss depends on ambient conditions. At the ambient temperature of 25 °C, both the evaporative heat loss and dry heat loss decrease with the air gap until 15 mm. At 35 and 45 °C, evaporative heat loss demonstrated a negative relationship with air gap. At 45 °C, dry heat gain was observed due to the negative temperature difference between the ambient air and hotplate. The presence of an air gap decreased dry heat gain.

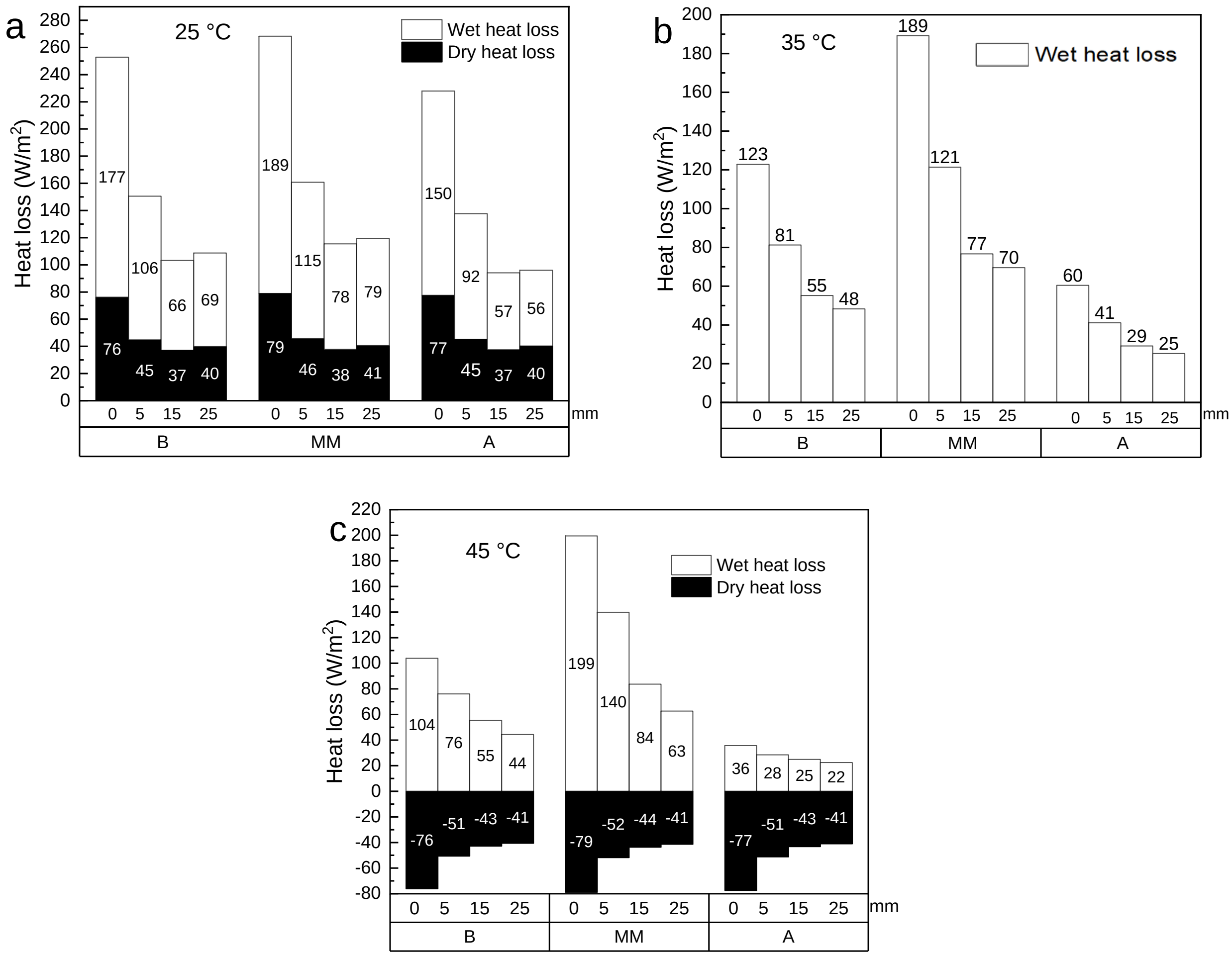

Figure 5-9. Dry and wet heat loss at (a) 25 °C, (b) 35 °C and (c) 45 °C at a constant vapor pressure difference of 3.57 kPa

5.4 Discussions

This study investigated of the effect of air gap size on heat transfer through firefighter clothing. At 25 °C, insulation of the air gap increased until 15 mm and then decreased. It was reported that the critical thickness for natural convection is 15 mm for a horizontally oriented air gap,[125] which is consistent with our study. Natural convection underneath the fabric was caused by the rise of warmer air (lighter due to lower density) to the top of air gap and sinking down of the cooler air (heavier due to higher density)[123]. A certain thickness threshold must be met before natural convection can occur because at a small air gap, the buoyancy force could not overcome the shear and tensile forces in the air gap[118, 122]. At 25 °C, the air close to the hotplate (35 °C) is lighter than the air near the facecloth of thermal liner, and this will induce natural convection, which may decrease thermal insulation. At 45 °C, an increasing trend of insulation was observed. This was due to the air near fabric being hotter and air near hotplate being colder, which prevented natural convection. For the same reason, during wet tests, as shown in Figure 5-7, the evaporative resistance of air gap increased consistently at 45 °C. At 35 °C, the increasing trend in evaporative resistance with air gap was observed, and this was because the absence of temperature difference between the hotplate and the inner surface of firefighter composite prevented the occurrence of natural convection. At 25 °C, due to the presence of natural convection, the evaporative resistance of the air gap increased up to 15 mm, and then became constant. This trend matched the vapor pressure profiles near the facecloth of the thermal liner, as shown in Figure 5-5.

This weight gain at 25 °C observed in Figure 5-4a was due to condensation of the moisture within the composite. Condensation occurs when water vapor pressure reaches the saturation point in the fabric due to lower local temperature[101, 150]. The amount of moisture uptake measured decreased with temperature, as was also observed by Rossi[151]. In addition to environmental factors, condensation was also affected by clothing properties[106, 157]. Moisture accumulation inside composite A was the highest, due to its high evaporative resistance (Figure 5-8). The amount of condensation decreased dramatically at 25 °C with the presence of an air gap. For example, at 25 °C a weight gain of 5.3 g was decreased to 1.1g with the presence of a 5 mm air gap. This may be due to the sharp decrease in vapor pressure and temperature difference when the air gap was created. With the 5 mm air gap, the vapor pressure beneath the firefighter composite decreased dramatically from 5.6 kPa (saturated vapor pressure at 35 °C on hotplate surface) to 4.2 kPa (Figure 5-5h) for composite A. A decrease of 1.9 °C in the temperature near thermal liner was also observed. Condensation was affected by the vapor pressure and temperature difference across the fabric[157]. With air gap, the dramatic decrease in both vapor pressure and temperature beneath the firefighter composite decreased the vapor pressure and temperature difference across the firefighter composite, which was responsible for the decrease in condensation. Condensation inside all composites at 15 mm reached steady state because of the occurrence of natural convection. At 35 °C, a constant reduction in weight with air gap was observed because the further away the composite is from the hotplate, the less humid the environment is, as shown in Figure 5-5e. At 45 °C, the decrease in water content was due to the increase in temperature and decrease in relative humidity with air gap. Water absorption is an exothermic reaction, and water uptake decreased as temperature increased. Weight loss was observed at 35 °C and 45 °C.

The most important finding in this paper is that the ambient conditions and air gap affected the moisture content inside bicomponent moisture barriers, and this further impacted the evaporative resistance. Bicomponent moisture barriers featured a non-porous hydrophilic coating on top of a microporous membrane. Moisture absorbed by the hydrophilic polymer can facilitate the transmission of water vapor by swelling the membrane (providing more free volume between polymer chains), and providing more hydrophilic sites[64]. When looking at Figure 5-4d-f and Figure 5-8a-c, for composites with bicomponent moisture barrier, their evaporative resistance increased with the decrease in moisture content. At 25 °C, the moisture content inside moisture barriers A and B decreased until 15 mm, corresponding to a gradual increase in evaporative resistance with the air gap. After 25 mm, the moisture content inside moisture barriers reached a steady state at 25 °C due to the occurrence of natural convection. The evaporative resistance was unchanged. At 35 °C, a consistent increase in evaporative resistance for composites A and B was observed as a result of the decline in moisture content with the air gap. At 45 °C, the evaporative resistance reached steady state at an air gap of 5 mm. This is because the moisture content loss at the moisture barrier has already reached its maximum value and will not change significantly with ambient temperature or air gap. For composites with microporous moisture barrier, its evaporative resistance is relatively consistent.

When the moisture content inside moisture barrier was plotted with the evaporative resistance of firefighter composites (Figure 5-10), it clearly demonstrated that the evaporation resistance of composites A and B dramatically changed when moisture barriers had less water inside and then reached a steady state. This implied that moisture barriers in composites A and B required a certain amount of moisture uptake to achieve their minimum evaporative resistance. For composite MM, its evaporative resistance is relatively independent of the moisture content inside the moisture barrier.

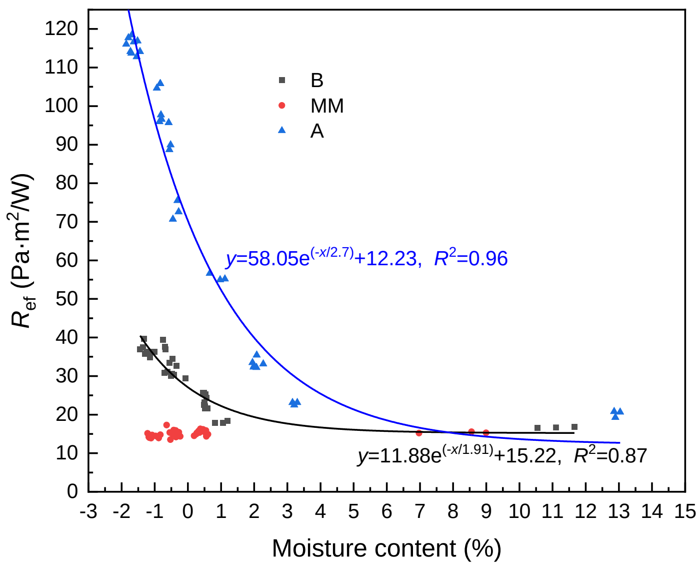

Figure 5-10. The relationship between evaporative resistances with water uptake inside moisture barriers

5.5 Conclusions

The evaluation of the heat loss through composites consisting of varied moisture barriers was performed using a dynamic hotplate for various air gap sizes and ambient conditions. Our results demonstrated that the existence of an air gap could add extra thermal and evaporative resistance and limit heat transfer. Moreover, a major finding in our research is that the presence of an air gap could change the water content inside moisture barriers, and this will affect the evaporative resistance of bicomponent moisture barrier dramatically. The findings from this study could be used to model heat transfer through firefighter clothing.

The following limitations should be considered: The air layer we studied is horizontal, while in most scenarios, air gap orientation is vertical. This may result in different moisture and heat transfer through air gap, but it will not change the fundamental findings from this study that air gap sizes affected the moisture content inside bicomponent moisture barriers, leading to increased evaporative resistance. It is important to study the effect of air gap orientations on evaporative heat loss. Another limitation is that we only considered air gaps in a still state. Forced convection could be created by human body movement (pumping effect)[41, 44-46, 127-130], incoming wind[44, 45, 128-130], or incorporating fans[131-133], which will influence moisture and heat transfer within air gaps. This will be addressed in our future research.

6 Effects of Outer Shell Fabric Color and Smoke Contamination on Heat Loss through Turnout Suit Systems

6.1 Introduction

The contribution of turnout clothing to firefighter heat strain is determined by many factors, including the breathability of the materials used in the construction, as well as the design and fit of the clothing itself[158, 159]. One of the least understood aspects of turnout suit design is the effect of the color of the outer shell fabric layer on heat strain-relieving heat loss through the turnout suits in solar exposure. Although studies have investigated the effects of solar radiation on heat transfer through protective clothing,[71, 114, 115] important questions remain about the influence of color and texture of outer shell fabrics on heat transfer through turnout systems in solar exposure. Additionally, researchers have used new fabric samples when studying solar effects on heat loss through turnout systems. This is significant because dirt, grime, and smoke contaminate firefighter PPE. Even when washed, turnout suits are rarely truly clean [160]. This means that the emissivity of the outer shell materials can change in use, potentially affecting the way the turnout system absorbs incident solar radiation. Significantly, no published studies exist on the effects of dirt and contaminants on turnouts on heat transfer through turnout fabric systems in solar exposure. Neither have the effects of the moisture barrier component on heat transfer through turnouts exposed to solar energy been explored.

Systematic research on the effects of solar radiation on heat loss through protective clothing has been limited to relatively few studies. A series of studies conducted by the European Union Project ThermProtect[71, 114] used low ambient air temperatures, high wind speed or low-intensity radiant load, testing conditions that would not produce heat stress in firefighters. To

---

Gao H, Deaton AS, Fang X, Barker R, DenHartog E, Watson K. Textile Research Journal 2021. (Submitted)

prevent hotplate overheating in solar-simulating radiant heat experiments, Fukazawa et al.[115] used very high clothing insulation that included five layers of underwear fabric in addition to an 8 mm air gap put under the protective clothing. None of these solar exposures or testing configurations realistically simulates exposure conditions encountered by firefighters. Shimazaki[161] investigated the temperature distribution of a single-layer fabric system exposed to different levels of solar radiation. Quintiere[52] and Collin et al.[19] used a spectrometer to measure the reflectivity of firefighter clothing fabrics in the range of visible and longwave radiation using a spectrometer. They found that fabric color has a strong effect on the solar heating load, although it has little effect in the range of flame radiation.

Other researchers have studied the comfort properties of firefighter clothing exposed to radiant heat from flames[53, 162-165]. Lei et al. used a sweating manikin to show that higher clothing insulation reduces the rate of core temperature rise in 3 kW/m^2 radiant heat exposure[162]. Bröde found that heat gain from long wave thermal radiation is relatively independent of fabric materials and color, except for fabrics with aluminized surfaces[53]. In regard to these findings, it is important to know that firefighters spend only 1 to 10% of their time actually fighting fires[166]. They spend much more of their time exposed to radiant heat from the sun[1].

The goal of this study was to explore the heat loss through firefighter materials under solar radiation. Effects of fabric color, and texture, as well as contamination and washing were studied. In addition, three different moisture barriers were selected, and their capability to release evaporative heat under simulated solar radiation was compared.

6.2 Experimental methods

A novel experimental setup was used to measure heat transfer through turnout suit composites exposed to incident radiant energy simulating sunlight (Figure 6-1). The sweating plate consists of a 20.3 cm × 20.3 cm heated test plate surrounded by a 5.1 cm guard ring to prevent lateral heat loss. Unlike a conventional sweating guarded hotplate, the system (DHS–8.2, Thermetrics, Seattle, Washington) uses a heat flux sensor embedded in the surface of the test plate to measure heat exchange from the plate and through the test material sample placed on the plate surface. Positive heat flux readings from the embedded thermal sensor indicate heat loss from plate to environment; negative values indicate net heat gain to the plate. The sweating plate is cooled by a water circulation system located under the hotplate. This feature is critical to the system functionality, enabling heat transfer measurements in tests that apply a solar-simulating incident radiant heat load to the test fabric.

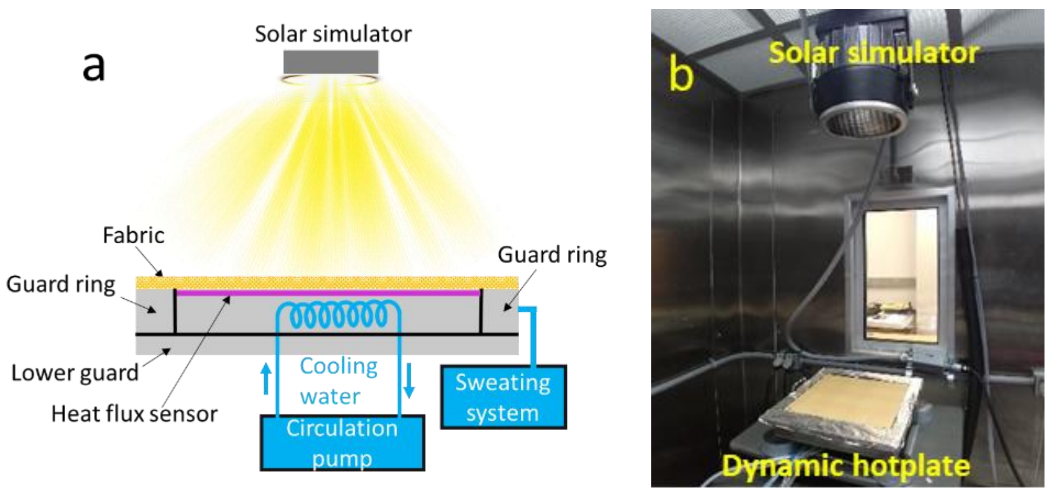

Figure 6-1. Novel sweating hot plate apparatus and solar simulator at climate chamber

The sweating hot plate simulates sweating by delivering volumetrically controlled water to 25 sweat ports distributed over the hotplate surface. The hotplate surface was maintained at 35 °C while measuring heat exchange between the plate surface and test sample. Heat exchange measurements were made in an insulation or dry plate condition and with the plate configured to simulate sweating and evaporative heat exchange. For evaporative resistance measurements in a wet condition, a liquid barrier consisting of fabric laminated with a water-resistant microporous e-PTFE (expanded polytetrafluoroethylene) membrane was placed on the sweating plate between the surface of the heated plate and test sample. Because it prevented liquid moisture transfer by wicking, the membrane ensured that only vapor phase evaporative heat transfer occurred from the sweating plate surface through the test sample. The plate surface was moisture saturated in evaporative resistance tests with incident radiation. The evaporative resistance tests proceeded for one hour to include a 30-minute period of thermal equilibrium. Heat loss measurements were averaged from readings taken after a condition of thermal equilibrium that occurred in the final 30 minutes of the test protocol.

A Thorn compact source sodium-iodide lamp (CSI, 1000 W) located above the hotplate simulated solar radiation incident on a turnout sample placed on the heated surface of the sweating guarded hotplate (Figure 6-1). The Thorn lamp produces radiant energy that simulates the solar spectrum[111, 167]. The incident radiant heat flux intensity was measured using a CMP 11, Kipp & Zonen Pyrometer. The testing system, including the Thorn solar simulator and sweating hot plate system, was housed in a climate chamber maintained at 25 °C, 65% RH with still air (< 0.4 m/s).

The intensity of the solar exposure was controlled by adjusting the distance between fabric surface and Thorn light source at 0.83, 1.07 and 1.88 meters. Radiation exposures of 216, 553, and 831 W/m^2 were achieved. The radiation levels represented the intensity of sunlight in different meteorological conditions of outside solar exposure.

Insulation tests (dry tests) and evaporative resistance tests (wet tests) were performed both with and without incident solar radiation. Heat gain from radiation was estimated by subtracting heat loss measured without incident radiation (HL_0, W/m^2) from that measured under radiation (HL_R, W/m^2), as:

$$\text{Heat gain} = HL_0 - HL_\mathrm{R} \tag{6.1}$$

The percentage of heat gain from radiation (%) was calculated as:

$$\%\ \text{Heat gain} = \frac{\text{Heat gain}}{\text{Radiation intensity}} \times 100\% \tag{6.2}$$

The intrinsic thermal resistance R_{cf} (K·m^2/W), intrinsic apparent evaporative resistance R_{ef}^{A} (Pa·m^2/W), and total heat loss (*THL*) through the test materials were calculated by equations 2.6-2.10.

After the wet test, each layer of the firefighter ensembles was weighed using a digital scale (Mettler PM460) immediately. The weight gain W (g) after wet test for each sample was calculated with:

$$W=W_2-W_1 \tag{6.3}$$

where W_1 (g) is the weight of preconditioned sample before wet test, and W_2 (g) is the sample weight after wet test.

6.3 Results and discussion

We used the experimental setup shown in Figure 6-1 to study the effects of outer shell fabric color, texture, and smoke contamination level on heat transfer through firefighter's composites with an applied solar load. Heat loss or heat gain measurements were made for turnout composite systems with shell fabric materials of different colors and conditions both with and without incident radiation. Radiation exposures, including 216, 553 and 831 W/m^2 simulated the intensity of sunlight typical of conditions from a cloudy day to a day with intense sunlight[168]. Presented results are the average reading of triplicate measurements for each test material and at each condition of radiant exposure.

6.3.1 Effects of outer shell fabric color and texture on heat loss with applied solar load

Layered fabric composites used as the primary construction material of firefighter turnout suits consist of an outer shell fabric combined with inner moisture barrier and thermal liner layers. We selected three different outer shell fabrics, layered in combination with the same inner moisture barrier and thermal liner components, to study the effects of outer shell fabric color and texture on turnout composite heat loss in solar exposure (Table 6-1). All the composites are NFPA 1971 compliant turnout systems incorporating state-of-the-art materials technologies.

Table 6-1. Physical properties of studied fabrics

	Fiber contents and structure	Weight (g/m^2)	Thickness (mm)
Outer shell GST	35% PBI (polybenzimidazole), 65% para-aramid, twill weave, golden color	239±0.6	0.40±0.01
Outer shell GSP	40% PBI, 60% para-aramid, plain weave, golden color	248±1.5	0.41±0.01
Outer shell BST	35% PBI, 65% para-aramid, twill weave, black color	242±0.7	0.41±0.01
Moisture barrier	Bicomponent e-PTFE membrane on woven meta-aramid fabric	163±1.4	0.36±0
Thermal liner	Two layers of meta-aramid and para-aramid spunlace nonwoven quilted to 60% meta-aramid filament / 40% spun yarn (meta-aramid, FR rayon) twill weave	272±2.2	1.39±0.04

GST: Golden Shell Twill; GSP: Golden Shell Plain; BST: Black Shell Twill.

To study the effects of outer shell color, we compared heat loss through sample GST, a turnout composite made with an undyed PBI/para-aramid golden brown-color twill weave fabric, with turnout composite sample BST that incorporated a shell fabric with the same fiber composition and twill weave construction, but dyed black by a solution dyeing process. To study the effects of outer fabric surface texture, we compared sample GST with sample GSP, a shell fabric with the same golden brown-colored PBI/para-aramid shell fabric, but made in a plain weave construction. We chose the smoother surface characteristic of twill weave construction in comparison to plain weave to create a difference in surface texture between the two shell fabrics used in composites GST and GSP. Twill weave fabrics are characteristically smoother than plain weave fabric because their weave design, or yarn-interlacing pattern, creates floats of yarn on the fabric surface, in comparison to the more frequent interlacing of warp and weft yarns in plain weave construction. The floats contribute to a smoother surface[169, 170]. In addition, the outer shell fabric in composite sample GST contained a higher percentage of smoother filament yarns, in comparison with a higher content of staple yarns used in the construction of sample GSP. The difference in the visual appearance of the outer shell fabric used in turnouts GST and GSP are evident in the photographs shown in Figure 6-2.

Figure 6-2. Photographs of outer shell fabrics with different color and surface texture

Figure 6-3 shows the total heat loss (*THL*) measured through turnout composites incorporating these three different outer shell fabrics when exposed to simulated solar radiation ranging in intensity up to 831 W/m^2. As points of reference, 216 W/m^2 is equivalent to solar intensity on a cloudy day; 831 W/m^2 is close to solar intensity on a sunny day[168].

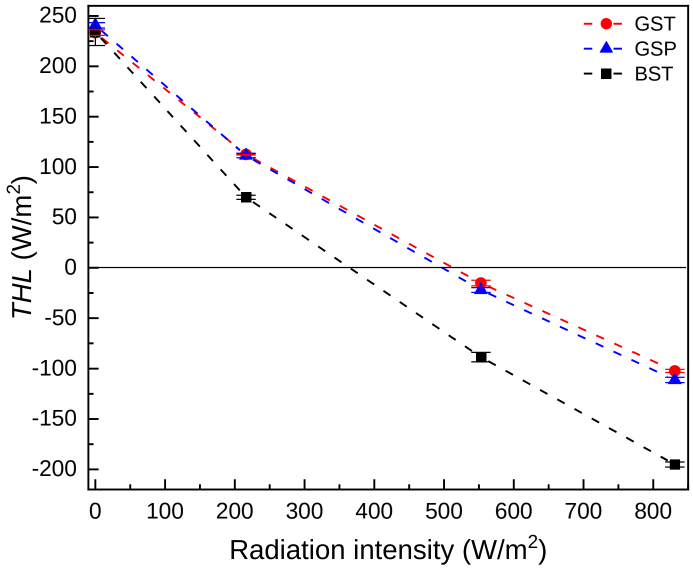

Figure 6-3. Effect of incident solar radiation on the *THL* of turnout composites made with outer shells having different colors and texture

These data indicate little difference in heat loss among the systems measured in the standard environmental testing conditions, without incident solar energy. However, they show that incident solar radiation had a profound effect on the heat loss of turnout systems. Heat transfer through all the turnouts dramatically decreased with applied solar heating, dropping from about 240 W/m^2 to less than 120 W/m^2 when the applied solar load is 216 W/m^2, or about the intensity of sunlight on a cloudy day. Most significantly, the color of the outer shell fabric had a major influence on the effect that solar radiation had on reducing turnout heat loss. Incident solar simulating exposure caused a much greater decrease in heat loss through the turnout composite sample that incorporated the black-dyed outer shell fabric (BST). Moreover, the magnitude of the difference related to shell fabric color increased with the intensity of the solar exposure. Figure 6-3 shows that measured total heat loss (*THL*) values fell below a positive level when the incident solar radiation reached 350-500 W/m^2. The specific intensity level at which the heat exchange transitions from heat loss to heat gain depended on the color of the outer shell layer used in the turnout composite construction. The turnout system with the black outer shell (BST) transitions from a net heat loss to heat gain when the solar exposure intensity was about 350 W/m^2, a lower intensity level than required to reverse the heat exchange for composites made with outer shell fabrics with a golden-brown hue (GST and GSP). In simulated intense sunlight (831 W/m^2), the turnout system with the black outer shell gained 93 W/m^2 more heat than a turnout with a golden-brown color. Unlike the differences observed with outer shell color, the texture of the shell materials caused by differences in fabric weave design and yarn type did not produce significant differences in the heat loss through the turnout composites in solar exposure.

The reflectivity of the outer shell fabric materials was measured in the spectral range between 0.25 and 3 μm using Jasco V670 with ILN-725 150 mm Integrating Sphere (0.25 to 2 μm), and Nicolet 6700 FTIR with Pike Technologies IntegratIR Diffuse Integrating Sphere (2 to 3 μm).

Spectrophotometric measurements revealed that measured heat gain associated with outer shell fabric color and texture are explained by measured differences in the reflectivity of turnout shell materials when exposed to radiant heat in wavelengths equivalent to sunlight (Figure 6-4).

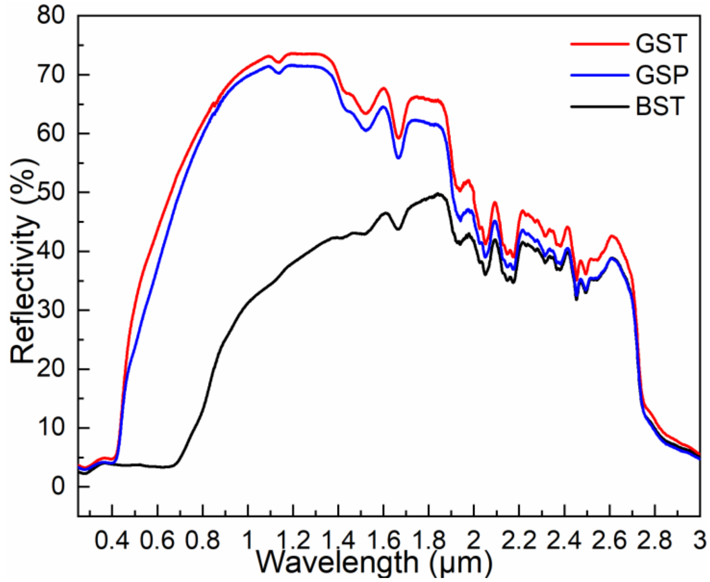

Figure 6-4. Effect of color and texture on the reflectivity of outer shell fabrics exposed to simulated solar radiation

A comparison of the reflectivity of the golden-brown outer shell (GST) with the black-dyed shell material (BST) shows that shell fabric color significantly affected solar reflectivity in wavelengths ranging from ~0.4 to 1.8 µm, or in the region of the spectrum where most solar radiant energy concentrates. On the other hand, shell fabric color had little effect on reflectivity in the ultraviolet (UV, 0.25-0.4µm) and medium infrared (MIR, 1.5-3µm) regions, an outcome consistent with studies that have reported color effect on radiation absorption in wavelengths below 1.5 µm[171]. Apart from color-related effects, we observed that the twill-weave golden-brown shell fabric made with filament yarns (GST) had a slightly greater reflectivity than the plain-weave golden-brown outer shell material (GSP), although these effects were much less significant than color-related differences.

Figure 6-5 shows how the measured heat loss during insulation test and evaporative resistance test were affected by incident radiation. These data indicate that incident radiation had a greater effect on reducing the heat transfer in the evaporative resistance test (Figure 6-5b.) in comparison to the insulation test (Figure 6-5a.) However, the marked difference in solar-influenced heat transfer reduction attributable to the color of the outer shell fabric was remarkable. Therefore, the black-dyed outer shell material (BST) suffered a much greater drop in outward heat transfer than did composites made with the golden-brown color shell materials (GST and GSP). Figure 6-6, which shows estimated heat gain from incident solar radiation in dry and wet tests reinforced the importance of the color of the outer shell fabric in solar influence on turnout composite heat transfer. Unlike the major differences caused by outer shell color, the texture of the outer shell materials related to differences in shell fabric weave and yarn type did not produce significant differences in the heat loss of these materials in solar exposure in either insulation test or evaporative resistance test.

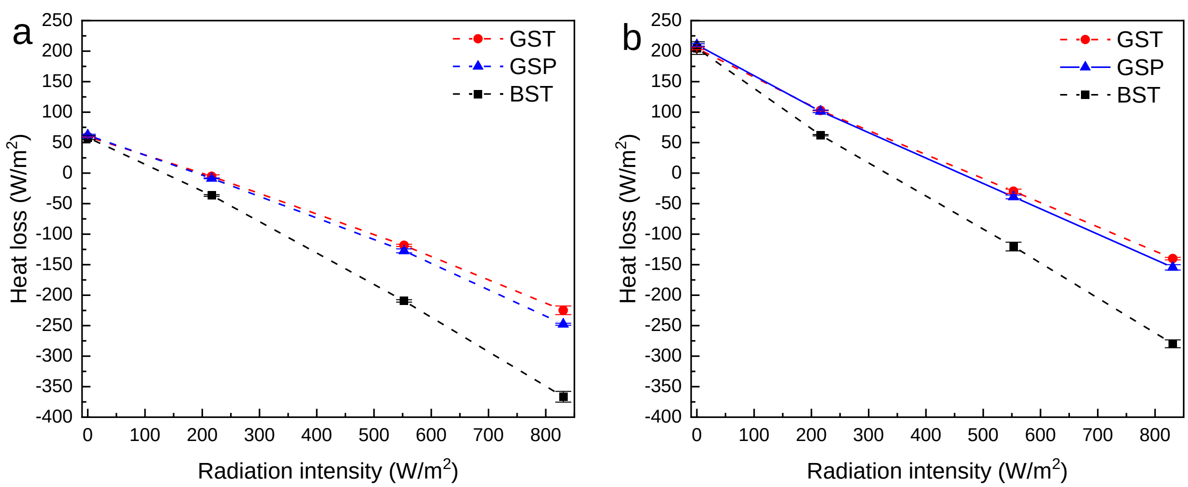

Figure 6-5. Measured heat loss by heat flux sensor for samples GST, GSP and BST in (a) insulation test and (b) evaporative resistance test under different levels of radiation

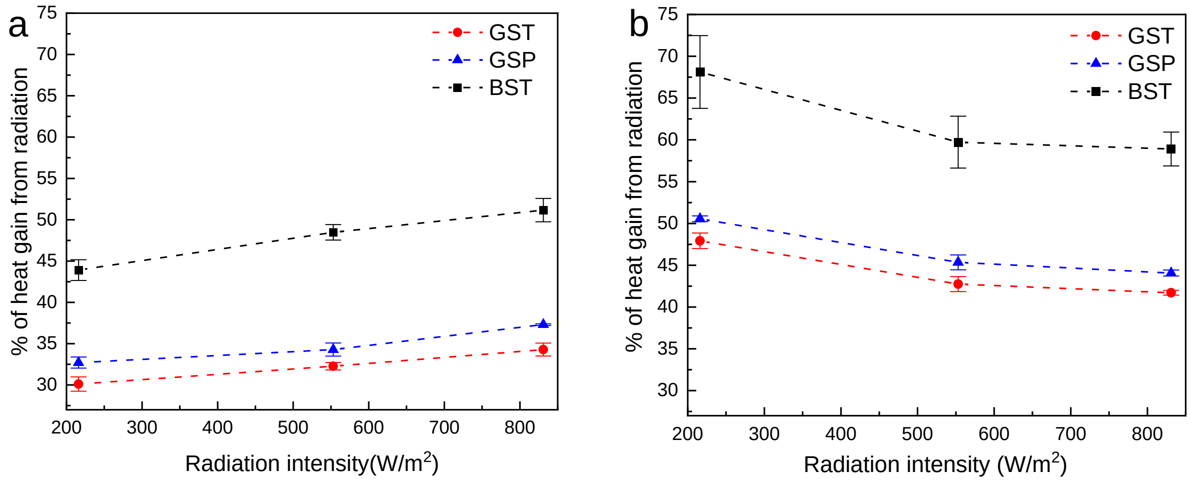

Figure 6-6. Relationship between heat gain and intensity of incident solar radiation for turnout composites with different outer shells in (a) insulation test and (b) evaporative resistance test

Figure 6-6 shows that percentage of heat gain from incident radiation was much higher in the evaporative resistance test than in the insulation (dry heat transfer) test regardless of the outer shell fabric used in the composite construction. The percentage heat gain decreased with the intensity of the solar exposure. Data displayed in Figure 6-7 also provide an explanation for this phenomenon. When tested in standard non-isothermal ambient conditions of temperature and humidity without incident solar radiation, turnout composites gained weight because of moisture condensation[156].

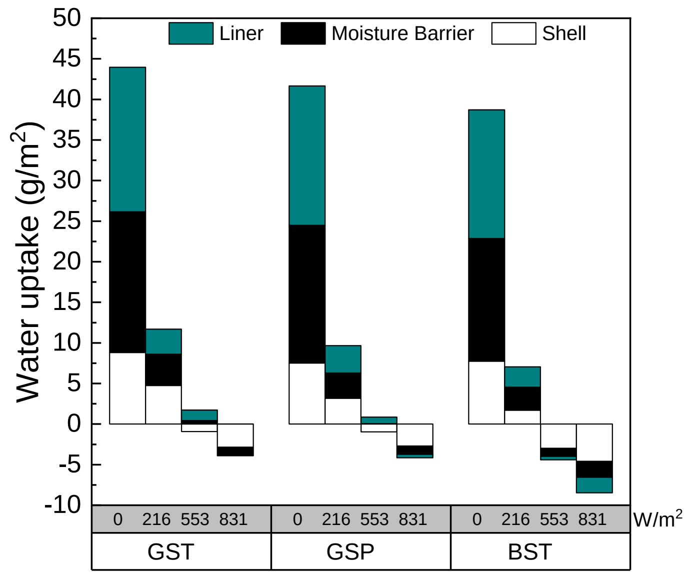

Figure 6-7. Water uptake of individual layer in turnout composites GST, GSP and BST under different levels of solar radiant loads after evaporative resistance test

However, incident solar radiation effectively dried the turnouts system reducing the amount of moisture absorbed in all layers of the composites, including the thermal liner and moisture barrier components. This effect increased their insulation against the applied solar load. The drying effects occurred in addition to the effect that the incident radiation had on increasing outward evaporative heat loss[53]. The combined effects produced the reduction in total heat loss with incident solar radiation previously show in Figure 6-3. The drying effect was greatest in the composite incorporating the black-dyed shell fabric (BST).

6.3.2 Effects of the moisture barrier component on turnout heat loss in incident solar radiation

We used three different turnout composite structures to study the influence of the moisture barrier component on heat loss and solar heat gain. The turnout constructions incorporated the same outer shell (GST shell in Table 6-1) and thermal liners (as in Table 6-1); however, they incorporated different moisture barrier technologies with different levels of moisture vapor resistance (Table 6-2).

Two of the samples used semipermeable, bicomponent barriers with different levels of evaporative resistance: high resistance (SP70) and lower moisture vapor resistance (SP27). The third turnout construction incorporated a vapor permeable, microporous e-PTFE barrier material with a very low evaporative resistance (MP17).

Table 6-2. Physical properties of turnout fabric system

ID	Moisture barrier structure	***THL*** **(W/m^2)**	***R*** **R_{ef} ($Pa \cdot m^2/W$)**
SP70	Prototype **bicomponent** e-PTFE membrane on meta-aramid woven fabric	213±8.5	70±6.4
SP27	Commercial **bicomponent** e-PTFE membrane on meta-aramid woven fabric	239±0.9	27±0.3
MP17	**Microporous** e-PTFE membrane on meta-aramid woven fabric	256±7.8	17±0.8

THL and intrinsic evaporative resistance (R_{ef}) were measured according to ASTM F1868 using standard sweating guarded hotplate.

Figure 6-8 shows that the heat loss through all these turnout constructions was dramatically lower when measured with incident solar radiation. However, solar heating had a more pronounced effect on lowering heat loss through semipermeable composites (SP70 and SP27), in comparison with the composite made up with the microporous membrane (MP17). Figure 6-9, showing moisture absorbed in the turnout constructions as a function of the intensity of applied solar radiation, explained these effects.

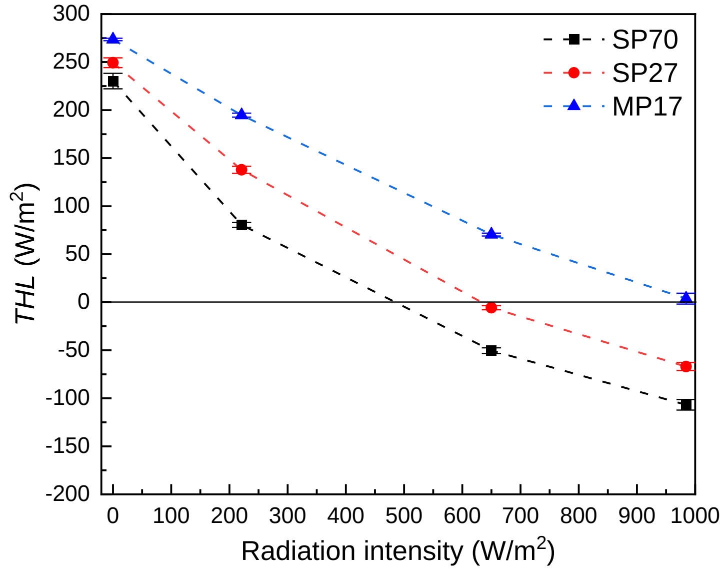

Figure 6-8. *THL* of composites with different moisture barriers under solar radiation

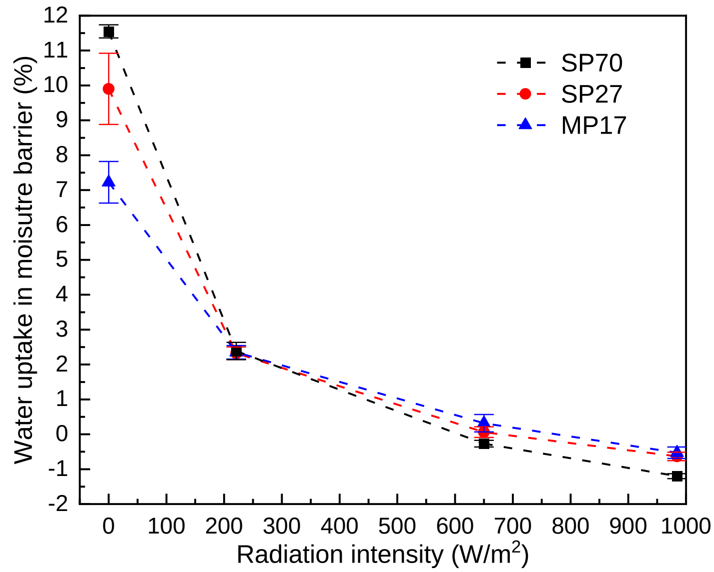

Figure 6-9. Effect of incident radiation intensity on water uptake in turnout moisture barriers

These data show that the applied solar radiation caused the systems to dry out, reaching equivalent states of moisture uptake with only about 200 W/m^2 of incident radiation. Because absorbed moisture in turnouts contributes heat loss through turnout systems in non-isothermal heat loss tests, we can conclude that solar radiation effectively negates the advantage in heat loss gained by using bicomponent barrier systems[156].

6.3.3 Effect of shell fabric contamination on heat loss in solar load

We used smoke-exposed turnout materials to investigate the effects of smoke contamination on heat loss in solar exposures (Table 6-3). The sample exposure protocol employed a fire-ground simulator located at the University of Illinois Fire Service Institute. The simulator consisted of a shipping container divided into 3 chambers, including two exposure chambers and a middle section containing a burning standard sofa[172, 173]. The exposed turnout samples hung vertically inside the smoke exposure chamber. After each exposure, the turnout composites were washed and dried following procedures described in the NFPA 1851 standard[174]. The protocol incorporated 40 cycles of smoke exposure followed by washing. References [172, 173] provide additional details of the smoke exposure protocol.

Table 6-3. Effect of washing and smoke exposures on turnout composite thickness and weight

	New condition		Washed only (40 cycles)		Smoke Exposed/Washed (40 cycles)	
	Weight (g/m^2)	Thickness (mm)	Weight (g/m^2)	Thickness (mm)	Weight (g/m^2)	Thickness (mm)
Outer shell: 60% para-aramid, 40% meta-aramid woven fabric	254	0.58 ±0.01	254	0.61±0.01	259	0.62±0.01
Moisture barrier: Bicomponent e-PTFE membrane on meta-aramid woven fabric	164	0.37±0.01	172	0.40±0.01	173	0.42±0.01
Thermal liner: Two layers of para-aramid/meta-aramid spunlace nonwoven quilted to a twill weave facecloth made with para-aramid, and FR rayon	265	1.40±0.02	281	1.71±0.06	280	1.68±0.03

Note: The weight standard deviation is not available as there is only one specimen each sample.

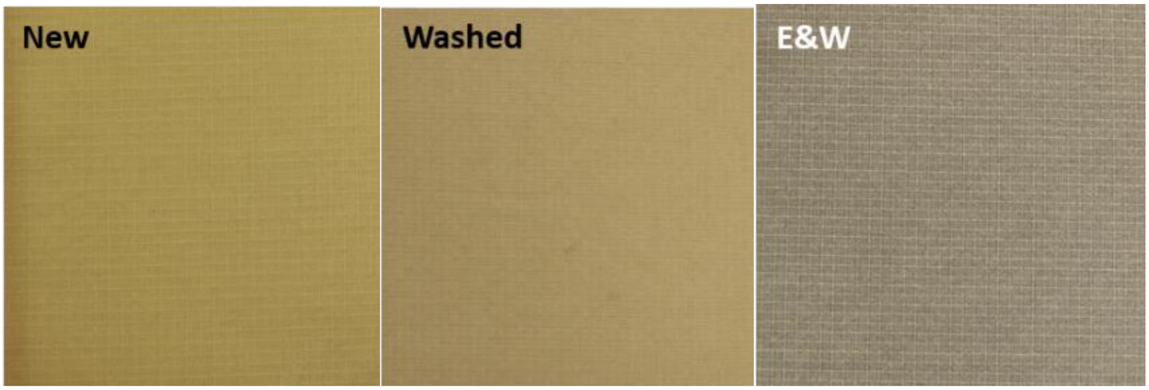

Figure 6-10. Appearance of turnout shell fabric: (a) new condition, (b) new sample after 40 cycles of washing and (c) new sample after 40 cycles of smoke exposure and washing

Guarded hot plate tests show that repeated washing or discoloration through smoke exposures had little effect on heat loss in this turnout system when measured without incident solar radiation (without radiation in Figure 6-11). However, measured in hot plate tests with intense incident sunlight (831 W/m^2), heat transport through the turnout samples changed from an outward heat loss to an inward heat gain (with radiation in Figure 6-11).

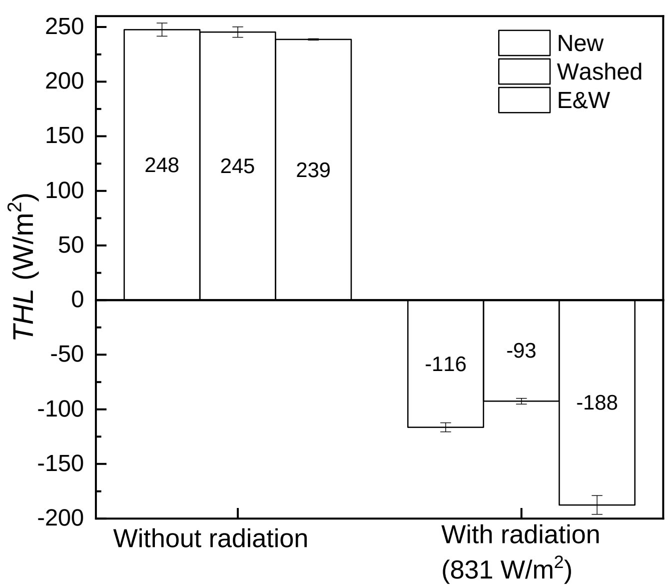

Figure 6-11. Effect of exposure to intense solar radiation (831 W/m^2) on total heat loss (*THL*) of turnout composite in new, washed and exposed and washed condition

The magnitude of incident solar-simulating radiation on heat gain is substantial, producing a heat exchange transition ranging from 338 to more than 400 W/m^2, depending on the smoke exposure and washing preconditioning. The washed only sample gained relatively less solar heat than the sample in a new condition, because of the effect of washing on lightening the shade of the turnout outer shell material (Figure 6-10). At the same time, the smoke contaminated turnout sample (E&W) gained 72 W/m^2 more heat from solar radiation than new gear when exposed to simulated sunlight (831 W/m^2).

Figure 6-12 shows that discoloration of the outer shell material caused by repeated smoke exposure has a significant effect on the reflectivity, even when normal cleaning procedures follow smoke exposure. This indicates that the soot remaining on the outer shell materials acted as an effective IR and visible light absorber. The measured spectral profiles were consistent with visually observable discoloration of the outer shell material.

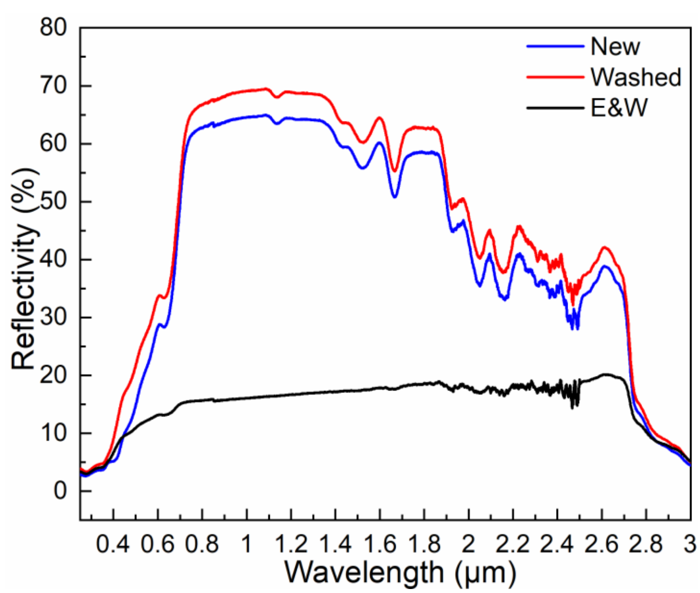

Figure 6-12. Effect of smoke exposure and washing on the reflectivity of outer shell fabric in the range of solar radiation

We observed that the washed turnout sample had slightly higher solar reflectivity in comparison to the sample in a new condition. We attributed this effect to the forty cycles of laundering on fading the color of the outer shell material (Figure 6-10). At the same time, smoke contamination reduced heat loss through the brown hued shell material to a level that is equivalent to the dyed-black shell fabric in solar exposure. Figure 6-13a shows the effect of outer shell smoke discoloration on the heat gained by the turnout system when exposed to incident solar radiation in radiant exposure (Figure 6-13a). Figure 6-13b shows that incident radiation dramatically reduced the amount of moisture absorbed by the thermal liner, moisture barrier and outer shell components of the turnout composite in the sweating hot plate test.

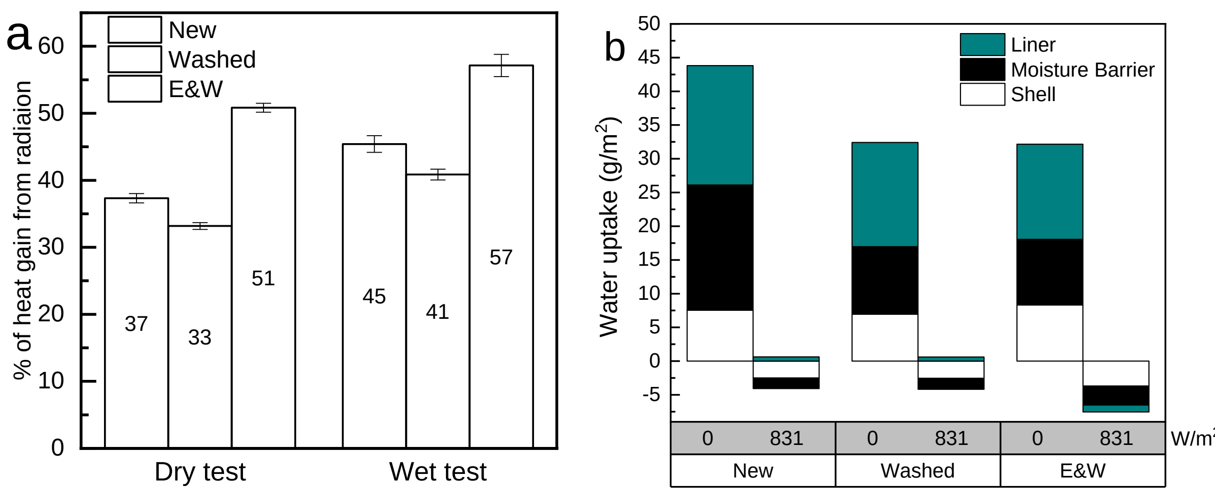

Figure 6-13. (a) Percentage heat gain from radiation (831 W/m^2) in insulation (dry) and evaporative (wet) hot plate test; (b) water uptake in composite layers after evaporative resistance test for composite in new condition, after washing, and smoke exposure followed by washing(E&W)

These data were consistent with the previously noted effect of shell fabric color on moisture absorption in turnout samples tested in a non-isothermal ambient environment (25 °C environmental temperature and 35 °C sweating plate temperature). They indicate that the effect that incident solar radiation had on drying the turnout test materials was a significant factor in solar heat gain; in not only reducing heat loss through composites with dark-colored shell layers, but also in lighter outer shells stained by smoke contaminants.

6.4 Conclusions

This study has shown that solar radiation could be a primary contributor to turnout related firefighter heat strain. Most significantly, the color of the outer shell fabric has a major influence on lowering turnout heat loss in solar exposures. Black-dyed outer shell fabrics absorb more solar energy than lighter colored shell materials. In addition, we have shown that smoke contamination of the turnout outer shell could contribute to heat-strain in solar exposure by dramatically reducing heat loss from the system to the ambient environment.

These findings support the heat-exchange hypothesis that, absent solar radiation, dry heat loss (conduction, convection, and radiation), and wet heat loss (wet conduction, evaporation) remain the major pathways for heat exchange from the sweating hot plate through the turnout composite test sample. For tests conducted in non-isothermal conditions (the hot plate is at higher temperature than the ambient environment), a significant fraction of the evaporative heat loss comes from moisture condensation in the turnout composite itself[104]. With applied solar load, the outer shell fabric, depending on its emissivity, reflects part of the incident energy. The remaining fraction of incident radiant energy is absorbed, leading to an increase in the temperature of outer shell fabric. Inner layers absorb radiation transmitted through outer shell, but the amount is tiny for protective clothing[19, 71]. However, the increase in fabric surface temperature caused by incident radiation can be expected to induce heat transfer from the top layer fabric to the hotplate through conduction and radiation, and to the environment by radiation, conduction, and convection. The ratio of the heat transferred to the hotplate is determined by the insulation of fabric, emissivity of outer layer, wind speed, and ambient temperature[71, 114]. Therefore, in the same environmental conditions and with similar thermal insulation value, composites with black-dyed outer shells, or lighter colored shells stained by smoke, absorb more thermal energy because of their lower reflectivity or high emissivity in the range of solar radiation. At the same time, evaporative heat loss is enhanced because of the effect of incident solar radiation on increasing the temperature of the fabric[53]. In turnout systems that contain hydrophilic bicomponent moisture barriers, our research has shown that the capability to transfer evaporative thermal energy is strongly dependent on the moisture absorbed by the turnout system[156]. Therefore, the effect that incident solar energy has on reducing the amount of absorbed moisture in turnout systems plays a major role in reducing their breathability.

7 Effect of Solar Radiation on Evaporative Heat Loss through Firefighter Composites

7.1 Introduction

Firefighters often work outdoors in direct sunlight while on a fire scene or doing other jobs, such as car extrication. This solar radiation intensity has been measured as high as 1000 W/m^2 on a day with clear sky[112], consisting of visible (45%), ultraviolet (5%) and infrared (50%) radiation[175]. Heating caused by solar radiation could cause significant strain on the human thermoregulatory system and may lead to heat illness[176]. It is necessary to understand the effect of solar radiation on the heat balance between the human body and the environment.

The radiation effect on dry heat loss has been well studied. It was reported that under longwave radiation (e.g. flame radiation), only the shell fabrics with special finishes, like aluminum coating, showed less heat gain[177], while materials and colors showed little difference[19, 52]. In contrast, under solar radiation, clothing with lighter color demonstrated less heat gain[19, 52, 178, 179]. In addition to the influence of surface properties, the amount of radiant heat absorbed by the human body increased with radiation intensity and ambient temperature, while attenuated with air velocity and clothing insulation[53, 71].

This heat gained by the human body from radiation constitutes a major part of heat stress, and has to be released from the body through evaporation[53]. Bröde et al. investigated the heat loss and evaporation rate of clothing with wet underwear and different outer layers under far infrared radiation using a thermal manikin[53, 177]. Higher heat gain was observed in less permeable garments and lower heat gain in a permeable system due to an elevated rate of evaporation under radiant load[53]. Guan et al. studied the thermal characteristics of protective clothing in continuous sweating conditions under infrared radiant heat exposure using sweating torso[164]. It was observed that the radiant heat increased the evaporation rate in most cases, which may due to increased vapor pressure difference from the torso surface to the environment by the radiant load[164]. For hydrophilic turnout gear, at a low sweat rate, the radiant heat increased evaporation rate, while at higher sweat rates, the radiant heat decreased evaporation. In contrast, for hydrophobic turnout gear, the radiant load enhanced evaporation[164].

Firefighter composites have different moisture barriers, including microporous, bi-component, and nonporous hydrophilic membranes, attached to a fire-resistant base fabric. The performance of different moisture barriers under radiant heat load is unknown. Current moisture barriers are mostly bicomponent membranes, featuring a thin hydrophilic layer coated on a microporous film. The purpose of the hydrophilic layer is to protect the porous structure from blocking by contaminants, to provide enough resistance to high-pressure water penetration, and to increase toughness of the film [65, 66]. Because of the surface hydrophilic nonporous layer in a bicomponent moisture barrier, it was reported that its water vapor resistance highly depends on moisture content in the membrane[61, 156]. It is possible that moisture barriers can dry out under solar radiation, increasing the evaporative resistance. However, the effects of the moisture barrier component on heat transfer through turnouts exposed to solar energy have never been explored.

The goal of this study was to explore the evaporative heat loss through firefighter composites under solar radiation, considering aspects related to outer shell color, and moisture barriers. In this paper, we investigated how radiation affects the outer shell surface temperature and water uptake in firefighter composites along with how cooling through evaporative heat loss changed. Three moisture barriers including two bicomponent and one microporous moisture barrier, and two outer shells (black and golden) were selected.

7.2 Experimental

7.2.1 Experimental design

Experiments were performed in a climate chamber maintained at 25 ± 0.2 °C, 65 ±3% RH, in still air (less than 0.4 m/s). A dynamic hotplate system (Thermetrics, Seattle, WA), with one test zone (8 × 8 inch) surrounded by a 2-inch guard ring (Figure 7-1), was used to characterize heat exchange between firefighter composites and the environment. Unlike a conventional sweating guarded hotplate, a heat flux sensor is embedded in the test zone that can be used to measure instantaneous heat flux through the dynamic hotplate surface. Positive heat flux values mean heat loss from plate to environment, and negative ones represent net heat gain from environment. Another feature of the dynamic hotplate system is the incorporation of an internal cooling system, where cold liquid is circulated through the hotplate to absorb extra heat. This feature allows it to work under intensive radiative heat load at a normal ambient condition without getting overheated. 25 sweat ports are evenly distributed on the hotplate surface and the sweating rate is controlled volumetrically.

To investigate the heat exchange in firefighter clothing under simulated sunlight, a Thorn Compact Source Iodide lamp (CSI, 1000 W) placed above the hotplate was employed to simulate solar radiation, as illustrated in Figure 7-1. The Thorn lamp produces radiant energy that simulates the solar spectrum[111, 167]. In this work, we kept the hotplate temperature at 35°C, and the overall heat flux through the plate surface was recorded by the heat flux sensor. The received radiant flux on the level of the fabric surface was measured by Pyranometer (Model CMP 11, Kipp & Zonen, The Netherlands).

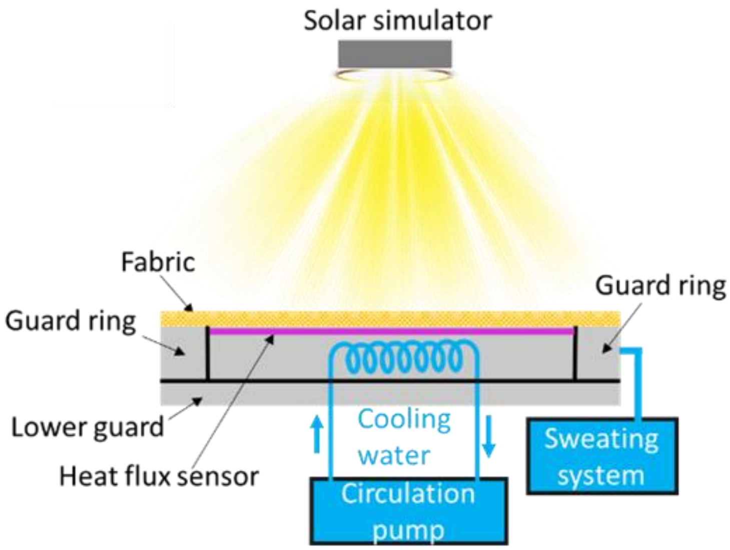

Figure 7-1. Schematic of experimental setup located at a climate chamber

The experiment was designed to investigate the effect of moisture barriers under solar radiation. For this study firefighter composites were measured with no radiation, and with the radiation exposures of 221, 650, and 984 W/m^2. These intensities were controlled by adjusting the distance between fabric surface and the light source at 1.88, 1.06, and 0.85 m, respectively. All tests were conducted in wet conditions, where a microporous membrane was used as a liquid barrier that only allows vapor to transfer through fabrics, and the plate surface was kept saturated. The duration for all wet tests was controlled as 1 hour, and the final 30 minutes of the data from the heat flux sensor were averaged. At the end of the test, an infrared thermometer (42510A, Extech) was used to measure the fabric surface temperature, and 10 measurements were conducted each time. After wet tests, each layer of the firefighter ensembles was weighed using a digital scale (Mettler PM460) immediately. The weight change could be obtained by comparing the weight after the wet tests with the samples preconditioned at the environment of 21 °C and 65% RH. All the experiments were repeated three times, and average values were used.

7.2.2 Materials

We constructed six different composite structures to study the influence of the moisture barrier component on solar heat gain (Table 7-1). These turnout constructions used the same thermal liners (two layers of aramid spunlace nonwoven quilted on twill facecloth woven from meta-aramid filament yarn and meta-aramid /FR rayon spun yarn, 272 g/m^2, 1.4 mm) and either black or golden outer shell with the same structure (twill weave, 65% para-aramid, 35% polybenzimidazole, 240 g/m^2, 0.4mm); however, they incorporated different moisture barrier technologies. Two of the samples used semipermeable, bicomponent barriers with different levels of evaporative resistance: high resistance (A) and lower moisture vapor resistance (B). The third turnout construction incorporated a vapor permeable, microporous PTFE barrier material with a very low evaporative resistance (MM). One of the semipermeable bicomponent membranes (Sample B) is a commercially available product compliant with the NFPA 1971 Standard for Structural Firefighter PPE[72]. Sample A is a specially designed bicomponent e-PTFE membrane coated with a proprietary nonporous layer. Sample MM is an example of a truly moisture vapor permeable e-PTFE microporous membrane (no hydrophilic coating). Membranes A and MM are special moisture barrier constructs specially obtained for this study.

Table 7-1. Physical properties of moisture barriers

Moisture barrier	Composition	Weight (g/m^2)	Thickness (mm)
A	Prototype bicomponent e-PTFE membrane on meta-aramid woven fabric	226±3.3	0.45±0.01
B	Commercial bicomponent e-PTFE membrane on meta-aramid woven fabric	163±1.4	0.36±0
MM	Microporous e-PTFE membrane on meta-aramid woven fabric	141±0.5	0.36±0

7.2.3 Calculations

Heat loss measured by hotplate H_t (W/m^2) is composed of dry heat loss H_{dry} and evaporative heat loss H_{eva}

$$H_{\mathrm{dry}} = \frac{35\ ^\circ\mathrm{C} - T_\mathrm{s}}{R_\mathrm{cf}} \tag{7.1}$$

where T_s (°C) is the surface temperature of outer shell, R_{cf} (K·m^2 /W) is the intrinsic thermal resistance of firefighter composite, and 35 °C is the hotplate surface temperature. If T_s is larger than 35 °C, H_{dry} becomes negative, meaning net heat gain.

$$H_{\mathrm{eva}} = H_\mathrm{t} - H_{\mathrm{dry}} \tag{7.2}$$

Total apparent evaporative resistance R_{et}^A (kPa·m^2/W), the sum of surface air layer and the intrinsic evaporation resistance of firefighter composites (R_{ef}^A, kPa·m^2/W), can be calculated by[75]:

$$R_{\mathrm{et}}^{\mathrm{A}} = \frac{\Delta P}{H_{\mathrm{eva}}} \tag{7.3}$$

where ΔP (kPa) is the vapor pressure difference between the hotplate surface and ambient.

Total heat loss (*THL*) was obtained with equation 2.10[75].

7.2.4 Statistical analysis

The statistical analysis was performed using JMP Pro 15 (SAS, Cary, NC, USA) and significance levels were set at $p < 0.05$. All data were compared using one-way analysis of variance (ANOVA), followed by Tukey's honestly significant difference (HSD).

7.3 Results

The thermal insulation and evaporative resistance were evaluated for composites with golden shells using the dynamic hotplate system, and the results are listed in Table 7-2. Since the only difference between the outer shells is color, the thermal insulation and evaporative resistance of composites with different colors were considered as the same. The study was mainly focused on the influence of radiation on the evaporative heat loss of firefighter composites with three different moisture barriers and two outer shells.

Table 7-2. Properties of firefighter ensembles

Ensemble Code	R_{cf} (K·m^2/W)	R_{ef}^A (Pa·m^2/W)	Weight (g/m^2)	Thickness (mm)
GSAL	0.083±0.002	19.7±1.2	736±2.5	2.24±0.02
GSBL	0.085±0.002	15.8±0.3	674±1.9	2.15±0.07
GSML	0.085±0.001	14.0±0.3	652±2.1	2.15±0.06
BSAL	0.083±0.002	19.7±1.2	740±3.3	2.25±0.05
BSBL	0.085±0.002	15.8±0.3	677±0.2	2.16±0.06
BSML	0.085±0.001	14.0±0.3	656±1.3	2.16±0.04

Note: GS: Golden shell, and BS: Black shell; the third letter refers to moisture barrier, and the end letter L is thermal liner. Intrinsic thermal resistance (R_{cf}) and intrinsic apparent evaporative resistance (R_{ef}^A) were measured according to ASTM F1868 part C.

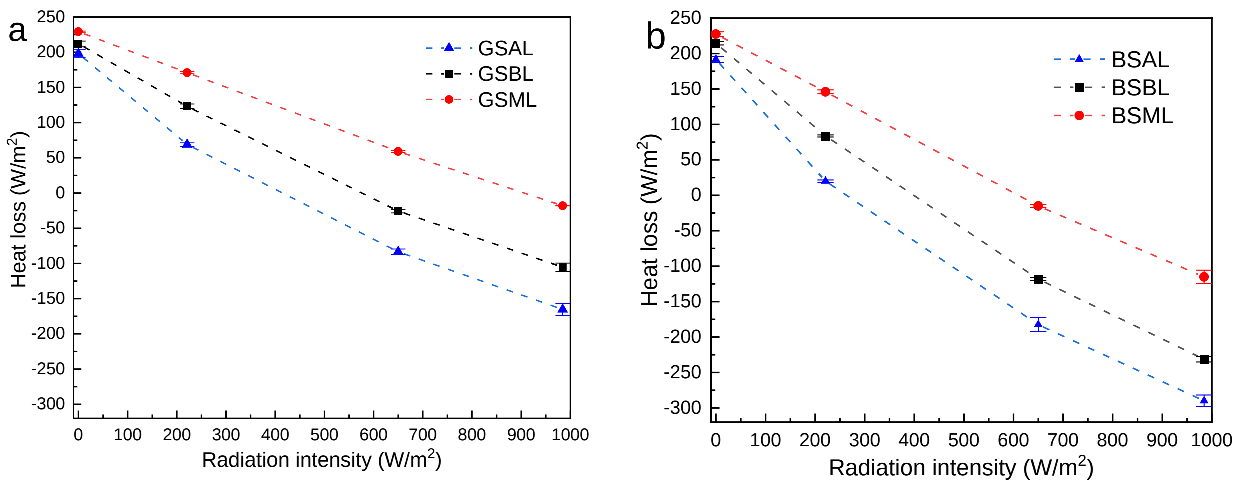

Figure 7-2. Heat loss measured from the hotplate for (a) composites with golden shells (GS), and (b) composites with black shells (BS).

Heat loss measured from the hotplate under radiation intensities from 0 to 984 W/m^2 was presented in Figure 7-1. The results show that the measured heat loss of all these turnout constructions was dramatically lower when measured with incident solar radiation. The gap in heat loss between ensembles with different moisture barriers widened. Without radiation, heat loss through GSAL and GSBL was 31 and 17 W/m^2 less than GSML, respectively, and the differences were increased dramatically to 151 and 91 W/m^2 under the radiation of 984 W/m^2. Heat loss of sample GSAL decreased at the fastest rate with radiation, as can be observed by Table 7-3. In addition to the moisture barrier, the color of outer shells also contributed to the difference in heat loss. Under the radiation of 984 W/m^2, the heat loss through BSAL is -231 W/m^2 (a net heat gain of 231 W/m^2), while its corresponding sample with golden shell, GSAL, showed 66 W/m^2 less heat gain (p<0.05). The slope of samples with black shells was larger than those with golden shells (Table 7-3).

Table 7-3. Linear fitting equations of heat loss (y, W/m^2) through firefighter composites with radiation intensity (x, W/m^2)

GSAL	GSBL	GSML	BSAL	BSBL	BSML
$y = -0.36x + 158$	$y = -0.34x + 203$	$y = -0.25x + 228$	$y = -0.49x + 138$	$y = -0.47x + 194$	$y = -0.37x + 227$
R^2=0.97	R^2=0.99	R^2=1.00	R^2=0.93	R^2=0.99	R^2=1.00

The individual layer in all ensembles was weighed after the one-hour-long wet tests under different levels of radiant load, and the results are shown in Figure 7-2a. Without radiation, a significant increase in weight in all the composites was found. As the radiation intensity increased, the moisture content in all composites dropped, and a loss of moisture was observed at the radiation of 650 and 984 W/m^2. Composite GSAL, GSBL, and GSML showed a total weight loss of 0.60, 0.37 and 0.29 g under the radiation of 984 W/m^2, respectively. It could also be observed that composites with black outer shells tended to lose more moisture. Under radiation of 984 W/m^2, BSAL lost 0.47 g more than GSAL. The percentage of water uptake in moisture barriers alone as a function of the intensity of applied solar radiation is illustrated in Figure 7-

2b,c. These data show that the applied solar radiation causes the systems to dry out, reaching equivalent states of moisture uptake with only about 221 W/m^2 incident radiation.

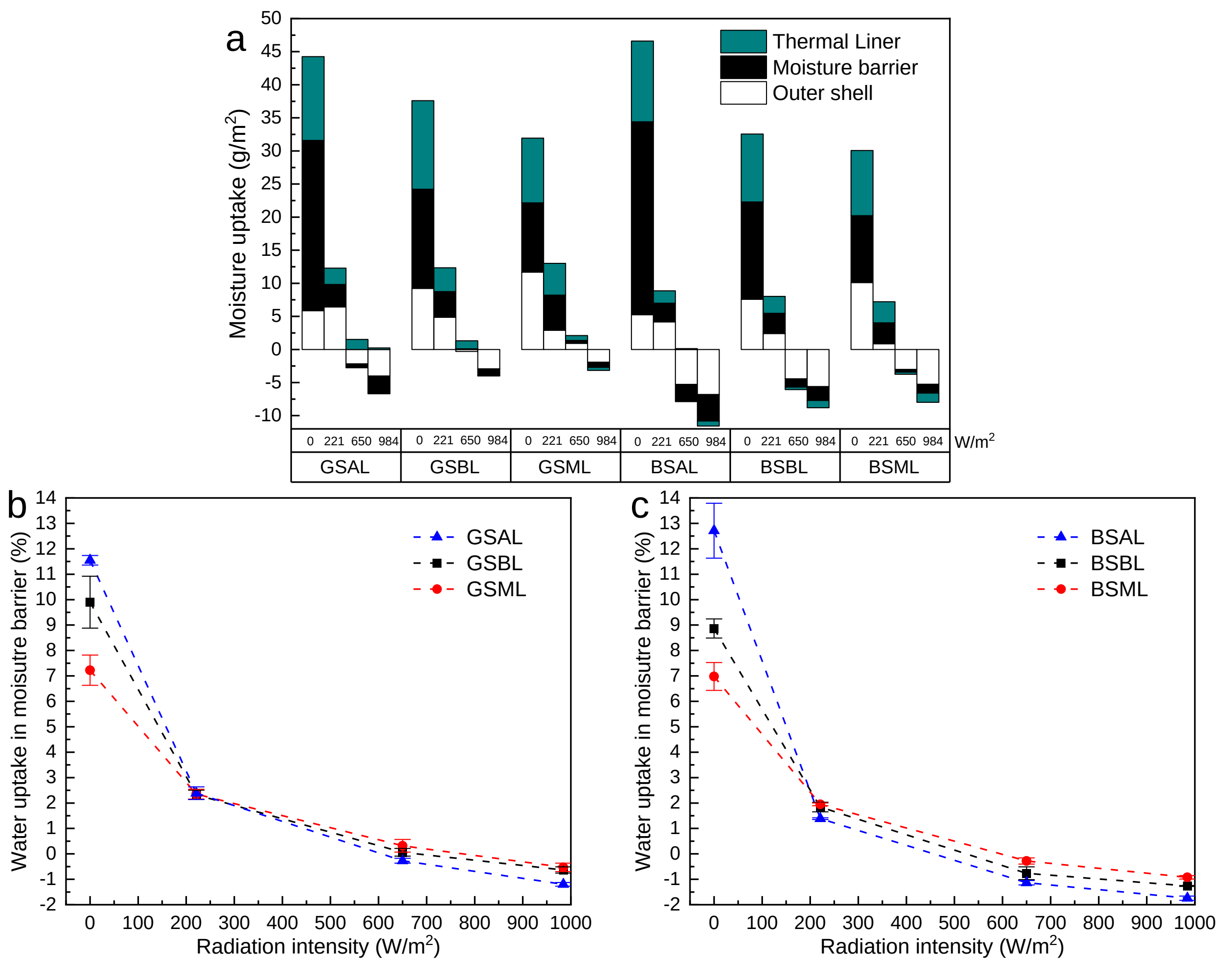

Figure 7-3. (a) Water uptake in all layers of firefighter composites, and the percentage of water uptake in (b) moisture barriers with golden outer shells, and (c) moisture barriers with black outer shells under various radiation intensities (0, 221, 650, and 984 W/m^2)

The surface temperature of outer shells was measured, and the results are displayed in Figure 7-4. Without radiation, a similar surface temperature was observed for all composites (p<0.05). As radiation increased, the surface temperature of all composites was raised. Ensembles with black outer shells (BSBL, BSML, BSAL) showed a higher surface temperature than composites with golden outer shells (GSBL, GSML, GSAL). Under the radiation of 984

W/m^2, the average surface temperature of composites with black shells is 10 °C higher than those with golden shells (p<0.05).

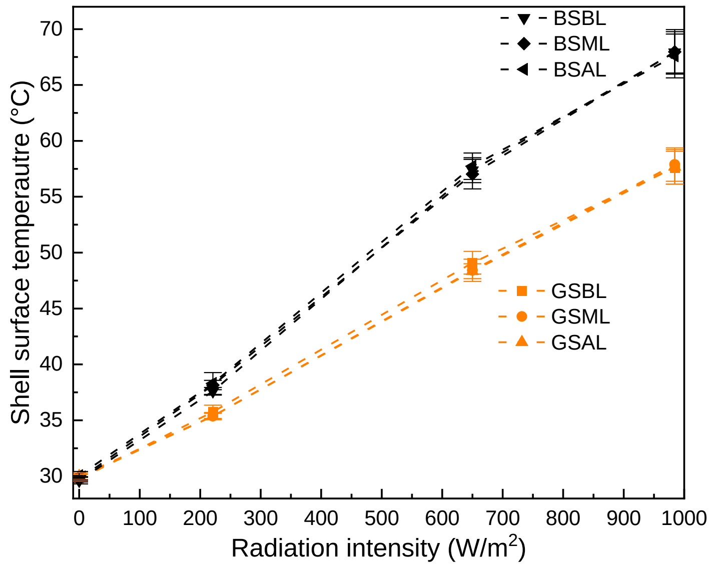

Figure 7-4. Effect of radiation intensity on outer shell surface temperature

Using the surface temperature of outer shells (Figure 7-4) and insulation value of composites (Table 7-2), dry heat loss was estimated using Equation 7.1. Then evaporative heat loss was separated from the measured heat loss using Equation 7.2. The results are displayed in Figure 7-5. The data show that dry heat loss decreased with radiation intensity and became negative starting from the radiation of 221 W/m^2, meaning a net heat gain from radiation. Samples with black shells showed a much higher heat gain from radiant heat load. Evaporative heat loss with radiation demonstrated different patterns. For composites with a microporous membrane (BSML & GSML), the evaporative heat loss was enhanced with the radiant heat load. For the composites with bicomponent moisture barrier A (GSAL, BSAL) and moisture barrier B (GSBL, BSBL), evaporative heat loss decreased under the radiation of 221 W/m^2, and then increased gradually with the radiation intensity. Outer shell color showed a detrimental effect on evaporative heat loss through composites with moisture barriers A and B under low radiant load. A difference of 18 W/m^2 between GSBL and BSBL, and 13 W/m^2 between GSAL and BSAL were observed under the radiation of 221 W/m^2. With increased radiation, the difference between composites with different outer shells became smaller.

Apparent evaporative resistance was calculated according to Equation 7.3, and its relationship with the radiation intensity was investigated (Figure 7-6). It could be observed that the evaporative resistance of composites with moisture barrier A and B (BSAL, GSAL, BSBL, GSBL) increased first and then decreased with radiation intensity. For example, evaporative resistance of BSAL increased from 26.8 to 60.7 Pa·m^2/W under radiation of 221 W/m^2, and then decreased to 34.9 Pa·m^2/W under radiation of 984 W/m^2. In contrast, the evaporative resistance for the composites with a microporous membrane (GSML and BSML) showed a consistent decreasing trend with radiation. The evaporative resistance of GSML and BSML decreased by 7.0 and 7.7 Pa·m^2/W under the radiation of 984 W/m^2, respectively, compared with the condition without radiation.

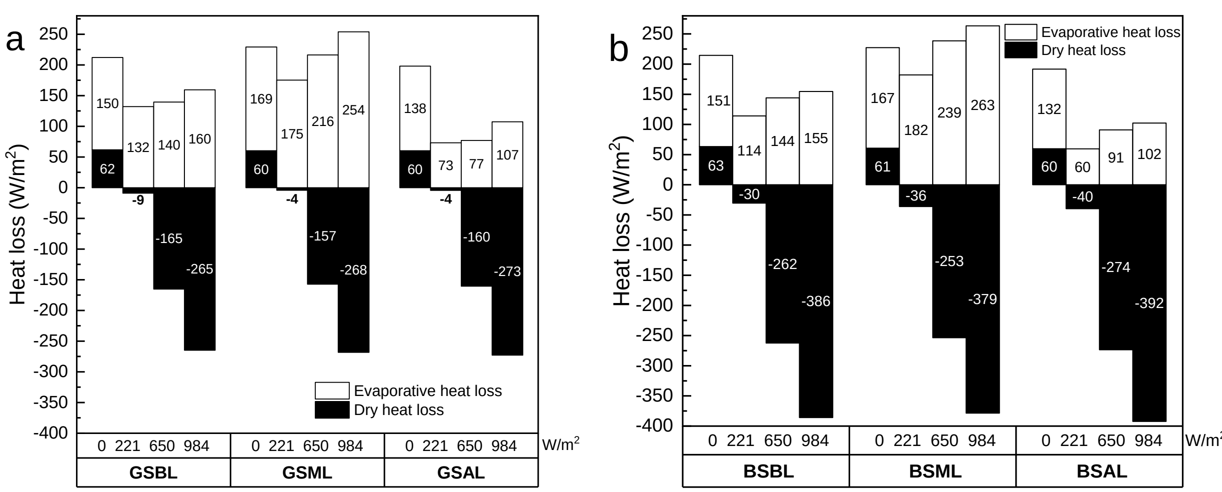

Figure 7-5. Dry heat loss and evaporative heat loss of firefighter composites under different radiation intensities with (a) golden shells, and (b) black shells

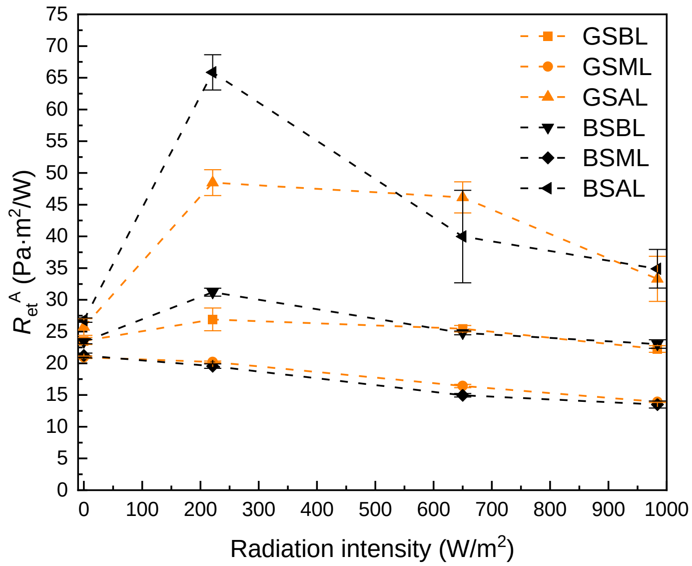

Figure 7-6. Effect of radiation intensity on apparent evaporative resistance

7.4 Discussions

The study used a dynamic hotplate system to investigate the effect of solar radiation on evaporative heat loss through firefighter composites with different moisture barriers. Color had a significant effect on heat loss (Figure 7-2): black samples absorbed more heat from solar radiation. This was also reflected by the higher surface temperature observed in black samples (Figure 7-4). The findings agreed well with previous publications stating that color has a strong effect on heat grain from solar radiation[19, 52, 178, 179].

The weight gain without radiation observed in Figure 7-3 was most likely due to condensation within the composites. Condensation happens when the moisture content at some region of clothing exceeds the saturated moisture content for the local temperature[99-101]. The increase in radiation heated the composites (Figure 7-3), and this increased the saturated vapor pressure in the fabric system, thus reducing the condensation effect. Under higher radiation levels, weight loss in firefighter composites was observed. This is because water absorption is an exothermic reaction, and water uptake decreases as temperature increases[152]. Due to the higher temperature observed in black samples (Figure 7-3), more weight loss in black samples was demonstrated.

Under solar radiation, heat balance on the surface of outer shells was established during steady state: solar radiation absorbed by outer shell equals to the heat transfer from the outer shell to the environment by radiation and convection plus the heat transfer from the outer shell to the hotplate by conduction. The heat from radiation was partially absorbed by the outer shell surface, and the rest were reflected. Under radiation from 221 to 984 W/m^2, the surface temperature of outer shells (Figure 7-3) surpassed hotplate surface temperature (35 °C), leading to heat transfer to the hotplate mainly by conduction, and this was measured by the hotplate as heat gain. A temperature difference was also created between the fabric surface and ambient air, resulting in heat release to the environment by radiation and convection. The heat gain from radiation can be attenuated by wind speed, ambient conditions, and insulation value[53, 71]. Since the environmental conditions were the same for all tests and insulation values were similar, composites with the same outer shell showed similar surface temperature (Figure 7-3).

Figure 7-4 revealed the significant influence of radiation on evaporative heat loss. For microporous membrane, radiation enhanced evaporative heat loss (Figure 7-4) or reduced evaporative resistance (Figure 7-5). The moisture transfer through the composites with microporous moisture barriers is through Fickian diffusion, whose water vapor diffusion coefficient has an Arrhenius dependence on temperature[59, 66]. Heating caused by radiation facilitated the transport of moisture vapor through firefighter composites. As a result, a consistent decrease in evaporative resistance was observed (Figure 7-5). Such temperature effects on evaporative resistance was also reported by Gibson[66]. The color of outer shells had a minor impact on evaporative resistance for samples with microporous membranes.

Bicomponent moisture barriers (A and B) have a nonporous hydrophilic layer coated on microporous e-PTFE film, making their evaporative resistance dependent on the moisture content inside the membrane[61]. The transmissions of vapors through the solid hydrophilic film occur by the absorption-diffusion-desorption mechanism[59]. Moisture absorbed by the hydrophilic layer can facilitate the transmission of water vapor by swelling membrane (creating more free volume between polymer chains), and providing more hydrophilic sites, etc[64]. Under radiation of 221 W/m^2, due to the large moisture loss in the moisture barrier (Figure 7-2), an increase in evaporative resistance was observed in Figure 7-5. Moisture transfer through other components, including the base fabric and the microporous film in moisture barrier, thermal liner, and outer shell in firefighter composites, is by vapor diffusion in air, whose diffusion rate is affected by temperature[59]. Under a higher radiation intensity, the moisture barrier effect on evaporative heat loss became less significant due to the little change in moisture content (Figure 7-2). Thus, further increase in radiation would mainly facilitate evaporation by heating fabrics and increasing moisture diffusion rate in other components of firefighter composites. As a result, the evaporative resistance of composites with moisture barrier A and B decreased first under low radiation, and then decreased gradually with the increase in radiation.

The NFPA 1971-2018 (Standard on protective ensembles for structural firefighting and proximity firefighting) establishes a minimum heat strain requirement for turnout suits materials based on measured Total Heat Loss or *THL*[72]. *THL* is measured by sweating hotplate in the environment of 25 °C, 65% RH, without considering the effect of solar radiation. Figure 7-6 shows the effects of moisture barriers on *THL* when measured in simulated solar exposures. Solar heating has a more pronounced effect on lowering the *THL* of the semipermeable composites (A and B), in comparison with the composite made up with the microporous membrane (MM), especially along with black outer shells. Data in Figure 7-2 show that solar radiation causes turnout systems to dry out, reaching equivalent states of moisture uptake when exposed to only 221 W/m^2 incident radiation. Because absorbed moisture in turnout maximizes heat loss in a non-isothermal *THL* test, solar radiation effectively offsets the advantage gained by turnout systems that incorporate bicomponent moisture barriers.

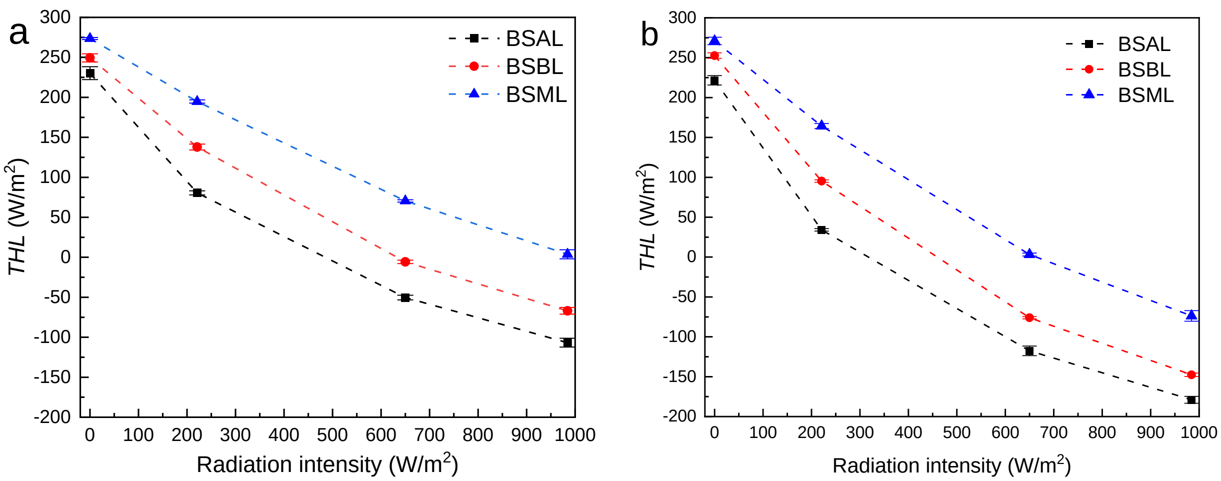

Figure 7-7. *THL* of composites with different moisture barriers under solar radiation (a) with golden outer shells and (b) with black outer shells

7.5 Conclusions

In summary, the effect of radiation on evaporative heat transfer through firefighter composites with different moisture barriers has been explored. This study revealed that radiation could increase composite temperature, causing different effects in relation to moisture barriers. For firefighter composites with microporous moisture barrier, evaporative resistance decreased consistently with radiation. In contrast, for composites with bicomponent moisture barriers, radiation showed a trade-off effect. At lower radiation, due to the reduction of the moisture content inside moisture barriers, evaporative resistance increased, especially for composites with a black shell. In contrast, with increased radiation, evaporative resistance decreased due to enhanced moisture diffusion rate. The property change of bicomponent moisture barriers under radiation must be addressed in order to mitigate heat strain in firefighters working outdoors.

To simplify the question, we assumed all water evaporated directly from the hotplate surface by covering a microporous film on hot plate surface, eliminating the wicking from the hotplate to thermal liner. In our future studies, the effect of wicking properties of thermal liner, as well the location of wet layer on heat gain from the radiation will be investigated. The underlying reason for the difference in evaporative resistance between the two bicomponent moisture barriers was not explored due to the lack of knowledge in these proprietary structures. It would be helpful to study how the chemical composition, thickness, and molecular structure of hydrophilic layer coating affect the water vapor diffusion capability through the bicomponent moisture barrier under various environmental conditions, but it is beyond the scope of our project.

8 Impact of Durable Water Repellent Finishing in Thermal Liner on Firefighter Heat Stress

8.1 Introduction

Firefighting is an extremely dangerous profession, and firefighters are exposed to various hazards, including thermal injuries, trauma, toxic liquids, etc[180]. To protect structural firefighters against external hazards, a 3-layer turnout clothing is required. The thick and bulky protective clothing adds large resistance to the dissipation of metabolic heat, causing potential heat stress[181]. It has been reported that heat stress is a major cause behind firefighters sudden cardiac deaths as well as numerous injuries[10].

Typical structural firefighter turnout clothing consists of an outer shell, moisture barrier, and thermal liner. The outer shell is the first line of protection, and is composed of woven fabrics made with blends of inherently flame-resistant fibers[51]. It provides basic protection against flame and heat, and has sufficient mechanical resistance to cuts, snags, tears and abrasion[50]. The moisture barrier is the next layer. Most moisture barriers contain a thin semipermeable membrane laminated to a flame-resistant base fabric. This layer is responsible for protecting the firefighter from water, biological materials and chemicals while still allowing the transmission of sweat vapor from the body[54]. The thermal liner, generally composed of thick nonwoven fabrics made of flame-retardant/resistant fibers quilted to a light-weight woven fabric, is the innermost layer[67]. It provides the majority of the thermal protection and protects the user from extreme heat[68].

During firefighting, it is essential to keep turnout gear dry for the purpose of thermal protection. Normally, durable water repellent finishing (DWR) is applied to the outer shell to repellent water from outside. Firefighters perspire enormously during intensive activities, and to limit water absorption from skin, some commercially available turnout gear has water repellent finishing in the thermal liner. Such turnout gear has gained much popularity among firefighters. In one of our workshops, some firefighters mentioned that they feel cooler when wearing such clothing. This prompts us to investigate the effect of DWR treatment on thermal comfort.

Gibson studied the effect of durable water repellent treatment in military uniforms and found that the uniform with or without DWR treatments showed similar air permeability and breathability, indicating no differences in heat strain potential[182]. However, it was reported that the DWR treatments negatively affected the perceived comfort[182]. This is consistent with a previous study on the influence of fabric sweat management properties on perceived tactile comfort by Barker[183]. However, the effect of DWR finishing in turnout clothing on firefighter thermal comfort is unknown.

The aim of this study was to evaluate the potential effect of DWR finishing inside turnout clothing on firefighter thermal comfort. To the best of our knowledge, this is the first systematic study on the physiological effect of DWR finishing using a hotplate, sweating manikin, and physiological manikin.

8.2 Experimental methods

8.2.1 Garments

Two turnout suits with the same outer shell and moisture barrier but different thermal liners A and B were selected. The two thermal liners have similar weight, thickness, and structure. In addition, the same face cloth with a good moisture wicking property was used in the two thermal liners. The only difference is that the 2 layers of spunlace nonwoven in the thermal liner of garment B were treated with DWR. More details for the composites are shown in Table 8-1.

Table 8-1. Physical properties of individual component

Components	Picture	Material structure	Weight (g/m^2)	Thickness (mm)
Outer shell	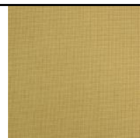	35% PBI, 65% para-aramid, twill weave	239±0.6	0.40±0.01
Moisture barrier		Bicomponent e-PTFE (expanded polytetrafluoroethylene) membrane on meta-aramid woven fabric	163±1.4	0.36±0
Thermal liner A		Two layers of aramid spunlace nonwoven quilted to 60% meta-aramid filament / 40% spun yarn twill weave (meta-aramid, FR rayon)	272±2.2	1.39±0.04
Thermal liner B	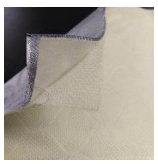	Two layers of durable water repellant (DWR) finished aramid spunlace nonwoven quilted to 60% meta-aramid filament / 40% spun yarn twill weave (meta-aramid, FR rayon)	263±1.1	1.44±0.04

Note: The garment area was estimated to be 5 m^2 based on the garment and fabric weight.

8.2.2 Sweating guarded hotplate test

Total heat loss (*THL*) is used to characterize the heat transfer through firefighter composites and regulated in the NFPA 1971[72]. It was obtained according to ASTM F1868 by measuring intrinsic thermal resistance (R_{cf}, K·m^2/W) and apparent evaporative resistance (R_{ef}^A, kPa·m^2/W) with a sweating guarded hotplate (Thermetrics, Seattle, USA) in the environment of 25 °C, 65% RH[75]. *THL* (Total heat loss, W/m^2) was calculated by equation 2.10[75].

8.2.3 Sweating manikin test

Compared to the sweating guarded hotplate test, the sweating manikin can capture the effect of garment design on heat loss. The tests were conducted with a 34-zone Newton sweating manikin (Thermetrics, Seattle, USA) according to ASTM F1291-16 (Standard Test Method for Measuring the Thermal Insulation of Clothing Using a Heated Manikin)[85] and ASTM F2370 -16

(Standard Test Method for Measuring the Evaporative Resistance of Clothing Using a Sweating Manikin)[87]. Insulation measurements were conducted at 15 °C, 50% RH, and evaporative resistance tests were performed at 35 °C, 40% RH. Manikin surface was kept as 35 °C to simulate skin temperature. Three replicates of each garment were tested.

To simulate total heat loss (*THL*) measured with sweating guarded hotplate, a predicted heat loss value (Q_{manikin}, W/m^2) in the environment of 25 °C, 65% RH was estimated using the total evaporative resistance (R_{et}, kPa·m^2/W) and thermal insulation value (R_{t}, K·m^2/W) measured by the manikin[88]:

$$Q_{\text{manikin}} = \frac{(T_{\text{s}} - T_{\text{a}})}{R_{\text{t}}} + \frac{(P_{\text{s}} - P_{\text{a}})}{R_{\text{et}}} \qquad (8.1)$$

where T_{s} and T_{a} is the manikin surface temperature (35 °C) and ambient temperature (25 °C), respectively. P_{s} and P_{a} is the vapor pressure (kPa) of water saturated skin surface and environment, respectively. The first part is dry heat loss mainly from conduction, convection, and radiation, and the second part is wet heat loss from evaporative heat loss.

8.2.4 Physiological manikin

The physiological manikin system composed of a 34-zone Newton sweating manikin (Thermetrics, Seattle, USA) coupled with TAITherm v.13.0.0 (Thermoanalytics, Calumet, MI USA) was used in this study. TAITherm implements the Fiala physiological model to predict physiological responses of an average 80 kg male, and more details can be found in papers by Burke[97, 184]. This system was proved to be a useful tool at predicting the physiological outputs of a firefighter wear trial in a recent study[185].

During the test, a short-sleeved cotton shirt (large size, 100% cotton), boxer brief (medium size, 100% cotton), socks (100% cotton), firefighting gloves, helmet, and athletic shoes were worn along with turnout suits. The bottom of the pants was taped up to simulate the pant to boot interface. Three replicates of each garment were tested. Figure 8-1 displays the pictures of a fully dressed manikin in walking and rest condition. All clothing items were preconditioned for at least 12 hours in an environment of 21 °C, 65% RH.

Figure 8-1. Picture of fully dressed physiological manikin in (a) rest and (b) walking condition

The ambient conditions of 25 °C, 65% RH with a wind speed of ~1m/s was selected to represent the environment that firefighters may experience. Before testing, the manikin was preheated to a set of starting skin temperatures inside the environmental chamber. After reaching the equilibrium condition (±0.05 °C of preset skin temperatures), the test protocol in Table 8-2 would be executed.

Table 8-2. Testing protocol

Period	Duration	Metabolic rates	Walking speed
1	10 mins	1 Met	0 DSPM*
2	20 mins	5 Mets	55 DSPM
3	20 mins	1 Met	0 DSPM
4	20 mins	5 Mets	55 DSPM
5	20 mins	1 Met	0 DSPM
6	20 mins	5 Mets	55 DSPM
7	20 mins	1 Met	0 DSPM

* DSPM means double step per minute. The manikin was driven by a mechanical system to simulate walking activities.

8.2.5 Statistical analysis

The statistical analysis was performed using JMP Pro 15 (SAS, Cary, NC, USA). The predicted core body temperature, sweating rate, skin temperature and cardiac output of garments A and B at the end of the protocol were compared using two sample t-tests. *P* <0.05 was considered significant.

8.3 Results

8.3.1 Basic properties on fabric level

Fabric-level *THL* tested by sweating guarded hotplate is the only index for evaluating materials related heat strain potential as specified in the NFPA 1971 Standard[72]. The *THL* of the three-layer base composite used in garments A and B is 238.9 and 230.8 W/m^2, respectively. (Figure 8-2a) Both are larger than the minimum requirement of 205 W/m^2 in NFPA 1971. In addition, the thermal protection performance (*TPP*) was also performed according to NFPA 1971, and the two composites exhibit values of 39.1 and 38.5 cal/cm^2. No significant difference was observed between the two composites on the fabric level regarding *TPP* or *THL* (p<0.05).

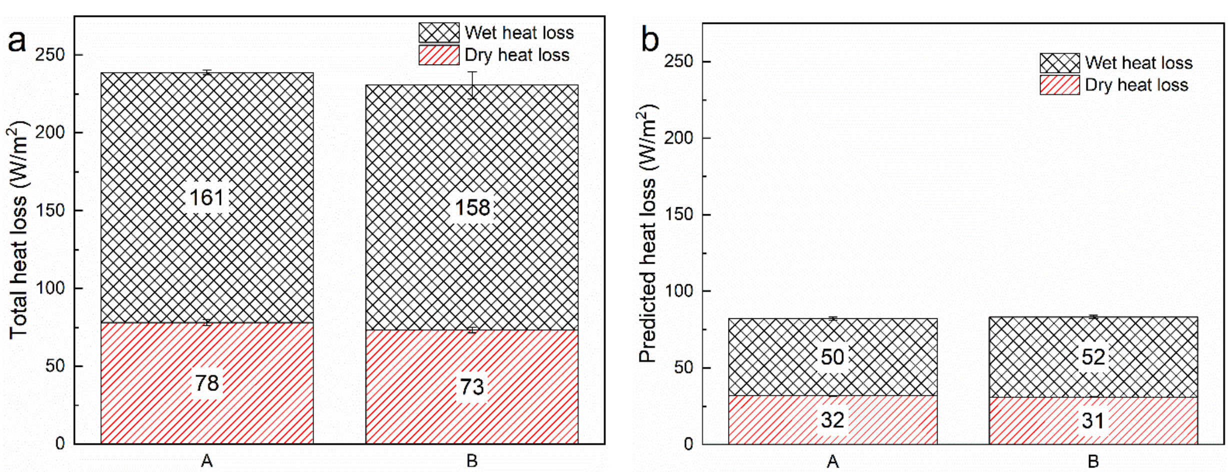

Figure 8-2. (a) Total heat loss measured by sweating guarded hotplate, and (b) predicted total heat loss measured from the sweating manikin

8.3.2 Predicted *THL* measured with the manikin

Compared to the bench level test, the manikin test allows the assessment of garment fit, design, and air layers[82]. A much lower amount of heat loss was observed from the manikin test than from the hotplate tests, as shown in Figure 8-2b. Garment A and B show a predicted total heat loss of 82 and 83 W/m^2, respectively. The heat loss was divided into dry and wet components and it could be found that wet heat loss through evaporation is a major pathway to release heat. No significant difference between heat loss in garment level was observed (p<0.05).

8.3.3 Physiological manikin results

The physiological manikin is a good alternative to a human wear trial and can be used to predict the physiological effects of clothing[98]. Core body temperature (*Tre*), skin temperature (*Tsk*), cardiac output (*CO*) and sweating rate (*Swa*) when wearing garments A or B (with DWR in thermal liner) were predicted over the 130-min-long protocol (Table 8-2).

8.3.3.1 Predicted core body temperature

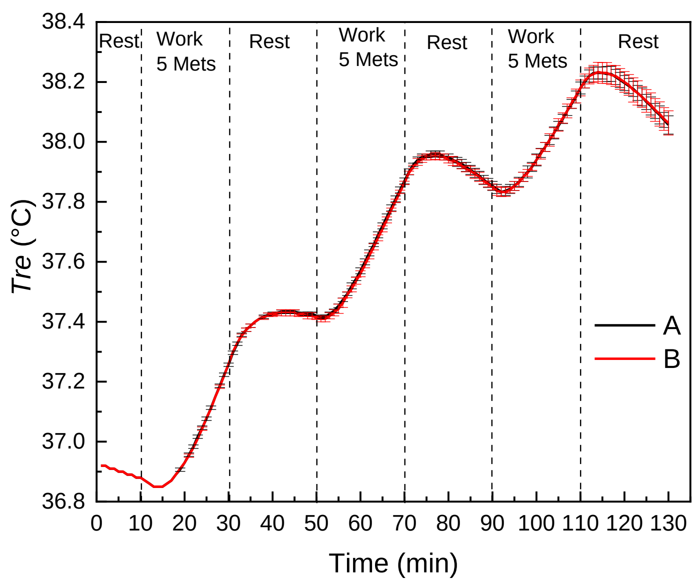

Figure 8-3. Predicted average core temperature (*Tre*) for turnout clothing in the environment of 25 °C, 65% RH

The body's core temperature is one of the most important indicators of heat stress and a normal core body temperature should be maintained within a 1°C range of ~ 37 °C by balancing the amount of heat produced in the body (metabolic activity) and heat loss to environment[5, 68, 181, 186]. Figure 8-3 displays the average predicted core temperature for garment A and garment B. The two garments showed no significant difference. The rises and falls of *Tre* correspond to the work and rest cycle. The predicted core body temperature for both garments reached the same maximum value of 38.2 °C after 113 mins into the protocol. This indicates slight heat stress.

8.3.3.2 Predicted skin temperature

Skin is the interface for heat exchange between the human body and environment. The starting skin temperature in a thermal equilibrium environment in this model is 32.6 °C. In Figure 8-4, the average predicted skin temperature for the garments A and B are displayed. No significant difference was identified.

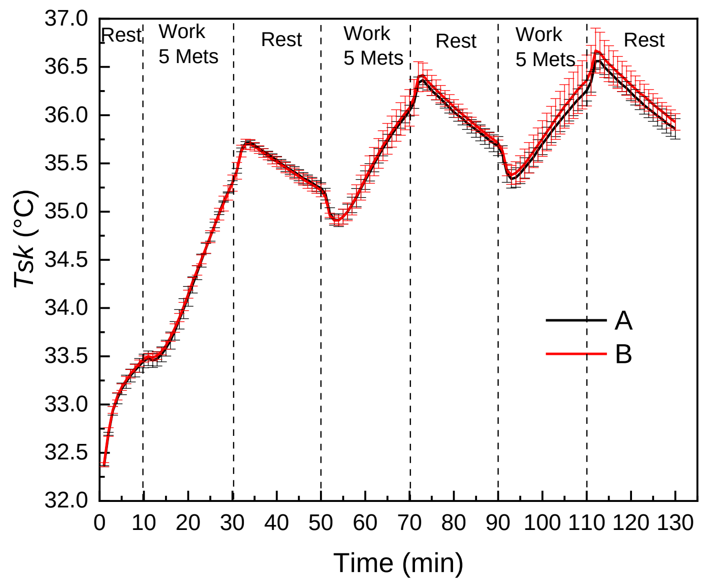

Figure 8-4. Predicted average skin temperature (*Tsk*) for turnout clothing in the environment of 25 °C, 65% RH

8.3.3.3 Predicted cardiac output

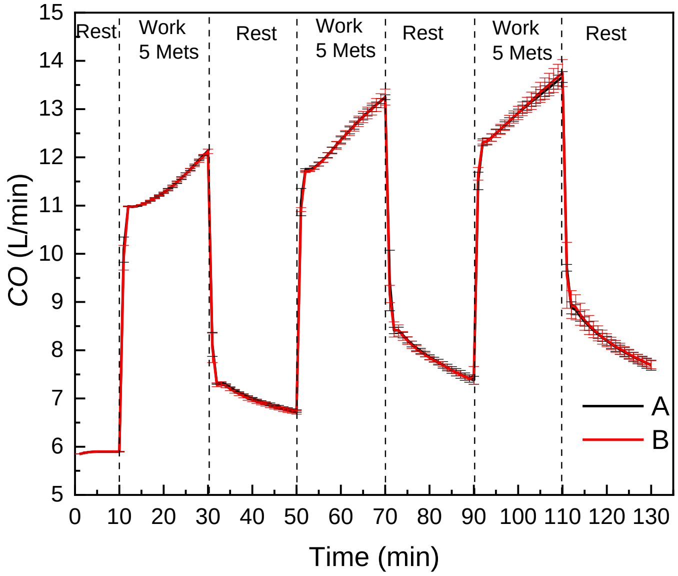

Figure 8-5. Predicted average cardiac output (*CO*) for turnout clothing in the environment of 25 °C, 65% RH

Cardiac output is the amount of blood the heart pumps per minute, and equals to the product of the stroke volume and heart rate[187]. The predicted cardiac outputs during test of each suit in mild conditions over the 130-min protocol are displayed in Figure 8-5. The sharp rises and falls observed in the graph were due to the change of metabolic rates during the work/rest cycle. At the end of the protocol, garments A and B both showed a predicted cardiac output of 7.7 L/min. Similar to predicted core body temperature and skin temperature, the two garments are statistically the same regarding cardiac output.

8.3.3.4 *Predicted sweating rate*

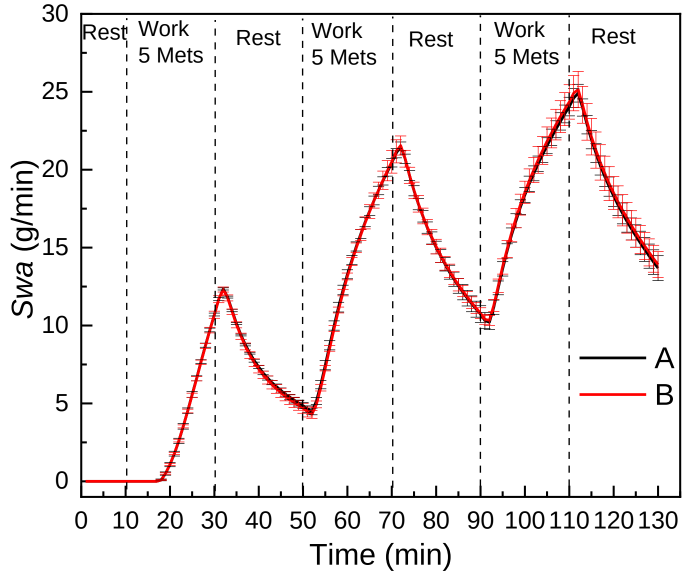

Figure 8-6. Predicted average sweating rates (*Swa*) for turnout clothing in the environment of 25 °C, 65% RH

Sweating is one of the main mechanisms that the human body uses to increase heat loss to the environment in order to maintain a stable body core temperature[188]. Average sweating rates for garments A and B were predicted, and the results are illustrated in Figure 8-6. For the first 17 mins, the sweating rate is zero. After 112 mins into the protocol, a maximum sweating rate of 25 g/min was reached for both turnout garments, close to the maximum allowable sweating rate of 30 g/min in this model. The two garments showed similar predicted sweating rates in the end of protocol (p<0.05).

8.3.3.5 *Weight gain*

The initial weight of garment A and B is 3622 g and 3576 g, respectively. After the physiological manikin test, the weight gain inside turnout clothing was measured immediately and the results are displayed in Figure 8-7. Garment A showed an average 156 g more weight gain than garment B with DWR finishing inside thermal liner (p<0.05).

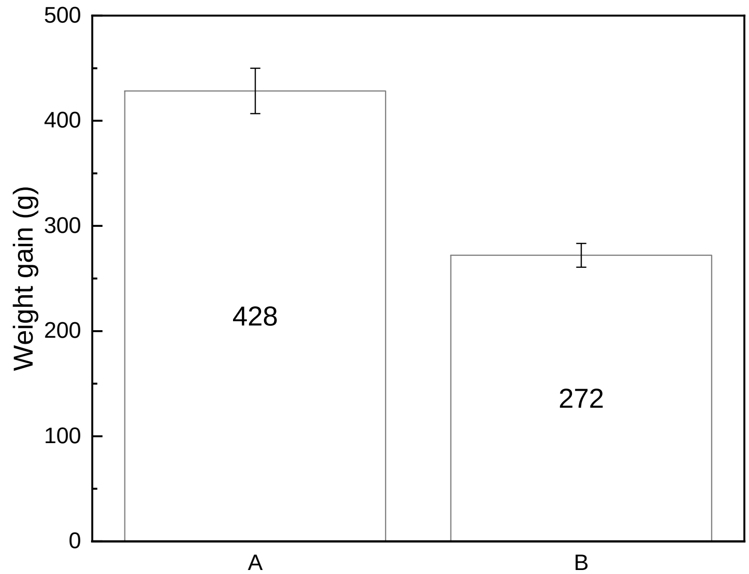

Figure 8-7. Weight gain inside clothing after physiological manikin test

8.4 Discussions

This study focused on the evaluation of the potential effect of DWR finishing inside the thermal liner on the thermal comfort of structural firefighters. The sweating guarded hotplate and sweating manikin tests showed no significant difference regarding the heat release properties in either bench level or garment level between garments A and B. Heat stress results from the imbalance between heat produced inside the body and the heat exchange with the environment. With the same metabolic rate and total heat loss, as expected, there is no significant difference in predicted physiological response between turnout clothing with or without durable water repellent finishing (DWR) in the thermal liner.

One of the key observations is that there is less water inside garment B. In the environment of 25 °C, 65% RH, the water present in turnout clothing may be due to the wicking of water from skin and condensation. The predicted sweating rates when wearing the two garments were similar and it is reasonable to conclude that the difference in wicking properties caused the difference in the weight gain. Thermal liner with DWR finishing could decrease the amount of water by wicking from the skin. Water absorbed by fabric will replace the air voids inside, and decrease the overall insulation since the thermal conductivity of water (0.6 W/m/K) is about 25 times higher than air (0.024 W/m/K)[105]. It is possible that garment A with more water inside could release more heat by conduction. However, this was not reflected as similar heat loss in the manikin test and predicted physiological responses were observed. It is because a slight change in moisture content of clothing only has a small effect on heat release by wet conduction[104].

In this paper, we assumed the metabolic rate to be the same when wearing each of the two garments, doing the same activities. However, it was reported that clothing weight could increase energy consumption[159, 189, 190]. When wearing garment B, the metabolic heat generation may be decreased since it has less weight gain and could cause less heat stress. But this needs further investigation as the weight gain difference is only 156g and may not cause any significant difference in metabolic cost of work.

Comfort is a complicated concept and it was defined by Slater as 'a pleasant state of psychological, physiological, and physical harmony between a human and the environment[191]. Thermophysiological and sensorial comfort are two main aspects of clothing comfort[192]. The first is related to the clothing heat and moisture release properties, as discussed in this paper, and the latter relates to the interaction of the clothing with the tactile response of the skin[169]. If the moisture released from the skin surface is transported by wicking action, a sensation of wetness can be generated that causes the garment to feel clammy[193]. Having DWR in thermal liner may limit the wicking activity and improve sensorial comfort.

Apart from the potential impact on clothing comfort, water trapped inside firefighter turnout gear could affect thermal protection. It was reported that moisture in firefighter protective gear could negatively impact thermal protective performance[143]. Steam burn is another concern. When exposed to thermal radiation, water inside clothing could re-evaporate, and condense on the skin, which may cause steam burns[194]. However, this is not within the scope of our study.

8.5 Conclusions

In this study, we compared the heat release properties of turnout clothing with or without DWR finishing in thermal liner with a sweating guarded hotplate and sweating manikin. The results show that there is no significant difference in heat release properties on fabric level or garment level. We also investigated the potential effect of DWR finishing on human physiological response using a physiological manikin. The two turnout garments showed similar predicted physiological responses in the environment of 25 °C, 65% RH when doing an alternating work/rest protocol of heavy intensity. However, the weight gain for garment B with DWR finishing was found to be significantly lower than for garment A, after the manikin test.

There are some limitations in this study. We only selected the environment of 25 °C, 65% RH due to cost and time. To fully understand the effect of DWR finishing on thermal physiological comfort, more environmental conditions should be selected. Sensorial comfort is of great importance and should also be assessed. In addition, the benefits of DWR finishing in the thermal liner on thermal protective performance should be investigated.

9 Investigation of the Impact of Clothing Reinforcement on Firefighter Heat Stress Using a Physiological Manikin

9.1 Introduction

Firefighting is a physiologically demanding and dangerous occupation. To protect structural firefighters against external hazards, especially thermal injuries, protective clothing consisting of an outer shell, moisture barrier, and thermal liner is required. The thick and bulky protective gear limits heat and moisture release from the human body to the environment. As a result, heat stress becomes a very critical problem among firefighters, and is an important factor behind sudden cardiac deaths, which accounted for 46% firefighter fatalities in 2019[12, 13].

Heat strain requirement is currently mandated in NFPA 1971 (Standard on Protective Ensembles for Structural Fire Fighting and Proximity Fire Fighting), and a minimum total heat loss (*THL*) of 205 W/m^2 through turnout gear base fabrics is required[72]. The total heat loss test, measured with a sweating guarded hotplate, only evaluates the properties of base composites. One of the key limitations is its inability to capture performance at the garment level. Due to the potential for higher heat exposure, certain areas of turnout clothing are reinforced,[195] using materials like foam, leather, and extra thermal liner layers[196]. For example, in a major USA metropolitan city, thick impermeable foam is used on arms and shoulders. Under the current standard, the turnout gear with or without reinforcement would be labeled as having the same *THL* value, as they use the same base composite. Firefighters may falsely assume that the two turnout garments have similar heat release properties, while the addition of the extra materials makes the heat stress worse as they lead to a significant decrease in heat loss[197].

The reinforcement effect on human physiological responses was investigated by Meredith et al. using a standard manikin test and virtual modeling[196]. Compared to control turnout gear, a

0.7 °C increase in core temperature was predicted when wearing a heavily reinforced suit working at 4 Mets (metabolic equivalents) for 1.5 hours in the environment of 21 °C, 50% RH[196]. This demonstrated the negative impact of clothing reinforcement on thermal comfort. One limitation of virtual physiological modeling is that it usually includes simplified clothing models that consider evaporation resistance and thermal resistance of garments are constant during simulation[90, 95].

Compared to virtual physiological modeling, the physiological manikin is a more realistic method. It includes sweating manikin coupled with a human physiological model. The manikin provides the boundary layer interface to the clothing and environment, and generates metabolic heating levels as requested by the regulation model[184, 198]. Burke et al. compared human subjects data with the response of a Newton thermal manikin incorporated with a physiological regulation system based on the Fiala model, and found generally good agreement[97].

The NFPA 1971 standard fails to account for the impact of reinforcement materials on heat loss through turnout gear. The impact of reinforcement materials on physiological response was not fully understood. In this paper, for the first time, we used a physiological manikin to evaluate the potential impact of clothing reinforcement on the human body. The results serve as a basis for improved heat strain requirement in NFPA 1971 and could help mitigate heat stress problems in firefighters.

9.2 Experimental methods

9.2.1 Garments

Two garments with the same base composites (Table 9-1) were selected. Garment B had foam reinforcement on arms and shoulders, as shown in Figure 9-1. The foam padding (3.85 mm thick) is a flame-resistant, impermeable, nonabsorbent, flexible silicone foam material. This garment is currently used by one of the largest metropolitan cities in the USA. The purpose of adding foam materials is to increase the thermal protection of certain body areas. The amount of foam reinforcement in the coat was estimated to be 37%.

Table 9-1. Physical properties of individual component

	Picture	Material structure	Weight (g/m^2)	Thickness (mm)
Outer shell	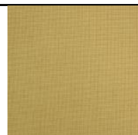	35% PBI (polybenzimidazole), 65% para-aramid, twill weave	239±0.6	0.40±0.01
Moisture barrier		Bicomponent e-PTFE (expanded Polytetrafluoroethylene) membrane on meta-aramid woven fabric	163±1.4	0.36±0
Thermal liner		Two layers of aramid spunlace nonwoven quilted to 60% meta-aramid filament / 40% spun yarn twill weave (meta-aramid, FR rayon)	272±2.2	1.39±0.04

Note: The garment area was estimated to be 5 m^2 based on the garment and fabric weight.

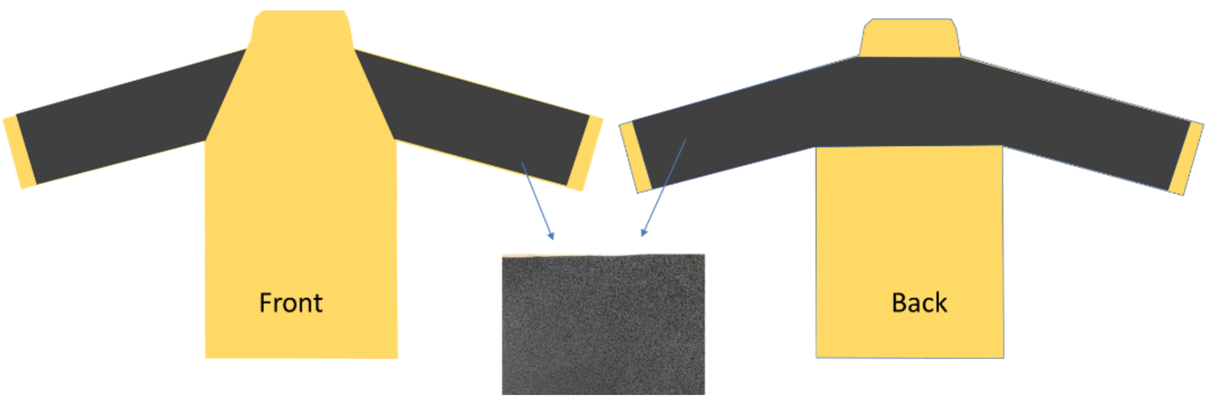

Figure 9-1. Coat of garment B with reinforcement

9.2.2 Sweating manikin test

Compared to a sweating guarded hotplate test, the sweating manikin test can capture the effect of garment design on heat release properties. Garment level tests were conducted with a

34-zone Newton sweating manikin (Thermetrics, Seattle, USA) according to ASTM F1291-16 (Standard Test Method for Measuring the Thermal Insulation of Clothing Using a Heated Manikin)[85] and ASTM F2370 -16 (Standard Test Method for Measuring the Evaporative Resistance of Clothing Using a Sweating Manikin) [87]. Insulation measurements were conducted at 15 °C, 50% relative humidity (RH), and evaporative resistance tests were performed at 35 °C, 40% RH. The manikin surface was kept at 35 °C to simulate skin temperature. Both static and dynamic manikin tests were performed. During the wet test in the static condition, we had to lower the ambient temperature from 35 °C to 32 °C in order to reach a steady state. During the dynamic test, the manikin was driven mechanically by the walking stand at a speed of 45 DSPM (double step per minute) and this could account for pumping effects. Three replicates of each garment were tested.

To simulate total heat loss (*THL*) measured with sweating guarded hotplate, a predicted heat loss value ($Q_{manikin}$, W/m^2) in the environment of 25 °C, 65% RH was estimated using the total evaporative resistance (R_{et}, kPa·m^2/W) and thermal insulation value (R_t, K·m^2/W) measured by the manikin, according to equation 8.1[88].

9.2.3 Physiological manikin

The physiological manikin system composed of a 34-zone Newton sweating manikin (Thermetrics, Seattle, USA) coupled with TAITherm v.13.0.0 (Thermoanalytics, Calumet, MI USA) was used in this study. TAITherm implements the Fiala physiological model to predict physiological responses of an average 80 kg male, and more details can be found in papers by Burke[97, 184]. This system was proved to be a useful tool at predicting the physiological outputs of a firefighter wear trial in a recent study[185]. During the tests, turnout suits were worn together with a short-sleeved cotton shirt, boxer brief, socks, firefighting gloves, helmet, and athletic shoes.

The bottom of the pants was taped up to simulate the pant to boot interface, a common practice in wear trial protocols[199]. Three replicates of each garment were tested. Figure 9-2 displays the pictures of the fully dressed manikin in rest condition and walking.

Figure 9-2. Picture of fully dressed physiological manikin in (a) rest and (b) walking condition

The ambient condition of 25 °C, 65% RH was selected to represent the environment that firefighters may experience. Before testing, the manikin was preheated to a set of starting skin temperatures inside the environmental chamber. After reaching the equilibrium condition (±0.05 °C of preset skin temperatures), the test protocol in Table 9-2 would be executed. The 130 min-long protocol included three work/rest cycles. Each test was repeated three times.

Table 9-2. Testing protocol

Period	Duration	Metabolic rates	Walking speed
1	10 mins	1 Met	0 DSPM*
2	20 mins	5 Mets	55 DSPM
3	20 mins	1 Met	0 DSPM
4	20 mins	5 Mets	55 DSPM
5	20 mins	1 Met	0 DSPM
6	20 mins	5 Mets	55 DSPM
7	20 mins	1 Met	0 DSPM

* DSPM means double step per minute. The manikin was driven by a mechanical system to simulate walking activities.

9.2.4 Statistical analysis

The statistical analysis was performed using JMP Pro 15 (SAS, Cary, NC, USA). The predicted heat loss from manikin, and the predicted physiological response at the end of protocol of garment A and B were compared using two sample t-tests. $P < 0.05$ was considered significant.

9.3 Results

9.3.1 *THL* from sweating guarded hotplate and manikin

Fabric-level *THL* tested by sweating guarded hotplate is the only index for evaluating materials related heat strain potential as specified in NFPA 1971 Standard. The *THL* of the three-layer base composite used in garment A and B is 238 W/m^2, larger than the minimum requirement of 205 W/m^2. This means both the turnout clothing with and without reinforcement meets the heat strain requirement In NFPA 1971. Compared with bench level tests, the manikin test allows the assessment of garment fit, design, and air layers[82]. The predicted heat loss from static and dynamic manikin test for the control suit (A) and the garment with foam reinforcement (B) are shown in Figure 9-3. The heat loss was divided into dry and wet components. It could be observed that wet heat loss through evaporation is a major pathway to release heat. The results indicate that the control turnout clothing (A) could release 5.3 W/m^2 and 11.7 W/m^2 more heat than the clothing with foam reinforcement (B) in the static and dynamic tests, respectively ($p<0.05$).

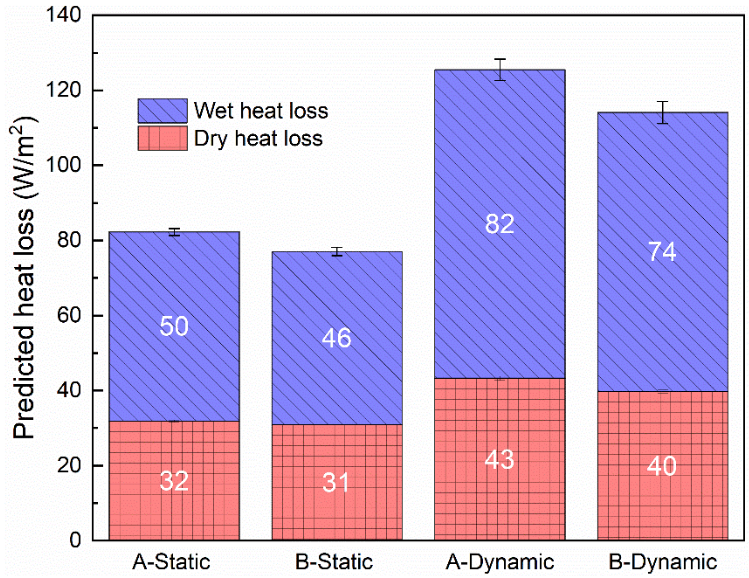

Figure 9-3. Predicted heat loss of turnout clothing (A & B) from static and dynamic manikin test

The predicted heat loss of each zone from the dynamic manikin test is shown in Figure 9-4. In garment B, the arms and shoulder parts have the thick impermeable foam reinforcement, and this can be reflected in the heat loss data. The average predicted heat loss in the arms is 67 W/m^2 less than wearing the control garment (A) without foam reinforcement.

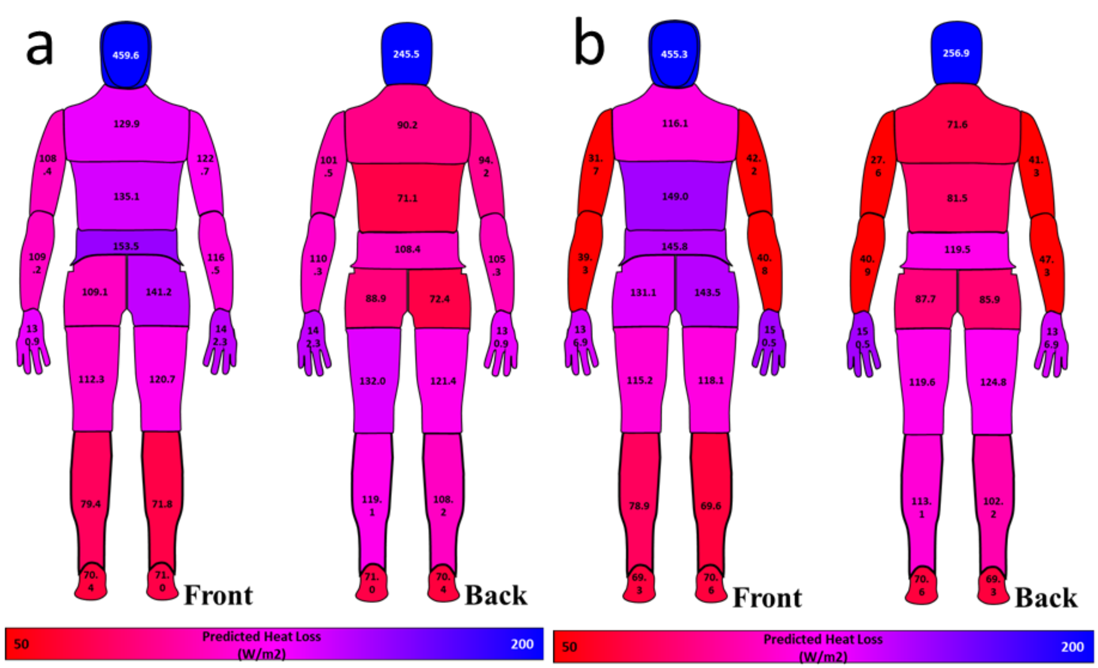

Figure 9-4. Predicted heat loss (W/m^2) of each body zone from dynamic manikin test: (a) garment A, and (b) garment B.

9.3.2 Physiological manikin results

The physiological manikin is a good alternative to human wear trial and can be used to predict the physiological effects of clothing. The physiological manikin acts like a real human and could generate reasonable results on both physiological responses and psychological perceptions[98]. Core body temperature (*Tre*), skin temperature (*Tsk*), cardiac output (*CO*) and sweating rate (*Swa*) when wearing the reinforced turnout gear (B) and control garment (A) in the environment of 25 °C, 65% RH were predicted.

9.3.2.1 Predicted core body temperature

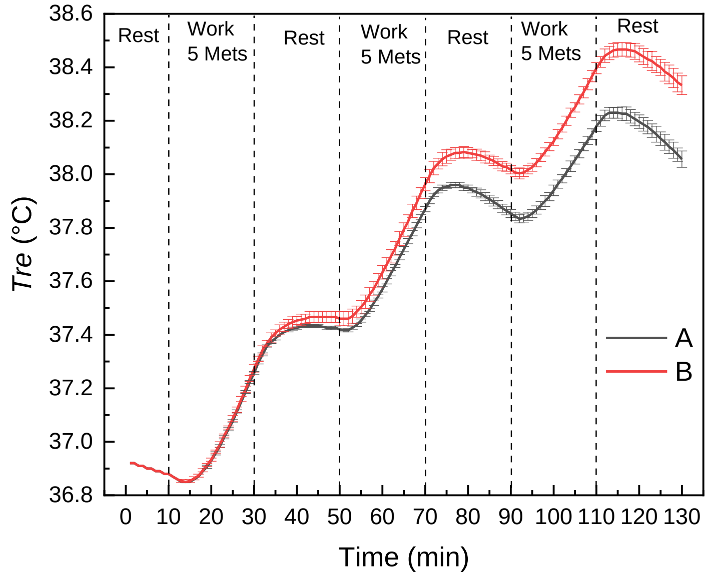

Figure 9-5. Predicted average core temperature (*Tre*) for turnout clothing

The human body tries to maintain a constant core temperature around 37 °C by balancing the amount of heat produced in the body (metabolic activity) and heat loss to environment. Core body temperature is a direct indicator of heat stress[5, 186]. Figure 9-5 displays the average predicted core temperature for control garment (A) and reinforced turnout clothing (B) in the environment of 25 °C, 65% RH. Core body temperature differences between the two suits emerges from ~40 mins into the protocol, and the gap between them become larger with time. At the end of the protocol, the difference in predicted core temperature between garment B and garment A is 0.28 °C (p<0.05).

9.3.2.2 Predicted skin temperature

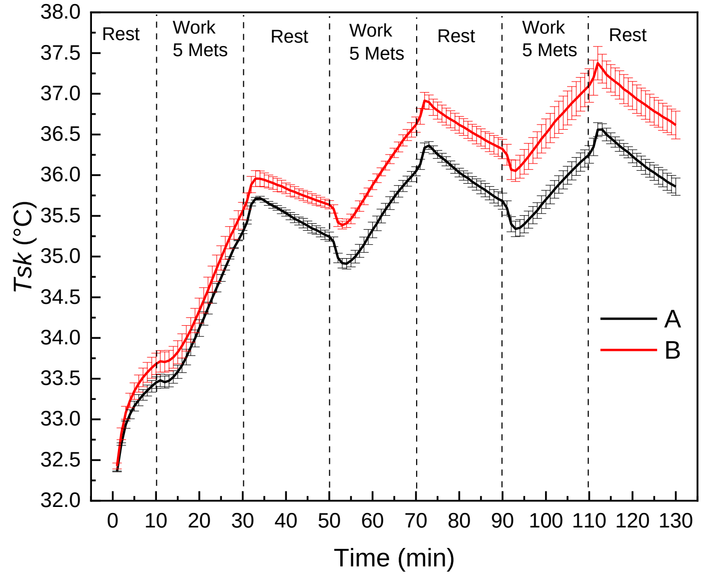

Figure 9-6. Predicted average skin temperature (*Tsk*) for turnout clothing

Skin temperature normally shows more pronounced changes compared with core body temperature[158]. The starting skin temperature in thermal equilibrium environment is 32.6 °C. In Figure 9-6, the average skin temperature for the garment A and B is displayed. The same trend is observed compared to Figure 9-5, where the garment with reinforcement shows a higher skin temperature than the control garment (p<0.05). The difference reaches 0.76 °C by the end of protocol.

9.3.2.3 Predicted cardiac output

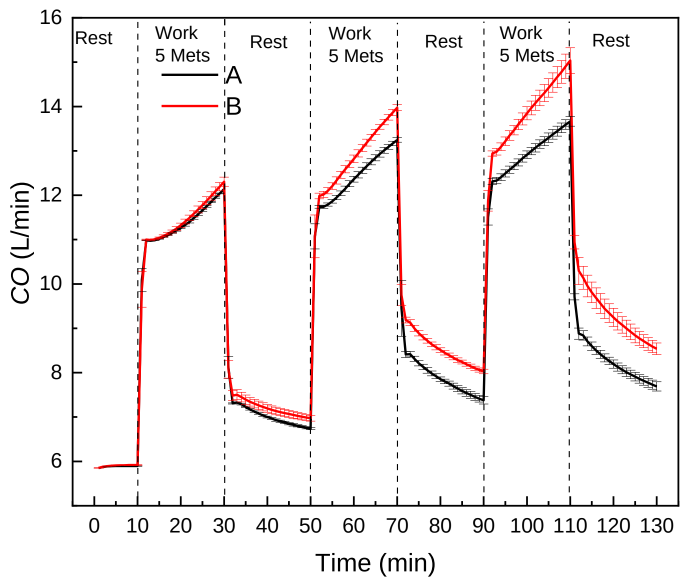

Figure 9-7. Predicted average cardiac output (*CO*) for turnout clothing

Cardiac output is the amount of blood the heart pumps per minute, and equals the product of the stroke volume and heart rate[187]. The predicted cardiac outputs of each suit over the 130-min protocol are displayed in Figure 9-7. The sharp rises and falls observed in the graph are due to the change of metabolic rates during the work/rest cycle. At the end of the protocol, the difference in predicted cardiac output between garment A and garment B is 0.85 L/min (p<0.05), indicating higher strain on the cardiovascular system when wearing garment B.

9.3.2.4 Predicted sweating rate

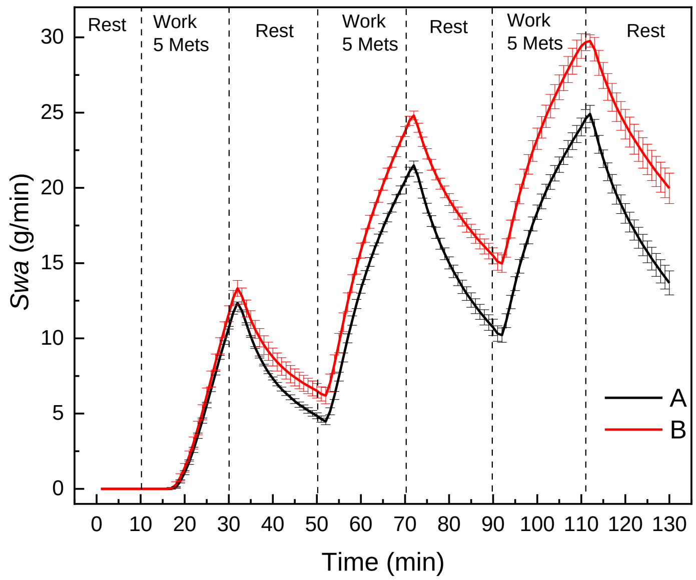

Figure 9-8. Predicted average sweating rates (*Swa*) for turnout clothing

Sweating is one of the main mechanisms that the human body uses to increase heat loss to the environment in order to maintain a stable body temperature. The average sweating rate for garment A and B in the environment of 25 °C, 65% RH was predicted, and the results are illustrated in Figure 9-8. The maximum sweating rate is 30 g/min in this model, and garment B shows a maximum predicted sweating rate of 29.8 g/min after 112 mins into the protocol. In the end, garment B exhibits a significantly higher sweating rate than garment A (p<0.05).

9.4 Discussions

This study focused on the evaluation of clothing reinforcement effect on the thermal comfort of structural firefighters. Fabric level testing of the three-layer base composite shows a much higher *THL* than either the static or dynamic manikin test. The reason is that the garment has air layers, reinforcement, pocket, and overlaps between coat and pant, etc., that add extra resistance to heat and moisture transfer. The predicted heat loss from the manikin (Figure 9-3) clearly reveals the significantly detrimental effect of clothing reinforcement on heat loss.

Evaporation of perspiration is a powerful mechanism for the human body to release heat[200]. The thick foam reinforcement not only decreases the dry heat loss by conduction, convection, and radiation, but also blocks the way to lose heat by evaporation due to its impermeability. As a result, incorporating a foam reinforcement on the arm and shoulder section would reduce an overall heat loss of 5.3 W/m^2 and 11.7 W/m^2 in the static and dynamic manikin test. The movements of the manikin could pump air between different clothing layers and force the air exchange with ambient air, which is called pumping effect[34]. In addition to the enclosed air layer, the movement could also decrease the resistance of surrounding air layer by increasing airflow[34]. As a result, a higher heat loss compared to the static condition was observed. The body sections with clothing reinforcement show significantly lower heat loss compared to the control garment. (Figure 9-4). However, the current standard (NFPA 1971) only mandates fabric-level *THL*, and the two garments would be labeled as having the same level of heat loss, which may cause potential heat stress issues among firefighters.

The negative effect of wearing turnout clothing with foam reinforcement was further demonstrated by predicted physiological responses using a physiological manikin. A significantly higher core body temperature, skin temperature, cardiac output, and sweating rate were observed for garment B (Figure 9-5 to 9-8) (p<0.05). Core body temperature is a direct indicator of heat stress,[201] and a small increase in internal temperature (~3 °C) can lead to injury and even death[202]. The difference between the two garments reaches 0.28 °C after the 130-min work/rest protocol in this study. When the human body is in a stressful condition, such a difference in core temperature could play a significant role. For example, in a recent firefighter wear trial involving 3 turnout clothing suits in the environment of 40 °C, 20 % RH, the garment with the lowest evaporative resistance resulted in a maximum difference of 0.19 °C compared with the worst turnout clothing[135]. Such a small difference in core temperature was demonstrated to be significant as 4 out of 10 firefighters wearing the worst turnout clothing were not able to finish the 95-min-long protocol due to high heart rates, associated with high-level heat strain[135]. Heat stress could add work to heart, as more blood needs to be delivered to skin for the heat release purpose[10]. This can be reflected by the cardiac output data in Figure 9-7 where wearing garment B would put more strain on the heart, increasing the risk of cardiac events. The skin temperature and sweating rate also tell the story that the garment with reinforcement would induce more heat stress.

This paper again reveals the benefits of manikin level testing compared to the bench level test using a sweating guarded hotplate. DenHartog et al. studied the heat loss properties of protective clothing for wildland firefighters from fabric level and garment level, as well as their impact on human thermal comfort through wear trial[88]. It was found that the manikin level test was more effective in predicting human responses[88]. Similar findings were also reported[82, 158, 196].

This study was not intended to discourage the use of reinforcement in the turnout gear, as reinforcement helps increase thermal protection in high-risk body sections[195]. Thermal protection and thermal comfort should be balanced by limiting the amount of reinforcement materials used. In addition, instead of using impermeable foam, an extra layer of breathable materials, such as thermal liner, may mitigate potential heat stress by allowing some evaporative heat loss. However, future studies are required to understand how different reinforcement materials could affect firefighters thermal comfort in various ambient environments.

9.5 Conclusions

For the first time, the physiological impact of clothing reinforcement was studied with both a standard manikin and physiological manikin in this paper. The results show that the foam reinforcement has a substantial effect on heat loss and thermal comfort. The turnout gear with foam reinforcement demonstrates a much higher sweating rate, skin temperature, cardiac output, and core temperature, and could cause more heat stress on the human body. The garment related heat strain requirement in the current standard (NFPA 1971) only relies on the total heat loss (*THL*) data from bench level testing, and lacks the ability to account for the effect of clothing reinforcement. It is important that the heat release properties based on the manikin test should be proposed. It is highly recommended that NFPA should regulate the maximum amount and the heat release properties of the reinforcement materials used in turnout clothing. Results from this study may also help designers and manufacturers make turnout gear with better heat loss properties, reducing the potential risk of heat stress.

10 Study the Influence of Turnout Materials on Firefighter Heat Stress in Mild and Hot Environments Using a Physiological Manikin

10.1 Introduction

Firefighting is one of the most strenuous occupations, and together with the requirement to wear protective clothing, substantial physiological demand can be placed on the body, leading to heat stress[3]. Sudden cardiac events have been a leading cause of firefighter fatalities, and accounted for 46% of firefighter deaths in 2019[12]. Heat stress can exacerbate the cardiovascular strain experienced by firefighters and is one of the leading factors of sudden cardiac events[13]. Turnout gear is considered as a significant contributor to firefighter heat stress.

The NFPA 1971 Standard for structural firefighter PPE establishes a minimum heat strain requirement for turnout suits materials based on measured Total Heat Loss or *THL*. Total heat loss (*THL*), measured at 25 °C, 65% RH with a sweating guarded hotplate, was first introduced to NFPA 1971 (Standard on Protective Ensembles for Structural Fire Fighting and Proximity Fire Fighting) in 2000. A minimum amount of 130 W/m^2 for total heat loss through firefighter composites was set. In 2007, the *THL* requirement was further raised to 205 W/m^2. Because the *THL* requirement is strictly valid only for predicting turnout suit related heat strain in mild environmental conditions (25 °C, 65% RH), there is interest in examining performance metrics in other environmental conditions[156]. This has led to consideration of R_{ef} requirement, which is evaporative resistance measured at 35 °C, 40% RH covered in ASTM F 1868, Part B[75]. It is critically important to examine the suitability of either *THL* or R_{ef} as heat strain index for firefighter turnout gear.

Previous studies have focused on defining the correlation between the total heat loss (*THL*) and heat strain in firefighter turnouts[77-79, 203]. These studies demonstrated that the *THL* could correlate with firefighter thermal comfort. Results of studies by Barker et al.,[77, 78] and Stull et al.[79] help set the performance limit of firefighter composites as total heat loss of 130 W/m^2 at 2000 and 205 W/m^2 at 2007, respectively. In a recent study by DenHartog et al.,[199] physiological response of firefighters wearing three different turnout gears with similar *THL* value but different R_{ef} values were investigated in an environment of 40 °C, 20% RH through a human wear trial. The results showed that under hot conditions, garments with different R_{ef} values induced significant differences in heat strain for the wearers. Firefighters work in a wide range of environments. Further studies are needed to investigate the performance of turnout gear in a range of environments. In addition, turnout gears with large distributions of *THL* and R_{ef} values should be selected.

Human wear trials are demanding due to high costs and ethical restrictions, and are often difficult to interpret due to intra- and inter-subject variability[89]. We chose to use a physiological sweating manikin methodology because of the advantages gained by minimizing the variability associated with garment fit, and the variability in the physiological response of human evaluators in a clothing wear trial. Burke[97] and Deaton[185] compared human subjects data with the response of a Newton thermal manikin incorporated with a physiological regulation system based on the Fiala model, and found general good agreement. It has been well established that the physiologically controlled sweating manikins act similar to a real human, and could generate reasonable results on both physiological response[98].

In order to answer the question whether *THL* or R_{ef} is better at predicting firefighter physiological responses, the physiological manikin was used to predict the physiological response of firefighters wearing five different turnout gears with a wide range of *THL* and R_{ef} distribution. Three environmental conditions were selected (25 °C, 65% RH; 35 °C, 40% RH;

and 40 °C, 28% RH). This study examines the correlation between the two thermal comfort indexes (*THL* and R_{ef}) and the human physiological responses in different environmental conditions.

10.2 Method

10.2.1 Material

Five turnout composites composed of the same outer shell, but different moisture barriers or thermal liners were selected. Table 10-1 lists the structure of each component used. Bi-CompA, Bi-CompD, and Bi-CompE were bicomponent e-PTFE (expanded-polytetrafluoroethylene) moisture barriers, featuring a thin solid hydrophilic film coated on top of e-PTFE microporous membrane. The evaporative resistance of bicomponent moisture barriers depends on moisture absorbed by the membrane[156]. Bi-CompA, and Bi-CompD were NFPA 1971 compliant and commercially available products. Bi-CompE was a specially designed bicomponent membrane with a proprietary coating of hydrophilic layer. Sample C contained a microporous e-PTFE membrane without any coating applied to the surface. Moisture barrier Bi-CompE and PTFE were special moisture barrier constructs obtained for this study. Turnout composite D had two 2-layer thermal liners, with a PTFE moisture barrier sandwiched between them. Composite B included a 1-layer thermal liner, and it was a thinner version of Garment A. Composites A and D were NFPA 1971 certified. We believed composite E was able to pass NFPA 1971 Standard. Garment C did not meet the *THL* (total heat loss) requirement and Garment B had a lower *TPP* value (thermal protective performance) than that required in NFPA 1971.

Table 10-1. Description of turnout materials

ID#	Thermal liner		Moisture Barrier		Weight (g/m^2)	Thickness (mm)
A	2-layer spunlace	Two layers of aramid spunlace nonwoven quilted to 60% meta-aramid filament / 40% spun yarn twill weave (meta-aramid, FR rayon) (278 g/m^2, 1.36mm)	Bi-CompA	Commercial bicomponent e-PTFE* membrane on meta-aramid woven fabric (163 g/m^2,0.36 mm)	674±1.9	2.15±0.07
B	1-layer spunlace	A thinner version of the liner in system 1 with one layer spunlace (219 g/m^2, 0.96mm)	Bi-CompA		621±1.4	1.72±0.05
C	2-layer spunlace /2-layer spunlace**		PTFE	e-PTFE microporous membrane on meta-aramid woven fabric (141 g/m^2, 0.36 mm)	924±4.1	3.54±0.08
D	2-layer spunlace		Bi-CompD	Commercial bicomponent e-PTFE membrane on meta-aramid nonwoven (155 g/m^2, 0.67 mm)	666±1.4	2.46±0.04
E	2-layer spunlace		Bi-CompE	Prototype bicomponent e-PTFE membrane on meta-aramid woven fabric (226 g/m^2, 0.45 mm)	736±2.5	2.24±0.02

Note: All constructions shared the same outer shell (twill weave, 65% para-aramid, 35% PBI, golden color, weight:241 g/m^2, thickness:0.39 mm) *e-PTFE: expanded-polytetrafluoroethylene. **Composite C had two 2 layer spunlace thermal liners, where the moisture barrier was sandwiched between them. The garment area was estimated to be 5 m^2 based on the garment and fabric weight.

10.2.2 Procedure

The physiological manikin system used a 34 zone Newton manikin (Thermetrics, Seattle, USA) coupled with the TAITherm (v.12.1.1, Thermoanalytics, Calumet, MI, USA) human comfort model. The articulated manikin is capable of flexible movement of its arms and legs.

The manikin system incorporates an external walking stand that can be used to simulate a walking motion. The model is based on the Fiala thermoregulation model[97, 185]. The system collects environmental data and measures changes in the temperature of the manikin surface every 900 milliseconds. We used these measurements, along with manually entered values of metabolic work rates, to predict the physiological response (core and skin temperature, sweating, cardiac output, etc.) of an average male weighing 80 kg. Burke et al. provided a detailed explanation of the physiological manikin model control system[97].

All the turnout suits were of identical design and sized to fit the sweating manikin. We conducted controlled chamber studies in three different environmental conditions: mild work environment (25 °C, 65% RH), and two hot ambient environments. We included hot conditions (35 °C, 40% RH, 40 °C, 28% RH) because they represent thermally stressful environments encountered by firefighters. The mild chamber condition was equivalent to the testing conditions used in the standard *THL* test method (25 °C, 65% RH). One of the hot environment conditions was equivalent to the conditions used in the R_{ef} test procedure (35 °C, 40% RH).

Table 10-2. Testing protocol

		25 °C, 65% RH		35 °C, 40% RH		40 °C, 28% RH	
Period	Duration	Metabolic rates	Walking speed	Metabolic rates	Walking speed	Metabolic rates	Walking speed
1	10 mins	1 Met	0 DSPM*	1 Met	0 DSPM	1 Met	0 DSPM
2	20 mins	5 Mets	55 DSPM	4 Mets	47 DSPM	4 Mets	47 DSPM
3	20 mins	1 Met	0 DSPM	1 Met	0 DSPM	1 Met	0 DSPM
4	20 mins	5 Mets	55 DSPM	3.5 Mets	40 DSPM	2.5 Mets	30 DSPM
5	20 mins	1 Met	0 DSPM	1 Met	0 DSPM	1 Met	0 DSPM
6	20 mins	5 Mets	55 DSPM	3.5 Mets	40 DSPM	2.5 Mets	30 DSPM
7	20 mins	1 Met	0 DSPM	1 Met	0 DSPM	1 Met	0 DSPM

* DSPM means double step per minute. The manikin was driven by a mechanical system to simulate walking activities.

Table 10-2 summarizes the work-rest protocol used to evaluate turnout related heat strain at different ambient environmental conditions. We designed the protocols to produce heat strain sufficient to cause core temperature to rise to between 38 °C and 39 °C. The work rate needed to produce this level of heat strain depended on environmental conditions. The protocols included environmental conditions, work rates and work rest cycles that reasonably represent firefighter activities and environmental conditions encountered in structural firefighting response scenarios.

We tested each turnout suit in triplicate in each of the environmental conditions maintained in a climate-controlled chamber. To enable maximum heat loss, we tested the turnout suits configured on the sweating manikin with the manikin wearing only a t-shirt (large size, 100% cotton), boxer brief (medium size, 100% cotton), and socks (100% cotton) as undergarments. (Figure 10-1a) The manikin wore the basic elements of a structural firefighter ensemble including turnout suit, helmet, and gloves. We replaced boots with tennis shoes for ease of dressing. We taped the pant-leg interface to limit air exchange, a common practice in wear trial protocols[199]. The manikin did not wear a self-contained breathing apparatus (SCBA) or facepiece (Figure 10-1b).

We operated the sweating manikin in dynamic mode during the working phase to enable realistic simulation of the effects of walking on air circulation in the microclimate formed between the manikin form and turnout suit (Figure 10-1c). Because the tested turnouts were of identical design, we expected garment effects to be the same for all of the study materials.

Figure 10-1. Picture of the physiological manikin in (a) undergarments; fully dressed and tested in (b) static condition during rest phase and (c) walking condition during the working phase

10.2.3 Statistical analysis

The statistical analysis was performed using JMP Pro 14 (SAS, Cary, NC, USA). The predicted physiological responses of different garments at the end of the protocol were compared using one-way analysis of variance (ANOVA), followed by Tukey's honestly significant difference (HSD). A *p*-value less than 0.01 indicates a significant difference**.**

10.3 Results and discussion

Basic properties of composites used in turnout garments are displayed in Table 10-3. NFPA 1971 has a minimum *TPP* (thermal protective performance) requirement of 35 cal/cm^2 [72]. Heat protection and thermal comfort have always been viewed as conflicting aspects[69]. *THL* can be increased by reducing the thickness and weight of firefighter composites, but this may be at the cost of *TPP*. For instance, garment B had a higher *THL* and lower *TPP* value (33 cal/cm^2) compared to garment A, due to its thinner thermal liner (Table 10-1). Garment C showed a *THL* of only 177 W/m^2, which was 28 W/m^2 less than the minimum *THL* requirement of 205 W/m^2 as in NFPA 1971. *TPP* is mainly determined by insulation, and garment C with two thermal liners showed the highest *TPP* level. R_{ef} measured at 35 °C, 40% RH showed a different ranking, demonstrating the change in material properties. In *THL* ranking, garment C was the worst, while in R_{ef} rating, garment C became the best one. Another example demonstrating the fundamental differences between heat strain indexes is composite E. It met the minimum *THL* requirements of the NFPA 1971 Standard while, with a R_{ef} rating of 70 Pa·m^2/W, having the highest measured evaporative resistance. The purpose of this research was to find out how *THL* or R_{ef} correlated with predicted human physiological responses in different environmental conditions.

Table 10-3. Properties of firefighter ensembles

Code	*THL* (W/m^2)	R_{ef} (Pa·m^2/W)	*TPP* (cal/cm^2)
A	239±0.9	27±0.3	39±0.8
B	271±4.3	24±0.8	33±1.2
C	177±7.6	24±0.7	>60
D	247±4.7	37±1.4	42±0.3
E	213±8.5	70±6.4	41±1.4

THL (total heat loss) and R_{ef} (intrinsic evaporative resistance) were conducted according to ASTM F 1868[75]. *TPP* (thermal protective performance) was conducted according to NFPA 1971[72].

10.3.1 Predicted physiological responses

10.3.1.1 Body core temperature (Tre)

The human body tends to maintain a core temperature around 37 °C by balancing the heat produced in the body (metabolic activity) and heat exchange with the environment[204]. Core temperature data directly indicates heat strain experienced by the wearers[158]. Figure 10-2 shows that the effects of the mild-climate work protocol on body core temperature are small and cumulative over the duration of the work and rest for all the turnout systems evaluated. Observable differences between different turnout systems emerge only near the end of the two-hour wear protocol with about 0.14 °C difference in *Tre* across all systems. These data show that producing a noticeable increase in core temperature in a mild environment required alternating periods of hard work. Most significantly, in a mild environment, the *THL* heat strain index accurately rates the expected effects on physiological heat strain for this group of turnout systems. It accurately predicts that the low *THL* turnout system C will produce the largest increase in body core temperature. This result indicates that the thicker, double thermal liner components incorporated in turnout system C produce a highly insulating composite structure that lowers non-evaporative heat loss through the system. At the same time, system C has a R_{ef} index of 24 Pa·m^2/W, indicating its ability to transmit evaporative heat.

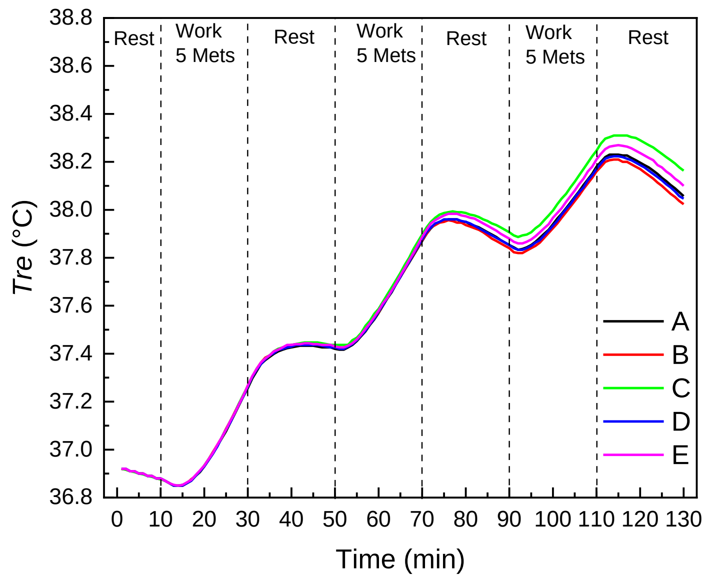

Figure 10-2. Predicted core temperature rise in a mild environment (25 °C, 65% RH)

Figure 10-3 shows the predicted effects of work protocols on body core temperature while wearing different turnout systems in hot environments. These graphs show that the core temperature rise produced by turnout systems with high R_{ef} heat strain ratings occurs more rapidly in the hot protocol wear simulations than observed in the mild-climate evaluation (Figure 10-2). Observed differences in core temperature (*Tre*) between turnout systems made with less breathable turnouts (systems D and E) emerge after about an hour in hot climate conditions, even though work needed to produce a heat stressful condition in the hot-climate protocols is less intense than required in the mild-climate protocol (Table 2). We observed that comparative differences in the core temperature at the end of protocol among systems with different evaporative resistance (R_{ef}) indexes are greater than observed in the mild-climate conditions: about 0.37 °C difference in the hottest condition (40 °C, 28% RH) vs. 0.14 °C difference in *Tre* among systems in the mild condition (25 °C, 65% RH). Most significantly, these data demonstrate that the R_{ef} heat strain index accurately ranks the heat strain performance of the study turnout systems. They also show that *THL* is not a useful predictive index of turnout heat strain in hot ambient conditions. Therefore, systems D and E have high R_{ef} ratings accurately indicative of their poor heat strain performance in hot environments. These turnout systems nevertheless pass the 205 W/m^2 *THL* heat strain requirements in the current edition of NFPA 1971 Standard. All the while, the worst performer in terms of *THL* (system C) which would not pass the NFPA 1971 requirements performs the best in these hot environments due to its low R_{ef} value.

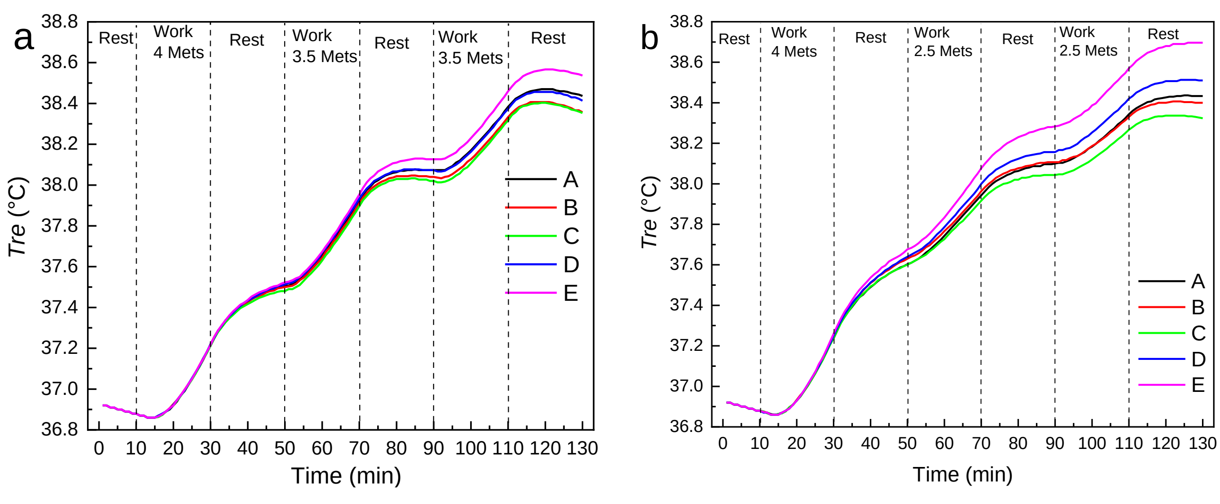

Figure 10-3. Predicted core temperature in hot conditions: (a) 35 °C, 40% RH, (b) 40 °C, 28% RH environment

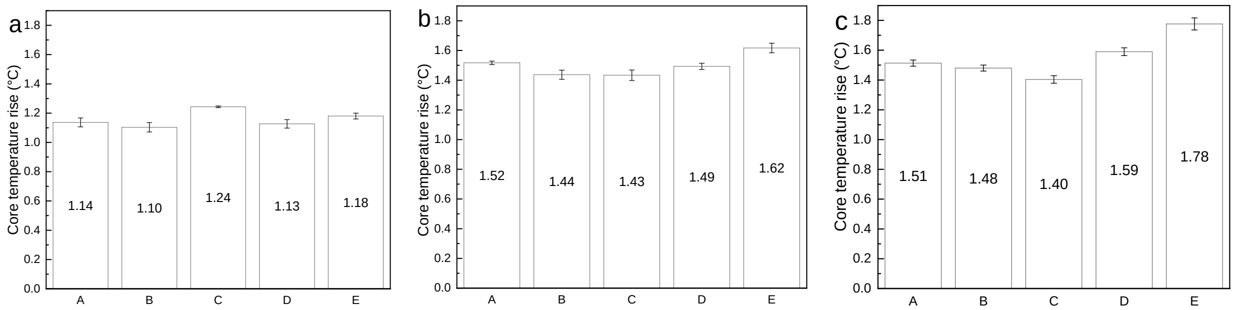

Figure 10-4. Predicted core body temperature rise at the end of the protocol in (a) 25 °C, 65% RH environment, (b) 35 °C, 40% RH environment, and (c) 40 °C, 28% RH environment

Figure 10-4 compares the core temperature rise at the end of the wear protocol for each of the turnout systems. We observed statistically significant differences in the predicted core temperature rise that is associated with the *THL* and R_{ef} ratings of the composite systems used in the construction of the otherwise identical turnout suits. The differences observed depend on the temperature and humidity of the test environment. Our previous research found that bicomponent moisture barriers showed a lower evaporative resistance when used in mild conditions due to large water uptake inside moisture barriers[156]. At 25 °C, 65% RH, all turnout garments, except garment C, demonstrate similar performance (p<0.01). It was likely that in a mild condition, moisture absorption in the moisture barrier equalized the evaporative resistance of turnout clothing with bicomponent moisture barriers (A, B, D and E), and made them perform similarly. At 35 °C, 40% RH, only turnout system E showed a significantly different predicted core temperature compared with other garments (p<0.01). At 40 °C, 28 % RH, significant differences in predicted core body temperature between most garments were found (p<0.01). One possible reason for the observed core temperature difference in Figure 10-4c was that bicomponent moisture barriers in garment A, B, D, and E were drier and less efficient in this condition, which led to the differentiation in evaporative resistance and physiological response.

10.3.2 Predicted skin temperature (*Tsk*)

Skin is the interface between the environment and the human body. The equilibrium mean skin temperature at room temperature is 32.4 °C in this model. Figure 10-5 depicts the predicted skin temperature for each turnout suit in mild and hot conditions, and the rise in skin temperature at the end of the protocol. Similar trends with core body temperature were found for predicted skin temperature. Under ambient conditions of 25 °C, 65% RH, garment C had the highest predicted skin temperature. By the end of the protocol, the skin temperature for garment C was 0.4 °C higher than garment B, while no significant difference was observed among other garments (p<0.01). At 35 °C, 40% RH, all turnout systems performed similarly (p<0.01). At the condition of 40 °C, 28% RH, garment E and C showed the highest and lowest skin temperature, with a difference of 0.6 °C at the end of the protocol (p<0.01). A significant difference between A and E, B and E were also observed (p<0.01). Compared with core body temperature in Figure 10-4, a less significant difference was observed in skin temperature between garments in all environmental conditions. This is due to a larger fluctuation in skin temperature[158].

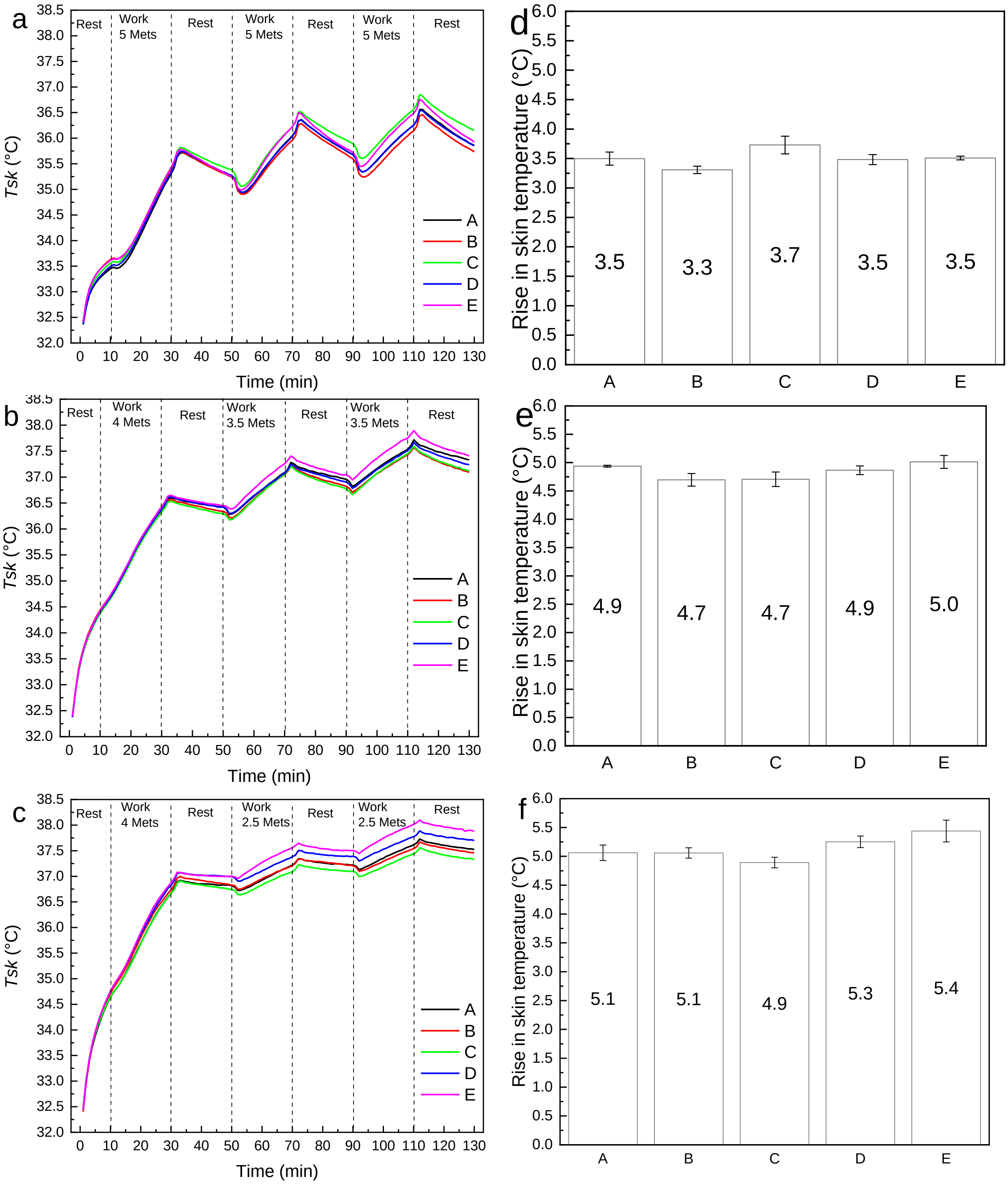

Figure 10-5. Predicted skin temperature at the environment of (a) 25 °C, 65% RH, (b) 35 °C, 40% RH, and (c) 40 °C, 28% RH; the rise of predicted skin temperature at the end of the protocol at the environment of (d) 25 °C, 65% RH, (e) 35 °C, 40% RH, and (f) 40 °C, 28% RH

10.3.3 Predicted cardiac output (*CO*)

Under heat stress, cardiac output increases in order to dissipate heat[204]. Cardiac output is determined by the product of stroke volume and heart rate. Stroke volume is maintained or only slightly increased during heat stress, and the increase in heart rate is the primary driving force behind the increases in cardiac output[205]. Figure 10-6 shows the predicted cardiac output response in different environmental conditions, as well as the value at the end of the protocol. In 25 °C, 65% RH, garment C showed the highest cardiac output, and it was 0.47 L/min more than garment B in the end of the protocol (p<0.01). In 35 °C, 40% RH, a difference of 0.80 L/min was observed between the garments with the highest and lowest cardiac output (garment E vs. C) in the end of protocol (p<0.01). In 40 °C, 28% RH, garment E had the highest cardiac output, followed by garments D, A, B, and C. In the end, the cardiac output of garment E was 1.77 L/min higher than garment C, indicating a higher burden on the cardiac system.

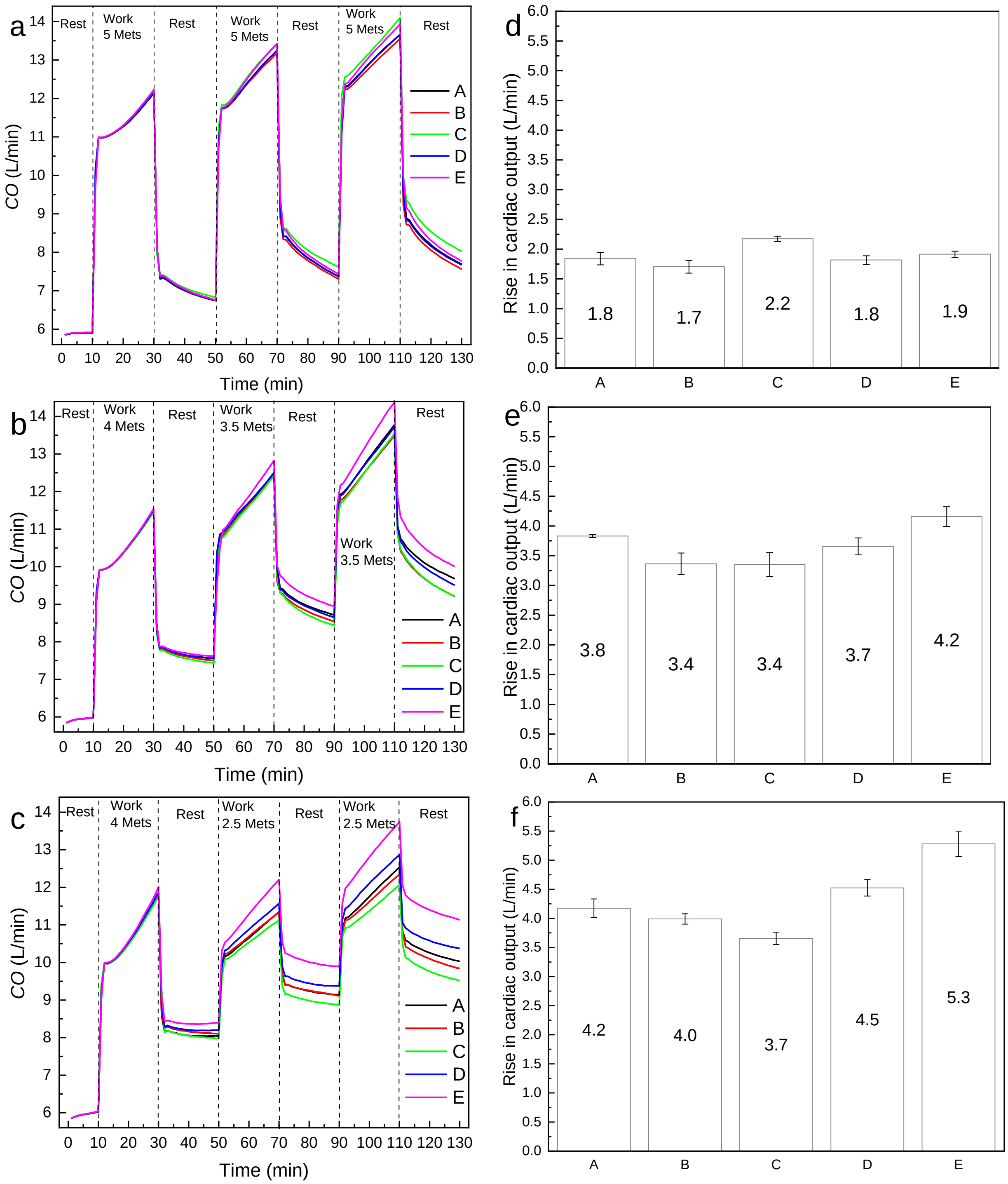

Figure 10-6. Predicted cardiac output at the environment of (a) 25 °C, 65% RH, (b) 35 °C, 40% RH, and (c) 40 °C, 28% RH; the rise of predicted cardiac output at the end of protocol at the environment of (d) 25 °C, 65% RH, (e) 35 °C, 40% RH, and (f) 40 °C, 28% RH

10.3.4 Predicted sweating rate (*Swa*)

Under heat stress, the human body sweats profusely in order to release body heat to the ambient environment by evaporation. The maximum sweating rate in this model is 30 g/min (1.8 L/h), close to the maximum sweating rate experienced by a person wearing protective clothing while doing light-intensity exercise[206]. In 25 °C, 65% RH, the sweating rate for garment C was the highest, about 3.7 g/min less than garment B (p<0.01). In 35 °C, 40% RH, garment E reached the maximum sweating rate from 105 mins and then started to decrease from 115 mins into the protocol. A difference of 3.6 g/min was observed compared to garment C in the end. In 40 °C, 28% RH, the sweating rate when wearing garment E reached the maximum amount at 105 mins, and maintained it for about 20 mins, indicating intensive heat stress. Garment D was the second worst and garment C was the best. The difference between garment E and Garment C reached 6.1 g/min at the end of the protocol (p<0.01).

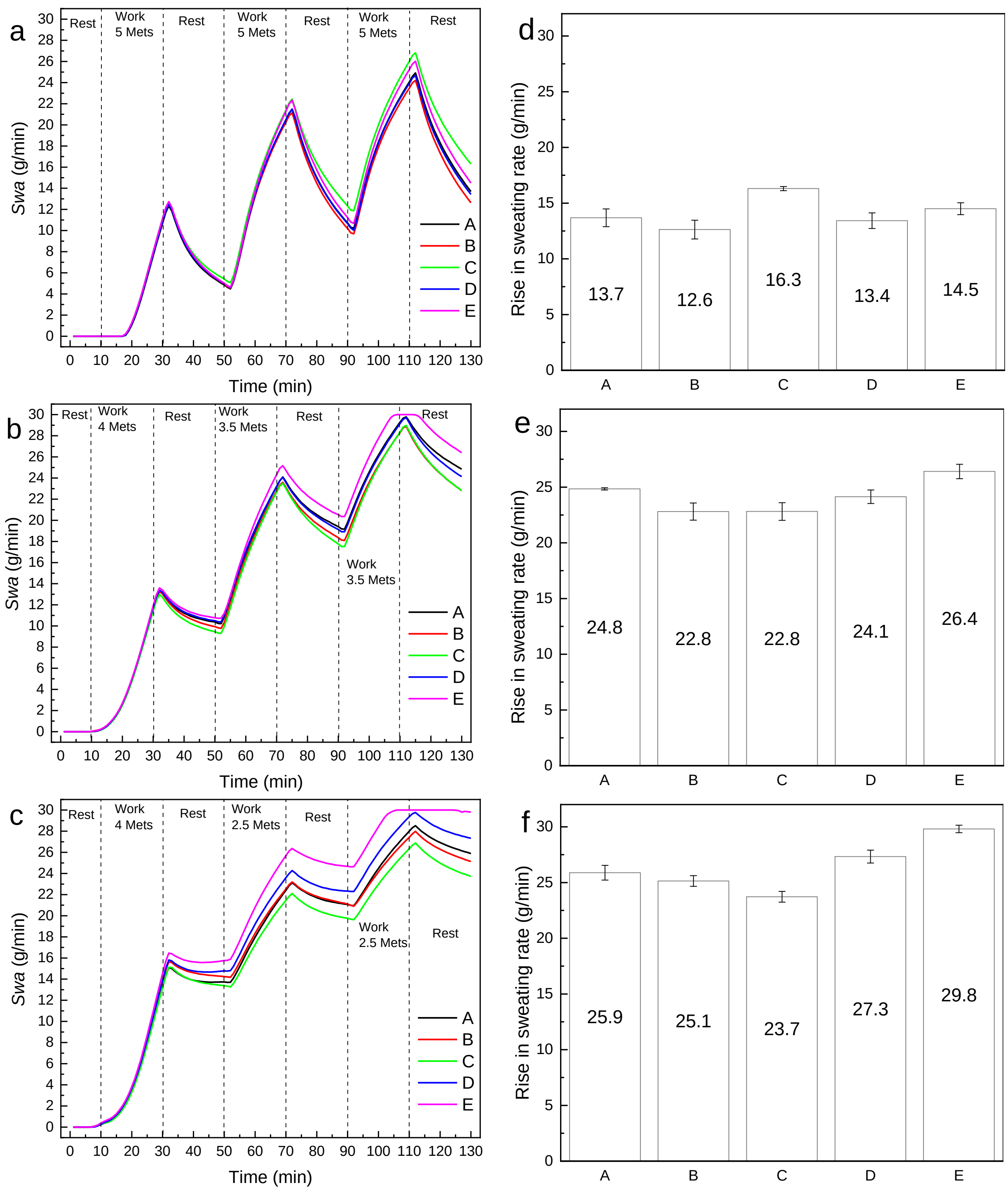

Figure 10-7. Predicted sweating rate in the environment of (a) 25 °C, 65% RH, (b) 35 °C, 40% RH, and (c) 40 °C, 28% RH, and the rise of sweating rate at the end of the protocol: (d) 25 °C, 65% RH, (e) 35 °C, 40% RH, and (f) 40 °C, 28% RH

This research revealed the influence of firefighter turnout suits on physiological responses in different environments. From Figures 10-2 to 10-7, it could be clearly observed that the performances of turnout garments depend on user environments. For example, garment C performed the best in hot conditions, and the worst in mild conditions. Another thing to be noted is that at the environments of 40 °C, 28% RH and 35 °C, 40% RH, even working less intensively than that at 25 °C, 65% RH, the predicted core temperature was much higher. This demonstrates that heat stress is more likely to occur in hot conditions. In addition, the benefit of using a thinner thermal liner on physiological comfort was not observed in this study as no physiological difference was found in the studied environmental conditions between garments A and B (p<0.01). This is likely due to the dominating effect of air layers inside turnout systems.

10.3.4.1 Correlation between THL/R_{ef} with predicted core temperature

Since core body temperature is a direct indicator of heat stress, we studied the relationship between predicted core body temperature and measured materials properties (*THL*, R_{ef}). Figure 10-8 shows the correlations observed between *THL* and R_{ef} heat strain indexes and core temperature rise predicted at the end of the protocol when wearing study turnouts in mild (25 °C, 65% RH) and in hot working conditions (35 °C, 40% RH; 40 °C, 28% RH). Pearson correlation analysis confirmed a strong negative correlation (r = -0.99) between *THL* and predicted core body temperature at 25 °C, 65% RH (Figure 10-8a). It shows a strong positive relationships (r = 0.92 and r = 0.96) between R_{ef} and predicted core body temperature at 35 °C, 40% RH and 40 °C, 28% RH (Figure 10-8e,f).

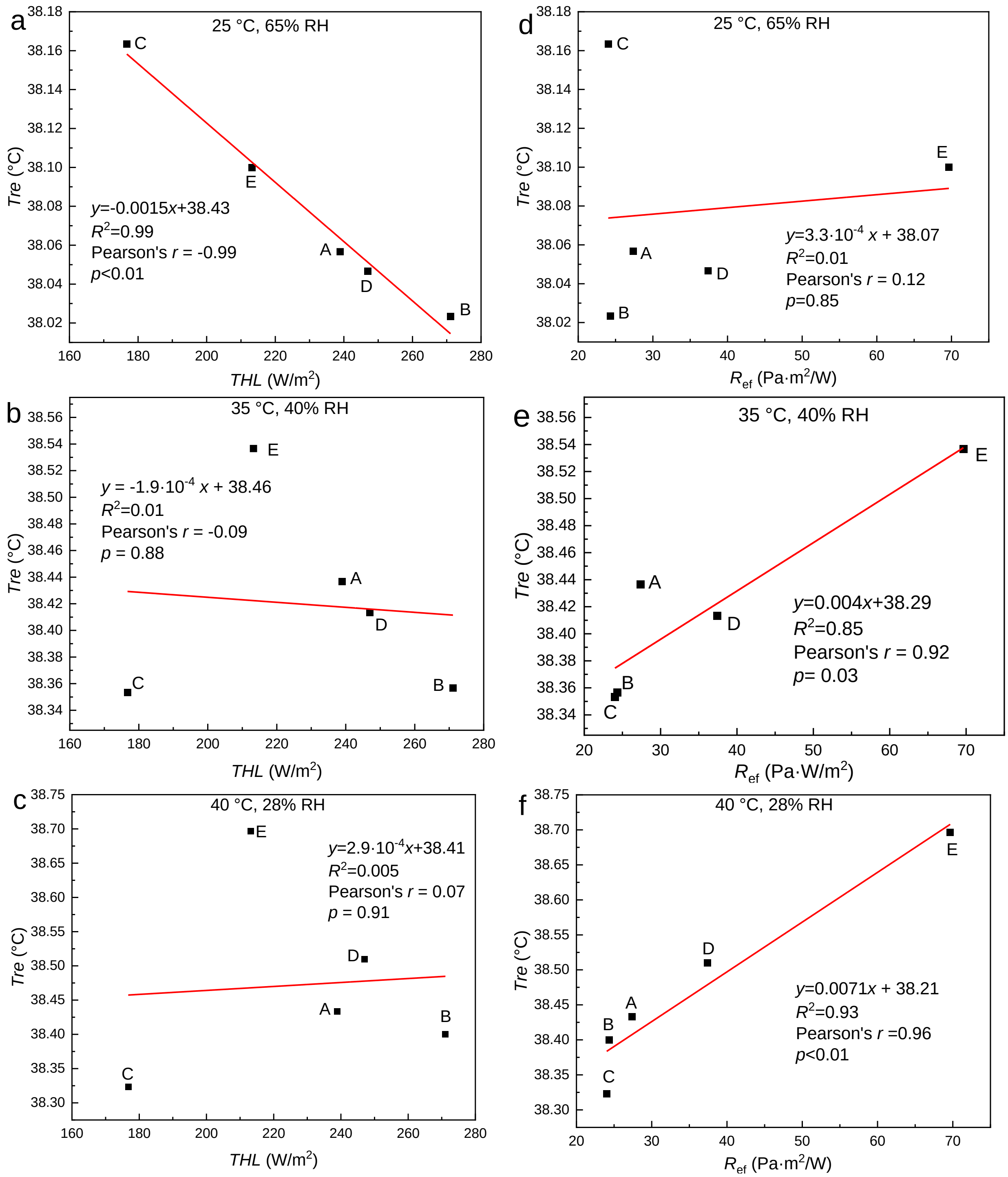

Figure 10-8. *THL*, R_{ef} correlations with core temperature in different ambient environments

These data show that the *THL* index correlates almost perfectly with predicted core temperature rise in mild conditions (Figure 10-8a); however, it has no value for predicting heat strain in hot conditions (Figure 10-8b and c). Conversely, the R_{ef} index correlates with core temperature increase in hot environments (Figure 10-8e and f), with no apparent correlation in the mild condition (Figure 10-8d). These graphs indicate that, within the limits of the simulation study, composite evaporative heat resistance (R_{ef}) less than about 45 Pa·m^2/W is a reasonable basis for predicting lower heat strain in turnout suits made from these materials.

Both *THL* and R_{ef} predict turnout related differences in heat strain. The comparative value of the indexes depends on the thermal stress level of the intended working environment: *THL* accurately forecasts heat strain in mild environments (< 25 °C); R_{ef} provides accurate prediction in hot environments (> 35 °C).

Several precautions are unavoidably present in relying on the *THL* index as the sole heat strain requirement for certifying turnout suit materials. Measured in non-isothermal test conditions, *THL* provides an inflated comparison of the ability of some systems to dissipate evaporative heat in hotter working conditions. Moisture absorbed in bicomponent moisture barriers aids in the evaporation of the moisture, thereby increasing evaporative heat loss. The evaporative heat loss advantage observed in mild environments is less in hot environments where the conditions promoting moisture absorption in the hydrophilic bicomponent barrier materials are not as prevalent. Exclusive reliance on *THL* as a heat strain performance criterion may preclude consideration of some thicker, high-*TPP* systems that fail the current NFPA 1971 criterion of 205 W/m^2, while having a low R_{ef} rating, predictive of normal range heat strain in hot environments (e.g., study turnout system C). It also allows high R_{ef} systems to be used that have shown significant physiological differences in this study and other human study[199].

In this work, we only considered the heat and moisture release properties of clothing in different environmental conditions. Human thermal physiological comfort is complicated, as it is influenced by interrelated variables, including environmental conditions, heat and moisture release properties of clothing materials, garment design, clothing fit, stiffness, workload, as well as the health status of the wearer[34, 203]. It suggests that human physiological wear trials involving a wide range of protective turnout clothing with different features should be conducted in multiple environmental conditions in order to comprehensively understand clothing related heat strain.

10.4 Conclusions

We found little difference in predicted physiological heat strain caused by turnout systems that incorporate breathable moisture barriers when worn in mild environmental conditions, even when high work rates produce metabolic heat sufficient to forecast heat strain in those conditions. Additionally, our studies showed that the *THL* index has no value for predicting heat strain in hot environments. Measured in non-isothermal test conditions, *THL* provides an inflated comparison of the ability of many turnout systems to dissipate evaporative heat in hotter working conditions. This is because moisture absorbed in hydrophilic bicomponent moisture barriers in mild environments contributes to maximal evaporative heat loss. The evaporative heat loss advantage found in mild environments decreases in hot environments where conditions promoting moisture absorption in systems containing semipermeable barrier materials are minimal. Exclusive reliance on *THL* as a performance criterion has allowed systems with high R_{ef} values to be certified. It may also preclude consideration of high-*TPP* systems that fail the current NFPA 1971 *THL* performance criterion of 205 W/m^2 yet perform well in hotter environments.

The comparative value of the total heat loss (*THL*) and R_{ef} indexes for predicting turnout related heat strain on firefighters depends on the thermal stress level of the intended working environment. *THL* accurately forecasts thermal burden in mild environments (<25 °C); R_{ef} provides accurate prediction in hot environments (>35 °C). Of the two indexes, R_{ef} index is more useful for evaluating turnout heat strain. The findings of this project support inclusion of a performance criterion in the NFPA 1971 Standard based on limiting the evaporative resistance (R_{ef}) of turnout materials to no more than 45 Pa·m^2/W with a minimum *THL* rating of 205 W/m^2.

11 Conclusions

This thesis investigated the heat strain indexes associated with firefighter turnout gear. The most important finding from this study is that *THL* could accurately forecast the thermal burden of firefighters in mild environments; R_{ef} provides accurate prediction in hot environments. *THL* overestimates the ability of many turnout systems to dissipate evaporative heat in hotter working conditions. Thus, it is recommended to incorporate R_{ef}, along with *THL*, as dual metrics for certifying the heat strain performance of turnout suits into the NFPA 1971 Standard.

The findings provide useful information on the effects of turnout materials on firefighter heat strain in different user environments. They showed that hydrophilic bicomponent barriers absorbed moisture in the mild, non-isothermal conditions of the standard *THL* test, giving them the advantage in heat loss that does not translate to more thermally stressful hot environments or applied with solar radiation. The evaporative resistance of turnout systems containing microporous barriers was relatively independent of the ambient testing environment. The outer shell color or discoloration due to smoke exposure had a major influence on lowering turnout heat loss in solar exposures. Outer shells with natural color, kept clean, could decrease heat stress in solar radiation. It was also found that a slight change in thermal liner had little effect on heat strain, while adding large portions of thick impermeable materials to the turnout garment could increase the risk of heat stress.

11.1 Research conclusions

11.1.1 The effects of turnout materials on heat transfer in different environmental conditions

The first objective was to understand how specific turnout materials, including outer shell color and texture, and thermal liner composites as well as air layers affect heat transfer in different environmental exposures encountered by firefighters. The standard *THL* test in NFPA 1971 only characterizes heat loss at the fabric level without an air gap in a mild condition (25 °C, 65% RH). To accomplish the objective, new testing procedures for measuring heat loss through turnout systems in various environmental conditions were developed, including the application of dynamic hotplate and simulated solar radiant exposure, as well as creating air gaps between the hotplate and fabric samples.

In the first study (Chapter 3), the relationship between thermal comfort indexes (*THL* and R_{ef}) was investigated by measuring fabric level properties of thirteen firefighter ensembles. The results showed that little correlation was found between *THL* and R_{ef}, meaning that firefighter composites performed differently with the environment. The influences of moisture barriers and test ambient environments on the evaporative resistance of firefighter composites were examined in Chapter 4. It was found that for the semipermeable moisture barriers with a non-porous coating of hydrophilic polymer, the evaporative resistance strongly depended on membrane water content. Testing at low temperature or high humidity could increase its moisture content, resulting in a significant enhancement in its transmission of water vapor. In contrast, for a microporous (uncoated) membrane, its evaporative resistance was relatively independent of environmental conditions. The exploration of the air gap effect on heat transfer in Chapter 5 demonstrated that the presence of an air gap could change the water content inside moisture barriers, and this affected the evaporative resistance of bicomponent moisture barriers dramatically.

In addition to temperature and humidity, the solar radiation effect was addressed as firefighters often need to work outdoors in direct sunlight. The effect of outer shells (color, texture, and discoloration by soot contamination) on heat loss when exposed to solar radiation was explored in Chapter 6. It showed that outer shell color played a vital role in the protection against solar radiation, while texture had a minor effect. Substantial heat gain was observed in the black or contaminated firefighter composites. The effect of solar radiation on evaporative heat loss through firefighter turnout composites with different moisture barriers was addressed in Chapter 7. It was found that radiation could increase the composite temperature, causing different effects in relation to moisture barriers. For firefighter composites with a microporous moisture barrier, evaporative resistance decreased consistently with radiation. In contrast, for composites with the bicomponent moisture barriers, radiation showed a trade-off effect. At lower radiation, due to the reduction of moisture content inside the moisture barrier, the evaporative resistance increased. With the increase of radiation, evaporative resistance decreased due to enhanced moisture diffusion rate.

11.1.2 The relationship between heat strain indexes with physiological heat strain

Since the fabric level testing cannot account for reinforcements, garment design and fit, or pumping effect, it is necessary to investigate the impact of turnout clothing on human physiological responses. A sweating manikin coupled with a validated physiological model was used to assess how the turnout systems performed in various working and environmental conditions.

In Chapter 8, the heat release properties of turnout clothing with or without durable water repellent (DWR) finishing in thermal liners was compared, and no significant difference in heat release properties on fabric level or garment level was found. This shows that fabric-level measurements could predict the performance of garments with or without DWR finishing.

The physiological impact of clothing reinforcement was addressed in Chapter 9. The results showed that the foam reinforcement had a substantial effect on heat loss and thermal comfort. The garment-related heat strain requirement in the current standard (NFPA 1971) only relied on the total heat loss (*THL*) data from the bench level testing, and lacked the ability to account for the effect of clothing reinforcement. It is important that the heat release properties based on the manikin test should be proposed.

The eligibility of using heat strain indexes (*THL* or R_{ef}) based on hotplate measurements to predict the garment performance was demonstrated in Chapter 10. The results revealed a clear trend of a reduction in predicted heat strain when wearing turnout suits with lower R_{ef} values in hot conditions, and higher *THL* in mild environments. At the mild condition, *THL* could predict firefighter heat stress well, whereas at hot conditions, R_{ef} is a better index.

11.2 Recommendations

Total Heat Loss (*THL*) is the only heat strain requirement for turnout materials in NFPA 1971. The research demonstrated that *THL* is a better index to predict firefighter physiological response in a mild environment, while R_{ef} is a good indicator of heat strain in a hot environment. It is highly recommended that R_{ef} be included as an additional index for heat strain management in the next version of the NFPA 1971 standard. The radiant heat load from the sun should be addressed. It is important that the heat loss under radiation or the emissivity of the outer shell fabrics should be tested. To limit the heat gain from solar radiation, outer shell fabrics should have a light color and be kept clean.

Adding large portions of thick impermeable materials to the turnout garment can impact physiological thermal comfort significantly. It is recommended that NFPA 1971 should regulate the maximum amount and the heat release properties of the reinforcement materials used in turnout clothing. Another solution is to test the heat release properties of turnout garments using a sweating manikin.

Although research was conducted thoroughly and many questions were answered regarding the effect of turnout materials and environments on firefighter heat strain, there is future work that is worth performing. Soot contaminated outer shell (E&W) has higher absorptivity in medium infrared radiation (Figure 11-1), which means more heat could be absorbed by the contaminated sample from the flame radiation. It is necessary to develop a sweating plate test method that incorporates flame radiant load.

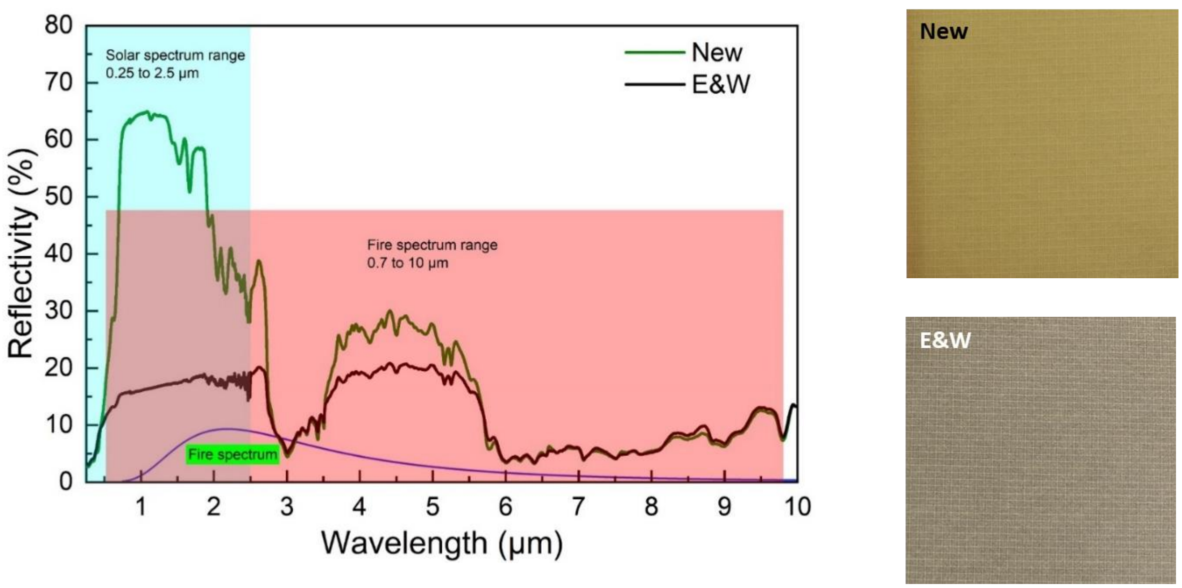

Figure 11-1. The reflectivity of new sample and dirty (E&W) sample in the range of flame radiation

Water is the primary agent used by firefighters to suppress fire and the vapor pressure in the environment may be higher than human skin surface during firefighting. As a result, the negative vapor pressure can cause an evaporative heat transfer from the environment to human skin, and may lead to steam burns. A preliminary experiment was conducted in the environment of 45 °C, 70% RH while maintaining the hotplate surface as 35 °C and water saturated. This created a negative 1.08 kPa vapor pressure difference between the hotplate surface and ambient environment. In this scenario, the composite with a low evaporative resistance (MM) brought in more heat and the composite with a bicomponent moisture barrier (A) and high evaporative resistance showed less heat gain (Figure 11-2). This needs more systematic study in the future.

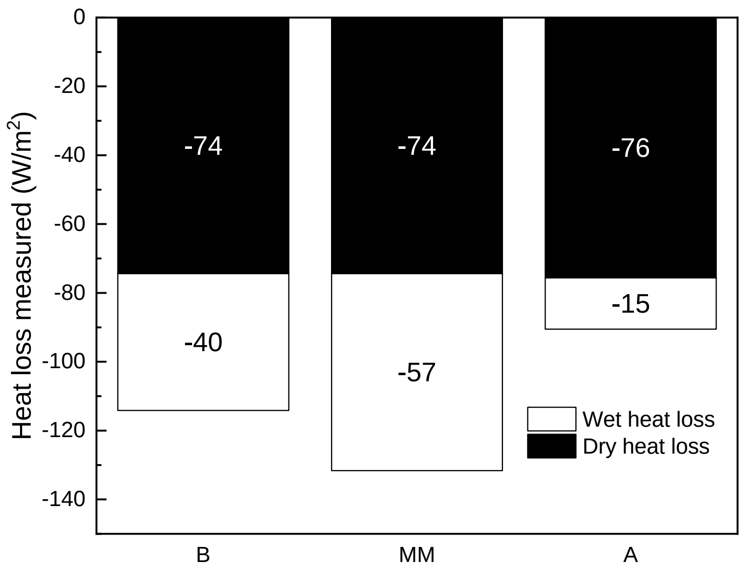

Figure 11-2. Heat loss measured during the experiment in the environment of 45 °C, 70% RH

The effect of solar radiation on heat loss was studied on bench-level using a hotplate, but it is not clear if solar radiation would have an impact on the human physiological response on the garment level. Our preliminary study shown in Figure 11-3 was not successful as a uniform distribution of solar radiation was not reached. In the future, a more uniform radiation source is needed to evaluate the solar radiation effect on human thermal comfort using a physiological manikin.

Figure 11-3. Preliminary study investigating the color effect using a physiological manikin

REFERENCES

1. Barker, R.; Fang,X.; Deaton, S.; DenHartog, E.; Gao, H.; Tutterow, R.; Schmid, M., Identifying factors that contribute to structural firefighter heat strain in North America. *Safety Science (submitted)* **2021**.
2. Smith, D. L., Firefighter fitness: improving performance and preventing injuries and fatalities. *Curr. Sports Med. Rep.* **2011,** *10* (3), 167-172.
3. Cheung, S. S.; Petersen, S. R.; McLellan, T. M., Physiological strain and countermeasures with firefighting: physiology of firefighting. *Scand. J. Med. Sci. Sports* **2010,** *20*, 103-116.
4. Parsons, K. C., *Human heat stress*. CRC Press, **2019**.
5. Havenith, G., Heat balance when wearing protective clothing. *Annals of occupational Hygiene* **1999,** *43* (5), 289-296.
6. Methner, M.; Eisenberg, J., Evaluation of heat stress and heat strain among employees working outdoors in an extremely hot environment. *J. Occup. Environ. Hyg.* **2018,** *15* (6), 474-480.
7. Criteria for a recommended standard: occupational exposure to heat and hot environments. National Institute for Occupational Safety and Health. **2016**.
8. Jardine, D. S., Heat illness and heat stroke. *Pediatr. Rev.* **2007,** *28* (7), 249.
9. Becker, J. A.; Stewart, L. K., Heat-related illness. *Am. Fam. Physician* **2011,** *83* (11), 1325-1330.
10. Smith, D. L.; Horn, G. P.; Goldstein, E.; Petruzzello, S. J., Firefighter fatalities and injuries: the role of heat stress and PPE. *Illinois Fire Service Institute*: **2008**.

11. Fahy, R. F.; Molis, J. L.,Firefighter fatalities in the US-2018. NFPA Research. **2019**, 1-26.

12. Fahy, R. F.; Petrillo J. T.; Molis, J. L., Firefighter fatalities in the US-2019. NFPA Research **2020**, 1-26.

13. Smith, D. L.; Barr, D. A.; Kales, S. N., Extreme sacrifice: sudden cardiac death in the US Fire Service. *Extrem Physiol Med* **2013,** *2* (1), 6.

14. National Fire Protection Association. https://www.nfpa.org/News-and-Research/Data-research-and-tools/Emergency-Responders/Firefighter-fatalities-in-the-United-States. (Accessed: July 2020)

15. Hur, P.; Rosengren, K. S.; Horn, G. P.; Smith, D. L.; Hsiao-Wecksler, E.T., Effect of protective clothing and fatigue on functional balance of firefighters. *Journal of Ergonomics* **2013**, S2.

16. Park, K.; Rosengren, K. S.; Horn, G. P.; Smith, D. L.; Hsiao-Wecksler, E. T., Assessing gait changes in firefighters due to fatigue and protective clothing. *Safety Science* **2011,** *49* (5), 719-726.

17. Abbott, N. J.; Schulman, S., Protection from fire: nonflammable fabrics and coatings. *Journal of Coated Fabrics* **1976,** *6* (1), 48-64.

18. Song, G.; Mandal, S.; Rossi, M. R., Fires and thermal environments. In *Thermal Protective Clothing for Firefighters*, Elsevier: **2017**; pp 5-15.

19. Collin, A.; Marchand, A.; Kadi, A.; Acem, Z.; Boulet, P.; Pageaux, J.; Pinson, S.; Lepelletier, M.; Van Waelfelghem, Y.; Magnolini, F.; Charette, H., Study on visible–IR radiative properties of personal protective clothings for firefighting. *Fire Safety Journal* **2015,** *71*, 9-19.

20. Rossi, R., Fire fighting and its influence on the body. *Ergonomics* **2003,** *46* (10), 1017-1033.

21. Hoschke, B. N., Standards and specifications for firefighters' clothing. 13. *Fire Safety Journal* **1981**, 4, 125-137.

22. Day, M.; Sturgeon, P. Z., Thermal radiative protection of fire fighters' protective clothing. *Fire Technol.* **1987,** *23* (1), 49-59.

23. Willi, J. M.; Horn, G. P.; Madrzykowski, D., Characterizing a firefighter's immediate thermal environment in live-fire training scenarios. *Fire Technol.* **2016,** *52* (6), 1667-1696.

24. Boulet, P.; Parent, G.; Acem, Z.; Kaiss, A.; Billaud, Y.; Porterie, B.; Pizzo, Y.; Picard, C., Experimental investigation of radiation emitted by optically thin to optically thick wildland flames. *Journal of Combustion* **2011,** *2011*, 1-8.

25. Smith, D. L.; DeBlois, J. P.; Kales, S. N.; Horn, G. P., Cardiovascular strain of firefighting and the risk of sudden cardiac events. *Exercise and Sport Sciences Reviews* **2016,** *44* (3), 90-97.

26. Boorady, L. M.; Barker, J.; Lee, Y.-A.; Lin, S.-H.; Cho, E.; Ashdown, S. P., Exploration of firefighter turnout gear part 1: identifying male firefighter user needs. *Journal of Textile and Apparel, Technology and Management* **2013,** *8*(1), 13.

27. Emergency Incident Rehabilitation. *U.S. Fire Administration.* **2008**.

28. Weather Underground.https://w2.weather.gov/climate/xmacis.php?wfo=psr (Accessed: July 2020)

29. ASTM G173-03:2012. Standard tables for reference solar spectral irradiances: Direct normal and hemispherical on 37 tilted surface.

30. Barker, R. L.; Heniford, R. C., Factors affecting the thermal insulation and abrasion resistance of heat resistant hydro-entangled nonwoven batting materials for use in firefighter turnout suit thermal liner systems. *Journal of Engineered Fibers and Fabrics* **2011,** *6* (1), 10.

31. Song, G. Modeling thermal protection outfits for fire exposures. **2003**.

32. Ghoshdastidar, P. S., Heat Transfer (2nd Edition). Oxford University Press: **2012**.

33. Holmér, I., Protective clothing and heat stress. *Ergonomics* **1995,** *38* (1), 166-182.

34. Havenith, G., Interaction of clothing and thermoregulation. *Exogenous Dermatology* **2002,** *1* (5), 221-230.

35. Bergman, T. L.; Incropera, F. P.; DeWitt, D. P.; Lavine, A. S., *Fundamentals of heat and mass transfer*. John Wiley & Sons: **2011**.

36. Ganji, D. D.; Sabzehmeidani, Y.; Sedighiamiri, A., *Nonlinear Systems in Heat Transfer: Mathematical Modeling and Analytical Methods*. Elsevier: **2017**.

37. Balaji, C.; Srinivasan, B.; Gedupudi, S., *Heat transfer engineering: fundamentals and techniques*. Academic Press: **2020**.

38. *ASHRAE Handbook—Fundamentals*, American society of heating, refrigerating and air-conditioning engineers. **2009**.

39. De Dear, R. J.; Arens, E.; Hui, Z.; Oguro, M., Convective and radiative heat transfer coefficients for individual human body segments. *Int. J. Biometeorol.* **1997,** *40* (3), 141-156.

40. Wang, F. Clothing evaporative resistance: its measurements and application in prediction of heat strain. Lund University, Lund, **2011**.

41. Havenith, G.; Heus, R.; Lotens, W. A., Resultant clothing insulation: a function of body movement, posture, wind, clothing fit and ensemble thickness. *Ergonomics* **1990,** *33* (1), 67-84.

42. Havenith, G.; Nilsson, H. O., Correction of clothing insulation for movement and wind effects, a meta-analysis. *Eur. J. Appl. Physiol.* **2004,** *92* (6), 636-640.

43. Nielsen, R.; Olesen, B. W.; Fanger, P. O., Effect of physical activity and air velocity on the thermal insulation of clothing. *Ergonomics* **1985,** *28* (12), 1617-1631.

44. Parsons, K.; Havenith, G.; Holmér, I.; Nilsson, H.; Malchaire, J., The effects of wind and human movement on the heat and vapour transfer properties of clothing. *Ann. Occup. Hyg.* **1999,** *43* (5), 347-352.

45. Qian, X.; Fan, J., Prediction of clothing thermal insulation and moisture vapour resistance of the clothed body walking in wind. *The Annals of occupational hygiene* **2006,** *50* (8), 833-842.

46. Wang, F., Effect of body movement on the thermophysiological responses of an adaptive manikin and human subjects. *Measurement* **2018,** *116*, 251-256.

47. Zhang, C.; Wang, F., Comfort Management of Fibrous Materials. *Handbook of Fibrous Materials* **2020**, 857-887.

48. Wang, F.; Annaheim, S.; Morrissey, M.; Rossi, R., Real evaporative cooling efficiency of one-layer tight-fitting sportswear in a hot environment. *Scand. J. Med. Sci. Sports* **2014,** *24* (3), e129-e139.

49. Park, H.; Park, J.; Lin, S.-H.; Boorady, L. M., Assessment of Firefighters' needs for personal protective equipment. *Fashion and Textiles* **2014,** *1* (1), 8.

50. Horrocks, A. R.; Price, D., *Advances in fire retardant materials*. Elsevier: **2008**.

51. Song, G.; Wang, F., *Firefighters' clothing and equipment: performance, protection and comfort*. CRC Press, **2019**.

52. Quintiere, J., Radiative characteristics of fire fighters' coat fabrics. *Fire Technol.* **1974,** *10* (2), 153-161.

53. Bröde, P.; Kuklane, K.; Candas, V.; Den Hartog, E. A.; Griefahn, B.; Holmér, I.; Meinander, H.; Nocker, W.; Richards, M.; Havenith, G., Heat gain from thermal radiation through protective clothing with different insulation, reflectivity and vapour permeability. *Int. J. Occup. Saf. Ergon.* **2010,** *16* (2), 231-244.

54. McQuerry, M.; Kwon, C.; Johnson, H. J. R. J. o. T.; Apparel, A critical review of female firefighter protective clothing and equipment workplace challenges. **2019,** *23* (2), 94-110.

55. McQuerry, M.; DenHartog, E.; Barker, R., Evaluating turnout composite layering strategies for reducing thermal burden in structural firefighter protective clothing systems. *Textile Research Journal* **2017,** *87* (10), 1217-1225.

56. Mukhopadhyay, A.; Midha, V. K., Waterproof breathable fabrics. In *Handbook of Technical Textiles*, Elsevier: **2016**; pp 27-55.

57. Özek, H. Z., Development of waterproof breathable coatings and laminates. In *Waterproof and Water Repellent Textiles and Clothing*, Elsevier: **2018**; pp 25-72.

58. Lomax, G. R., The Design of waterproof, water vapour-permeable fabrics. *Journal of Coated Fabrics* **1985,** *15* (1), 40-66.

59. Lomax, G. R., Breathable polyurethane membranes for textile and related industries. *J. Mater. Chem.* **2007,** *17* (27), 2775.

60. Tehrani-Bagha, A. R., Waterproof breathable layers–A review. *Advances in Colloid and Interface Science* **2019**, 268,114-135.

61. Mukhopadhyay, A.; Midha, V. K., A Review on Designing the Waterproof Breathable Fabrics Part I: Fundamental Principles and Designing Aspects of Breathable Fabrics. *Journal of Industrial Textiles* **2008,** *37* (3), 225-262.

62. Schledjewski, R.; Schultze, D.; Imbach, K.-P., Breathable Protective Clothing with Hydrophilic Thermoplastic Elastomer Membrane Films. *Journal of Coated Fabrics* **1997,** *27* (2), 105-114.

63. Gretton, J. C.; Brook, D. B.; Dyson, H. M.; Harlock, S. C., A Correlation between Test Methods Used to Measure Moisture Vapour Transmission through Fabrics. *Journal of Coated Fabrics* **1996,** *25* (4), 301-310.

64. Osczevski, R., *Diffusion of water vapour through cold Gore-Tex*. Defence Research Establishmnt Ottawa:**1993**.

65. Finn, J. T.; Sagar, A. J. G.; Mukhopadhyay, S. K., Effects of Imposing a Temperature Gradient on Moisture Vapor Transfer Through Water Resistant Breathable Fabrics. *Textile Research Journal* **2000,** *70* (5), 460-466.

66. Gibson, P. W., Effect of temperature on water vapor transport through polymer membrane laminates. *Polymer Testing* **2000,** *19* (6), 673-691.

67. Song, G.; Mandal, S.; Rossi, S.M., Development of high performance thermal protective clothing. In *Thermal Protective Clothing for Firefighters*, Elsevier: **2017**; pp 27-55.

68. McQuerry, M.; Barker, R.; DenHartog, E., Functional design and evaluation of structural firefighter turnout suits for improved thermal comfort: thermal manikin and physiological modeling. *Clothing and Textiles Research Journal* **2018,** *36* (3), 165-179.

69. Jin, L.; Cao, M. L.; Yu, W.; Hu, J. Y.; Yoon, K. J.; Park, P. K.; Li, Y., New approaches to evaluate the performance of firefighter protective clothing materials. *Fire Technol.* **2018,** *54* (5), 1283-1307.

70. Lin, L.-Y.; Jou, G. T., A study on total heat loss of clothing materials for firefighters' protective clothing. The 9th Asian Textile Conference. **2007.**

71. DenHartog, E. A.; Havenith, G., Analytical study of the heat loss attenuation by clothing on thermal manikins under radiative heat loads. *Int. J. Occup. Saf. Ergon.* **2010,** *16* (2), 245-261.

72. NFPA 1971:2018. Standard on protective ensembles for structural fire fighting and proximity fire fighting.

73. EN469:2020. Protective clothing for firefighters—performance requirements for protective clothing for firefighters.

74. ISO 11999-3:2015. PPE for firefighters—test methods and requirements for PPE used by firefighters who are at risk of exposure to high levels of heat and/or flame while fighting fires occurring in structures—part 3.

75. ASTM F1868:2017. Standard test method for thermal and evaporative resistance of clothing materials using a sweating hot plate.

76. Gohlke, D., History of the development of the total heat loss test method. In *Performance of Protective Clothing: Sixth Volume*, Stull, J.; Schwope, A., Eds. ASTM International: 100 Barr Harbor Drive, PO Box C700, West Conshohocken, PA 19428-2959, **1997**; pp 190-190-17.

77. Barker, R.; Myhre, L.; Scruggs, B.; Shalev, I.; Prahsarn, C.; Miszko, T., Effect of measured heat loss through turnout materials on firefighter comfort and heat stress. Part I:

performance in a mild environment. In *Performance of Protective Clothing: Issues and Priorities for the 21*, Nelson, C.; Henry, N., Eds. ASTM International: 100 Barr Harbor Drive, PO Box C700, West Conshohocken, PA 19428-2959, **2000**; pp 519-519-16.

78. Myhre, L.; Barker, R.; Scruggs, B.; Shalev, I.; Prahsarn, C.; Miszko, T., Effect of measured heat loss through turnout materials on firefighter comfort and heat stress. part II: performance in a warm environment. In *Performance of Protective Clothing: Issues and Priorities for the 21*, Nelson, C.; Henry, N., Eds. ASTM International: 100 Barr Harbor Drive, PO Box C700, West Conshohocken, PA 19428-2959, **2000**; pp 535-535-11.

79. Stull, J.; Duffy, R., Field evaluation of protective clothing effects on fire fighter physiology: predictive capability of total heat loss test. In *Performance of Protective Clothing: Issues and Priorities for the 21*, Nelson, C.; Henry, N., Eds. ASTM International: 100 Barr Harbor Drive, PO Box C700, West Conshohocken, PA 19428-2959, **2000**; pp 481-481-23.

80. Huang, J., Sweating guarded hot plate test method. *Polymer Testing* **2006,** *25* (5), 709-716.

81. Howe, D. B.; Blood, K. R.; Burke, R. R.; Lanci, N., Development of a human sensation-relevant method for measuring phase change materials. In *Performance of Protective Clothing and Equipment: 10th Volume, Risk Reduction Through Research and Testing*, Shiels, B.; Lehtonen, K., Eds. ASTM International: 100 Barr Harbor Drive, PO Box C700, West Conshohocken, PA 19428-2959, **2016**; pp 331-350.

82. Ross, K.; Barker, R.; Deaton, A. S., Translation between heat loss measured using guarded sweating hot plate, sweating manikin, and physiologically assessed heat stress of

firefighter turnout ensembles. In *Performance of Protective Clothing and Equipment: 9th Volume, Emerging Issues and Technologies*, Shepherd, A. M., Ed. ASTM International: 100 Barr Harbor Drive, PO Box C700, West Conshohocken, PA 19428-2959, **2012**; pp 27-47.

83. Holmér, I., Thermal manikin history and applications. *Eur. J. Appl. Physiol.* **2004,** *92* (6), 614-618.

84. Mandal, S.; Annaheim, S.; Camenzind, M.; Rossi, R. M., Evaluation of thermo-physiological comfort of clothing using manikins. In *Manikins for Textile Evaluation*, Elsevier: **2017**; pp 115-140.

85. ASTM F1291:2016. Standard test method for measuring the thermal insulation of clothing using a heated manikin.

86. Kuklane, K.; Gao, C.; Wang, F.; Holmér, I., Parallel and serial methods of calculating thermal insulation in European manikin standards. *International journal of occupational safety and ergonomics* **2012,** *18* (2), 171-179.

87. ASTM F2370:2016. Standard test method for measuring the evaporative resistance of clothing using a sweating manikin.

88. DenHartog, E. A.; Walker, M. A.; Barker, R. L., Total heat loss as a predictor of physiological response in wildland firefighter gear. *Textile Research Journal* **2016,** *86* (7), 710-726.

89. Psikuta, A.; Allegrini, J.; Koelblen, B.; Bogdan, A.; Annaheim, S.; Martínez, N.; Derome, D.; Carmeliet, J.; Rossi, R. M., Thermal manikins controlled by human thermoregulation models for energy efficiency and thermal comfort research – A review. *Renewable and Sustainable Energy Reviews* **2017,** *78*, 1315-1330.

90. Katić, K.; Li, R.; Zeiler, W., Thermophysiological models and their applications: A review. *Build. Environ.* **2016,** *106*, 286-300.

91. Havenith, G.; Fiala, D., Thermal indices and thermophysiological modeling for heat stress. *Comprehensive Physiology*. **2015**, *6* (1), 255-302.

92. Fiala, D., Physiological modeling for technical clinical and research applications. *Front. Biosci.* **2010,** *S2* (3), 939-968.

93. Fiala, D.; Lomas, K. J.; Stohrer, M., A computer model of human thermoregulation for a wide range of environmental conditions: the passive system. *J. Appl. Physiol.* **1999,** *87* (5), 1957-1972.

94. Fiala, D.; Lomas, K. J.; Stohrer, M., Computer prediction of human thermoregulatory and temperature responses to a wide range of environmental conditions. *Int. J. Biometeorol.* **2001,** *45* (3), 143-159.

95. Veselá, S.; Kingma, B.; Frijns, A., Local thermal sensation modeling—a review on the necessity and availability of local clothing properties and local metabolic heat production. *Indoor Air* **2017,** *27* (2), 261-272.

96. Psikuta, A.; Koelblen, B.; Mert, E.; Fontana, P.; Annaheim, S., An integrated approach to develop, validate and operate thermo-physiological human simulator for the development of protective clothing. *Ind. Health* **2017,** *55* (6), 500-512.

97. Burke, R.; Blood, K.; Deaton, A. S.; Barker, R., Application of model-controlled manikin to predict human physiological response in firefighter turnout gear, 8th International Meeting for Thermal Manikin and Modeling (8I3M), Victoria, Canada, **2010**.

98. Wang, F., Physiological Model Controlled Sweating Thermal Manikin: Can it replace human subjects? *Journal of Ergonomics* **2011,** *01* (01).

99. Fan, J.; Cheng, X.; Chen, Y.-S., An experimental investigation of moisture absorption and condensation in fibrous insulations under low temperature. *Experimental Thermal and Fluid Science* **2003,** *27* (6), 723-729.

100. Fukazawa, T.; Kawamura, H.; Tochihara, Y.; Tamura, T., Experiment and analysis of combined heat and water vapor transfer through clothes with condensation. *Textile Research Journal* **2003,** *73* (9), 774-780.

101. Ren, Y. J.; Ruckman, J. E., Condensation in three-layer waterproof breathable fabrics for clothing. *International Journal of Clothing Science and Technology* **2004,** *16* (3), 335-347.

102. Fu, M.; Weng, W.; Han, X., Effects of moisture transfer and condensation in protective clothing based on thermal manikin experiment in fire environment. *Procedia Engineering* **2013,** *62*, 760-768.

103. Richards, M. G. M.; Rossi, R.; Meinander, H.; Broede, P.; Candas, V.; DenHartog, E.; Holmér, I.; Nocker, W.; Havenith, G., Dry and wet heat transfer through clothing dependent on the clothing properties under cold conditions. *Int. J. Occup. Saf. Ergon.* **2008,** *14* (1), 69-76.

104. Havenith, G.; Richards, M. G.; Wang, X.; Bröde, P.; Candas, V.; DenHartog, E.; Holmér, I.; Kuklane, K.; Meinander, H.; Nocker, W., Apparent latent heat of evaporation from clothing: attenuation and “heat pipe” effects. *J. Appl. Physiol.* **2008,** *104* (1), 142-149.

105. Mangat, M. M.; Hes, L.; Bajzík, V., Thermal resistance models of selected fabrics in wet state and their experimental verification. *Textile Research Journal* **2015,** *85* (2), 200-210.

106. Yoo, S.; Kim, E., Effects of multilayer clothing system array on water vapor transfer and condensation in cold weather clothing ensemble. *Textile Research Journal* **2008,** *78* (3), 189-197.

107. Fukazawa, T.; Lee, G.; Matsuoka, T.; Kano, K.; Tochihara, Y., Heat and water vapour transfer of protective clothing systems in a cold environment, measured with a newly developed sweating thermal manikin. *Eur. J. Appl. Physiol.* **2004,** *92* (6), 645-648.

108. Brake, D. J.; Bates, G. P., Limiting metabolic rate (thermal work limit) as an index of thermal stress. *Appl. Occup. Environ. Hyg.* **2002,** *17* (3), 176-186.

109. Rossi, R., Clothing for protection against heat and flames. In *Protective Clothing*, Elsevier: **2014**; pp 70-89.

110. Su, Y.; Yang, J.; Song, G.; Li, R.; Xiang, C.; Li, J., Development of a numerical model to predict physiological strain of firefighter in fire hazard. *Sci. Rep.* **2018,** *8* (1).

111. Tawfik, M.; Tonnellier, X.; Sansom, C., Light source selection for a solar simulator for thermal applications: a review. *Renewable and Sustainable Energy Reviews* **2018,** *90*, 802-813.

112. Grantham, A.; Pudney, P.; Ward, L.; Belusko, M.; Boland, J. J. S. E., Generating synthetic five-minute solar irradiance values from hourly observations. **2017,** *147*, 209-221.

113. Kuklane, K.; Gao, C.; Holmér, I., Effects of natural solar radiation on manikin heat exchange. In 3rd European Conference on Protective Clothing and NOKOBETEF 8.

Protective clothing-towards balanced protection. Central Institute for Labour Protection, Warszawa, Poland, **2006**.

114. Havenith, G.; Wang, X.; DenHartog, E. A.; Griefahn, B.; Holmer, I.; Meinander, H.; Richards, M., Interaction effects of radiation and convection measured by a thermal manikin wearing protective clothing with different radiant properties. **2005**.

115. Fukazawa, T.; DenHartog, E. A.; Daanen, H. A.; Penders-van Elk, N.; Tochihara, Y.; Havenith, G., Radiant heat transfer network in the simulated protective clothing system under high heat flux. The Third International Conference on Human-Environment System ICHES'05 in Tokyo, Japan, 12-15 Sep., **2005**.

116. Fukazawa, T.; DenHartog, E. A.; Daanen, H. A.; Tochihara, Y.; Havenith, G., Water vapour transfer in the simulated protective clothing system with exposure to intensive solar radiation. The Third International Conference on Human-Environment System ICHES'05 in Tokyo, Japan, 12-15 Sep., **2005**.

117. Udayraj; Talukdar, P.; Das, A.; Alagirusamy, R., Numerical investigation of the effect of air gap orientations and heterogeneous air gap in thermal protective clothing on skin burn. *International Journal of Thermal Sciences* **2017,** *121*, 313-321.

118. Deng, M.; Wang, Y.; Li, P., Effect of air gaps characteristics on thermal protective performance of firefighters' clothing: A review. *International Journal of Clothing Science and Technology* **2018,** *30* (2), 246-267.

119. Su, Y.; Li, J.; Wang, Y., Effect of air gap thickness on thermal protection of firefighter's protective clothing against hot steam and thermal radiation. *Fibers and Polymers* **2017,** *18* (3), 582-589.

120. He, H.; Yu, Z., Effect of air gap entrapped in firefighter protective clothing on thermal resistance and evaporative resistance. *Autex Research Journal* **2018,** *18* (1), 28-34.

121. Ding, D.; Tang, T.; Song, G.; McDonald, A., Characterizing the performance of a single-layer fabric system through a heat and mass transfer model-Part I: Heat and mass transfer model. *Textile Research Journal* **2011,** *81* (4), 398-411.

122. Mert, E.; Psikuta, A.; Bueno, M.-A.; Rossi, R. M., Effect of heterogenous and homogenous air gaps on dry heat loss through the garment. *International Journal of Biometeorology* **2015,** *59* (11), 1701-1710.

123. Phelps, H. L.; Watt, S. D.; Sidhu, H. S.; Sidhu, L. A., Using phase change materials and air gaps in designing fire fighting suits: a mathematical investigation. *Fire Technol.* **2019,** *55* (1), 363-381.

124. Cain, B.; Farnworth, B., Two new techniques for determining the thermal radiative properties of thin fabrics. *Journal of Thermal Insulation* **1986,** *9* (4), 301-322.

125. Morozumi, Y.; Akaki, K.; Tanabe, N., Heat and moisture transfer in gaps between sweating imitation skin and nonwoven cloth: effect of gap space and alignment of skin and clothing on the moisture transfer. *Heat and Mass Transfer* **2012,** *48* (7), 1235-1245.

126. Chen, Y.; Fan, J.; Qian, X.; Zhang, W., Effect of garment fit on thermal insulation and evaporative resistance. *Textile Research Journal* **2004,** *74* (8), 742-748.

127. Morrissey, M. P.; Rossi, R. M., The effect of wind, body movement and garment adjustments on the effective thermal resistance of clothing with low and high air permeability insulation. *Textile Research Journal* **2014,** *84* (6), 583-592.

128. Lu, Y.; Wang, F.; Wan, X.; Song, G.; Shi, W.; Zhang, C., Clothing resultant thermal insulation determined on a movable thermal manikin. Part I: effects of wind and body movement on total insulation. *Int. J. Biometeorol.* **2015,** *59* (10), 1475-1486.

129. Lu, Y.; Wang, F.; Wan, X.; Song, G.; Zhang, C.; Shi, W., Clothing resultant thermal insulation determined on a movable thermal manikin. Part II: effects of wind and body movement on local insulation. *Int. J. Biometeorol.* **2015,** *59* (10), 1487-1498.

130. Bouskill, L.; Havenith, G.; Kuklane, K.; Parsons, K.; Withey, W., Relationship between clothing ventilation and thermal insulation. *AIHA journal* **2002,** *63* (3), 262-268.

131. Wan, X.; Wang, F., Numerical analysis of cooling effect of hybrid cooling clothing incorporated with phase change material (PCM) packs and air ventilation fans. *International Journal of Heat and Mass Transfer* **2018,** *126*, 636-648.

132. Sun, Y.; Jasper, W. J., Numerical modeling of heat and moisture transfer in a wearable convective cooling system for human comfort. *Build. Environ.* **2015,** *93*, 50-62.

133. Sun, W. J. J. Y.; Jasper, W. J., Effects of air velocity, air gap thickness and configuration on heat transfer of a wearable convective cooling system. *Journal of Textile Science & Engineering* **2015,** *5* (6).

134. Cui, Z.; Zhang, W., Study of the effect of material assembly on the moisture and thermal protective performance of firefighter clothing. *Fibres & Textiles in Eastern Europe* **2009,** *17* (6), 77.

135. DenHartog, E.; Fang, X.; Deaton, A., Effects of total heat loss versus evaporative resistance of firefighter garments in a physiological heat strain trial. *Performance of Protective Clothing and Equipment: 11th Volume, Innovative Solutions to Evolving Challenges*, **2021**, 204-221.

136. Kim, J.-H.; Kim, D.-H.; Lee, J.-Y.; Coca, A., Relationship between total heat loss and thermal protective performance of firefighter protective clothing and consequent influence on burn injury prediction via flame-engulfment manikin test. *Proceedings of the Human Factors and Ergonomics Society Annual Meeting* **2017,** *61* (1), 1468-1471.

137. Xin, L.; Li, J., The relation between thermal protection performance and total heat loss of multi-layer flame resistant fabrics with the effect of moisture considered. *Fibers and Polymers* **2016,** *17* (2), 289-297.

138. Stoll, A. M.; Chianta, M. A., Method and rating system for evaluation of thermal protection. *Aerosp. Med.* **1969,** *40* (11), 1232-8.

139. Matusiak, M., Investigation of the thermal insulation properties of multilayer textiles. *Fibres & Textiles in Eastern Europe* **2006,** *14* (5), 98-102.

140. Song, G.; Paskaluk, S.; Sati, R.; Crown, E. M.; Doug Dale, J.; Ackerman, M., Thermal protective performance of protective clothing used for low radiant heat protection. *Textile Research Journal* **2011,** *81* (3), 311-323.

141. Naeem, J.; Mazari, A.; Volesky, L.; Mazari, F., Effect of nano silver coating on thermal protective performance of firefighter protective clothing. *The Journal of The Textile Institute* **2018**, 1-12.

142. Lee, Y. M.; Barker, R. L., Effect of moisture on the thermal protective performance of heat-resistant fabrics. *Journal of Fire Sciences* **1986,** *4* (5), 315-331.

143. Barker, R. L.; Guerth-Schacher, C.; Grimes, R. V.; Hamouda, H., Effects of moisture on the thermal protective performance of firefighter protective clothing in low-level radiant heat exposures. *Textile Research Journal* **2006,** *76* (1), 27-31.

144. Lu, Y.; Li, J.; Li, X.; Song, G., The effect of air gaps in moist protective clothing on protection from heat and flame. *Journal of Fire Sciences* **2013,** *31* (2), 99-111.

145. Su, Y.; Yang, J.; Li, R.; Song, G.; Li, J., Effect of compression on thermal protection of firefighting protective clothing under flame exposure. *Fire and Materials* **2019**, *43*, 802–810.

146. Shaid, A.; Wang, L.; Padhye, R., Textiles for Firefighting Protective Clothing. *Firefighters' Clothing and Equipment: Performance, Protection, and Comfort* **2018**, 1.

147. McQuerry, M.; Kwon, C.; Johnson, H., A critical review of female firefighter protective clothing and equipment workplace challenges. *Research Journal of Textile and Apparel* **2019**.

148. Osczevski, R., *Diffusion of water vapour through cold Gore-Tex*. Defence Research Establishment Ottawa: **1993**.

149. Ding, D.; Tang, T.; Song, G.; McDonald, A., Characterizing the performance of a single-layer fabric system through a heat and mass transfer model-Part II: thermal and evaporative resistances. *Textile Research Journal* **2011,** *81* (9), 945-958.

150. Yoo, S.; Kim, E., Wear trial assessment of layer structure effects on vapor permeability and condensation in a cold weather clothing ensemble. *Textile Research Journal* **2012,** *82* (11), 1079-1091.

151. Rossi, R. M.; Gross, R.; May, H., Water vapor transfer and condensation effects in multilayer textile combinations. *Textile Research Journal* **2004,** *74* (1), 1-6.

152. Hearle, J. W.; Morton, W. E., *Physical properties of textile fibres*. Elsevier: **2008**.

153. Akcagun, E.; Bogusławska-Bączek, M.; Hes, L., Thermal insulation and thermal contact properties of wool and wool/PES fabrics in wet state. *Journal of Natural Fibers* **2017**, 1-10.

154. Romeli, D.; Barigozzi, G.; Esposito, S.; Rosace, G.; Salesi, G., High sensitivity measurements of thermal properties of textile fabrics. *Polymer Testing* **2013,** *32* (6), 1029-1036.

155. Wang, Y.-y.; Lu, Y.-h.; Li, J.; Pan, J.-h., Effects of air gap entrapped in multilayer fabrics and moisture on thermal protective performance. *Fibers and Polymers* **2012,** *13* (5), 647-652.

156. Gao, H.; Deaton, S.; Fang, X.; Watson, K.; DenHartog, E.; Barker, R.L., Effects of environmental temperature and humidity on evaporative heat loss through firefighter suit materials made with semipermeable and microporous moisture barriers. *Textile Research Journal* **2021** (Accepted).

157. Lotens, W. A.; Van De Linde, F. J. G.; Havenith, G., Effects of condensation in clothing on heat transfer. *Ergonomics* **1995,** *38* (6), 1114-1131.

158. McQuerry, M.; Barker, R.; DenHartog, E., Relationship between novel design modifications and heat stress relief in structural firefighters' protective clothing. *Appl. Ergon.* **2018,** *70*, 260-268.

159. Barker, R., Evaluating the heat stress and comfort of firefighter and emergency responder protective clothing. In *Improving comfort in clothing*, Elsevier: **2011**; pp 305-319.

160. Banks, A. P. W.; Wang, X.; Engelsman, M.; He, C.; Osorio, A. F.; Mueller, J. F., Assessing decontamination and laundering processes for the removal of polycyclic

aromatic hydrocarbons and flame retardants from firefighting uniforms. *Environ. Res.* **2021,** *194*, 110616.

161. Shimazaki, Y.; Goto, S.; Yoshida, A.; Yamamoto, T., Transfer, M., The effect of solar radiation on temperature distribution in outdoor human–clothing–environment systems. *International Journal of Heat and Mass Transfer* **2017,** *104*, 1-6.

162. Lei, Z.; Qian, X.; Zhang, X., Assessment of thermal protective performance of firefighter's clothing by a sweating manikin in low-level radiation. *International Journal of Clothing Science and Technology* **2019,** *31* (1), 145-154.

163. Bröde, P.; Kuklane, K.; Candas, V.; DenHartog, E. A.; Griefahn, B.; Holmér, I.; Meinander, H.; Nocker, W.; Richards, M.; Havenith, G., Heat transfer through protective clothing under symmetric and asymmetric long wave thermal radiation. Zeitschrift für Arbeitswissenschaft **2008**, *62*(4), 267-276.

164. Guan, M.; Annaheim, S.; Camenzind, M.; Li, J.; Mandal, S.; Psikuta, A.; Rossi, R. M., Moisture transfer of the clothing–human body system during continuous sweating under radiant heat. *Textile Research Journal* **2019**, 004051751983576.

165. Guan, M.; Psikuta, A.; Camenzind, M.; Li, J.; Mandal, S.; Michel Rossi, R.; Annaheim, S., Effect of perspired moisture and material properties on evaporative cooling and thermal protection of the clothed human body exposed to radiant heat. *Textile Research Journal* **2018**, 004051751881706.

166. DenHartog, E. A., Challenges in future personal protective equipment–an overview of developments in user needs. *Research Journal of Textile and Apparel* **2010**, *14(4)*, 22-37.

167. Krusi, P.; Schmid, R., The CSI 1000 W lamp as a source for solar radiation simulation. *Solar Energy* **1983,** *30* (5), 455-462.

168. Al-Aboosi, F. Y., Models and hierarchical methodologies for evaluating solar energy availability under different sky conditions toward enhancing concentrating solar collectors use: Texas as a case study. *International Journal of Energy and Environmental Engineering* **2020,** *11* (2), 177-205.

169. Yoo, S.; Barker, R. L., Comfort properties of heat-resistant protective workwear in varying conditions of physical activity and environment. Part I: Thermophysical and sensorial properties of fabrics. *Textile Research Journal* **2005,** *75* (7), 523-530.

170. Akgun, M.; Becerir, B.; Alpay, H. R., The effect of fabric constructional parameters on percentage reflectance and surface roughness of polyester fabrics. *Textile Research Journal* **2012,** *82* (7), 700-707.

171. Rezazadeh, M.; Bespflug, C. J.; Torvi, D. A.; Noble, S. D.; Fulton, M., Predicting Mechanical Strength of In-Use Firefighter Protective Clothing Using Near-Infrared Spectroscopy. *Fire Technol.* **2018,** *54* (6), 1759-1781.

172. Horn, G. P.; Kerber, S.; Andrews, J.; Kesler, R. M.; Newman, H.; Stewart, J. W.; Fent, K. W.; Smith, D. L., Impact of repeated exposure and cleaning on protective properties of structural firefighting turnout gear. *Fire Technol.* **2020**, 1-23.

173. Mayer, A. C.; Horn, G. P.; Fent, K. W.; Bertke, S. J.; Kerber, S.; Kesler, R. M.; Newman, H.; Smith, D. L., Impact of select PPE design elements and repeated laundering in firefighter protection from smoke exposure. *J. Occup. Environ. Hyg.* **2020,** *17* (11-12), 505-514.

174. NFPA 1851:2020. Standard on selection, care, and maintenance of protective ensembles for structural fire fighting and proximity fire fighting.

175. Hodder, S. G.; Parsons, K., The effects of solar radiation on thermal comfort. *Int. J. Biometeorol.* **2006,** *51* (3), 233-250.

176. Otani, H.; Kaya, M.; Tamaki, A.; Goto, H.; Maughan, R. J., Exposure to high solar radiation reduces self-regulated exercise intensity in the heat outdoors. Physiology & behavior **2019,** *199*, 191-199.

177. Bröde, P.; Candas, V.; Kuklane, K., Effects of heat radiation on the heat exchange with protective clothing – a thermal manikin study. In Proceedings of 3rd European Conference on Protective Clothing (ECPC), Poland, May **2006**.

178. Shimazaki, Y.; Goto, S.; Yoshida, A.; Yamamoto, T., The effect of solar radiation on temperature distribution in outdoor human–clothing–environment systems. *International Journal of Heat and Mass Transfer* **2017,** *104*, 1-6.

179. Clark, J. A.; Cena, K., Net radiation and heat transfer through clothing: the effects of insulation and colour. *Ergonomics* **1978,** *21* (9), 691-696.

180. Mandal, S.; Camenzind, M.; Annaheim, S.; Rossi, R. M., Firefighters' protective clothing and equipment. In *Firefighters' Clothing and Equipment*, 1 ed.; Song, G.; Wang, F., Eds. CRC Press:**2018**; pp 31-59.

181. Yang, J.; Su, Y.; Song, G.; Li, R.; Xiang, C., A new approach to predict heat stress and skin burn of firefighter under low-level thermal radiation. *International Journal of Thermal Sciences* **2019,** *145*, 106021.

182. Gibson, P., Water-repellent treatment on military uniform fabrics: physiological and comfort implications. *Journal of Industrial Textiles* **2008,** *38* (1), 43-54.

183. Yoo, S.; Barker, R. L., Comfort properties of heat resistant protective workwear in varying conditions of physical activity and environment. Part II: perceived comfort

response to garments and its relationship to fabric properties. *Textile Research Journal* **2005,** *75* (7), 531-539.

184. Burke, R.; Curran, D. A.; Hepokoski, M., Integrating an active physiological and comfort model to the Newton sweating thermal manikin. *Proceedings of the 13th International Conference on Environmental Ergonomics (ICEE)*. University of Wollongong, Wollongong. **2009**.

185. Deaton, A.S.; Watson, K.; DenHartog, E.; Barker, R. L., Effectiveness of using a Thermal Sweating Manikin Coupled with a Thermoregulation Model to Predict Human Physiological Response to Different Firefighter Turnout Suits. *11th Symposium on Performance of Protective Clothing and Equipment: Innovative Solutions to Evolving Challenges* **2020**.

186. Hunt, A. P.; Buller, M. J.; Maley, M. J.; Costello, J. T.; Stewart, I. B., Validity of a noninvasive estimation of deep body temperature when wearing personal protective equipment during exercise and recovery. *Military Medical Research* **2019,** *6* (1), 1-11.

187. Vincent, J.-L., Understanding cardiac output. *Critical Care* **2008,** *12* (4), 174.

188. Havenith, G., Temperature regulation, heat balance and climatic stress. In *Extreme weather events and public health responses*, Springer: **2005**; pp 69-80.

189. Dorman, L. E.; Havenith, G., The effects of protective clothing on energy consumption during different activities. *Eur. J. Appl. Physiol.* **2009,** *105* (3), 463-470.

190. Dorman, L.; Havenith, G., The influence of clothing weight and bulk on metabolic rate when wearing protective clothing. The Third International Conference on Human-Environment System ICHES'05 in Tokyo, Japan, 12-15 Sep., **2005**.

191. Slater, K., *Human comfort*. Charles C. Thomas Publisher. **1985**.

192. Barker, R. L.; Tang, T.; Song, G.; McDonald, A., Multilevel approach to evaluating the comfort of functional clothing. *J. Fiber Bioeng. Inform* **2008,** *1* (3), 173-176.

193. Yoo, S.; Barker, R. L., Moisture management properties of heat-resistant workwear fabrics— effects of hydrophilic finishes and hygroscopic fiber blends. *Textile Research Journal* **2004,** *74* (11), 995-1000.

194. Keiser, C.; Rossi, R. M., Temperature analysis for the prediction of steam formation and transfer in multilayer thermal protective clothing at low level thermal radiation. *Textile Research Journal* **2008,** *78* (11), 1025-1035.

195. Stull, J. O., Comparative thermal insulative performance of reinforced knee areas of firefighter protective clothing. In *Performance of Protective Clothing: Issues and Priorities for the 21 st Century: Seventh Volume*, ASTM International: **2000**.

196. McQuerry, M.; DenHartog, E.; Barker, R., Impact of reinforcements on heat stress in structural firefighter turnout suits. *The Journal of The Textile Institute* **2018,** *109* (10), 1367-1373.

197. McQuerry, M.; Barker, R.; Hummel, A.; Deaton, S., The cost of a pocket: how additional reinforcements impact THL & TPP. *Fire Engineering* **2015,** *168*, 78-79.

198. Blood, K.; Burke, R. Further validation of the model-controlled Newton thermal manikin against historical human studies. 8th International Meeting for Thermal Manikin and Modeling (8I3M), Victoria, Canada, **2010**.

199. DenHartog, E.; Fang, X.; Deaton, A., Effects of total heat loss versus evaporative resistance of firefighter garments in a physiological heat strain trial. *Performance of Protective Clothing and Equipment: 11th Volume, Innovative Solutions to Evolving Challenges* **2020**, 204-221.

200. Nunneley, S. A., Heat stress in protective clothing: interactions among physical and physiological factors. *Scandinavian journal of work, environment & health* **1989**, 52-57.

201. Cheshire Jr, W. P., Thermoregulatory disorders and illness related to heat and cold stress. *Auton. Neurosci.* **2016,** *196*, 91-104.

202. Crandall, C.; Gonzalez-Alonso, J., Cardiovascular function in the heat-stressed human. *Acta physiologica* **2010,** *199* (4), 407-423.

203. Barker, R. L., A Review of gaps and limitations in test methods for first responder protective clothing and equipment: a final report presented to National Personal Protection Technology Laboratory, National Institute for Occupational Safety and Health. **2005**.

204. Parsons, K. C., *Human thermal comfort*. CRC Press, **2020**.

205. Wilson, T. E.; Crandall, C. G. Effect of thermal stress on cardiac function. *Exercise and sport sciences reviews* **2011,** *39* (1), 12.

206. Sawka, M. N.; Montain, S. J., Fluid and electrolyte supplementation for exercise heat stress. *The American journal of clinical nutrition* **2000**, 72 (2), 564S-572S.